ProQuest LLC.
789 East Eisenhower Parkway
P.O. Box 1346
Ann Arbor, MI 48106 – 1346

Speciation of Chromium in Environmental Matrices

Michelle Derbyshire BSc (Hons)

A thesis submitted in partial fulfilment of the requirements of

Sheffield Hallam University

for the degree of Doctor of Philosophy

June 2001

Collaborating Organisation: European Commission, Joint Research Centre, Institute for Reference Materials and Measurements, Geel, Belgium

ACKNOWLEDGMENTS

Work was carried out at the Joint Research Centre, Institute for Reference Materials and Measurements (IRMM), Geel, Belgium as part of a Community Training Project financed by the Commission Programme "Reference Materials and Measurements".

Supervisors:
Dr. P. Gardiner & Dr. N. Bricklebank
(Sheffield Hallam University, Sheffield, United Kingdom)

Advisor:
Dr. A. Lamberty
(IRMM, Geel, Belgium, Management of Reference Materials Unit)

I would like to thank the following people without whose help this thesis would not have been possible:
Dr. Håkan Emteborg for help with the ETAAS analysis and the chemiluminescence as well as endless encouragement.
Dr. Magnus Johansson again for help with the ETAAS analysis, assistance with the use of experimental modelling and valuable discussions about ion chromatography.
Dr. Einar Pontin and Dr. Malin Stigbrand for help with the chemiluminescence analysis and for the loan of a chemiluminescence instrument.
Mr. Paul De Vos, Mr. Albert Oostra and Mr. Kramer for help with carrying out the production procedures for a typical soil reference material.
Jørgen Nørgaard for help with the writing and editing of this work and for constant encouragement.
Stefan Rückold and Patrick Conneely for help with the theory and practice of the Karl Fischer analysis.
Nineta Majcen for assistance with the understanding of chemometrics.
Andrew Dobney, Simon Nelms and Christophe Quetel for assistance with the operation and theory of the ICP-MS instrument.

LIST OF ABBREVIATIONS

Techniques

CL.....Chemiluminescence

AAS.....Atomic Absorption Spectrometry

FAAS.....Flame AAS

ETAAS.....Electrothermal AAS

HPLC.....High Performance Liquid Chromatography

ICP.....Inductively Coupled Plasma

AES.....Atomic Emission Spectrometry

MS.....Mass Spectrometry

IC.....Ion Chromatography

UV.....Ultraviolet

Chemicals

EDTA.....Ethylene Diamine Tetraacetic Acid

APDC.....Ammonium Pyrrolidine Dithiocarbamate

PDCA.....Pyridine Dicarboxylic Acid

DPC.....Diphenylcarbazide

Luminol.....5-amino-2,3-dihydro-1,4-phthalazine dione

Miscellaneous

GTF.....Glucose Tolerance Factor

RM.....Reference Material

CRM.....Certified Reference Material

HETP.....Height Equivalent to a Theoretical Plate

TABLE OF CONTENTS

Page No.

ABSTRACT

Published methods for single and sequential extraction, separation and determination of chromium(III) and (VI) in sewage sludge, soil and dried plant material were critically evaluated. The results obtained illustrate the difficulties of speciation analysis in such complex matrices.

A method based on single extraction with 0.43 mol L^{-1} acetic acid followed by on-line ion chromatography with chemiluminescence detection was found to be simple, sensitive, free of interferences, and more importantly the integrity of the chromium species was maintained. Instrumental parameters affecting the sensitivity of the chemiluminscence signals were optimised using a multivariate optimisation approach. A linear calibration was obtained from 0.01 to 50 μg L^{-1}. Limits of detection were found to be 0.002 μg L^{-1} for both Cr(III) and Cr(VI). Limits of determination were found to be 0.02 μg L^{-1} for both Cr(III) and Cr(VI). The precision, determined using a 10 μg L^{-1} solution of Cr(III) and Cr(VI) was 10.6 ± 0.52μg L^{-1} (4.9%) for Cr(III) and 10.1 ± 0.50 μg L^{-1} (4.9%) for Cr(VI) (n=6). Validation of the method was carried out using two water reference materials certified for total chromium content; LGC CRM 6010 49 μg L^{-1} ± 4 μg L^{-1} and NIST SRM 1643d 18.53 μg L^{-1} ± 0.20 μg L^{-1}. Results obtained showed good agreement with the certified values; 49.21 μg L^{-1} ± 1.81 μg L^{-1} and 19.03 μg L^{-1} ± 1.50 μg L^{-1} respectively.

The developed method was used to study the distribution of Cr(III) and Cr(VI) species in soils. The species extraction procedure was validated using a certified reference material (CRM): BCR CRM 483. The changes in the distribution of both species in soil that had been through similar pre-treatment steps as in the production of reference materials were studied. This investigation showed that contamination or chemical oxidation could alter the chromium species present within a natural sample during production steps such as milling, homogenisation and sieving. As a result the metal speciation in the product is different from that in the starting material. In order to limit the effect of oxidation jet rather than ball milling is recommended.

CHAPTER 1 INTRODUCTION

1.1 Chemical Speciation

Chemical speciation can be defined as the process of identifying and quantifying the different species, forms or phases present in a material, or the description of these. The species can be defined in several different ways[1,2]:

- Functionally i.e. according to their function e.g. 'plant available species', 'mobile forms' or 'exchangeable cations'.
- Operationally i.e. according to the reagents or procedures used in their isolation e.g. 'EDTA-extractable', 'moderately reducible' or 'soil solution'.
- As particular compounds or oxidation states of an element e.g. Fe^{2+} and Fe^{3+}, CH_3Hg^+ and Hg^{2+} or Cr(III) and Cr(VI).

There are inherent problems associated with the application of each of these definitions particularly in cases where functionally or operationally defined chemical species are extracted from solid samples. Therefore only weak methods of extraction may be used and consequently the result is often not related to the total species content[3,4,5]. However these methods normally relate better to what is actually occurring in natural soil-water systems, as they determine the amount of species available to plants[6], and are therefore useful in bioavailability studies. The study of the distribution of actual chemical species without modifying them in any way is difficult to achieve. However, this approach is useful when an understanding of the behaviour of the chemical species at a molecular level is required.

It has been stated that the toxicity of metals to plants and animals depends on their physicochemical form (i.e. speciation)[7]. The term "speciation" has become widely accepted as appropriate to describe the distribution of an element between different physicochemical forms. In the context of this study, speciation may be regarded as the differentiation between different chemical forms of the analyte of interest, for example chromium (III) and chromium (VI).

Chemical speciation is important in assessing the availability of plant nutrients, plant uptake of potentially toxic elements and the movement of both nutrient and toxic substances into waterways or other parts of an ecosystem[8]. An element that is present in, for example soil, may be sorbed by a range of mechanisms such as precipitation, ion exchange and complexation. They may also be associated with different components of the soil e.g. metal hydrous oxides, silicates, carbonates or soil organic matter etc. This makes for a very complex analysis.

The techniques used in speciation analysis generally involve several analytical steps (e.g. extraction, derivatisation, separation and detection). Each of these steps can introduce errors to the analysis. Results reported in the literature are often difficult to compare and there is therefore a need for appropriate reference materials certified for the chemical species content. During the preparation of these environmental and biological reference materials it is possible that changes in the distribution of the chemical species could occur. Investigations into the nature of these changes therefore need to be carried out so that reference materials with properties closely related to the natural materials can be produced.

1.2 Chromium (Cr) - General Properties

Chromium, a member of group 6 of the periodic table, is widely distributed in the environment and is found in varying concentrations in air, soil, water and biological matter. Chromium can occur in any of the oxidation states from -II to +VI, but it is only commonly found in the oxidation states 0 (the metallic form), III and VI.

Chromium (III) is regarded as an essential element and is required for normal glucose and lipid metabolism[9] in man. The chromium content in all tissues decreases with age and it has been postulated that this decline in chromium may be involved in the development of disease states related to ageing[10]. The recommended daily intake for chromium is 50-200 μg. Studies have shown that insufficient dietary intake of chromium is prevalent in the USA and Europe[11]. Chromium is essential for the normal glucose tolerance factor (GTF) in man[12]. GTF is essential for insulin activity and chromium is prescribed as a dietary supplement where impaired glucose tolerance is diagnosed. The signs of chromium deficiency are often similar to those of maturity-onset diabetes and cardiovascular diseases.

In contrast, chromium (VI), in the form of chromate (CrO_4^{2-}) and dichromate ($Cr_2O_7^{2-}$), has been found to be harmful to living organisms[13]. Chromium (VI) compounds are allergens and irritants, which can cause dermatitis. They can enter the body via the respiratory tract, by ingestion or through the skin. The toxic effects are wide ranging from lachrymation to the formation of malignant growths[14]. Inhalation can cause asthma, ulceration and damage to the mucus membranes of the respiratory system and respiratory cancer[15]. In the event of ingestion, damage is caused to the mucous membranes of the gastrointestinal tract, accompanied by damage to the kidneys and liver, which can lead to shock and death. Soluble salts such as chromate (CrO_4^{2-}) and

dichromate ($Cr_2O_7^{2-}$) when absorbed through the skin cause damage to mucous membranes, as well as various proteins and nucleic acids and lead to mutation and carcinogenesis[16,17].

In the natural environment, chromium occurs principally as the mineral chromite ($FeO.Cr_2O_3/FeCr_2O_4$) which is an extremely stable trivalent state. The majority of atmospheric chromium emissions are produced from ferrochromium or chromium metal alloy production, smelting, roasting and extraction processes used to produce chromate and dichromate chemicals, and the casting by electric furnaces of refractory bricks[18]. Hexavalent chromium species are found mainly in liquid emissions from electroplating, the manufacture of alloys, the leather tanning industry and water pipes, to which it is added as a corrosion inhibitor[19,20,21].

1.3 Redox Chemistry of Chromium

The toxicity and the mobility of chromium are dependent upon its oxidation state. Hexavalent chromium is a strong oxidising agent and is readily reduced in the presence of an appropriate electron donor[22].

Equation 1

$$HCrO_4^- + 7H^+ + 3e^- \rightarrow Cr^{3+} + 4H_2O$$

Due to the high redox potential of the Cr(VI)/Cr(III) couple, there are few oxidants in natural systems capable of oxidising Cr(III) to Cr(VI). The main oxidants are the higher valent manganese oxides, Mn (III, IV), such as birnessite (δ-MnO_2) and dissolved oxygen, although oxidation by dissolved oxygen is reported to be very slow[23].

Equation 2

$$2Cr^{3+} + 3MnO_2 + 2H_2O \rightarrow 2CrO_4^{2-} + 3Mn^{2+} + 4H^+$$

On the other hand, Cr(VI) is strongly oxidising, as shown by its stability at high redox potentials (Figure 1) and there are therefore numerous reductants for the Cr(VI) to Cr(III) process. Examples include Fe(II), S^{2-} and organic matter[23,24]. For example in the case of iron, weathering of Fe(II)-containing minerals such as biotite, haematite and some clays, as well as industrial wastes, can generate dissolved Fe(II) ions. These ions are then capable of reducing Cr(VI)[25].

Equation 3

$$3FeO + 14H^+ + CrO_4^{2-}{}_{(aq)} \rightarrow Cr^{3+}{}_{(aq)} + 3Fe^{3+}{}_{(aq)} + 7H_2O$$

This process is very rapid, taking only a few minutes. Reduction of Cr(VI) by organic matter such as simple amino acids[23] or humic or fulvic acids[26] results in intermediate Cr(IV) and (V) species (see Equation 4) which then decay slowly (over several days) to Cr(III)[27].

Equation 4

$$H_2A + Cr(VI) \rightarrow Cr(IV) + A \text{ (slow - rate determining step)}$$

$$Cr(IV) + Cr(VI) \rightarrow 2Cr(V)$$

$$Cr(V) + H_2A \rightarrow Cr(III) + A \text{ (where A represents the acid)}[28]$$

Reduction of Cr(VI) by sulphides, in contrast, is rapid for the first five minutes, but then slows down and reaches completion within a day[23]. Discharge of industrial wastes, decomposition of organic matter and sulphate reduction provide the dissolved sulphides for this reduction.

Ferrous iron and organic matter are ubiquitous in soils and groundwaters. Therefore, in many natural environments, Cr(VI) would be reduced to Cr(III).

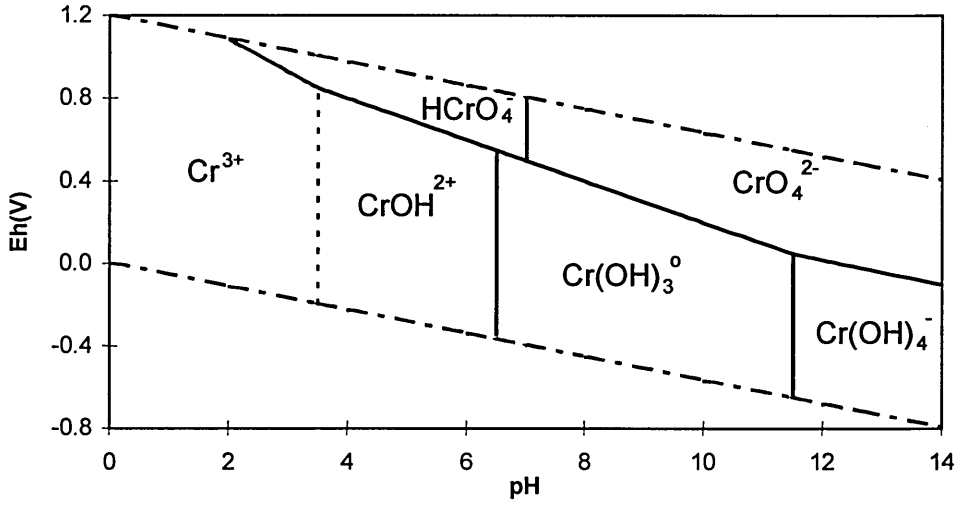

Figure 1: Eh-pH diagram for aqueous chromium species. Based on data from Palmer and Wittbrodt[29].

Figure 1 shows that chromium can exist in many different forms depending upon pH. In aqueous solution Cr(III) can exist as $Cr_3(OH)_4^{5+}$, $Cr_2(OH)_2^{4+}$, $Cr(H_2O)_6^{3+}$, $CrOH^{2+}$, $Cr(OH)_2^+$, $Cr(OH)_3^0$ and $Cr(OH)_4^-$. Under acidic conditions (at a pH lower than 3.6) Cr(III) exists primarily as $Cr(H_2O)_6^{3+}$ (i.e. Cr^{3+}). With increasing pH the hydrolysis of Cr(III) occurs. A review of this hydrolysis has been carried out by Rai et al.[30]. The distribution of species depends mainly upon the pH of the environment. Trivalent chromium behaves as a typical "hard" Lewis acid and forms complexes with a variety of ligands e.g. hydroxyl, sulphate, ammonium cyanide and natural and synthetic organic ligands. The rate of formation of Cr(III) complexes is slow, but they are thermodynamically very stable once formed.

As shown in Figure 2, at pH values above 6.5, the predominant Cr(VI) species is CrO_4^{2-}. Between pH 1 and 6.5, $HCrO_4^-$ is the main species at concentration levels below 1 g L^{-1}, whereas at higher levels $Cr_2O_7^{2-}$ is formed.

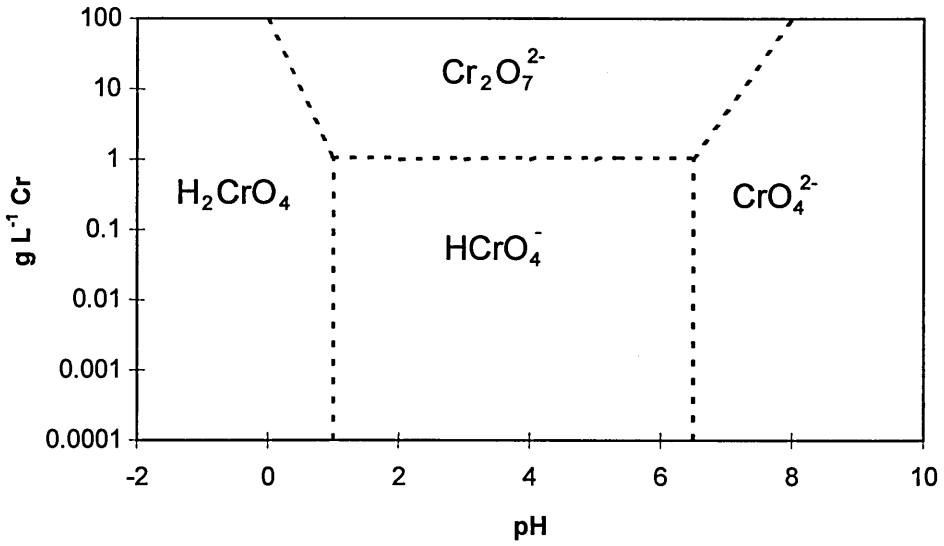

Figure 2: Relative distribution of Cr(VI) species in water as a function of pH and Cr(VI) concentration[31].

Trivalent chromium is only sparingly soluble in soils. Therefore the reduction of Cr(VI) to Cr(III) in alkaline soils minimises potential migration of Cr(VI) and as a result reduces the potential hazard to human health. It has been found, however, that manganese oxides in moist, aerobic soils at a pH above 6 can convert cationic Cr(III) species into $HCrO_4^-$ and CrO_4^{2-}[32]. These conditions are prevalent in many field soils. This has implications for the interpretation of the results from studies carried out on dried soil samples. It has been found that when the soil is dried the oxidised Mn (III, IV) is reduced to Mn(II)[32]. Under these conditions, the Cr(III) is not oxidised.

1.4 Extraction of Chromium

The choice of method is determined by the sample type and the requirements of the detection technique. The most important consideration in a speciation study such as this is that the method of extraction removes the chemical species without loss or contamination and does not change the distribution of species. Extraction procedures may be applied individually or as part of a sequence.

1.4.1 Extraction of Chromium from Water

In the analysis of water samples very little sample preparation is normally necessary. This usually amounts to filtration and possibly buffering in order to maintain the integrity of the species. Acidification is not recommended as this is likely to cause the reduction of Cr(VI) to Cr(III).

1.4.2 Extraction of Chromium from Solid Matrices

Determination of chromium species in soils, sediments and sewage sludges represents much more of a challenge. Complete extraction of the chromium species from the sample matrix without changes in the oxidation states is essential to the overall success of the operation.

Metal cations in soils may be bound in different ways: as simple or complex ions, easily exchangeable ions, organically bound, occluded by or co-precipitated with metal oxides or carbonates or phosphates and secondary minerals, or as ions in the crystal lattices of primary minerals. Any sequential extraction schemes that are proposed must therefore reflect these differences in binding of the metal to the matrix. In this way a number of fractions are obtained, each of which is associated with a particular type of binding of

the metal ion[33,34]. Table 1 shows some of the chemical extractants used and the metal containing fractions extracted.

Table 1: Extraction of fractions from soil samples.

Nature of Extractant	Metal Species Extracted	Chemical Extractant
Exchangeable	adsorbed metals	$CaCl_2$, $MgCl_2$, CH_3COOH
Carbonate	bound to carbonates	EDTA
Reducible	bound to Fe and Mn oxides	NH_3OHCl, citrate
Oxidisable	bound to organic & sulphidic compounds	H_2O_2,H_2O_2/HNO_3, $H_2O_2/CH_3CO_2NH_4$
Residual	bound to the mineral lattice	mixtures of strong acids such as $HNO_3/HClO_4/HF$

Extraction media for soil, sludge or sediment can be neutral electrolytes such as $CaCl_2$[35] or $MgCl_2$, buffers of weak acids e.g. acetic and oxalic acids, chelating agents such as EDTA, redox agents e.g. NH_2OH, strong acids e.g. HCl, HNO_3[36] or bases such as Na_2CO_3 and NaOH[37]. Electrolytes, weak acids and chelating agents release metals from coordination sites, while strong acids and other redox agents are capable of releasing additional quantities of metal ions as the mineral and organic soil constituents are broken down[38].

Sequential extraction procedures are also often employed, in order to successively extract more strongly bound fractions from the soil matrix. Tessier et al.[39] developed such a procedure for the partitioning of particulate trace metals into five fractions. The total extractable content was determined with a coefficient of variation of better than ± 10%. Davidson et al.[40] also used a sequential extraction scheme in order to obtain information about the mobilities of the constituents of soil with reference to their

availability to plants. Problems with this type of extraction scheme, however, are that the extractants are selective, but not specific. Therefore each extractant normally extracts more than one type of metal species. Consequently, the same species may be removed by two different extractants. Also, the use of strong acids or redox agents, which are often used in these extraction schemes, can alter the form of the chromium species. The stronger extraction media can cause reduction or oxidation of the species present, and therefore are not suitable for the proposed study.

Methods are available for the extraction of Cr(VI) only, such as the alkaline digestion method reported by James[41] and also Vitale et al.[42] using 0.28 mol L^{-1} Na_2CO_3 /0.5 mol L^{-1} NaOH heated with the soil for 60 minutes to solubilise all forms of Cr(VI). In a later paper, Vitale et al.[43] compared this method to four other methods for the solubilisation of $PbCrO_4$ spiked into four diverse soil materials. The other extractants investigated were water, phosphate buffer, sodium carbonate/hydroxide solution without heating and sodium hydroxide solution with sonication. The hot sodium carbonate/hydroxide solution was found to be superior to all the other methods with respect to the amount of $PbCrO_4$ extracted. These extraction techniques were also compared by James et al.[44] for total Cr(VI) extraction. Here the hot sodium carbonate/hydroxide solution was also found to be superior. Methods, such as that of Nivas et al.[45], employing surfactants, e.g. Dowfax-8390 [$C_{16}H_{33}C_{12}H_7O(SO_3Na)_2$], have also been used in order to selectively extract Cr(VI) with some success (2.0 to 2.5 times better than water). This success rate was increased when a complexing agent e.g. diphenylcarbazide was used in conjunction with the surfactant (3.7 to 5.7 times greater than the surfactant alone).

Other methods are available which extract operationally defined fractions, such as that of Houba et al.[46]. In this method 0.01 mol L^{-1} $CaCl_2$ was evaluated. This extractant removes exchangeable or adsorbed metals from the soil matrix. They found that the amount of extractable metal ions changed with storage. Phosphate extraction has also been used in this way to extract soluble and exchangeable forms of Cr(VI) from soils[44].

1.5 Methods of Analysis

A commonly used analysis technique for chromium determination is that of atomic absorption spectrometry (AAS). This technique may be performed using a flame (FAAS), or a graphite furnace (electrothermal) (ETAAS) for atomisation. Using FAAS, complexation and pre-concentration on an iminodiacetate resin, Pasullean et al.[47] were able to determine Cr(III) and total chromium in sea waters. One problem with the use of FAAS is that it is often subject to interferences, which may be either spectral or chemical[48]. Spectral interferences occur when particulate matter scatter the incident radiation or when the absorption of an interfering species either overlaps or lies so close to the analyte absorption that resolution by the monochromator becomes impossible. Chemical interferences result from various chemical processes occurring during atomisation that alter the absorption characteristics of the analyte. Addition of a chemical modifier can help to counteract these, for example in the case of Kabil[49]. Here determination of both Cr(III) and Cr(VI) in aqueous solutions was achieved using butylamine (BA) as a modifier to obtain reproducible results, even in the presence of a range of organic and inorganic interfering species. The modifier was suggested to protect the chromium from any contaminant effects by the formation of Cr^{III}-$(BA)_4$ and by creating a suitable reducing environment in the flame. Zybin et al.[50] obtained a detection limit of 30 pg mL^{-1} when they used high performance liquid chromatography

(HPLC) coupled to diode laser FAAS to determine Cr(VI) in tap water. In another method, Oktavec et al.[51] determined Cr(III) and Cr(VI) in groundwater and wastewater using both flame and graphite furnace AAS after their separation with cation and anion exchangers. The method was found to be suitable for detection of both species in the range from 0.06 μg L^{-1} to 5 mg L^{-1}. Both Cr(III) and Cr(VI) were determined by difference, in river water, by Manzoori et al.[52] using ETAAS and an alumina micro-column, which retained Cr(VI). Limits of detection were found to be 0.57 μg mL^{-1} and 0.61 μg mL^{-1} for Cr(III) and Cr(VI) respectively. Other methods using ETAAS include those by Kubrakova et al.[53] and Beceiro-Gonzalez et al.[54]. Kubrakova used sorption pre-concentration in a microwave field in order to determine Cr(III) and Cr(VI) at a detection limit of 30 ng L^{-1}. Beceiro-Gonzalez on the other hand used complexation with 8-hydroxyquinoline in order to determine Cr(III) in mineral water samples and Cr(VI) by difference. A more difficult matrix (UHT milk) was successfully analysed for both total chromium and Cr(VI) by Lameiras et al.[55] using ETAAS. Due to the matrix, more complex pre-treatment was required involving the use of surfactants, chemical modifiers and precipitation procedures. The procedure involved determination of total chromium directly in the milk by the addition of a surfactant and a mixture of Pd and Mg as a chemical modifier. For the selective separation of Cr(VI), the sample pre-treatment consisted of the precipitation of proteins and elution of the supernatant through a solid phase extraction column (Chromabond NH_2). This complicated procedure underlines the problems encountered when more complex matrices are encountered.

Inductively coupled plasma (ICP) sources can be an important tool in determining trace levels of an element in a sample. It can be used with an atomic emission spectrometry (AES) or mass spectrometry (MS) detector. The drawback with this technique is that it

can only measure total chromium, not the individual forms and therefore there has to be a separation step prior to the analysis in order to determine Cr(III) and Cr(VI) separately. In a method by Manzoori and Shemirani[56], Cr(VI) and total chromium were determined using ICP-AES after solvent extraction with tributylphosphate, and back extraction of Cr(VI) using ammonium acetate. Total chromium was detected after oxidation of Cr(III) to Cr(VI) by $KMnO_4$ in acid media. Limits of detection were found to be 1.0 $\mu g\ L^{-1}$ and 0.9 $\mu g\ L^{-1}$ for Cr(VI) and total chromium respectively. Isozaki et al.[57] used ettringite to effect a separation of Cr(III) and Cr(VI), followed by analysis by ICP-AES. Another procedure developed by Cox and McCleod[58] for water samples incorporated isolation of the desired species on activated alumina micro-columns and subsequent analysis by flow injection ICP-AES. This technique proved to be both simple and robust, and therefore ideal for field sampling with later analysis. Water samples, on collection, were immediately passed through the microcolumns in order to isolate and retain the desired species. These were then returned to the laboratory and inserted into a flow injection ICP-AES for elution and quantitation. Another type of plasma, a microwave induced plasma (MIP), can also be used as a source for AES. In a method by Heltai et al.[59], a microwave induced plasma was used to determine Cr(III) and Cr(VI). By using HPLC-MIP-AES absolute detection limits of 13 ng and 18 ng were achieved for Cr(III) and Cr(VI) respectively, although significant matrix effects were observed in real samples.

In order to obtain information on the distribution of various chemical species the ICP-MS instrument is coupled to a chromatographic technique. High performance liquid chromatography (HPLC) and ion chromatography (IC) are the two most commonly used. An important consideration when using hyphenated methods is the mode of sample introduction, as if sample is lost then sensitivity may be lost also. Sample

introduction to the ICP-MS can be achieved using concentric nebulisers, ultrasonic, direct injection or hydraulic high-pressure nebulisers. Alternatively thermospray introduction is also possible. The thermospray sample introduction method was used by Tomlinson and Caruso[60] to determine Cr(III) and Cr(VI) by IC-ICP-MS. Cr(III) was complexed with pyridine dicarboxylic acid (PDCA) in order to effect a separation of the two species. They found improved results with the use of this sample introduction technique compared to previous results obtained for the same separation[61]. Direct injection nebulisation was used by Powell and Boomer[62] in their detection of Cr(III), Cr(VI) and total chromium using HPLC-ICP-MS. A microcolumn specifically designed for chromium was both characterised and optimised with a mobile phase of 0.25% HNO_3. Detection limits of 30, 60 and 180 ng L^{-1} were found for total chromium, Cr(III) and Cr(VI) respectively. Analysis of industrial effluent samples proved problematic due to changes in oxidation state of the chromium species present. Pantsar-Kallio and Manninen[63] also used IC-ICP-MS with a nitric acid mobile phase, but in this case a concentric nebuliser was used. In order to effect a separation of the two species of chromium a cation guard column and an anion analytical column were utilised. Species conversion was prevented in the aquatic samples analysed by use of a nitric acid mobile phase and by minimising pre-treatment. This method enabled quantitation of chromium species down to values of 0.3 and 0.5 μg L^{-1} respectively for Cr(III) and Cr(VI). Other methods can be found in the literature employing IC-ICP-MS with EDTA chelation[64,65]. More recent modifications to the use of ICP-MS for chromium speciation have been demonstrated by Saverwyns et al.[66]. Detection limits of less than 1 μg L^{-1} were obtained using a microbore anion exchange column, coupled with a microconcentric nebuliser. The results obtained from the analysis of an aqueous reference material were in good agreement with the certified values. A further development has been direct speciation without the need for pre-separation. This was

achieved by Zhang et al.[67] by the use of thermospray sample introduction in to the ICP-MS. This method selectively deposited Cr(III) in the presence of Cr(VI) to give a rapid, sensitive chromium speciation with limits of detection at the 0.5 ng mL^{-1} level.

The two chromium species have also been analysed by isotope dilution mass spectrometry (IDMS) after separation using the liquid anion exchanger, Amberlite LA-2[68] and re-extraction of Cr(VI) with an ammonia solution. Using this method, fresh and wastewater samples were analysed for Cr(III) in the range of 2-55 ng g^{-1} and Cr(VI) concentrations of less than 2.4 ng g^{-1}. The accuracy of the IDMS method was shown in two interlaboratory comparisons. The disadvantage with the use of IDMS is the necessity of spiking with radioactive isotopes, making this technique somewhat specialised.

It can therefore be seen that in most cases the concentration of one of the species, either Cr(III) or Cr(VI), and the total chromium content is determined, enabling the concentration of the remaining species to be obtained by difference. HPLC or IC with spectrometric detection on the other hand is a convenient technique that enables the simultaneous determination of both species. The advantages these methods have over others are that the separation, identification and detection of the species of interest down to trace levels can be performed in a single procedure. In a method by Andrle and Broekaert[69] a HPLC system with ultra-violet (UV) detection was used to determine both Cr(III) and Cr(VI) in galvanic wastewaters after derivatisation with ammonium pyrrolidinedithiocarbamate (APDC) and extraction with ethyl acetate. The limits of detection were found to be improved (2.4 μg L^{-1} for Cr(III) and 2.1 μg L^{-1} for Cr(VI)) compared to the literature[70,71], and linear calibration curves between 5 μg L^{-1} and 5000 μg L^{-1} were obtained. APDC was demonstrated to be a more suitable chelating

agent than the more commonly used sodium diethyldithiocarbamate[72]. Padarauskas and Schwedt[73], used reversed phase ion pair chromatography for the simultaneous detection of Cr(III) and Cr(VI), along with common anions by using a C_{18} column and an acetonitrile-water mobile phase at pH 6.5. Complexation with trans-1,2-diaminecyclohexane-N,N,N',N'-tetraacetic acid (DCTA) was used in this case along with UV detection, to give detection limits of 8 μg L^{-1} for Cr(III) and 35 μg L^{-1} for Cr(VI). A major drawback of this method was the slow rate of formation of the Cr(III)-DCTA complex, requiring off-line pre-complexation. The use of elevated temperature or long periods of time is not ideal in speciation analysis, due to the increased danger of conversion occurring between different species. Tian and Schwedt[74] also used HPLC, with visible detection in order to determine chromate after derivatisation with diphenylcarbazide (DPC). The linear range of the method was found to be 0.05-2 mg L^{-1} and a detection limit of 2 μg L^{-1} was estimated. Four geological samples were analysed and these showed good agreement with the results obtained by photometry, however a reference material was not analysed with the samples. Sikovec et al.[75] used on-line thermal lens spectrometric detection of Cr(III) and Cr(VI) after ion chromatography separation. In this method pre-column derivatisation of Cr(III) with pyridine-2,6-dicarboxylic acid (PDCA) and post-column derivatisation of Cr(VI) by diphenylcarbazide (DPC) were used to enable the separation and detection of the two species. Using a 200 μL sample loop and an argon laser operating at 514.5 nm, detection limits of 30 μg L^{-1} for Cr(III) and 0.3 μg L^{-1} for Cr(VI) were achieved. These proved to be superior to those previously obtained by spectrophotometric methods[76]. Gammelgaard et al.[77] developed a method for the simultaneous determination of Cr(III) and Cr(VI), in a flow injection system, using ion exchange chromatography with chemiluminescence detection (IC-CL). A cation exchange guard column was used to separate the two species and Cr(VI) was reduced by potassium sulphite, in order to

detect both species on-line using a luminol-hydrogen peroxide chemiluminescence system. The linear calibration range for both species was found to be 1-1000 μg L^{-1} and the detection limit was 0.5 μg L^{-1} for both species. A National Institute of Standards and Technology (NIST) water reference material was analysed and showed good agreement with the certified values. The method was also evaluated by ETAAS, which also showed good agreement with those results obtained by IC-CL. Flow injection systems have also been used with the use of chemiluminescence to determine Cr(III) in tap water[78], blood serum[79], urine, and hair[80] with extremely sensitive results. The advantages with the use of chemiluminescence over the more conventional techniques include speed, simplicity, sensitivity and low cost of the equipment.

After reviewing the literature and taking into account what instrumentation was available it was decided to initially investigate the following techniques for the determination of chromium species:

- Inductively coupled plasma – mass spectrometry (ICP-MS)
- High performance liquid chromatography (HPLC)
- Ion chromatography (IC).

Electrothermal atomic absorption spectrometry (ETAAS) would be used as a reference method to validate the results obtained from these methods.

1.6 Mass Spectrometry (MS)

Positive rays were first discovered by Goldstein, in 1886, in a low pressure electrical discharge tube. His discovery, along with that of Wien, who deflected these rays in magnetic and electrical fields, led to the development of the modern mass spectrometer.

A mass spectrometer analyses samples by first ionising them. This can be achieved in the following ways[81]:

- Loss of an electron → $M^{+\bullet}$
- Addition of an electron → $M^{-\bullet}$
- Loss of a proton → $(M-H)^-$
- Addition of a proton → $(M+H)^+$

The products of the ionisation process are then separated according to their mass to charge ratio (m/z) and a mass spectrum is produced which can give both qualitative and quantitative information on the compound analysed. Figure 3 is a typical representative diagram of the essential components of a mass spectrometer[81].

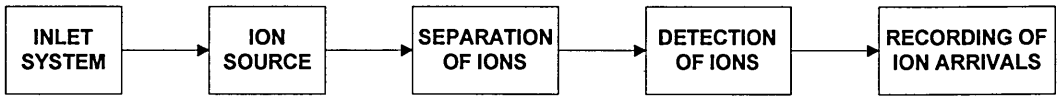

Figure 3: Essential features of a mass spectrometer.

A vacuum is used, as otherwise collisions with air molecules occur and sensitivity is lost. The most commonly used ion sources are the electron impact device or inductively coupled plasma (ICP)[82]. Other types of ion sources include fast atom bombardment, secondary ion, spark source and thermal, field and chemical ionisation[83,84]. The advantage with the use of an ICP ion source is that it can operate outside of the vacuum, which simplifies the sample introduction mechanism. This is the type of ion source that was used in this study and the details of the mechanism will be discussed later. Detection of ions is normally carried out by the use of an electron multiplier, followed by recording by computer software.

1.6.1 Mass Analysers

Ions produced in the ion source are extracted and focused into the mass analyser where they are separated according to their mass to charge ratio. The types of mass analysers commonly used are listed below:

- Double focusing magnetic sector
- Quadrupole mass analyser
- Ion trap
- Time of flight

All make use of the fact that as charged particles, ions may be deflected and/or accelerated by magnetic and/or electrostatic fields. The quadrupole mass analyser was used in this study and will therefore be discussed further. This instrument was chosen as it is smaller than the other instruments, rugged and relatively inexpensive.

1.6.1.1 Quadrupole Mass Analyser

The quadrupole mass analyser, is a device in which ions can be separated according to their m/z ratio without the need for a large, heavy and costly magnet. It employs four short, parallel metal rods arranged symmetrically around the beam (see Figure 4).

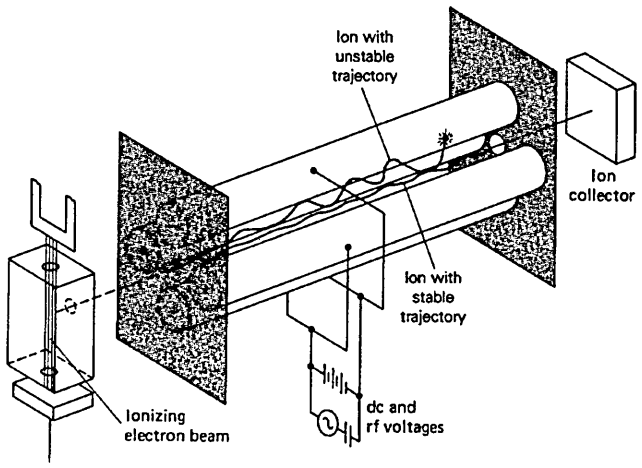

Figure 4: A quadrupole mass spectrometer. Adapted from Lichtman[85].

Diagonally opposite rods are connected electrically, one pair to the positive terminal and the other to the negative terminal of a variable dc source. In addition, variable frequency ac potentials (also termed rf), which are 180 degrees out of phase, are applied to each pair of rods. This creates a complex electrostatic field within the area bound by the rods. Neither the dc nor ac fields act to accelerate the positive particles ejected from the ion source. The combined fields, however, cause the particles to oscillate about their central axis of travel; only those with a particular m/z ratio can pass through the array, without being removed by collision with one of the rods. Those ions that pass through the array are termed stable ions and those lost, unstable. Hence by varying the Rf and dc voltages a mass spectrum can be obtained.

1.7 Inductively Coupled Plasma (ICP)

By definition, a plasma is a conducting gaseous mixture containing a significant concentration of cations and electrons. In the argon plasma, normally employed, argon ions and electrons are the principal conducting species, although cations from the sample also contribute. Argon ions, once formed in the plasma, are capable of absorbing sufficient power from an external source to maintain the temperature at a level at which further ionisation sustains the plasma indefinitely[86]. The mechanism is termed inductive coupling. Argon ions (Ar^+), are "seeded" by applying a high voltage spark. These ions move into the field induced inside the load coil region around the torch, thereby causing further ionisation and kinetic energy transfer. Temperatures up to 10,000 K can be generated. Three power sources have been employed in the generation of argon plasmas. One is a dc electrical source capable of maintaining a current of several amperes between electrodes immersed in the argon plasma. The second and third are powerful radio-frequency and microwave-frequency generators through which

the argon flows. Of the three, the radio-frequency, or inductively coupled plasma (ICP), source offers the greatest advantages in terms of sensitivity and freedom from interference, the main disadvantage being cost, although cheaper than the microwave-frequency generators.

The exact conditions occurring in the plasma remain the subject of current research. This is complicated by the fact that there is probably no thermodynamic equilibrium. However the plasma is a particularly good ion source; the incoming sample aerosol is rapidly desolvated, atomised and ionised by the high temperatures. Gas flows, the induced electric field and some approximate temperatures at various positions in the plasma are shown in Figure 5.

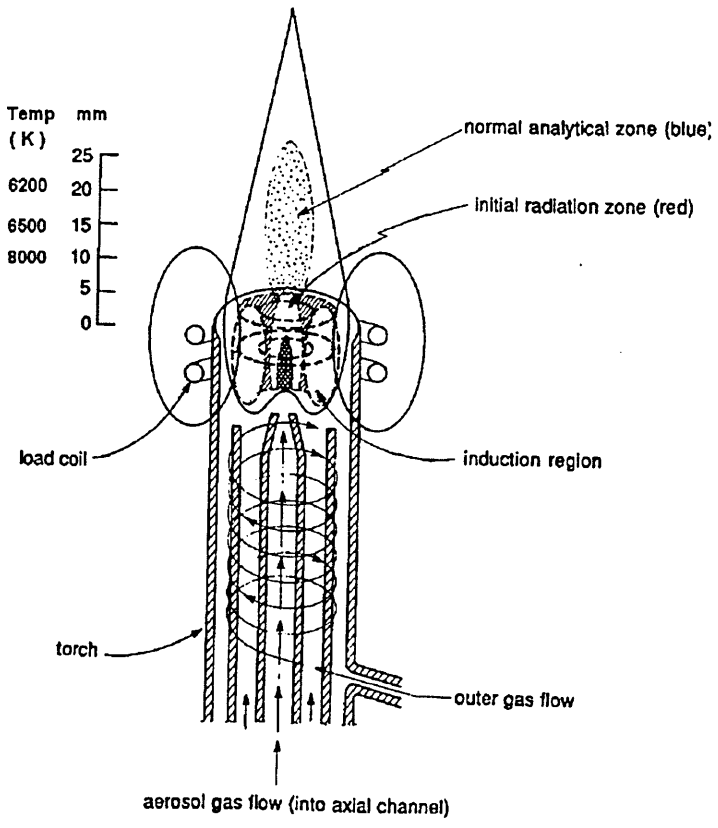

Figure 5: Inductively coupled plasma torch. Adapted from Jarvis et al.[87,88] and Fassel[89].

Figure 5: Inductively coupled plasma torch. Adapted from Jarvis et al.[87,88] and Fassel[89].

1.7.1 Inductively Coupled Plasma Mass Spectrometry

Since commercial instrumentation first became available in the 1980s[90,91], inductively coupled plasma mass spectrometry (ICP-MS) has been widely recognised as a versatile and powerful analytical technique for the determination of trace elements.

In ICP-MS, solutions of analyte are introduced into the ion source as a gas-borne aerosol, most commonly by the use of a pneumatic nebuliser[92], at atmospheric pressure. The aerosol punches a hole through the plasma and the high temperatures dry the aerosol, volatilise and atomise the particles, then excite and ionise atoms with ionisation energies below about 16 eV. That includes nearly all of the elements, except fluorine, helium and neon[93]. Once the atoms have been ionised they are transferred to the mass analyser. This is carried out using a plasma sampling interface (see Figure 6).

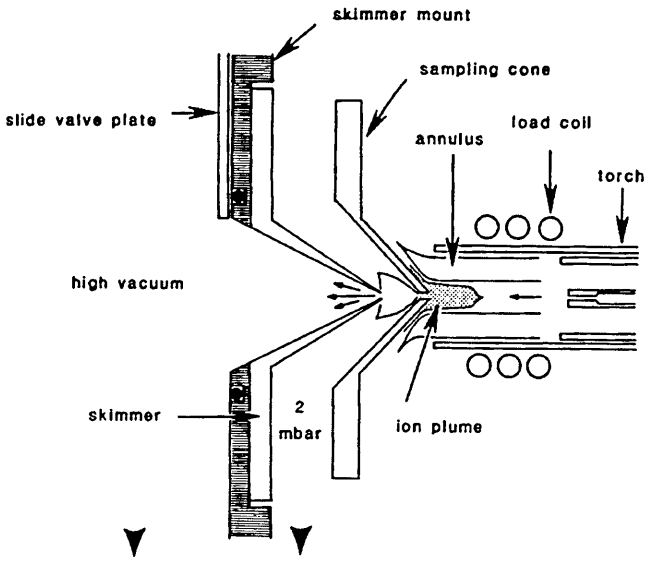

Figure 6: Plasma sampling interface. From Jarvis et al.[87].

The function of the plasma interface is to transfer a representative sample of the ions in the plasma, at near atmospheric pressure, to the MS under high vacuum (typically 10^{-5} torr)[94]. The ions are sampled from the central channel of the plasma by a water-cooled metal cone (the sampler), and are then separated from the bulk of the argon and transmitted into the mass spectrometer by another water-cooled metal cone (the skimmer). Ions are then focused by the lens system and subsequently filtered by the quadrupole mass analyser[95].

The high number of ions produced, with very low background, provides the best detection limits available for most elements[96]. However, drawbacks of the ICP-MS technique include matrix effects[97], and for quadrupole MS the occurrence of spectral interferences, due to polyatomic ions and doubly charged ions[98].

1.8 Electrothermal Atomic Absorption Spectrometry

Atomic absorption spectrometry (AAS) relies on the principle of absorption of radiation by atoms[99]. The first documented observation of such absorption was by Fraunhofer[100], who observed dark lines in the radiation from the sun. These lines were later identified as the absorption lines of metal atoms and were found to correspond with the emission lines of those same atoms[101].

AAS can be achieved by use of either a flame[102] or a graphite furnace[103]. Flames are not ideal, since they are somewhat dangerous to operate and necessitate the use of potentially hazardous fuel and oxidiser gases. Flames are also relatively expensive to employ, due to their consumption of large volumes of fuel and oxidiser gases. In addition, spectroscopic techniques based on flames require relatively large volumes of

sample solution, are often troubled by interferences, and are generally restricted to samples of low concentration.

A cheaper, safer and more efficient atomisation of the sample can be achieved by the use of electrothermal atomic absorption spectrometry (ETAAS). In ETAAS, also known as graphite furnace atomic absorption spectrometry (GFAAS), a small graphite tube[104], electrically heated to a temperature up to 3000°C, is used to evaporate the solution and dissociate the sample into its component atoms. This is generally achieved by the use of a temperature programme. The temperature is first raised to about 100°C, and held there for perhaps a minute, to evaporate the solvent. Any organic matter is then removed by charring at between 400-1100°C for another minute or so. Only after this is the temperature increased to the point needed to dissociate inorganic compounds into atoms (up to 3000°C)[105]. An inert gas, such as argon, surrounds the graphite tube in order to prevent oxidation of both the sample and the hot carbon. In order to improve the efficiency of atomisation a graphite platform called a L'vov platform is inserted into the tube. The L'vov platform is often used in graphite furnaces, in order to delay the atomisation slightly, due to the sample no longer being in contact with the furnace wall. As a consequence, atomisation occurs in an environment in which the temperature is not changing so rapidly and enables more reproducible peaks to be obtained. Another modification of the graphite tube is to pyrolytically coat the furnace walls. This prevents sample losses by diffusion through the porous graphite walls[106]. Figure 7 shows the graphite tube[107], around 50 mm long, with the L'vov platform[108] in place. Sample solutions are introduced through a 2 mm hole in the centre of the tube with a micropipette[109].

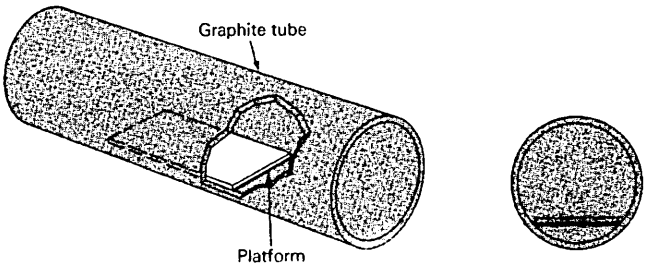

Figure 7: Graphite furnace tube and cross-sectional view of the L'vov platform. Adapted from Skoog[110] and Slavin[111].

When light from a hollow cathode lamp passes through the cloud of atoms, the atoms of interest absorb the light from the lamp. This is measured by a detector, and used to calculate the concentration of that element in the original sample (see Figure 8).

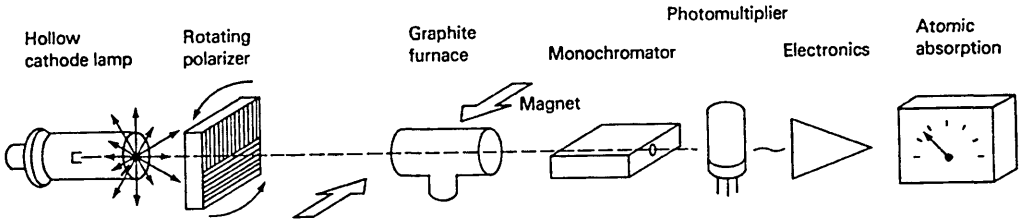

Figure 8: Schematic diagram of an electrothermal atomic absorption spectrometer with Zeeman background correction.

In the hollow cathode lamp, a low-power electrical discharge is sustained between an inert electrode (anode) and a second electrode (cathode) made from the element to be determined. Atoms from the cathode are thereby excited, to produce a very pure line spectrum of the desired element in addition to the line spectrum of the inert fill-gas (argon or neon) present in the hollow cathode lamp. Because of inter-element influences, a hollow cathode lamp is rarely made to emit the spectra of more than four elements; the most stable and intense lamps are made for a single element[112].

To correct for background absorption, a second light source, typically a deuterium arc, may be used. This type of correction is termed a continuum source. The radiation from the second light source (continuum source) and the hollow cathode lamp are passed alternately through the graphite tube atomiser with the use of a chopper. The absorbance of the deuterium radiation is then subtracted from that of the analyte beam. This dual lamp system, in turn requires very precise alignment and does not work well in the visible region[113]. To avoid this problem the Zeeman effect[114] may be used. The Zeeman background correction[115,116] provides a more accurate correction for background than most of the others available e.g. continuum source or two line corrections. It is particularly useful in combination with electrothermal atomisers and permits the direct determination of elements in samples such as blood and soil solutions. The decomposition of organic material in these samples can produce large background corrections and significant errors when using other methods[117].

The better efficiencies of atomisation of ETAAS compared to FAAS improve detection limits by a factor of up to 1000, so reaching the sub ppb range[96]. As well as high sensitivity, ETAAS also allows the determination of a large number of elements with selectivity, accuracy and speed. This coupled with the simplicity and relatively low cost of the apparatus makes ETAAS an excellent choice for trace and ultratrace analysis[118].

1.9 Chromatography

Generally, methods for chemical analysis are at best selective, with few, if any, being truly specific. Consequently, the separation of the analyte from potential interferences or indeed from other analytes in a mixture is an essential step in many analytical procedures. Without question, the most widely used means of performing analytical

separations is chromatography. Chromatography is a 'blanket' term applied to a wide variety of very powerful separation techniques applicable to molecular mixtures. The technique was first employed by the Russian botanist Mikhail Tswett[119] in the early 1900s. He observed coloured bands when he separated plant pigments by passing solutions through glass columns packed with finely divided calcium carbonate.

The mixture to be separated is equilibrated between two phases, one of which remains stationary while the other, mobile phase, percolates through interstices or over the surface of the stationary phase. The *stationary phase* is a solid or a liquid immobilised on a solid, and the *mobile phase* is either a liquid or a gas. The movement of the mobile phase results in differential migration of the individual components of the mixture, because different components spend different times in the stationary phase. While traversing a given length of chromatographic medium, all components spend the same amount of time in the mobile phase, but those that spend least time in the stationary phase are eluted first.

The most common way of achieving a chromatographic separation is by *column elution chromatography*. Here successive fresh portions of mobile phase or *eluent* are applied to a column after the addition of the mixture to be separated. In this way the mixture is forced down the column or eluted. This process is illustrated in Figure 9.

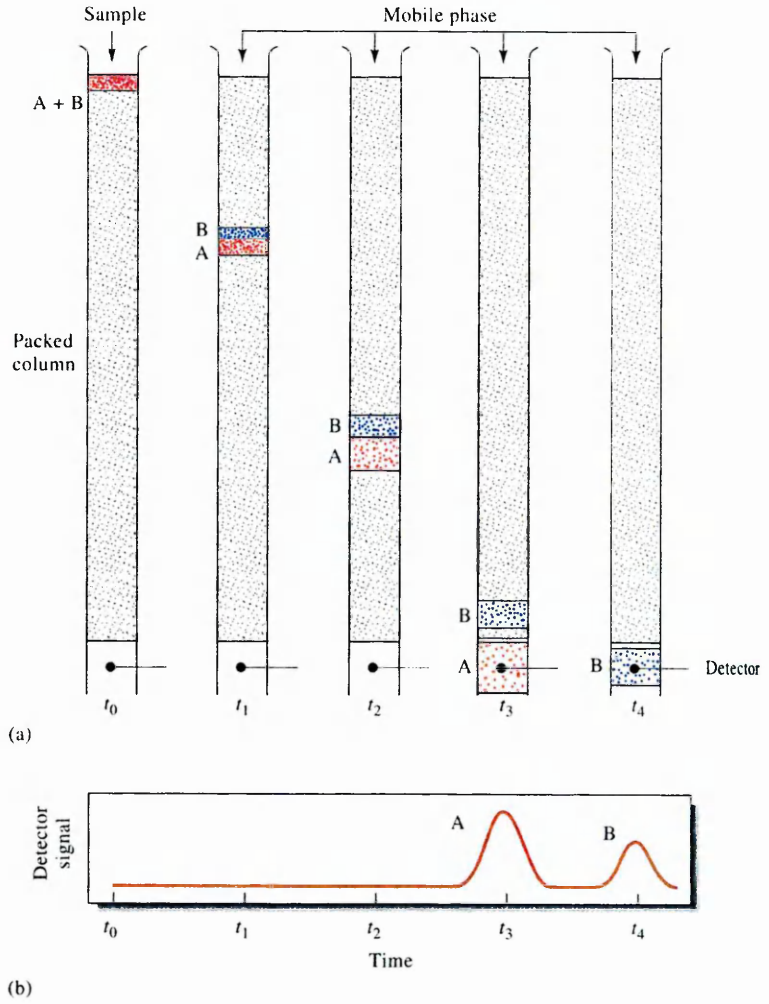

Figure 9: (a) Elution chromatography. (b) Signal of the detector at each stage of elution. Adapted from Skoog et al.[110].

1.9.1 Basic Concepts of Chromatography

During the set up and optimisation of a chromatographic system there are four main factors which need to be considered. The first of these, *resolution*, is defined as the ability to separate components of a mixture and is closely related to retention times and peak shapes. Secondly, the *sensitivity* of the detection system must be adequate for the application. Thirdly, the technique must give *reproducible* results, and finally the *analysis time* should be reasonable. In order to select the optimum conditions for a

particular analysis the factors that influence retention, peak shape, sensitivity and efficiency must be considered.

1.9.1.1 Retention Time

The retention of a compound is defined as the volume of the mobile phase required to elute that compound compared with the volume of the column. This value however is difficult to measure and therefore time is used. Figure 10 shows a simple chromatogram of two components. The smaller peak represents a species that is not retained by the stationary phase. The time from injection to the elution of such a peak is termed the *dead time* or *void volume*. The retention time of this peak, t_M, is therefore approximately equal to the time required for a molecule of the mobile phase to travel the column. The time from injection to the elution of the larger analyte peak is called the *retention time* (t_R).

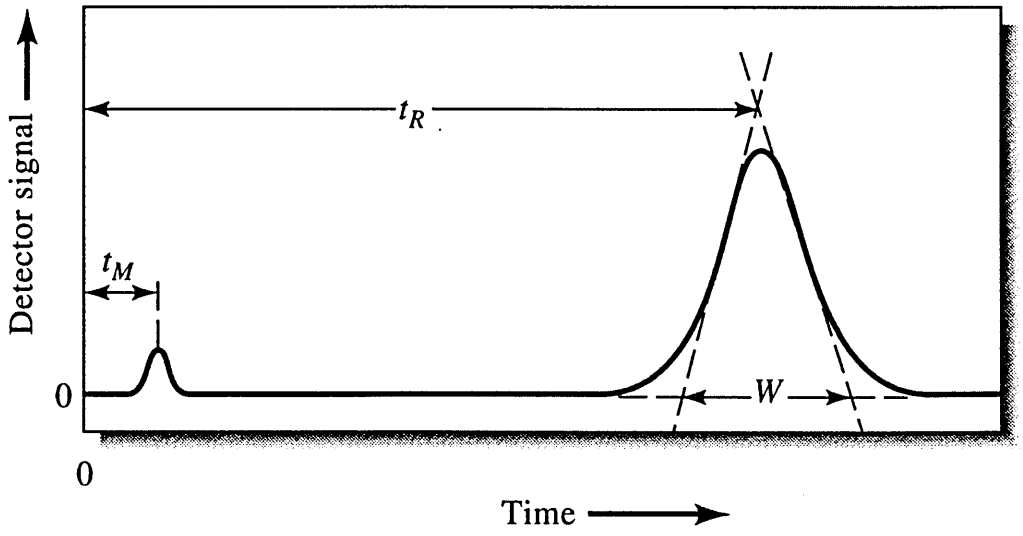

Figure 10: Typical chromatogram for a two component mixture. Taken from Skoog et al.[110].

The *adjusted retention time*, t'_R, is the difference between the retention time (t_R) and the void volume (or dead time) (t_M).

Equation 5

$$t'_R = t_R - t_M$$

Equation 5 therefore represents the time that the analyte has spent in the stationary phase.

Therefore the factor which governs the retention time is how long it takes for the sample to be distributed between the mobile and stationary phases. Analytes interact with the stationary phase in different ways and are therefore distributed differently. Differences in retention times result in the separation of mixtures. The distribution, or partitioning, of the sample between the mobile and stationary phases is represented by the *partition ratio*, K.

Equation 6

$$\mathrm{K} = \frac{\text{concentration in unit volume of stationary phase}}{\text{concentration in unit volume of mobile phase}}$$

K depends on the structure of the analyte and the nature of the mobile and stationary phases.

The proportion of the analyte present in each phase is termed the *capacity factor* (k'). This is an important experimental factor that is used to describe the migration rates of analytes on columns. It can be represented as follows:

Equation 7

$$k' = \frac{K \cdot Vs}{Vm}$$

where Vs and Vm are the volumes of the stationary and mobile phases respectively. The capacity factor can be shown to be related to retention time i.e.

Equation 8

$$k' = \frac{t_R - t_M}{t_M} \qquad \text{i.e.} \qquad \frac{t'_R}{t_M} = \frac{K \cdot Vs}{Vm}$$

There is therefore a direct relationship between the partition ratio and the retention time of an analyte. Since the partition ratio is a property of the compound, the retention time of that particular analyte should remain unchanged in the presence of other compounds.

For two different analytes to be separated on the same column they must have different partition ratios i.e. their retention times must be different. However, some analytes have the same or very similar partition ratios. To overcome this problem the separation conditions can be changed e.g. mobile phase, stationary phase or temperature.

1.9.1.2 Efficiency

The chromatographic band typically has a Gaussian shape. This is due to the fact that individual molecules of analyte have random motions (see Figure 11). As individual molecules travel down a column random motions determine the amount of time they spend in the stationary phase (the molecule is only eluted during residence in the mobile phase). The average rate at which each molecule moves relative to the mobile phase varies depending on the path they travel. The consequence of this is that there is a

symmetrical spread of velocities around a mean value, which represents the behaviour of the average and most common molecule.

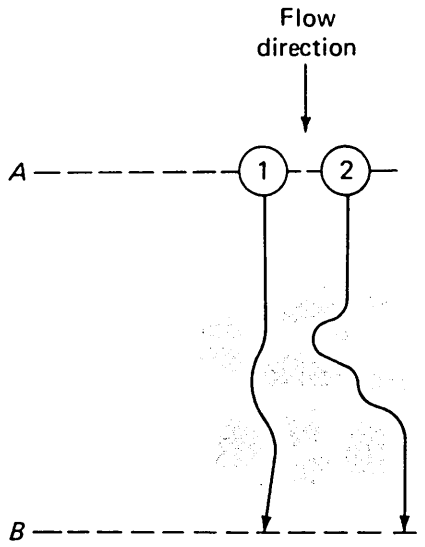

Figure 11: Random pathways of two analyte molecules during elution.

When a sample is injected onto a column the analyte bands should ideally spread as little as possible during the separation and thus should result in sharp peaks. The breadth of a band increases as it moves down the column because more time is allowed for spreading to occur. Thus, the band width is directly related to residence time in the column and inversely related to the velocity at which the mobile phase flows. The efficiency of the separation can be described according to the *plate theory*. This theory, originally adapted by Martin and Synge from the theory of distillation columns[120], envisages a chromatography column as being composed of a series of narrow horizontal layers, termed *theoretical plates*. At each plate, equilibration of the analyte molecules between the mobile and stationary phases is assumed to take place. Movement of the analyte and the mobile phase is then viewed as a series of stepwise transfers from one plate to the next.

The efficiency of a chromatographic column as a separation device improves as the number of equilibrations increases i.e. as the *number of theoretical plates*, N, increases e.g.

Equation 9

$$N = \frac{L}{H}$$

where L = column length and H = height equivalent to a theoretical plate (HETP) which is the thickness of one plate. HETP enables a comparison of the efficiencies of columns of different length to be carried out.

H and N can be determined experimentally using the following expressions:

Equation 10

$$H = \frac{L \cdot W^2}{16 \cdot t_R{}^2} \qquad N = 16 \cdot \left(\frac{t_R}{W} \right)^2$$

Thus, N can be calculated from measurement of the retention time, t_R and the width of the peak, W, and H can be obtained using the length of the column packing. Another method for approximating N is to determine $W_{1/2}$, the width of a peak at half its maximum height. The number of theoretical plates is then given by

Equation 11

$$N = 5.54 \cdot \left(\frac{t_R}{W_{1/2}} \right)^2$$

In comparing two columns, it is essential that N is determined using the same compounds.

The most important experimental variables affecting separation efficiency and band broadening of the peaks are particle size of the packing, thickness of the adsorbed film (when the stationary phase is an adsorbed liquid), viscosity of the mobile phase, temperature and linear velocity of the mobile phase. Decreases in the first three of these variables generally lead to improved separations or decreased plate heights, while decreases in temperature have the opposite effect.

1.9.1.3 Resolution

Resolution is a measure of the degree of separation of adjacent peaks. When a chromatogram contains two components their resolution is determined from the differences in their retention times and their peak widths. Figure 12 shows chromatograms for species A and B on three columns having different resolving powers. The resolution, Rs, for each of these columns is defined as:

Equation 12

$$Rs = \frac{2 \cdot [(t_R)_B - (t_R)_A]}{W_A + W_B}$$

It is evident from Figure 12 that a resolution of 1.5 gives an essentially complete separation of A and B, whereas a resolution of 0.75 does not. At a resolution of 1.0, B contains about 4% of A, whereas at a resolution of 1.5 the overlap is only around 0.3%. The resolution for a given stationary phase can be improved by lengthening the column, thus increasing the number of theoretical plates. An adverse consequence of the added plates, however, is an increase in the time required for the separation, thus leading to an increase in band broadening.

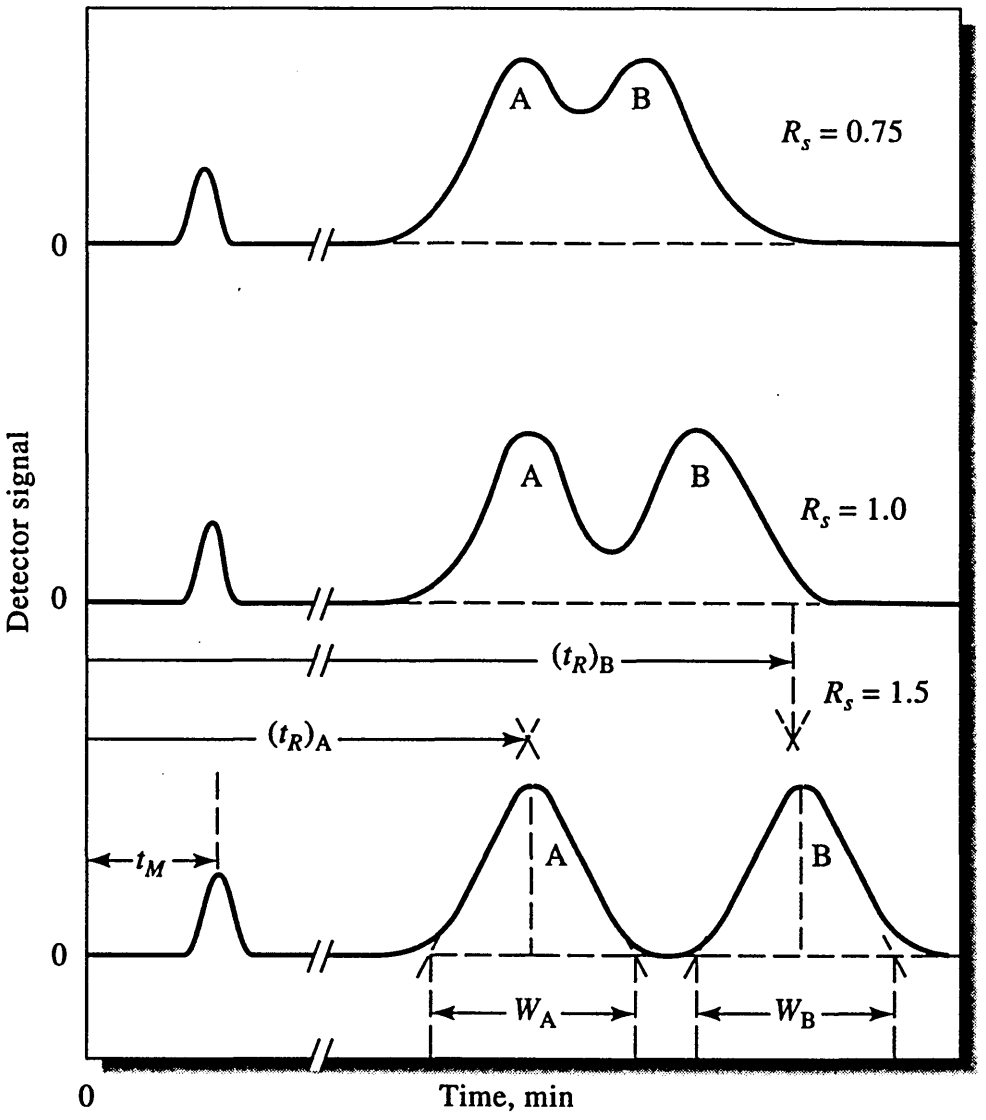

Figure 12: Separation of a two component mixture at three resolutions. Adapted from Skoog et al.[110].

The equations for efficiency and resolution can be combined, i.e.

Equation 13

$$Rs = \frac{\sqrt{N}}{4} \cdot \left(\frac{a - 1}{a} \right) \cdot \left(\frac{k'_B}{1 + k'_B} \right)$$

where α is the ratio of the capacity factors, i.e.

Equation 14

$$\alpha = \frac{k'_B}{k'_A}$$

This equation shows that the resolution of a separation depends on the square root of the efficiency. Since efficiency is directly proportional to column length, to double the resolution of a separation, the column length would have to increase four fold.

1.9.2 Chromatography Classification

Chromatographic techniques are split into two main categories based on the type of mobile phase used. Gas and liquid chromatography, use gas and liquid mobile phases respectively. More recently, supercritical fluid chromatography, which uses a supercritical fluid as the mobile phase, has been introduced combining the properties of both a gas and a liquid. The different techniques which can be classified under these headings are shown in Table 2.

The advantage of using liquid chromatography is that the analyte of interest need not be volatile, as is the case in gas chromatography. The techniques used in this study were based on liquid chromatography, namely high performance liquid chromatography and ion chromatography and therefore these will be discussed further.

Table 2: Classification of column chromatographic methods.

General Classification	Specific Method	Stationary Phase	Separation Medium
Liquid chromatography (LC) (mobile phase: liquid)	Liquid-liquid, or partition	Liquid absorbed on solid	Partition between immiscible liquids
	Liquid-bonded phase	Organic species bonded to a solid surface	Partition between liquid and bonded surface
	Liquid-solid or adsorption	Solid	Adsorption
	Ion exchange	Ion-exchange resin	Ion exchange
	Size exclusion	Liquid in interstices of a polymeric solid	Partition/sieving
Gas chromatography (GC) (mobile phase: gas)	Gas-liquid	Liquid adsorbed on a solid	Partition between gas and liquid
	Gas-bonded phase	Organic species bonded to a solid surface	Partition between liquid and bonded surface
	Gas-solid	Solid	Adsorption
Supercritical-fluid chromatography (SFC) (mobile phase: supercritical fluid)		Organic species bonded to a solid surface	Partition between supercritical fluid and bonded surface

1.9.3 High Performance Liquid Chromatography (HPLC)

The first modern liquid chromatograph was developed by Csaba Horváth at Yale University, in 1965[121], and used for the investigation of biological substances. It is extremely popular as a separation technique due to its sensitivity, adaptability and applicability to substances that are of prime interest to industry[122]. A typical schematic diagram for an HPLC is shown in Figure 13.

This type of chromatography employs a liquid mobile phase and a finely divided (3-10 μm particle size) stationary phase. In order to obtain a satisfactory flow through the stationary phase the liquid must be pressurised. Figure 14 illustrates the five most popular types of HPLC and their separation mechanisms. These can be carried out on a

flat surface, where the method is termed *planar chromatography* or in a column, which is by far the most popular, where the method is termed *column chromatography.*

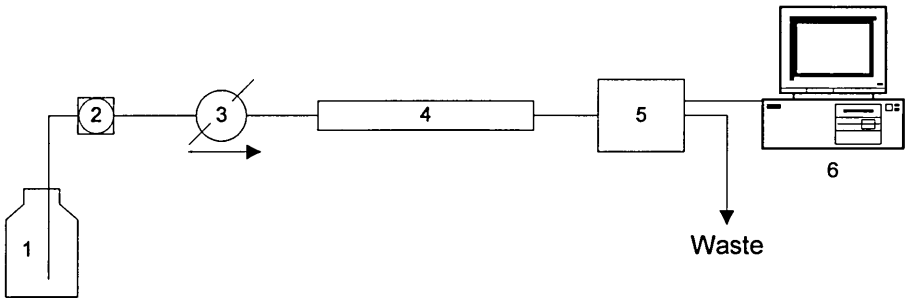

1 Eluent
2 Pump
3 Injection port
4 Column
5 Detector
6 Data processor (Computer)

Figure 13: Schematic diagram of an HPLC instrument.

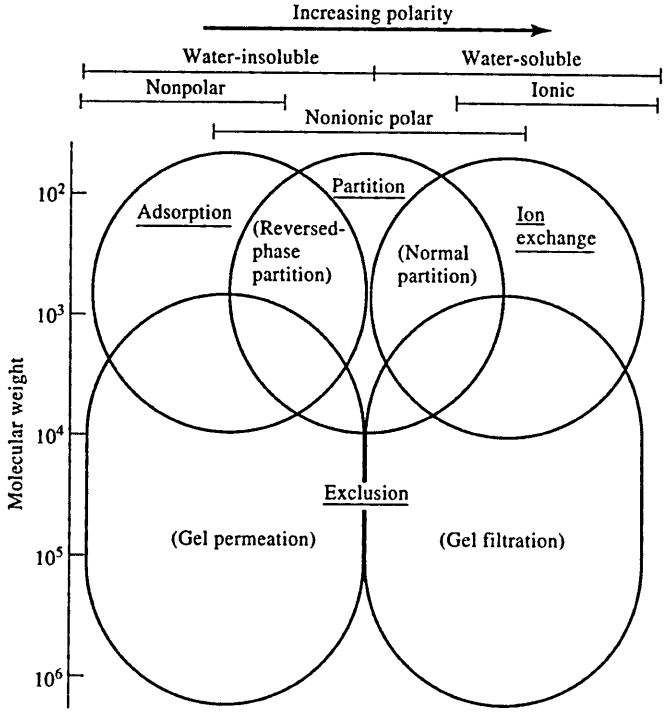

Figure 14: Types of HPLC. Taken from Heftmann[123].

1.9.3.1 Column Packings

Two types of column packings for liquid chromatography exist; *pellicular* and *porous particle*. Pellicular phases consist of spherical, nonporous, glass or polymer beads on which a thin porous layer of silica, alumina or ion-exchange resin has been deposited. Porous phases, on the other hand, are solely composed of silica, alumina or an ion-exchange resin. The use of silica is by far the most common.

1.9.3.2 Detectors

The ideal detector for liquid chromatography should have the following properties.

1. Adequate sensitivity.
2. Good stability and reproducibility.
3. A linear response.
4. A short response time that is independent of flow rate.
5. High reliability and ease of use.
6. Similarity in response to all analytes, or alternately a highly predictable and selective response toward one or more classes of analyte.
7. Minimal internal volume in order to reduce band broadening.

The most common detectors for HPLC are UV, fluorescence, refractive index, electrochemical, conductometric and mass spectrometry. Other less commonly used detectors include IR absorption, radioactivity, bioluminescence and chemiluminescence.

1.9.3.3 Mobile Phases

The desirable properties for a mobile phase are as follows.

1. Good solvent for the sample being studied.

2. High purity to avoid introduction of peaks that may overlap analyte peaks.
3. Readily available at a reasonable cost.
4. A boiling point that is 20-50°C above the column temperature.
5. Low viscosity.
6. Low reactivity to avoid interactions with the sample or the packing.
7. Compatibility with the detector.
8. Low flammability and toxicity.

These requirements greatly reduce the number of mobile phases available for liquid chromatography. This list is further reduced by the need for a solvent in which the capacity factors for the sample components lie in a suitable range. For a two or three component sample, it is realistic to select a solvent where the capacity factor is in the range 2-5. For multi-component mixtures this range must be extended to allow time for the separation.

HPLC can be further subdivided into normal phase and reversed phase. The reversed phase chromatography, using an essentially non polar stationary phase with polar mobile phase, has become the predominant technique.

1.9.4 Ion-exchange Chromatography (IC)

Ion-exchange chromatography was first described by Taylor and Urey, in 1938, for the separation of lithium and potassium isotopes, using inorganic zeolites as the stationary phase[124]. The application of ion-exchange for the separation of amino acids was first automated in the early 1960s.

This type of chromatography is based upon the differential affinity of ions for the stationary phase. The rate of migration of the ion through the column is directly dependent upon the type and concentration of the ions that comprise the eluent.

1.9.4.1 Resins

Ion exchange resins are made up of high molecular weight polymeric materials, containing ionic functional groups. Natural ion-exchangers, such as clays and zeolites, have been recognised and used for several decades. Synthetic ion-exchange resins were first produced in the 1930s for water softening, deionisation and purification of solutions. These materials are classified as either cation-exchange (separating simple cations) or anion-exchange resins (separating anions)[125] depending upon the ionic functional groups that they contain. They can also be classed as a weak or strong exchanger. For example cation-exchange resins containing sulphonic acid groups ($RSO_3^-H^+$) and carboxylic acid groups (RCOOH) are classified as strong and weak respectively. Anion-exchange resins contain basic amine functional groups, with quaternary amines ($RN(CH_3)_3^+OH^-$) classified as strong-base anion-exchangers, and secondary or tertiary amines being classified as weak-base anion-exchangers.

Figure 15 shows the typical structure of a cross-linked polystyrene resin. Similar resins are also used in which the $-SO_3^-H^+$ group is replaced by $-COO^-H^+$, $-NH_3^+OH^-$ or $N(CH_3)_3^+OH^-$ groups. Some applications for the different types of resins are shown in Table 3.

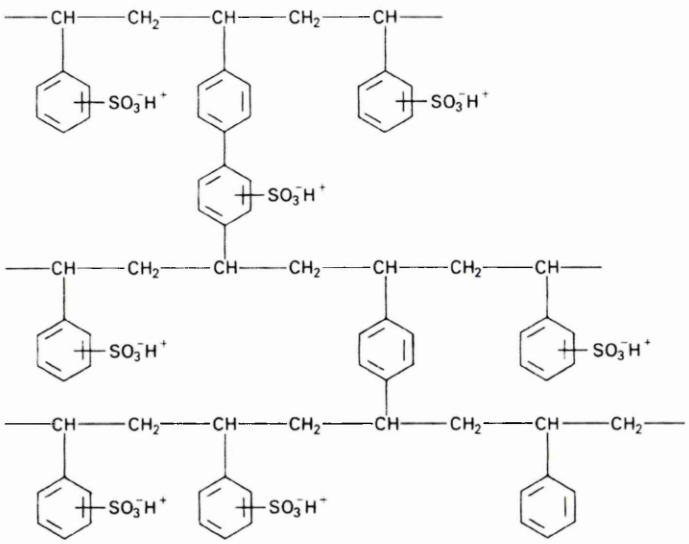

Figure 15: Structure of an ion-exchange resin. Adapted from Skoog et al.[110].

Table 3: Ion-exchange resins for chromatography. Adapted from Ewing[105].

Resin Class	Functional group	Nature of resin	Effective pH range	Applications
Strong-acid cation-exchanger	$RSO_3^-H^+$	Sulphonated polystyrene	1-14	Fractionation of cations; inorganic separations; lanthanides; B vitamins; peptides; amino acids
Weak-acid cation-exchanger	$RCOO^-H^+$	Carboxylic polymethacrylate	5-14	Fractionation of cations; biochemical separations; transitional elements; amino acids; organic bases; antibiotics
Strong-base anion-exchanger	$RN(CH_3)_3^+OH^-$	Quaternary ammonium polystyrene	0-12	Fractionation of anions; halogens; alkaloids; vitamin B complexes; fatty acids
Weak-base anion-exchanger	$RNH_3^+OH^-$	Polyamine polystyrene or phenol formaldehyde	0-9	Fractionation of anionic complexes of metals; anions of differing valencies, amino acids; vitamins

The pH ranges are important, for example for weak-acid resins if a pH below 5 is employed then the dissociation is so slight that cation exchange is negligible. The converse is true for the weak-base resin above pH 9.

1.9.4.2 Equilibria

An important attribute of the ion-exchange resins is that they are essentially insoluble in aqueous media. Therefore when a strong-acid cation exchanger (sulphonic acid) is brought into contact with an aqueous solvent containing a cation $M^{\chi+}$, an exchange equilibria is set up as follows:

Equation 15

$$\underset{\text{solid}}{\chi RSO_3^-H^+} + \underset{\text{solution}}{M^{\chi+}} \rightleftharpoons \underset{\text{solid}}{(RSO_3^-)_\chi M^{\chi+}} + \underset{\text{solution}}{\chi H^+} \quad \text{CATION-EXCHANGE}$$

where $RSO_3^-H^+$ represents one of the many sulphonic groups attached to a large polymer molecule. Similarly a strong-base anion-exchanger interacts with the anion $A^{\chi-}$ as shown by the reaction:

Equation 16

$$\underset{\text{solid}}{\chi RN(CH_3)_3^+OH^-} + \underset{\text{solution}}{A^{\chi-}} \rightleftharpoons \underset{\text{solid}}{[RN(CH_3)_3^+]_\chi A^{\chi-}} + \underset{\text{solution}}{\chi OH^-} \quad \text{ANION-EXCHANGE}$$

The law of mass action can be applied to the separation of ions using ion-exchange chromatography. The equilibrium established between a singly charged ion B^+ with a sulphonic acid resin at the head of a chromatographic column can be described by Equation 17:

Equation 17

$$RSO_3^-H^+(s) + B^+(aq) \rightleftharpoons RSO_3^-B^+(s) + H^+(aq)$$

Elution with a dilute solution of hydrochloric acid shifts the equilibrium to the left causing part of the B^+ ions in the stationary phase to be transferred to the mobile phase. These ions then move down the column in a series of transfers between the stationary and mobile phases. The equilibrium constant, K' for the exchange reaction takes the form:

Equation 18

$$\frac{[RSO_3^-B^+]_s[H^+]_{aq}}{[RSO_3^-H^+]_s[B^+]_{aq}} = K'$$

Here, $[RSO_3^-B^+]_s$ and $[RSO_3^-H^+]_s$ are concentrations of B^+ and H^+ on the solid surface. Rearranging yields:

Equation 19

$$\frac{[RSO_3^-B^+]_s}{[B^+]_{aq}} = K'\frac{[RSO_3^-H^+]_s}{[H^+]_{aq}}$$

The aqueous concentration of hydrogen ions is much higher than the concentration of the singly charged B^+ ions in the mobile phase, during the elution. Furthermore, the exchanger has a greater number of exchange sites relative to the number of B^+ ions being retained. Thus, the overall concentrations $[H^+]_{aq}$ and $[RSO_3^-H^+]_s$ are not affected significantly by shifts in the equilibrium in Equation 17. Therefore when $[RSO_3^-H^+]_s$ is much larger than $[RSO_3^-B^+]_s$ and $[H^+]_{aq}$ is much larger than $[B^+]_{aq}$ the right hand side of Equation 19 is constant, hence:

Equation 20

$$\frac{[RSO_3^-B^+]_s}{[B^+]_{aq}} = K\frac{C_s}{C_M}$$

where K is a constant that corresponds to the distribution coefficient. In Equation 19, K' represents the affinity of the resin for the ion B^+ relative to another ion, in this case H^+. When K' is large, there is a large tendency for the stationary phase to retain B^+; when K' is small, the reverse is true. By selecting a common reference ion such as H^+, distribution ratios for different ions on a given type of resin can be experimentally compared. Such experiments reveal that polyvalent ions are much more strongly held than singly charged species. Within a given charge group, however, differences appear that are related to the size of the hydrated ion as well as to other properties. Thus, for a typical sulphonated cation exchange resin, values for K' decrease in the order $Tl^+ > Ag^+ > Cs^+ > Rb^+ > K^+ > NH_4^+ > Na^+ > H^+ > Li^+$. For divalent cations, the order is $Ba^{2+} > Pb^{2+} > Sr^{2+} > Ca^{2+} > Ni^{2+} > Cd^{2+} > Cu^{2+} > Co^{2+} > Zn^{2+} > Mg^{2+} > UO_2^{2+}$. For anions, K' decreases in the order $SO_4^{2-} > C_2O_4^{2-} > I^- > NO_3^- > Br^- > Cl^- > HCO_2^- > CH_3CO_2^- > OH^- > F^-$. It should be noted that this sequence is somewhat dependent upon resin type and reaction conditions. However, using this information, separations can be achieved due to differing charges and also due to the differences in affinities within a charge group.

1.10 Aims of Study

The aims of this study were the following:

- To critically review methods for the chemical speciation of chromium in environmental samples.
- To find a sensitive, selective, reproducible, robust and simple method that enabled the simultaneous determination of Cr(III) and Cr(VI) in environmental samples.

- To optimise the developed method using both univariate and multivariate optimisation procedures.
- To validate the method using certified water reference materials.
- To investigate methods for the extraction of Cr(III) and Cr(VI) from soil samples, and to find a method that extracted Cr(III) and Cr(VI) from soil samples without affecting the species' integrity
- To validate a chromium extraction method using certified soil reference materials.
- To use the extraction method for the determination of the Cr(III) and Cr(VI) content in a field soil sample.
- To compare the extraction results obtained with those from published methods.
- To study changes in chromium speciation in field soil taken through the production stages of a reference material.

CHAPTER 2 PRELIMINARY INVESTIGATIONS

2.1 Reagents

2.1.1 Ion Chromatography-ICP-MS

All chemicals were obtained from BDH, Poole, Dorset, UK, and were of Aristar grade unless otherwise stated. Nitric acid [HNO_3], 69%; acetic acid [CH_3COOH] (100%); Chelex 100 chelating resin (iminodiacetic acid), sodium form; sodium dichromate [$Na_2Cr_2O_7.H_2O$], AnalaR reagent; hydroxylammonium chloride [$HO.NH_3Cl$] (99%), spectrosol grade; hydrogen peroxide [H_2O_2] (30%), general purpose reagent; chromium(III)nitrate nonahydrate [$Cr(NO_3)_3.9H_2O$] (99.99+%), Aldrich, Bornem, Belgium; ammonium acetate [$CH_3CO_2NH_4$] (99.999%), Aldrich, Bornem, Belgium; 18MΩ deionised water, MilliQ Plus 185 Ultrapure Water System, Millipore, Milford, MA, USA.

2.1.2 HPLC

All chemicals were obtained from BDH, Poole, Dorset, UK unless otherwise stated. Sodium dichromate [$Na_2Cr_2O_7.H_2O$], AnalaR reagent; ammonium pyrrolidine-dithiocarbamate (APDC) [$CH_2(CH_2)_2CH_2NCSSNH_4$] (99%); acetonitrile [CH_3CN], hypersolv reagent for HPLC; 18MΩ deionised water, MilliQ Plus 185 Ultrapure Water System, Millipore, Milford, MA, USA.; acetic acid [CH_3COOH] (100%), Normapur AR, Rhone-Poulenc Ltd., Ongar, UK; sodium acetate [CH_3COONa] (99% min), SLR, Fisons, Manchester, UK; chromium(III)nitrate nonahydrate [$Cr(NO_3)_3.9H_2O$], 99.99%, Aldrich, Bornem, Belgium.

2.1.3 Ion Chromatography with Visible Detection

All chemicals were obtained from Aldrich, Bornem, Belgium, and were of ACS reagent grade unless otherwise stated. 2,6-Pyridine dicarboxylic acid (PDCA) [$C_5H_3N(CO_2H)_2$] (99%); sodium phosphate dibasic heptahydrate [Na_2HPO_4] (98%); sodium iodide [NaI] (99.99%); ammonium acetate [$CH_3CO_2NH_4$] (99.999%); lithium hydroxide mono-hydrate [LiOH] (99.95%); 1,5-diphenylcarbazide (DPC) [$C_6H_5NHNHCONHNHC_6H_5$]; HPLC grade methanol [CH_3OH] (99.9%); sulphuric acid sub-boiled [H_2SO_4]; sodium hydroxide [NaOH], P.A. grade, Janssen, Beerse, Belgium; hydrochloric acid fuming [HCl] (37%), G.R., Merck, Darmstadt, Germany; 18MΩ deionised water, MilliQ Plus 185 Ultrapure Water System, Millipore, Milford, MA, USA.

2.1.4 Single Extraction Procedures with ICP-MS

All chemicals were obtained from Aldrich, Bornem, Belgium and were of ACS reagent grade unless otherwise stated. Sodium carbonate anhydrous [Na_2CO_3], 99.0%, SigmaUltra; Potassium chromate [$KCrO_4$], 99.7%; Potassium phosphate dibasic anhydrous [K_2HPO_4], 99.6%; Potassium phosphate monobasic anhydrous [KH_2PO_4], 99.3%; chromium(III)nitrate nonahydrate [$Cr(NO_3)_3.9H_2O$], 99.99%; 18MΩ deionised water, MilliQ Plus 185 Ultrapure Water System, Millipore, Milford, MA, USA; Nitric acid [HNO_3], sub-boiled; Sodium hydroxide [NaOH] P.A. grade, Janssen, Beerse, Belgium; Hydrogen peroxide [H_2O_2], 27%, Mobilab, Zutendaal, Belgium.

2.2 *Instrumentation*

2.2.1 Ion Chromatography with ICP-MS

The ion chromatography instrument (see Figure 16) used was a Dionex metal free system Ion Chromatograph (Dionex n.v., Mechelen, Belgium), consisting of an eluent degas module, a GP 40 gradient pump and a metal free injector with a 25 µL PEEK sample loop. Connections between the injector and column were made using PEEK tubing (i.d 0.03 cm).

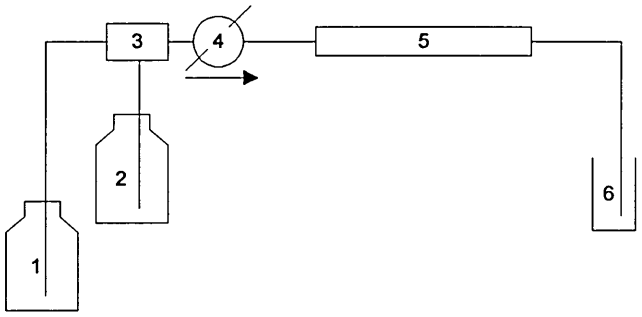

1 Eluent (0.5 mol L^{-1} HNO_3)
2 Eluent (0.075 mol L^{-1} HNO_3)
3 Gradient Pump
4 Injection port
5 Column: AG4A guard column
6 Autosampler

Figure 16: Schematic diagram of the ion chromatograph used for IC with ICP-MS.

2.2.2 HPLC

The HPLC instrument incorporated a Philips Pye Unicam PU4010 pump and PU4020 UV detector, a Waters 746 Data Module Integrator and a Rheodyne 7125 Injection Valve fitted with a 20 µL loop. Separation was carried out on a C_{18} Spherisorb S5 ODS 1 column and detection was at 259 nm.

2.2.3 Ion Chromatography with Visible Detection (IC-Vis)

The ion chromatography instrument used was a Dionex metal free system Ion Chromatograph (Dionex n.v., Mechelen, Belgium), consisting of a GP40 gradient pump with vacuum degasser, AS3500 autosampler, PC10 pneumatic controller (postcolumn module), 375 µL reaction coil (mixing device) and equipped with a variable wavelength UV/Visible AD20 absorbance detector. Figure 17 shows a schematic diagram of the ion chromatography system with the post-column manifold coupled to the UV/visible detector.

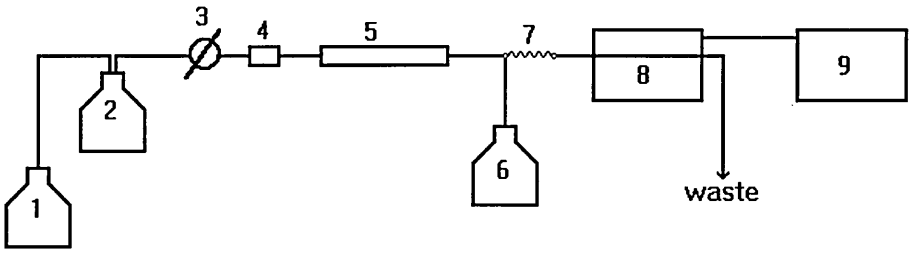

1 Helium
2 Eluent (PDCA + counter ions)
3 Injection port
4 Guard column
5 Analytical column
6 Post-column reagent (DPC)
7 Mixing device
8 UV/Visible detector
9 Data processor (Computer)

Figure 17: Schematic diagram of the ion chromatograph used for IC-Vis.

2.2.4 ICP-MS Instrumentation

The ICP-MS instrument used was a Fisons PQ2+ quadrupole instrument with a micro concentric nebuliser, for sample introduction at a flow rate of 50 µL min^{-1}, and a Meinhard concentric ICP torch with a double pass spray chamber and recirculating pump. Operating conditions are shown in Table 4.

Table 4: ICP-MS operating conditions.

Parameter	Setting
Forward Power	1400 watts
Reflected Power	0 watts
Torch	Meinhard concentric torch
Spray Chamber	Double Pass
Nebuliser	Micro Concentric
Sample introduction	Peristaltic pump
Solution uptake rate	50 μL min^{-1}
Coolant gas flow rate	15 L min^{-1} Argon
Nebuliser gas flow rate	0.7 L min^{-1} Argon
Nebuliser gas pressure	207 Pa (30 psi)
Sample cone material	Nickel
Skimmer cone material	Nickel
No. of sweeps per replicate	50
No. of replicates	6
Masses	^{53}Cr
Measurement mode	Peak jumping
Integration time	3 s
Detector mode	Pulse counting

Tuning of this instrument was carried out daily using a multielement standard (Merck, Darmstadt, Germany) containing Be, Mg, Co, In, Ce, Tm, Pb and U at a concentration of 10 μg L^{-1} in 2% nitric acid. The determination of chromium was carried out at m/z 53. Although this isotope is of low abundance it suffers much less from interferences (see Table 5).

Table 5: Chromium isotopes, relative abundances and interferences[126,127].

Isotope Mass	Occurrence(%)	Interference
50	4.345	$^{32}S^{18}O$
		^{50}Ti
		^{50}V
52	83.789	$^{38}Ar^{14}N$
		$^{35}Cl^{16}O^{1}H$
		$^{36}Ar^{16}O$
		$^{40}Ar^{12}C$
53	9.501	$^{36}Ar^{16}O^{1}H$
		$^{40}Ar^{13}C$
54	2.365	^{54}Fe
		$^{40}Ar^{14}N$

2.3 Chromatographic Conditions

2.3.1 Ion Chromatography - ICP-MS

The column used was an AG4A guard column (Dionex n.v., Mechelen, Belgium). The mobile phase was a linear gradient of nitric acid, changing from 0.075 mol L^{-1} HNO_3 to 0.5 mol L^{-1} over 10 minutes as shown in Table 6. The flow rate through the column was 0.5 mL min^{-1}. Before each run the column was conditioned with 0.075 mol L^{-1} nitric acid for 5 minutes.

Table 6: Gradient for ion chromatography (IC with ICP-MS).

Time (minutes)	% 0.075 mol L^{-1} HNO_3	% 0.5 mol L^{-1} HNO_3
0.0	100	0
10.0	0	100
22.0	0	100

Column fractions were collected immediately after sample injection and at two minute intervals for a period of 22 minutes. The 1 mL fractions were collected in sample vials and then aspirated into the ICP-MS. A calibration graph was produced using Cr(III) standard solutions in 0.075 mol L^{-1} HNO_3.

2.3.2 Ion Chromatography with Visible Detection

The chromatographic conditions, which were optimised and used in this method are given in Table 7. Both the guard and analytical columns were obtained from Dionex n.v., Mechelen, Belgium.

Table 7: Chromatographic conditions for ion chromatography with visible detection.

Parameter	Setting
Sample loop volume	200 µL
Guard Column	HPIC-CG5 (4 x 50 mm) Guard Column
Analytical Column	HPIC-CS5 (4 x 250 mm) Analytical Column
Eluent	0.002 mol L^{-1} PDCA; 0.002 mol L^{-1} Na_2HPO_4; 0.01 mol L^{-1} NaI; 0.05 mol L^{-1} $CH_3CO_2NH_4$; 0.0028 mol L^{-1} LiOH
Eluent Flow Rate	1.0 mL min^{-1}
Postcolumn reagent:	0.002 mol L^{-1} DPC; 10% CH_3OH; 1.8 mol L^{-1} H_2SO_4
Postcolumn Flow Rate:	0.5 mL min^{-1}
Detector wavelength:	520 nm

2.4 Chelex 100

Chelex 100 was used during the IC with ICP-MS analysis in order to remove any metal contaminants in the mobile phase. Approximately 25 g of Chelex 100 in its sodium

form was mixed with deionised water and poured into a column 20 cm x 1 cm. The column was equilibrated by passing through 60 mL of deionised water followed by 20 mL of 0.075 mol L^{-1} HNO_3. The 0.075 mol L^{-1} HNO_3 mobile phase was then passed through the column and collected. This was then used to make the calibration solutions and mixtures as well as the mobile phase. The 0.5 mol L^{-1} HNO_3 was cleaned in the same way.

2.5 Measurement of pH

A Metrohm 744 pH meter with a KCl glass electrode (Metrohm Belgium n.v., Berchem, Belgium) was used. The instrument was calibrated daily using Metrohm pH 4 and 7 buffer solutions (Metrohm Belgium n.v., Berchem, Belgium).

2.6 Centrifugation

The centrifuge used was a Heraeus Sepatech Megafuge 1.0R (Kendro Laboratory Products GmbH, Hanau, Germany).

2.7 Preparation of Solutions for Ion Chromatography with Visible Detection

ELUENT STOCK SOLUTION:

Known weights of pyridine-2,6-dicarboxylic acid (PDCA) (0.02 mol L^{-1}, 3.34 g), disodium hydrogen phosphate heptahydrate (0.02 mol L^{-1}, 5.36 g), sodium iodide (0.1 mol L^{-1}, 15.0 g), ammonium acetate (0.5 mol L^{-1}, 38.5 g) and lithium hydroxide monohydrate (0.028 mol L^{-1}, 1.10 g) were dissolved in 1 L of deionised water. PDCA is

slow to dissolve so the solution was heated gently (30-40°C) on a hot plate before adding the remaining reagents.

ELUENT:

One hundred mL of the stock solution was transferred to a 1 L flask and the volume made up to 1 L with deionised water. The pH of the eluent was then checked to ensure that it was between 6.70 and 6.80.

POSTCOLUMN REAGENT:

The postcolumn reagent was prepared by dissolving 0.5 g of 1,5-diphenylcarbazide (DPC) in 100 mL of HPLC grade methanol. This was then added to about 500 mL of deionised water containing 25 mL of 96% spectrophotometric grade sulphuric acid and diluted to 1 L with the deionised water.

2.8 Procedures

2.8.1 Extraction Procedure for Ion Chromatography-ICP-MS

A modified version of the sequential extraction procedure developed by Davidson et al.[128] was used for this study. Half volumes and mass of material and a platform shaker instead of an end-over-end mixer were used. The centrifuge tubes were also loosely capped instead of covering with a watch glass.

Step one. Twenty millilitres of 0.11 mol L^{-1} acetic acid was added to 0.5 g of sewage sludge amended soil: BCR CRM 597 in a 30 mL polypropylene centrifuge tube. The tube was then shaken at a speed of 40 rpm, on an Innova 2000 Platform Shaker (New Brunswick Scientific), for 16 hours (overnight) at room temperature (approx. 20°C).

The extract was separated from the solid residue by centrifugation at 4000rpm (Heraeus Sepatech Megafuge 1.0R; Kendro Laboratory Products GmbH, Hanau, Germany) for 15 minutes. The supernatant liquid was decanted into a clean polypropylene container and stored at 4°C prior to IC and analysis. The residue was washed with 20 mL of deionised water by shaking for 15 minutes, centrifuged and the washings discarded.

Step two. Twenty millilitres of 0.1 mol L^{-1} hydroxylammonium chloride (pH adjusted to 2 with nitric acid) was added to the residue from step one. The extraction procedure was repeated as described in step one, i.e. the sample was shaken overnight, the extract separated by centrifugation and the residue washed with deionised water.

Step three. Five millilitres of 8.8 mol L^{-1} hydrogen peroxide was carefully added, in small aliquots, to the residue from step two. The centrifuge tube was loosely capped and the contents digested at room temperature for one hour with occasional manual shaking. Digestion was continued by heating the tube to 85°C in a water bath for one hour. The lid was then removed and the tube contents reduced to about 1 mL. A second 5 mL aliquot of H_2O_2 was added and the tube again covered and heated for one hour. The volume was then reduced as before. A 25 mL volume of 1 mol L^{-1} ammonium acetate (pH adjusted to 2 with nitric acid) was added to the cool moist residue. The sample was then shaken, centrifuged and the extract separated as described in step one.

The extracted solutions were collected and injected onto the ion chromatography column, followed by ICP-MS analysis as described previously.

2.8.2 HPLC

This method is based on the application of reversed phase HPLC with UV detection as described by Andrle and Broekaert[69].

For the quantitative precipitation of the chromium compounds, 10 mL of an aqueous solution containing 1g L^{-1} Cr(VI) or Cr(III) was transferred into a 250 mL beaker. Ten millilitres of an acetate buffer solution (pH 4.66) and 20 mL of a saturated ammonium pyrrolidinedithiocarbamate (APDC) solution (~0.5 mol L^{-1}) were added to the solution. The reaction mixture was stirred at 60°C for 1 h, after which the solution was allowed to cool. The resulting violet precipitate was filtered using a scintered glass filter, washed with 50 mL of pure water and dried to constant weight at 40°C. The resulting complexes were then analysed by HPLC.

2.8.3 Ion Chromatography with Visible Detection

In this method[129] the Cr(III) and Cr(VI) complexes formed are detected by visible detection after separation by ion chromatography.

A 10 mL aliquot of sample was added to 20 mL of eluent stock solution in a 100 mL beaker and the pH adjusted to 4 (at higher pH the precipitation of chromium oxide hydroxide occurs)[75]. The beaker was then covered with a watch glass and heated for one hour. At this point the colour of the solution should become purple. After cooling, the pH of the solution was adjusted to 6.8, transferred to a 100 mL volumetric flask and made up to the mark with deionised water. The sample was then analysed by ion chromatography.

2.8.4 Single Extraction Procedures with ICP-MS

Two certified reference materials: BCR CRM 597 and BCR CRM 596; sewage sludge amended soil and aquatic plant material respectively, were subjected to different extraction procedures as detailed below.

2.8.4.1 Nitric Acid/Hydrogen Peroxide Extraction

This method developed by Krishnamurty et al.[130] was used for the extraction of total chromium.

The sample (500 mg) was weighed into a 50 mL beaker and 0.5 mL of water added in order to minimise sample splash and facilitate rapid reaction with the acid. A 10 mL volume of concentrated nitric acid was then added to the slurry and the beaker covered with a watch glass. This was then heated at approximately 100°C on a hot plate for 2 h. The beaker was then removed from the hot plate and cooled for 15 minutes. A 4 mL aliquot of 27% v/v hydrogen peroxide was then added dropwise to the contents of the beaker. Heating was then continued with occasional stirring (by swirling the beaker) for a further 1 h. The cooled digest was then transferred to a centrifuge tube. The beaker was rinsed with deionised water and the washings transferred to the centrifuge tube. The sample was then centrifuged at 4000 rpm (Sorvall TC6 Bench Top Centrifuge) for 5 minutes, and the volume made up to 100 mL with deionised water, before ICP-MS analysis. All samples were prepared in duplicate.

2.8.4.2 Nitric Acid Extraction

This method adapted from Greene et al.[37] uses a (3+7) nitric acid and deionised water mixture to extract total chromium from solid matrices. This extraction solution is made

from 300 mL of concentrated (d=1.42 g mL^{-1}) nitric acid and 700 mL of deionised water.

About 500 mg of sample (soil or plant) was weighed into a 50 mL beaker and 10 mL of the nitric acid solution was added. The beaker, covered with a watch glass, was transferred to a hot plate, heated to approximately 100°C and left for one hour. The contents of the beaker were transferred to a clean, dry FEP centrifuge tube, along with washings using deionised water. The sample was centrifuged at 4000 rpm (Sorvall TC6 Bench Top Centrifuge) for 5 minutes and the supernatant was then decanted into a 50 mL volumetric flask. A 2 mL aliquot of the hot nitric acid solution was added to the residue in the centrifuge tube. The tube was shaken to mix the contents and then centrifuged as previously described. After transfer of the supernatant to the 50 mL volumetric flask, a further 2 mL of the hot nitric acid solution was added to the residue and the process repeated. The flask and contents were allowed to cool to room temperature before the solution was made up to volume with deionised water. The sample was then analysed by ICP-MS. All samples were prepared in duplicate.

2.8.4.3 Sodium Carbonate/Sodium Hydroxide Extraction

This method[37] extracts chromium(VI) only. At high pH (9-10) Cr(III) is precipitated as chromium hydroxide [$Cr(OH)_3$], whereas the Cr(VI) remains in solution. This is confirmed by the Eh-pH diagram for chromium (Figure 1).

EXTRACTING SOLUTION: A mixture of 30 g sodium carbonate and 20 g sodium hydroxide was transferred to a 1 L volumetric flask, dissolved in deionised water and the final volume made up to 1 L with further addition of deionised water.

NEUTRALISING SOLUTION: A 30 mL aliquot of concentrated (d = 1.42 g mL^{-1}) nitric acid was transferred to a 500 mL flask containing 300 mL of deionised water and the resulting solution made up to 500 mL with deionised water.

Approximately 500 mg of sample was weighed into a 50 mL beaker and 10 mL of the extracting solution was added. The watch glass covered beaker was transferred to a hot plate and heated at just below boiling for one hour. The contents of the beaker were transferred to a clean, dry FEP (Teflon fluorinated ethylene propylene) centrifuge tube, along with washings using hot extracting solution. The sample was centrifuged at 4000 rpm (Sorvall TC6 Bench Top Centrifuge) for 5 minutes and the supernatant was then decanted into a 25 mL volumetric flask. The contents of the volumetric flask were then neutralised with 5 mL of neutralising solution (HNO_3). This was then diluted to 25 mL with deionised water after cooling to room temperature. All samples were prepared in duplicate. Further dilutions were carried out as required.

2.8.4.4 Phosphate Extraction

This method extracts Cr(VI) only and was adapted from a method by James et al.[36].

PHOSPHATE BUFFER: A solution of phosphate buffer at pH 7.0 was prepared from a mixture of 0.005 mol L^{-1} dibasic potassium phosphate [K_2HPO_4] and 0.005 mol L^{-1} monobasic potassium phosphate [KH_2PO_4].

To a 50 mL beaker was added 500 mg of sample and 10 mL of phosphate buffer. The beaker was then allowed to stand for one hour with occasional swirling. The contents of

the beaker were then transferred to a clean, dry FEP centrifuge tube, along with washings using deionised water. The sample was centrifuged at 4000 rpm (Sorvall TC6 Bench Top Centrifuge) for 5 minutes and the supernatant was then decanted into a 25 mL volumetric flask and diluted to 25 mL with deionised water. All samples were prepared in duplicate. Further dilutions were carried out as required.

2.8.4.5 Recovery Procedure

In order to determine the extraction efficiency and to establish whether the form of chromium had changed, Cr(VI), in the form of potassium chromate [K_2CrO_4], was added to the soil and plant samples. Measured aliquots of either 0.0385 mol L^{-1} or 0.00192 mol L^{-1} standard solutions were added to the plant or soil samples to give a final concentration of 200 mg Cr(VI) per kg of sample. Spiked samples were incubated overnight or for 1 week before analysis.

2.8.4.6 Calibration

Calibration solutions of Cr(III) were prepared in 0.14 mol L^{-1} nitric acid.

A 100 mg L^{-1} stock solution of Cr(III) was first prepared by weighing 0.07695 g of chromium(III) nitrate nonahydrate [$Cr(NO_3)_3.9H_2O$] and diluting to 100 mL with deionised water. Calibration standards of 1, 5, 10 and 20 µg L^{-1} Cr(III) were prepared from the stock solution.

2.9 Results and Discussion

These preliminary experiments were carried out in order to determine which method could be used for the determination of chromium species in environmental matrices,

such as the aquatic plant material or the sewage sludge amended soil, BCR CRM 596 and BCR CRM 597 respectively.

The suitability of both sequential and single extraction procedures for Cr(III) and Cr(VI) were investigated. The most important consideration here was that the distribution of the species in the sample should be retained i.e. that the extraction method used should not alter the species present.

For separation of the species, two chromatographic techniques were investigated; high performance liquid chromatography (HPLC) with ammonium pyrrolidinedithio-carbamate (APDC) derivatisation and ion chromatography (IC) both with and without derivatisation.

2.9.1 Ion Chromatography - ICP-MS

Chromium Abundances

Isotope abundances and possible interferences for the major isotopes of chromium are shown in Table 5. Measurements for chromium were carried out at both m/z 52 and 53, since 52 is the most abundant and 53 suffers from the least interferences.

Figure 18 is a typical calibration graph at m/z 52 which shows that the linearity of this method was satisfactory at the levels investigated (n=10), giving a straight-line graph ($y = 19823x + 49530$, $r^2 = 0.9935$). This calibration graph was used to convert the response (counts) into chromium concentration in Figure 19 to Figure 23.

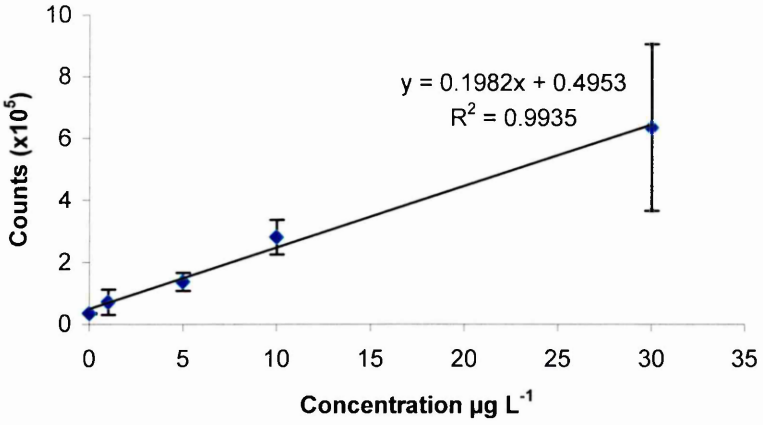

Figure 18: Calibration graph of chromium in the range 0 - 30µg L^{-1} using ICP-MS detection at ^{52}Cr. Error bars give the standard deviation of 10 measurements.

As can be seen from Figure 19, it is possible to resolve the two chromium species using this method, however it is not a baseline separation.

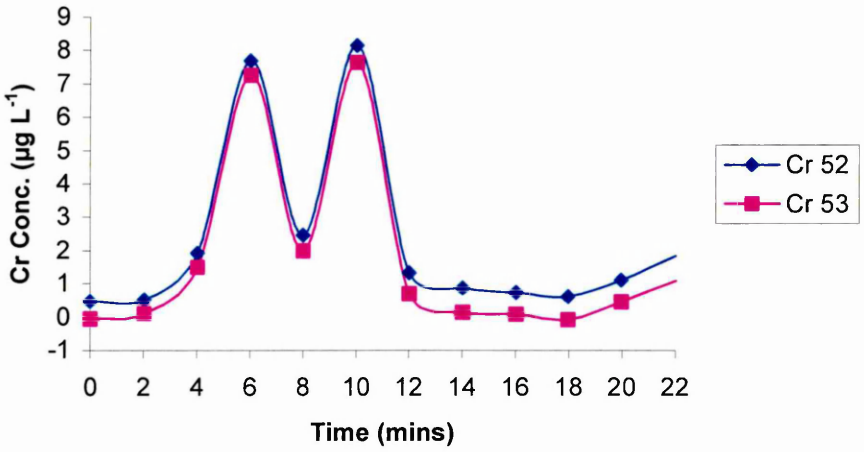

Figure 19: Chromatogram of 10 µg L^{-1} Cr(III)/Cr(VI) in deionised water using an AG4A column and ICP-MS detection at ^{52}Cr (♦) and ^{53}Cr (■).

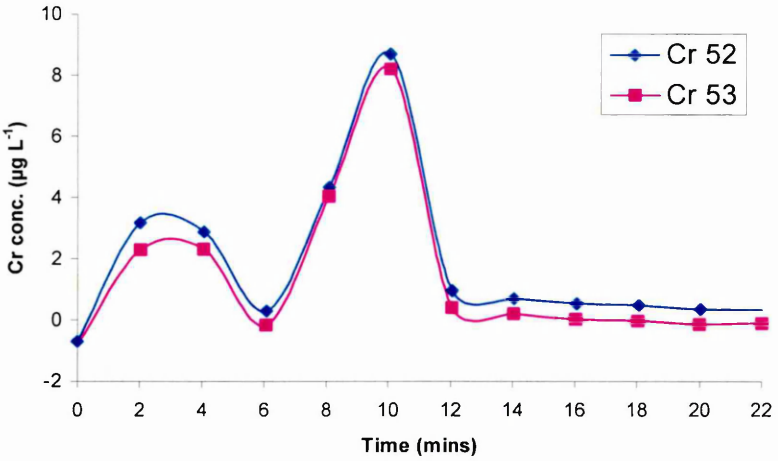

Figure 20: Chromatogram of 10 µg L^{-1} Cr(III) in deionised water using an AG4A column and ICP-MS detection at ^{52}Cr (♦) and ^{53}Cr (■).

Figure 20 and Figure 21 are the chromatograms of Cr(III) and Cr(VI) respectively. As can be seen in Figure 20, some Cr(III) is converted to Cr(VI) under the experimental conditions. In contrast there is very little conversion of Cr(VI) to Cr(III). This conversion may be occurring either whilst the samples are in storage or during the ion chromatography itself.

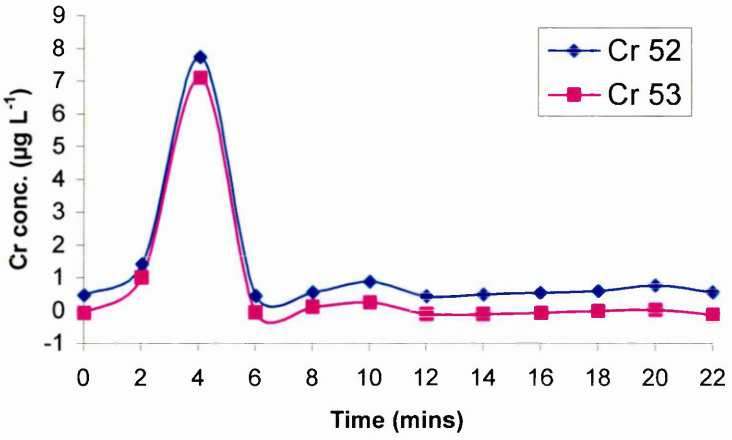

Figure 21: Chromatogram of 10 µg L^{-1} Cr(VI) in deionised water using an AG4A column and ICP-MS detection at ^{52}Cr (♦) and ^{53}Cr (■).

In order to further investigate the nature of the conversion, samples were prepared in acetate buffer and in 0.075 mol L^{-1} nitric acid, to see if these solutions affected the species present. When the samples were prepared in these solutions a further peak was detected and differences in the peak areas were apparent, as can be seen in Figure 19, Figure 22 and Figure 23.

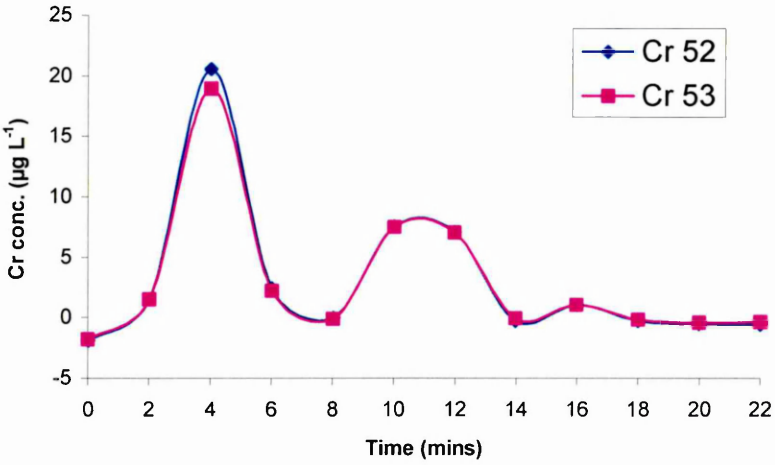

Figure 22: Chromatogram of 10 µg L^{-1} Cr(III)/Cr(VI) in acetate buffer using an AG4A column and ICP-MS detection at ^{52}Cr (♦) and ^{53}Cr (■).

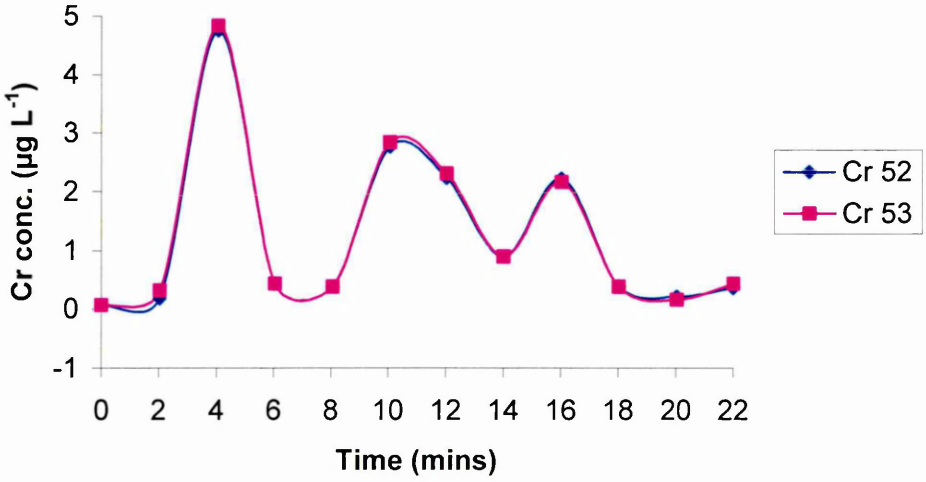

Figure 23: Chromatogram of 10 µg L^{-1} Cr(III)/Cr(VI) in 0.075 mol L^{-1} nitric acid using an AG4A column and ICP-MS detection at ^{52}Cr (♦) and ^{53}Cr (■).

The pH of the deionised water, the acetate buffer and the 0.075 mol L^{-1} HNO_3 were measured as 5.5, 4.3 and 1.4 respectively. The chromatograms show that there is a tendency for Cr(VI) to convert to Cr(III) as pH decreases. This is to be expected, since it is known that in acidic solutions dichromate is a strong oxidising agent[131]:

Equation 21

$$Cr_2O_7^{2-} + 14H^+ + 6e^- \quad 2Cr^{3+} + 7H_2O \qquad E° = 1.33V$$

These findings suggest that the distribution of chromium species is largely determined by the pH of the solution, an observation confirmed by the stability diagram for chromium species (see Figure 1). This is an extremely important consideration when deciding what methods to use for the extraction, separation and determination of chromium species.

2.9.1.1 Sewage Sludge Amended Soil Extraction by IC with ICP-MS

A conventional soil extraction scheme was investigated to determine its suitability for extraction of chromium species. A sewage sludge amended soil certified reference material, BCR CRM 597, was used. This was extracted successively with the extractants shown in Table 8.

Table 8: A soil extraction scheme.

Extractant	Type of Chromium Species
Step one. Acetic acid [CH_3COOH]	Exchangeable
Step two. Hydroxylammonium chloride [$HONH_3Cl$]	Reducible
Step three. H_2O_2/ammonium acetate [$CH_3CO_2NH_4$]	Oxidisable

Hydrogen peroxide (H_2O_2) releases ions from the organic phase by oxidation. Ammonium acetate was added to the H_2O_2 in order to prevent readsorption of these ions[2].

Step one. Acetic acid extraction

In this step, exchangeable chromium is extracted, i.e. only loosely bound chromium will be extracted.

Figure 24 shows that both Cr(III) and Cr(VI) have been extracted from the sample, although in small amounts. Detected concentrations of 1.45 and 0.7 ng mL^{-1} were obtained for Cr(VI) and Cr(III) respectively at mass 52.

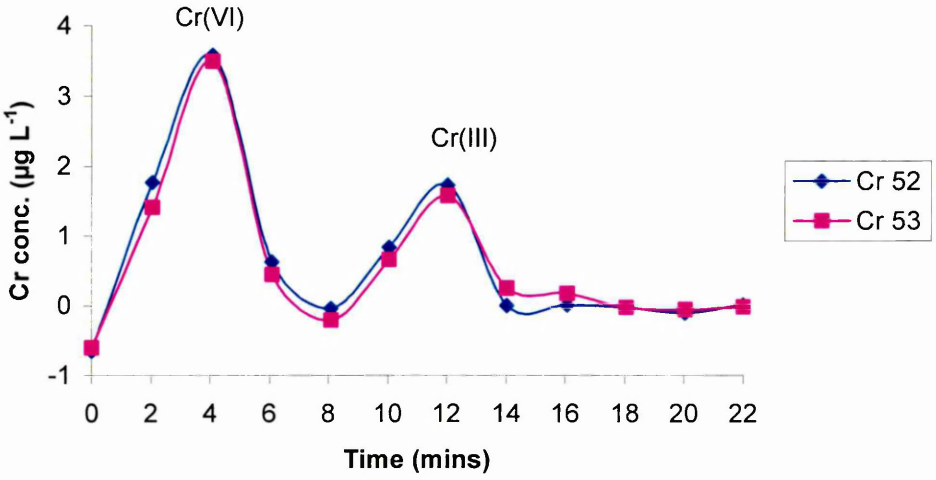

Figure 24: Blank corrected chromatogram of 0.11 mol L^{-1} acetic acid extraction from sewage sludge amended soil using an AG4A column and ICP-MS detection at ^{52}Cr and ^{53}Cr.

Step two. Hydroxylammonium chloride extraction

In this extraction step reducible forms of chromium will be extracted, i.e. Cr(VI) will be extracted and in the process will be reduced to Cr(III). Hydroxylammonium chloride acts as an electron donor[22]:

Equation 22

$$HCrO_4^- + 7H^+ + 3e^- \rightarrow Cr^{3+} + 4H_2O$$

Therefore a peak should appear at the position expected for Cr(III) (around 12 minutes).

The chromatogram for this sewage sludge amended soil sample (Figure 25), once corrected for the blank chromium concentration, shows a peak for Cr(III), however this corresponds to Cr(VI) that has been reduced to Cr(III) upon extraction from the sample. The concentration of Cr(VI) was measured as 1.23 ng mL^{-1}.

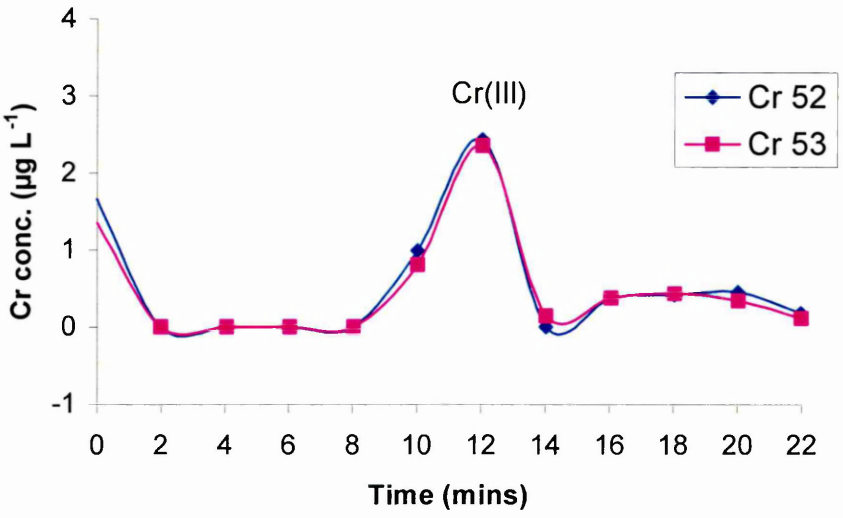

Figure 25: Blank corrected chromatogram of 0.1 mol L^{-1} hydroxylammonium chloride extraction from sewage sludge amended soil using an AG4A column and ICP-MS detection at ^{52}Cr and ^{53}Cr.

Step three. H_2O_2/ammonium acetate extraction

This extractant solution extracts oxidisable forms of chromium, i.e. Cr(III) will be extracted and in the process will be oxidised to Cr(VI):

Equation 23

$$Cr^{3+} + 2H_2O_2 \rightarrow CrO_4^{2-} + 4H^+$$

The peak seen in Figure 26 represents Cr(III) that has been oxidised to Cr(VI) during extraction. The concentration of Cr(III) was measured as 67 ng mL^{-1}.

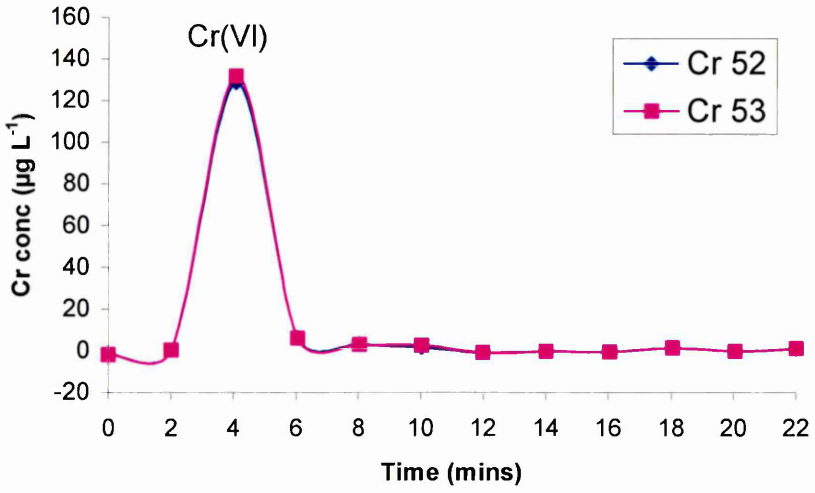

Figure 26: Blank corrected chromatogram of 8.8 mol L^{-1} hydrogen peroxide /1 mol L^{-1} ammonium acetate extraction from sewage sludge amended soil using an AG4A column and ICP-MS detection at ^{52}Cr and ^{53}Cr.

This clearly shows that this approach does not work for the speciation of Cr(III) and Cr(VI), since the species are changed by the extractants used.

2.9.2 High Performance Liquid Chromatography

This method uses a chelating agent in order to produce two chromium species which can be separated from each other by reversed phase HPLC and subsequently detected using UV detection[69]. HPLC has several advantages over many other methods, as separation, identification and quantitation of the different species down to trace concentration levels can be performed in a single procedure.

2.9.2.1 Complex Binding Reactions

The Cr(III) and Cr(VI) complexes formed are thought to be as follows in Equation 24 and Equation 25[132,133,134].

Equation 24: Cr(III):

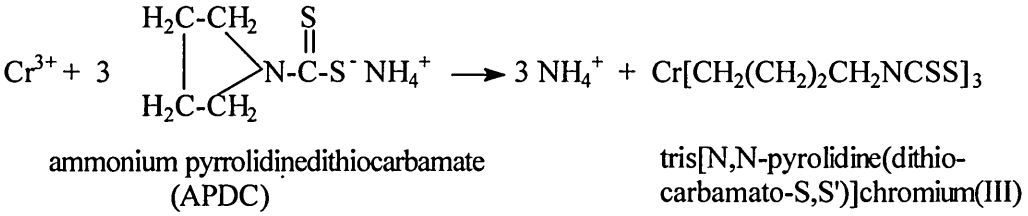

Equation 25: Cr(VI):

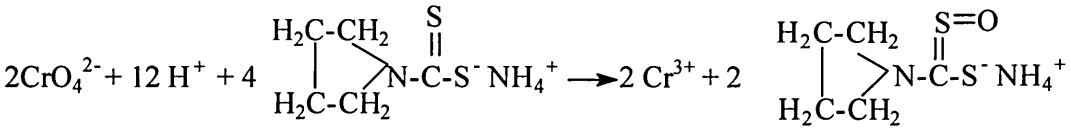

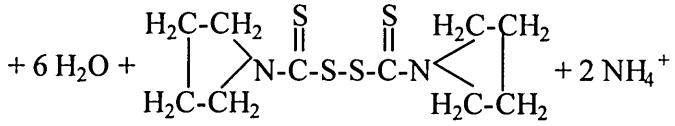

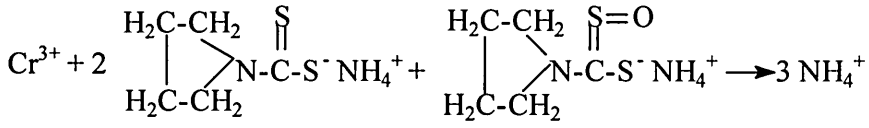

+ $Cr[CH_2(CH_2)_2CH_2NCSS]_2[CH_2(CH_2)_2CH_2NCSSO]$
bis[N,N-pyrrolidine(dithiocarbamato-S,S')][N,N-pyrrolidine(dithioperoxycarbamato-O,S)]chromium(III) **Main Product**

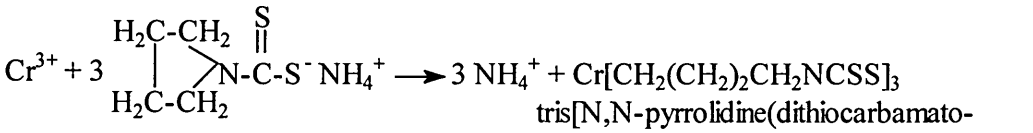

tris[N,N-pyrrolidine(dithiocarbamato-S,S')]chromium(III) **By Product**

Cr(VI) $Cr[CH_2(CH_2)_2CH_2NCSS]_2\ [CH_2(CH_2)_2CH_2NCSSO]$

bis[N,N-pyrrolidine(dithiocarbamato-S,S')][N,N-pyrrolidine(dithioperoxycarbamato-O,S)]chromium(III)

Cr(III) $Cr[CH_2(CH_2)_2CH_2NCSS]_3$

tris[N,N-pyrrolidine(dithiocarbamato-S,S')]chromium(III)

As can be seen from Figure 27 there is clearly one major peak and a small peak obtained for the Cr(III) complex with APDC, but the Cr(VI) complex with APDC gives a chromatogram with four peaks. One of the species (eluting at 8.24 minutes) corresponds to the major Cr(III) species. The by product of the Cr(VI)-APDC reaction is the same as the main product for Cr(III).

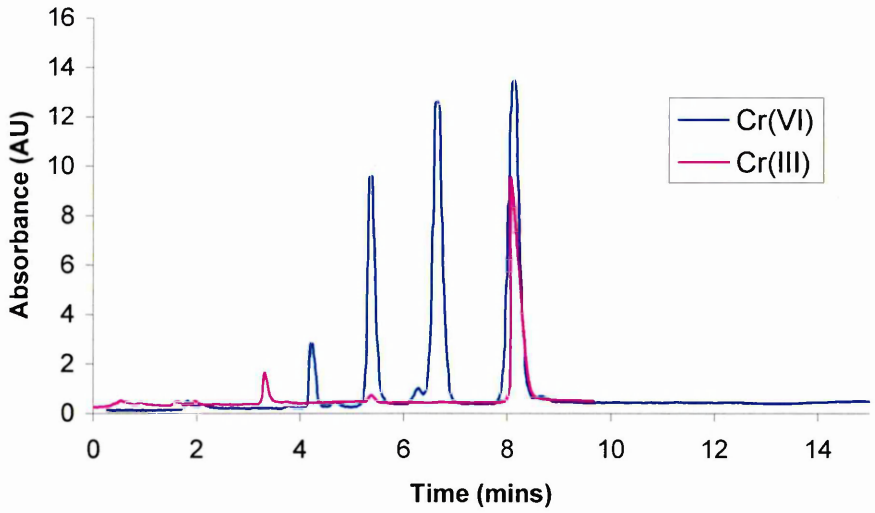

Figure 27: Overlaid plot of Cr(III) and Cr(VI) complexes with APDC.

From the evidence of these preliminary experiments it appears that the two species cannot be determined in a single run. It is possible that with careful optimisation of the reaction conditions it may be possible to limit the number of products formed.

2.9.3 Ion Chromatography with Visible Detection

In this method[135] complexes are formed between Cr(III) and pyridine dicarboxylic acid (PDCA) and also between Cr(VI) and diphenylcarbazide (DPC), and their absorbances measured at 520 nm. The method involves pre-derivatisation of Cr(III) to give the $Cr(PDCA)_2^-$ complex and separation from Cr(VI) as the chromate ion $[CrO_4^{2-}]$ on an

ion exchange column. The Cr(VI) does not form a complex with PDCA but is detected by a post-column derivatisation with DPC. Because of the slow kinetics of the ligand exchange for Cr(III) it is necessary to derivatise the sample with PDCA prior to separation, although the eluent also contains the PDCA ligand. At the pH of the eluent (6.8) the Cr(VI) exists as divalent chromate and the Cr(III)-PDCA complex is a stable monovalent anion, this enabling a separation of the two complexes to be achieved. The pH of 6.8 was chosen because below this value chromate can convert to dichromate and above this value inhibition of the formation of the Cr(III)-PDCA complex was observed[135].

2.9.3.1 Cr(VI)-DPC Complex

Diphenylcarbazide has the following chemical structure[74]:

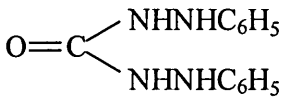

In acid solutions diphenylcarbazide reacts with Cr(VI) to form a red-violet complex. This process is preceded by a 2:3 ratio redox reaction[136] as shown below:

Equation 26

$$2Cr(VI) + 3DPC \rightarrow 2Cr(III) + 3 \text{ diphenylcarbazone (DPCO)}$$

In this way Cr(III) is formed, which is then capable of forming a coloured complex with the DPCO in a 1:1 ratio:

Equation 27

$$Cr(III) + DPCO \rightarrow [Cr(III)\text{-}DPCO]^{(3-n)+} + nH^{+}$$

where n represents the unknown number of protons released in the complex formation.

Only the Cr(VI) in the sample is measured in this way as, even though the complex is formed with the Cr(III), the Cr(III) previously in the sample is already complexed with PDCA and is therefore unavailable for this reaction.

A good peak shape and response is observed for the Cr(VI) standard (see Figure 28) and the calibration graph (see Figure 29) shows good linearity, $r^2 = 0.9997$.

The chromatogram shown below (Figure 28) is for a 50 mg L^{-1} Cr(III) standard and a 1 mg L^{-1} Cr(VI) standard in water, along with a blank run of deionised water with the pH adjusted for comparison.

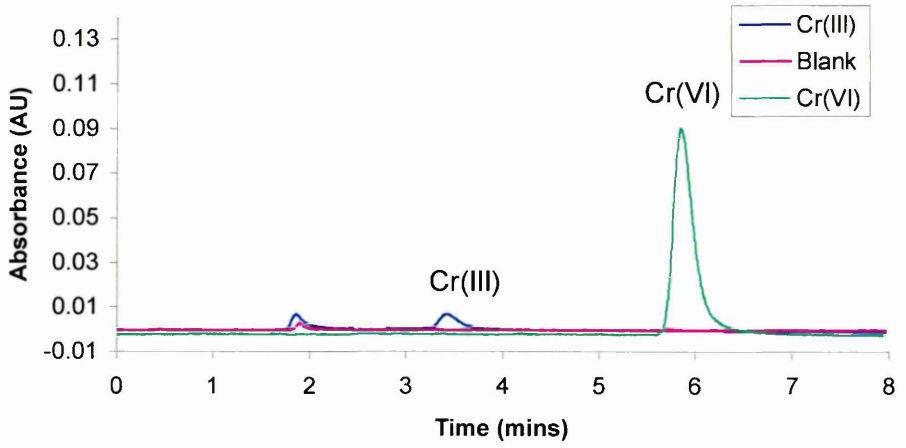

Figure 28: Chromatogram of a 50 mg L^{-1} Cr(III) standard and a 1 mg L^{-1} Cr(VI) standard, along with a blank run of deionised water (pH adjusted) using CS5 column and visible detection at 520 nm.

In the case of the Cr(III) standards the response is much lower and also an impurity that absorbs at 520 nm was observed. This was thought to be due to either the sodium

hydroxide or hydrochloric acid, which were used for pH adjustments, since when a blank solution with the pH adjusted to 6.8 was analysed a similar chromatogram was obtained (see Figure 28). Samples of the deionised water used and also the eluent were also run to see if any impurities were present in these, but no peaks were observed. This impurity could be due to a chromium species, but could also be due to some other species that forms a coloured complex with either DPC or PDCA. The presence of other metal ions is known to interference with this method[137]. Since the impurity peak is well resolved from both the Cr(III) and Cr(VI) peaks this was not viewed as being a problem. Much lower responses for Cr(III) were observed compared to those obtained for Cr(VI) (see Figure 29). It is likely that the difference in sensitivity is due to the nature of the complexes formed. It is also possible that the Cr(VI) has been reduced to Cr(III), however this is unlikely at the relatively neutral pH of 6.8 at which the reaction was carried out.

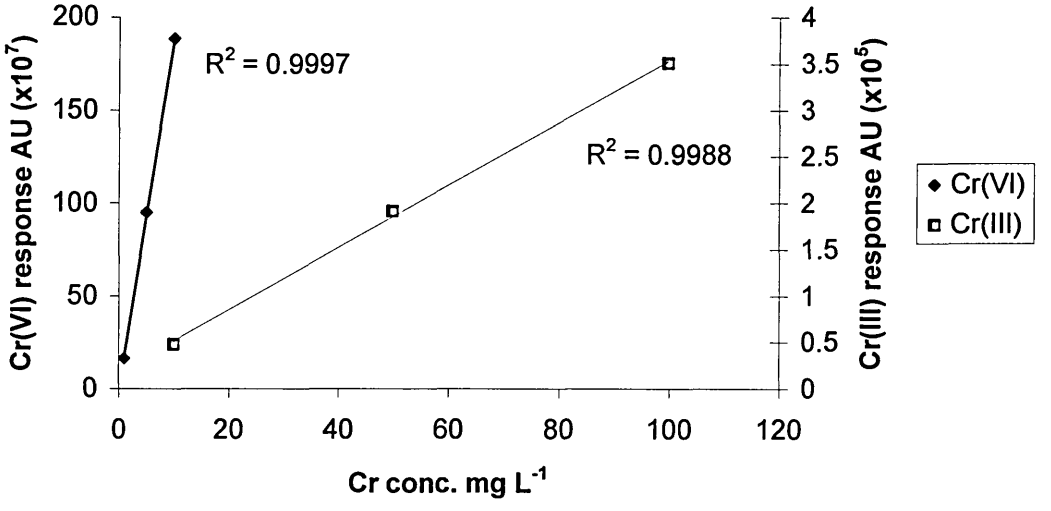

Figure 29: Cr(III) calibration from 10-100 mg L^{-1} and Cr(VI) calibration from 1-10 mg L^{-1} using a CS5 column and visible detection at 520 nm.

The calibration graph for Cr(III) (Figure 29) also shows good linearity, $r^2 = 0.9921$, although at much higher concentration levels than for Cr(VI). Due to the poorer response for Cr(III) lower concentrations could not be measured.

Detection limits were found to be approximately 1 mg L^{-1} and 10 µg L^{-1} for Cr(III) and Cr(VI) respectively using the criteria of three times the background response. These values are much higher than 30 µg L^{-1} and 0.3 µg L^{-1} reported for Cr(III) and Cr(VI) respectively[135] using a similar method.

2.9.4 Single Extraction Procedures with ICP-MS

Two certified reference materials; BCR CRM 596 and 597, with chromium contents of 203 ± 6 and 36.3 ± 1.7 mg kg^{-1} respectively were subjected to a number of extraction procedures. Single extraction procedures were considered, as it was clear from the previously attempted sequential extraction procedure (see paragraph 2.9.1.1) that changes in the species present occurred when successively stronger extractants were used. The amount of chromium extracted by the various procedures is summarised in Table 9 to Table 19.

Key for Table 9 to Table 19

Key	Explanation
[1]	total recovery i.e. both first extraction and subsequent extractions
[2]	second extraction; the residue from the first extraction taken and the HNO_3 extraction procedure carried out again.
[3]	the average value for the first extraction has been subtracted.
[4]	concentrated spike used (if not marked then dilute spike was used)
[5]	spike left overnight before analysis.
[6]	spike left for 1 week before analysis.
[7]	stirring was employed during the extraction.

Table 9: ICP-MS analysis of soil samples extracted using HNO_3/H_2O_2.

SAMPLE	TYPE	EXTRACTION METHOD	Cr CONC (mg kg^{-1})	RECOVERY (%)
Sample 1	Soil	HNO_3/H_2O_2	134.4	66.2
Sample 2	Soil	HNO_3/H_2O_2	134.4	66.2
Sample 3	Soil	HNO_3/H_2O_2	387.7	191.0
Sample 4	Soil	HNO_3/H_2O_2	131.0	64.5
Sample 5	Soil	HNO_3/H_2O_2	124.5	61.3
Sample A	Soil	HNO_3/H_2O_2	126.2	62.2
Sample A	$Soil_{[2]}$	(3+7) HNO_3	49.3 ($175.5_{[1]}$)	86.5 (total)
Sample B	Soil	HNO_3/H_2O_2	135.2	66.6
Sample B	$Soil_{[2]}$	(3+7) HNO_3	45.7 ($180.9_{[1]}$)	89.1 (total)
Sample C	Soil	HNO_3/H_2O_2	147.9	72.9
Sample C	$Soil_{[2]}$	(3+7) HNO_3	35.5 ($183.4_{[1]}$)	90.3 (total)
Spike 1	$Soil_{[4]}$	HNO_3/H_2O_2	340.6 ($204.2_{[3]}$)	102.1
Spike 2	$Soil_{[4]}$	HNO_3/H_2O_2	341.3 ($204.9_{[3]}$)	102.4
Spike 3	$Soil_{[4]}$	HNO_3/H_2O_2	290.5 ($162.7_{[3]}$)	81.35
Spike 4	$Soil_{[4]}$	HNO_3/H_2O_2	301.4 ($173.6_{[3]}$)	86.8
Spike 5	$Soil_{[7]}$	HNO_3/H_2O_2	348.9 ($193.8_{[3]}$)	96.9
Spike 6	$Soil_{[7]}$	HNO_3/H_2O_2	326.6 ($171.5_{[3]}$)	85.8
Spike 7	Soil	HNO_3/H_2O_2	348.2 ($193.1_{[3]}$)	96.6
Spike 8	Soil	HNO_3/H_2O_2	329.4 ($174.3_{[3]}$)	87.2

Sample 1, 2 etc... = separate 500 mg samples of soil extracted with HNO_3/H_2O_2. See section 2.8.4.1 for details.
Sample A, B etc... = separate 500 mg samples of soil extracted with HNO_3/H_2O_2, then subsequently extracted with HNO_3. See section 2.8.4.1 and 2.8.4.2 for details.
Spike 1, 2 etc... = soil samples with added Cr(VI)spike. See section 2.8.4.5 for details.
Each analysis was carried out in triplicate.

Average extraction yields of 65.7 ± 3.5% (n = 48) were obtained when the samples were subjected to one extraction using the HNO_3/H_2O_2 method. However improved extraction yields of 88.6 ± 10.9% (n = 9) were obtained when a further (3+7) HNO_3 extraction was carried out. This indicates that after the first extraction there is still some extractable chromium remaining in the sample. The average extraction for the spiked

samples agrees well with that obtained for the second extraction, 92.4 ± 7.5% compared with 88.6%. However it is likely that the spiked chromium is not as tightly bound as the original chromium in the sample.

Table 10: ICP-MS analysis of soil samples extracted using HNO_3.

SAMPLE	TYPE	EXTRACTION METHOD	Cr CONC ($mg\ kg^{-1}$)	RECOVERY (%)
Sample 1	Soil	(3+7) HNO_3	115.5	56.8
Sample 2	Soil	(3+7) HNO_3	98.8	48.7
Sample 3	Soil	(3+7) HNO_3	79.4	39.1
Sample 4	Soil	(3+7) HNO_3	121.3	59.8
Sample 5	Soil	(3+7) HNO_3	126.0	62.1
Sample 6	Soil	(3+7) HNO_3	123.5	60.8
Sample 7	Soil	(3+7) HNO_3	122.2	60.2
Sample 8	Soil[7]	(3+7) HNO_3	152.3	75.0
Sample 9	Soil[7]	(3+7) HNO_3	154.5	76.1
Sample 10	Soil	(3+7) HNO_3	159.0	78.3
Sample 11	Soil	(3+7) HNO_3	154.8	76.3
Sample A	Soil	(3+7) HNO_3	165.0	81.3
Sample A	Soil[2]	(3+7) HNO_3	20.6 (185.6[1])	91.4 (total)
Sample B	Soil	(3+7) HNO_3	175.7	86.6
Sample B	Soil[2]	(3+7) HNO_3	16.1 (191.8[1])	94.5 (total)
Sample C	Soil	(3+7) HNO_3	165.7	81.6
Sample C	Soil[2]	(3+7) HNO_3	21.7 (187.4[1])	92.3 (total)
Soil 1	Soil	Conc. HNO_3	113.9	56.1
Soil 2	Soil	Conc. HNO_3	118.3	58.3
Spike 1	Soil[4]	(3+7) HNO_3	205.7 (36.9[3])	18.5
Spike 2	Soil[4]	(3+7) HNO_3	213.6 (44.8[3])	22.4
Spike 3	Soil[4]	HNO_3	219.6 (95.9[3])	48.0
Spike 4	Soil[4]	HNO_3	210.4 (86.7[3])	43.4
Spike 5	Soil[4,6]	Conc. HNO_3	317.6 (201.5[3])	100.8

SAMPLE	TYPE	EXTRACTION METHOD	Cr CONC (mg kg^{-1})	RECOVERY (%)
Spike 6	$Soil_{[4,6]}$	Conc. HNO_3	366.8 ($250.7_{[3]}$)	125.4
Spike 7	$Soil_{[4,5]}$	(3+7) HNO_3	328.3 ($205.4_{[3]}$)	102.7
Spike 8	$Soil_{[4,5]}$	(3+7) HNO_3	400.4 ($277.5_{[3]}$)	138.7
Spike 9	$Soil_{[7]}$	(3+7) HNO_3	367.4 ($212.3_{[3]}$)	106.2
Spike 10	$Soil_{[7]}$	(3+7) HNO_3	362.7 ($207.6_{[3]}$)	103.8
Spike 11	Soil	(3+7) HNO_3	367.4 ($212.3_{[3]}$)	106.2
Spike 12	Soil	(3+7) HNO_3	351.8 ($196.7_{[3]}$)	98.4

Sample 1, 2 etc... = separate 500 mg samples of soil extracted with (3+7) HNO_3. See section 2.8.4.2 for details.
Sample A, B etc... = separate 500 mg samples of soil extracted with (3+7) HNO_3, then subsequently extracted again with (3+7) HNO_3. See section 2.8.4.2 for details.
Spike 1, 2 etc... = soil samples with added Cr(VI)spike. See section 2.8.4.5 for details.
Soil 1, 2 etc... = separate 500 mg samples of soil extracted as detailed in section 2.8.4.2, but replacing the (3+7) HNO_3 with concentrated HNO_3. Spiked samples 5 and 6 were also extracted using concentrated HNO_3.
Each analysis was carried out in triplicate.

From Table 10 it can be seen that significantly more chromium was extracted from the sewage sludge amended soil, 92.7 ± 14.9%, compared to 66.1 ±14.5% when two extractions as opposed to one were used. These results show that more than one extraction is required to remove most of the chromium in the sewage sludge amended soil samples. In this case the second extraction step has extracted even more chromium on average than from the spiked samples, which only extracted 84.5 ± 38.7%.

Table 11: ICP-MS analysis of soil samples extracted using Na_2CO_3/NaOH.

SAMPLE	TYPE	EXTRACTION METHOD	Cr CONC (mg kg^{-1})	RECOVERY (%)
Sample 1	Soil	Na_2CO_3/NaOH	5.5	2.7
Sample 2	Soil	Na_2CO_3/NaOH	7.5	3.7
Spike 1	$Soil_{[4]}$	Na_2CO_3/NaOH	20.8 ($14.3_{[3]}$)	7.2
Spike 2	$Soil_{[4]}$	Na_2CO_3/NaOH	21.1 ($14.6_{[3]}$)	7.3
Sample A	Soil	$NaCO_3$/NaOH	4.5	2.2
Sample A	$Soil_{[2]}$	(3+7) HNO_3	138.2 (142.7_1)	70.3 (total)

SAMPLE	TYPE	EXTRACTION METHOD	Cr CONC (mg kg^{-1})	RECOVERY (%)
Sample B	Soil	$NaCO_3$/NaOH	1.5	0.7
Sample B	$Soil_{[2]}$	(3+7) HNO_3	140.8 (142.3_1)	70.1 (total)
Sample C	Soil	Na_2CO_3/NaOH	3.0	1.5
Sample C	$Soil_{[2]}$	(3+7) HNO_3	92.1 ($92.4_{[1]}$)	45.5 (total)
Sample D	Soil	$NaCO_3$/NaOH	1.0	0.5
Sample D	$Soil_{[2]}$	(3+7) HNO_3	103.1 ($104.1_{[1]}$)	51.3 (total)
Spike A	$Soil_{[4]}$	$NaCO_3$/NaOH	9.9 ($6.9_{[3]}$)	3.5
Spike A	$Soil_{[2]}$	(3+7) HNO_3	217.4 ($224.3_{[1]}$)	112.1 (total)
Spike B	$Soil_{[4]}$	$NaCO_3$/NaOH	9.3 ($6.3_{[3]}$)	3.2
Spike B	$Soil_{[2]}$	(3+7) HNO_3	206.3 ($212.6_{[1]}$)	106.3 (total)
Spike C	$Soil_{[4,6]}$	$NaCO_3$/NaOH	16.8 ($14.8_{[3]}$)	7.4
Spike C	$Soil_{[2]}$	(3+7) HNO_3	331.9 ($348.7_{[1]}$)	174.4 (total)
Spike D	$Soil_{[4,6]}$	$NaCO_3$/NaOH	31.6 ($29.6_{[3]}$)	14.8
Spike D	$Soil_{[2]}$	(3+7) HNO_3	134.3 ($165.9_{[1]}$)	83.0 (total)
Spike E	Soil	$NaCO_3$/NaOH	14.6 ($12.6_{[3]}$)	6.3
Spike E	$Soil_{[2]}$	(3+7) HNO_3	288.1 ($302.7_{[1]}$)	151.4 (total)
Spike F	Soil	$NaCO_3$/NaOH	8.3 ($6.3_{[3]}$)	3.2
Spike F	$Soil_{[2]}$	(3+7) HNO_3	291.0 ($299.3_{[1]}$)	149.7 (total)

Sample 1, 2 etc... = separate 500 mg samples of soil extracted with Na_2CO_3/NaOH. See section 2.8.4.3 for details.
Sample A, B etc... = separate 500 mg samples of soil extracted with Na_2CO_3/NaOH, then subsequently extracted with (3+7) HNO_3. See section 2.8.4.3 and 2.8.4.2 respectively for details.
Spike 1, 2 etc... = soil samples with added Cr(VI)spike. See section 2.8.4.5 for details.
Spike A, B etc... = spiked samples extracted with Na_2CO_3/NaOH, then subsequently extracted with (3+7) HNO_3. See section 2.8.4.3 and 2.8.4.2 respectively for details.
Each analysis was carried out in triplicate.

From Table 11, the average recovery of chromium using Na_2CO_3/NaOH, after one extraction and from the spiked samples, were only 2.6 ± 1.6% and 7.2 ± 3.8%, respectively. Subsequent extraction of the same samples with HNO_3 released all of the remaining chromium i.e. to give 100% yield. The Na_2CO_3/NaOH extracting solution is reported to remove only Cr(VI), with the Cr(III) being precipitated as chromium oxide hydroxide[75], whereas the HNO_3 removes total chromium. This indicates that there is

only a small amount of Cr(VI) present in the sewage sludge amended soil sample and that almost all the chromium in the sample is present in the form of Cr(III).

Table 12: ICP-MS analysis of soil samples extracted using phosphate buffer.

SAMPLE	TYPE	EXTRACTION METHOD	Cr CONC ($mg\ kg^{-1}$)	RECOVERY (%)
Sample 1	Soil	Phosphate	3.5	1.7
Sample 2	Soil	Phosphate	2.0	1.0
Sample 3	Soil	Phosphate	4.4	2.2
Sample 4	Soil	Phosphate	4.0	1.9
Spike 1	$Soil_{[4]}$	Phosphate	48.8 ($46.0_{[3]}$)	23.0
Spike 2	$Soil_{[4]}$	Phosphate	68.8 ($66.0_{[3]}$)	33.0
Spike 3	$Soil_{[4]}$	Phosphate	47.5 ($43.3_{[3]}$)	21.7
Spike 4	$Soil_{[4]}$	Phosphate	38.8 ($34.6_{[3]}$)	17.3

Sample 1, 2 etc... = separate 500 mg samples of soil extracted with phosphate. See section 2.8.4.4 for details.
Spike 1, 2 etc... = soil samples with added Cr(VI)spike. See section 2.8.4.5 for details.
Each analysis was carried out in triplicate.

From Table 12, low recoveries of Cr(VI), 1.7 ± 0.4%, were also obtained when phosphate buffer was used on the sewage sludge amended soil sample. Only Cr(VI) was extracted from the samples, when phosphate buffer was used[138]. This would again appear to indicate that there is very little Cr(VI) in the sewage sludge amended soil samples. This is to be expected since the soil will contain numerous reductants of Cr(VI) e.g. Fe(II), S^{2-} and organic matter. However any Mn(III) or (IV) present in the soil, which is capable of oxidising Cr(III) to Cr(VI), will most likely have been converted to Mn(II) in the process of drying and will therefore be unavailable for oxidation. Also for the spiked extraction very low recoveries were obtained (23.8 ± 5.7%). It is probable that the Cr(VI) spike is reduced to Cr(III) by constituents in the soil thereby making it unavailable for extraction.

Table 13: ICP-MS analysis of plant samples extracted using HNO_3/H_2O_2.

SAMPLE	TYPE	EXTRACTION METHOD	Cr CONC (mg kg^{-1})	RECOVERY (%)
Sample 1	Plant	HNO_3/H_2O_2	8.0	21.9
Sample 2	Plant	HNO_3/H_2O_2	8.0	21.9
Spike 1	Plant[7]	HNO_3/H_2O_2	242.2 (229.8[3])	114.9
Spike 2	Plant[7]	HNO_3/H_2O_2	195.4 (183.0[3])	91.5
Spike 3	Plant	HNO_3/H_2O_2	217.1 (204.7[3])	102.4
Spike 4	Plant	HNO_3/H_2O_2	139.4 (127.0[3])	63.5

Sample 1, 2 etc... = separate 500 mg samples of aquatic plant material extracted with HNO_3/H_2O_2. See section 2.8.4.1 for details.
Spike 1, 2 etc... = aquatic plant samples with added Cr(VI)spike. See section 2.8.4.5 for details.
Each analysis was carried out in triplicate.

From Table 13, an average of only 21.9% of the chromium from the aquatic plant material was extracted using HNO_3/H_2O_2, but this may have been improved with a second extraction. With the spiked samples a much better recovery was obtained (93.1 ± 19.0%). It is possible that the chromium present in the sample is tightly bound to the matrix and is therefore unavailable for extraction.

Table 14: ICP-MS analysis of plant samples extracted using HNO_3.

SAMPLE	TYPE	EXTRACTION METHOD	Cr CONC (mg kg^{-1})	RECOVERY (%)
Sample 1	Plant	(3+7) HNO_3	10.9	30.0
Sample 2	Plant	(3+7) HNO_3	8.0	22.0
Sample 3	Plant	(3+7) HNO_3	5.3	14.6
Sample 4	Plant	(3+7) HNO_3	5.4	14.9
Sample 5	Plant	(3+7) HNO_3	17.3	47.7
Sample 6	Plant	(3+7) HNO_3	16.0	44.1
Sample 7	Plant[7]	(3+7) HNO_3	8.6	23.7
Sample 8	Plant[7]	(3+7) HNO_3	7.6	20.9
Plant 1	Plant	Conc. HNO_3	6.7	18.5

SAMPLE	TYPE	EXTRACTION METHOD	Cr CONC ($mg\ kg^{-1}$)	RECOVERY (%)
Plant 2	Plant	Conc. HNO_3	8.5	23.4
Spike 1	$Plant_{[4]}$	(3+7) HNO_3	162.7 ($153.2_{[3]}$)	76.6
Spike 2	$Plant_{[4]}$	(3+7) HNO_3	165.3 ($155.8_{[3]}$)	77.9
Spike 3	$Plant_{[4,6]}$	Conc. HNO_3	234.9 ($227.3_{[3]}$)	113.7
Spike 4	$Plant_{[4,6]}$	Conc. HNO_3	205.0 ($197.4_{[3]}$)	98.7
Spike 5	$Plant_{[4,5]}$	(3+7) HNO_3	185.6 ($180.2_{[3]}$)	90.1
Spike 6	$Plant_{[4,5]}$	(3+7) HNO_3	196.2 ($190.8_{[3]}$)	95.4
Spike 7	$Plant_{[7]}$	(3+7) HNO_3	211.1 ($198.7_{[3]}$)	99.4
Spike 8	$Plant_{[7]}$	(3+7) HNO_3	196.4 ($184.0_{[3]}$)	92.0
Spike 9	Plant	(3+7) HNO_3	205.7 ($193.3_{[3]}$)	96.7
Spike 10	Plant	(3+7) HNO_3	196.9 ($184.5_{[3]}$)	92.3

Sample 1, 2 etc... = separate 500 mg samples of aquatic plant material extracted with (3+7) HNO_3. See section 2.8.4.2 for details.
Spike 1, 2 etc... = aquatic plant samples with added Cr(VI)spike. See section 2.8.4.5 for details.
Plant 1, 2 etc... = separate 500 mg samples of aquatic plant material extracted as detailed in section 2.8.4.2, but replacing the (3+7) HNO_3 with concentrated HNO_3. Spiked samples 3 and 4 were also extracted using concentrated HNO_3.
Each analysis was carried out in triplicate.

From Table 14, again with this HNO_3 extraction technique only 26.0 ± 10.9% of the chromium was extracted compared to 93.3 ± 10.1% for the spiked sample. These findings highlight the difficulties of chromium extraction, especially from natural matrices.

Table 15: ICP-MS analysis of plant samples extracted using Na_2CO_3/NaOH.

SAMPLE	TYPE	EXTRACTION METHOD	Cr CONC ($mg\ kg^{-1}$)	RECOVERY (%)
Sample A	Plant	$NaCO_3$/NaOH	1.0	2.8
Sample A	$Plant_{[2]}$	(3+7) HNO_3	12.3 ($13.3_{[1]}$)	36.6 (total)
Sample B	Plant	$NaCO_3$/NaOH	5.5	15.2
Sample B	$Plant_{[2]}$	(3+7) HNO_3	11.7 ($17.2_{[1]}$)	47.4 (total)
Sample C	Plant	$NaCO_3$/NaOH	0.5	1.4
Sample C	$Plant_{[2]}$	(3+7) HNO_3	8.1 ($8.6_{[1]}$)	23.7 (total)

SAMPLE	TYPE	EXTRACTION METHOD	Cr CONC (mg kg^{-1})	RECOVERY (%)
Sample D	Plant	$NaCO_3$/NaOH	0.9	2.5
Sample D	$Plant_{[2]}$	(3+7) HNO_3	2.1 ($3.0_{[1]}$)	8.3 (total)
Spike A	$Plant_{[4]}$	$NaCO_3$/NaOH	17.5 ($14.2_{[3]}$)	7.1
Spike A	$Plant_{[2]}$	(3+7) HNO_3	65.9 ($80.1_{[1]}$)	40.1 (total)
Spike B	$Plant_{[4]}$	$NaCO_3$/NaOH	6.5 ($3.2_{[3]}$)	1.6
SpikeB	$Plant_{[2]}$	(3+7) HNO_3	69.6 ($72.8_{[1]}$)	36.4 (total)
Spike C	$Plant_{[4,5]}$	$NaCO_3$/NaOH	58.7 ($58.0_{[3]}$)	29.0
Spike C	$Plant_{[2]}$	(3+7) HNO_3	67.1 ($125.8_{[1]}$)	62.9 (total)
Spike D	$Plant_{[4,5]}$	$NaCO_3$/NaOH	98.5 ($97.8_{[3]}$)	48.9
Spike D	$Plant_{[2]}$	(3+7) HNO_3	93.3 ($191.8_{[1]}$)	95.9 (total)
Spike E	$Plant_{[4,6]}$	$NaCO_3$/NaOH	70.1 ($69.4_{[3]}$)	34.7
Spike E	$Plant_{[2]}$	(3+7) HNO_3	115 ($185.1_{[1]}$)	92.6 (total)
Spike F	$Plant_{[4,6]}$	$NaCO_3$/NaOH	86.5 ($85.8_{[3]}$)	42.9
Spike F	$Plant_{[2]}$	(3+7) HNO_3	111.1 ($197.6_{[1]}$)	98.8 (total)

Sample A, B etc... = separate 500 mg samples of aquatic plant material extracted with Na_2CO_3/NaOH, then subsequently extracted with (3+7) HNO_3. See section 2.8.4.3 and 2.8.4.2 respectively for details.
Spike A, B etc... = aquatic plant samples with added Cr(VI)spike. See section 2.8.4.5 for details. Extracted with Na_2CO_3/NaOH, then subsequently extracted with (3+7) HNO_3. See section 2.8.4.3 and 2.8.4.2 respectively for details.
Each analysis was carried out in triplicate.

From Table 15 very low yields on average are observed for the first extraction using Na_2CO_3/NaOH (5.5 ± 5.6%) as well as for the extraction of the spiked samples (27.4% ± 17.5%), with much more being recovered by the second extraction with HNO_3 (54.3 ± 30.3%). The Na_2CO_3/NaOH method extracts Cr(VI), with Cr(III) being precipitated as chromium oxide hydroxide[75]. These results again show that most of the chromium present in the aquatic plant material is in the form of Cr(III), and any Cr(VI) spike being added is being converted by the reductants (e.g. organic matter) present within the sample to Cr(III). This result is similar to that found for the sewage sludge amended soil samples when the extraction solution was used.

Table 16: ICP-MS analysis of plant samples extracted using phosphate buffer.

SAMPLE	TYPE	EXTRACTION METHOD	Cr CONC (mg kg^{-1})	RECOVERY (%)
Sample 1	Plant	Phosphate	0.3	0.8
Sample 2	Plant	Phosphate	0.3	0.8
Spike 1	Plant[4]	Phosphate	1.5 (1.2[3])	0.6
Spike 2	Plant[4]	Phosphate	0.5 (0.2[3])	0.01

Sample 1, 2 etc... = separate 500 mg samples of aquatic plant material extracted with phosphate. See section 2.8.4.4 for details.
Spike 1, 2 etc... = aquatic plant samples with added Cr(VI)spike. See section 2.8.4.5 for details.
Each analysis was carried out in triplicate.

From Table 16, it can be seen that using phosphate buffer as extractant, only Cr(VI) is extracted from the samples[138] and again very low recoveries are obtained, 0.8 and 0.3 ± 0.3%, for the sample and the spike respectively. This points to a very low concentration of Cr(VI) in the sample and reduction of the Cr(VI) in the spike solution to Cr(III) making it unavailable for extraction.

2.9.4.1 Stirring and Spiking Trials

Table 17 and Table 18 show that no improvement in recoveries was obtained when the samples were stirred. Results of trials in which spikes were left in contact with samples overnight and for one week (see Table 14 and Table 15) also showed no significant differences.

Table 17: ICP-MS analysis of soil samples after spiking trials.

SAMPLE	TYPE	EXTRACTION METHOD	Cr CONC (mg kg^{-1})	RECOVERY (%)
Sample 1	Soil[7]	(3+7) HNO_3	152.3	75.0
Sample 2	Soil[7]	(3+7) HNO_3	154.5	76.1
Sample 3	Soil	(3+7) HNO_3	159.0	78.3

SAMPLE	TYPE	EXTRACTION METHOD	Cr CONC (mg kg^{-1})	RECOVERY (%)
Sample 4	Soil	(3+7) HNO_3	154.8	76.3
Spike 1	$Soil_{[7]}$	(3+7) HNO_3	367.4 ($212.3_{[3]}$)	106.2
Spike 2	$Soil_{[7]}$	(3+7) HNO_3	362.7 ($207.6_{[3]}$)	103.8
Spike 3	Soil	(3+7) HNO_3	367.4 ($212.3_{[3]}$)	106.2
Spike 4	Soil	(3+7) HNO_3	351.8 ($196.7_{[3]}$)	98.4
Spike 5	$Soil_{[7]}$	HNO_3/H_2O_2	348.9 ($193.8_{[3]}$)	96.9
Spike 6	$Soil_{[7]}$	HNO_3/H_2O_2	326.6 ($171.5_{[3]}$)	85.8
Spike 7	Soil	HNO_3/H_2O_2	348.2 ($193.1_{[3]}$)	96.6
Spike 8	Soil	HNO_3/H_2O_2	329.4 ($174.3_{[3]}$)	87.2

Sample 1, 2 etc... = separate 500 mg samples of soil extracted with (3+7) HNO_3. See section 2.8.4.2 for details.
Spike 1, 2 etc... = soil samples with added Cr(VI)spike. See section 2.8.4.5 for details.
Each analysis was carried out in triplicate.

Table 18: ICP-MS analysis of plant samples after spiking trials.

SAMPLE	TYPE	EXTRACTION METHOD	Cr CONC (mg kg^{-1})	RECOVERY (%)
Sample 1	Plant	(3+7) HNO_3	17.3	47.7
Sample 2	Plant	(3+7) HNO_3	16.0	44.1
Sample 3	$Plant_{[7]}$	(3+7) HNO_3	8.6	23.7
Sample 4	$Plant_{[7]}$	(3+7) HNO_3	7.6	20.9
Spike 1	$Plant_{[7]}$	(3+7) HNO_3	211.1 ($198.7_{[3]}$)	99.4
Spike 2	$Plant_{[7]}$	(3+7) HNO_3	196.4 ($184.0_{[3]}$)	92.0
Spike 3	Plant	(3+7) HNO_3	205.7 ($193.3_{[3]}$)	96.7
Spike 4	Plant	(3+7) HNO_3	196.9 ($184.5_{[3]}$)	92.3
Spike 5	$Plant_{[7]}$	HNO_3/H_2O_2	242.2 ($229.8_{[3]}$)	114.9
Spike 6	$Plant_{[7]}$	HNO_3/H_2O_2	195.4 ($183.0_{[3]}$)	91.5
Spike 7	Plant	HNO_3/H_2O_2	217.1 ($204.7_{[3]}$)	102.4
Spike 8	Plant	HNO_3/H_2O_2	139.4 ($127.0_{[3]}$)	63.5

Sample 1, 2 etc... = separate 500 mg samples of aquatic plant material extracted with phosphate. See section 2.8.4.4 for details.
Spike 1, 2 etc... = aquatic plant samples with added Cr(VI)spike. See section 2.8.4.5 for details.
Each analysis was carried out in triplicate.

From Table 17, the mean chromium recoveries for unspiked and spiked soil samples were 76.4 ± 1.2% and 97.6 ± 7.3% respectively. From Table 18, the recoveries of chromium from the unspiked and spiked plant samples were 34.1 ± 11.9% and 94.1 ± 13.6% respectively. Stirring did not improve the recoveries in either the spiked or the unspiked samples.

Experiments using known concentrations of Cr(VI) and Cr(III) were carried out in order to determine if the method of extraction was affecting the results. Solutions containing 2 mg L^{-1} and 4 mg L^{-1} Cr(VI) were used to test the HNO_3 and HNO_3/H_2O_2 methods and the Na_2CO_3/NaOH and phosphate methods respectively. The procedures were carried out exactly as before, but without the addition of any sample.

The purpose of this experiment was to determine if the extractant solutions caused any reduction of Cr(VI) to Cr(III). This therefore had to be carried out without the addition of sample, as this may also contain elements that may cause reduction of the chromium species present.

Table 19 shows that 100% of the Cr(VI) was recovered using the total chromium extractants and 85-90% of the Cr(VI) was recovered in the methods used to extract Cr(VI) only. Results obtained which were greater than 100% could be due to contamination by the extractant, although blank extraction was carried out. It could also be due to the 'memory effect' which may occur in ICP-MS, although rinsing was carried out with HNO_3 between injections.

Table 19: Results of the ICP-MS analysis of standard Cr(VI) solutions after extraction.

Extractant	Expected Cr conc. ($\mu g\ L^{-1}$)	Found Cr Conc. ($mg\ L^{-1}$)	Recovery (%)
HNO_3 I	2.0	2.36	118.0
HNO_3 II	2.0	2.41	120.5
HNO_3/H_2O_2 I	2.0	2.22	111.0
HNO_3/H_2O_2 II	2.0	2.17	108.5
Na_2CO_3/NaOH I	4.0	3.6	90.0
Na_2CO_3/NaOH II	4.0	3.5	87.5
Phosphate I	4.0	3.4	85.0
Phosphate I	4.0	3.4	85.0

Conclusions - Preliminary Investigations

2.9.5 Ion Chromatography - ICP-MS (IC with ICP-MS)

- A method was developed which gave a satisfactory separation of a mixture of the two chromium species, Cr(III) and Cr(VI), although a baseline separation was not achieved.
- It was found that the pH of the solution was very important and that in acidic solutions conversion of Cr(VI) to Cr(III) occurred rapidly. The least conversion of the sample to other species was observed in deionised water (pH 5.5).
- A sequential extraction procedure was carried out which gave good reproducibility between the duplicates carried out. However the usefulness of this procedure is not certain, as many of the extractants change the species present by either oxidation or reduction and are therefore more suited to a total extraction analysis where speciation information is not required.

- When the sequential extraction procedure was carried out on a sewage sludge amended soil sample it was found that most of the chromium was extracted by the final extractant (hydrogen peroxide) and that the chromium present in the sewage sludge amended soil sample BCR CRM 597 was in the form of Cr(III).
- Baseline separation of the peaks was not achieved. This is a problem as quantification of the two peaks cannot then be carried out.
- The method suffers from high blank levels for many of the extractant solutions, which could be a problem for samples containing low concentrations of chromium. The use of higher grade chemicals could solve this problem.

2.9.6 High Performance Liquid Chromatography (HPLC)

- A satisfactory complexation procedure was developed which gave a major peak and a small peak for the Cr(III) complex, however the Cr(VI) complex gave four peaks.
- Further development is needed in order to optimise the formation of the Cr(VI) complex and reduce the number of side products.
- The HPLC method used gave sharp peaks with baseline separation (see Figure 27), however the Cr(VI)-APDC complex contains a significant amount of the Cr(III)-APDC complex. This makes separation and quantitation of the two species impossible.
- The time taken for this procedure was lengthy; each run was 10 minutes with around 2 hours required for the preparation of each chromium complex.

2.9.7 Ion Chromatography with Visible Detection (IC-Vis)

- A good peak shape and sensitivity was observed for the Cr(VI) standards.
- The calibration graph for Cr(VI) showed good linearity.

- Two peaks for the Cr(III) standards were observed. The first may be due to the impurities in the NaOH or HCl used for pH adjustments.
- The use of higher grade NaOH and HCl is recommended.
- The calibration graph for Cr(III) also showed good linearity.
- Detection limits were 1 mg L^{-1} and 10 μg L^{-1} for Cr(III) and Cr(VI) respectively. There is obviously some room for improvement here since the expected values (from literature[135]) are 30 μg L^{-1} and 0.3 μg L^{-1} for Cr(III) and Cr(VI) respectively.

2.9.8 Single Extraction Procedures with ICP-MS

- It was found that most of the chromium present within either the aquatic plant or sewage sludge amended soil reference materials was in the form of Cr(III).
- It is probable that Cr(VI) present within the samples would have been reduced by Fe(II), S^{2-} or organic matter. This observation was supported by the finding that on addition of Cr(VI) spikes, Cr(III) was detected.
- Any ability of the samples to oxidise Cr(III) to Cr(VI) is likely to have been destroyed, because Mn(III) or (IV) would have been reduced to Mn(II).
- The HNO_3/H_2O_2 and HNO_3 methods both give good recoveries for the total chromium content. However, these methods cannot be used to study the distribution of chromium species in the samples, because of the changes in chromium speciation.
- Both the Na_2CO_3/NaOH method and the phosphate method gave similar recoveries of Cr(VI) from the samples. For example 2.6 ± 1.6% of chromium was extracted from the sewage sludge amended soil by $NaCO_3$/NaOH compared to only 1.7 ± 0.4% when the phosphate method was used. No statistically significant difference was found using both one and two-tailed students' t test.

2.9.9 Overall Conclusion

The resolution of the IC with ICP-MS method was poor. The HPLC method was slow (10 minutes per run plus 2 hours sample preparation) and in addition a number of side products were formed giving rise to several peaks in the chromatogram. The ion chromatography with visible detection method appeared to be the most promising method, however the limit of detection was not acceptable, with a more sensitive detector being required. In order to obtain sensitive detection of the chromium species without the use of an expensive detector such as ICP-MS, a chemiluminescence detector was investigated.

CHAPTER 3 ION CHROMATOGRAPHY WITH CHEMILUMINESCENCE DETECTION

3.1 Introduction to Chemiluminescence

Chemiluminescence (CL) is a phenomenon that has interested mankind for several centuries. Aristotle (384–322 BC) wrote about "cold light"[139], but it was not until 1888 that the term was defined by Eilhard Wiedemann as light emitted from chemical reactions[140]. If CL occurs within a living organism, the term bioluminescence is used. Different functions have been ascribed to bioluminescence, most often it is connected with such necessities in life as obtaining food, defence or reproduction[141]. Luminescence is defined as emissions of electromagnetic radiation in the ultra violet (UV), visible and infrared regions of the spectrum, derived from electronically excited atoms or molecules, which return to the ground state. Fluorescence is luminescence from a singlet excited state whereas phosphorescence originates from a triplet state (see Figure 30). Most molecules do not emit luminescence, but rather relax from the excited state by energy loss through rotation or vibration. Molecules that are rigid in structure (especially aromatic rings) cannot relax in this way and therefore return to the ground state by the emission of electromagnetic radiation i.e. luminescence.

There is a fundamental difference between photoluminescent processes i.e. when the excited state is reached through absorption of light and chemiluminescent processes, in which the excited state is reached through a chemical reaction[142]. In chemiluminescence the electronically excited state is generated by a chemical reaction. As a result the excited molecule, the product of the reaction, has a different molecular structure compared to the reactant.

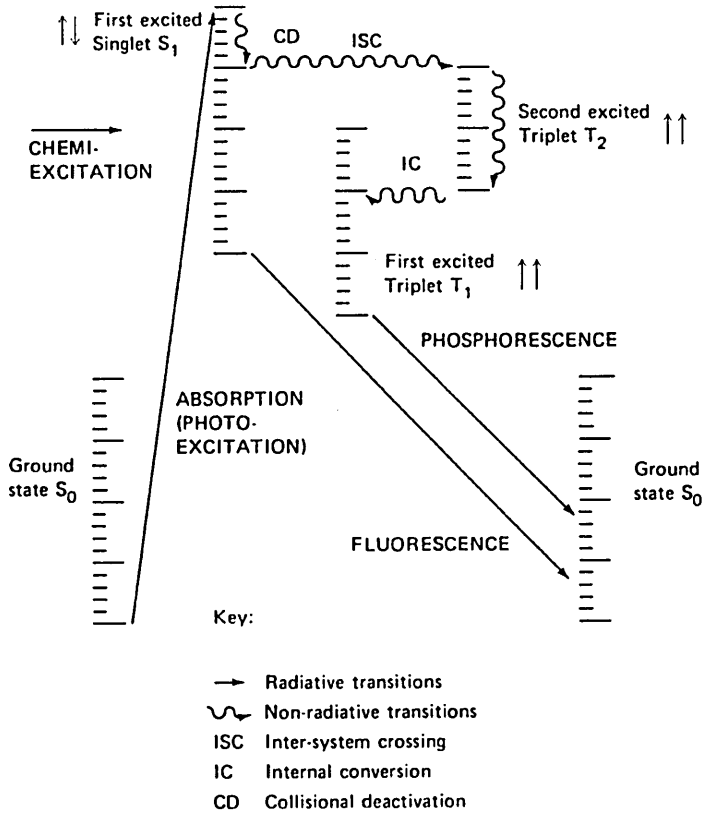

Figure 30: Jablonski diagram, showing excited state energetics. Adapted from Campbell[141].

A chemiluminescent chemical reaction can be written as follows[143]:

Equation 28

$$A + B \rightarrow P^* \rightarrow P + h\nu$$

where A and B are reactants and P is the excited state product. Three criteria need to be fulfilled for a reaction to generate light.

i) The chemical reaction must supply sufficient energy to produce an excited state.

ii) There must be a reaction path that favours production of excited state products.

iii) The excited state must be able to produce luminescence, or transfer its energy to a molecule capable of doing so.

A wide variety of chemiluminescent reactions are known, although only a limited number have been employed in analytical chemistry. CL can occur in liquids, gases and on solid surfaces. The latter two will not be discussed further in this thesis, the focus will rather be on a specific liquid-phase CL reaction, the luminol reaction. An overview of the wide array of liquid-phase CL reactions, can be found in two excellent reviews covering the field[143,144]. There are two main types of CL; *direct* or *indirect*. Direct CL occurs when the excited molecule emits light itself. In contrast, if the excited molecule transfers the excess energy to a sensitiser, which then emits light, the CL is indirect or *sensitised*. In the first case the light always has the same spectrum, while in the second case it is dependent on the properties of the sensitiser. Luminol is an example of direct mode CL and follows the general scheme outlined in Equation 28. The luminol chemiluminescence reaction is discussed in more detail in section 3.2. The peroxyoxalate chemiluminescence reaction on the other hand is an example of indirect mode CL, since the product of the primary reaction does not emit light. Instead the intermediate transfers its energy to a fluorophore (F) which becomes electronically excited and subsequently emits light as follows[145]:

Equation 29

$$\text{oxalic compound} + H_2O_2 \rightarrow \text{intermediates}$$

$$\text{intermediates} + F \rightarrow F^*$$

$$F^* \rightarrow F + h\nu$$

CL is characterised by four main parameters: light intensity, spectral characteristics, speed of light production and polarisation of light. The intensity of the light produced is

dependent on both the reaction kinetics and the efficiency in generating excited products, as described in Equation 30. The CL emission intensity, I, is directly proportional to the rate of the chemical reaction, dP/dt. ϕ_{CL} is the chemiluminescent quantum yield, defined as the number of molecules emitting light divided by the number of reacting molecules. This ratio is in turn the product of the excitation quantum yield, ϕ_{EX} (defined as the number of excited states formed per reacting molecule) and the emission quantum yield, ϕ_{EM} (defined as the number of photons emitted per excited state). As a consequence, ϕ_{CL} is sometimes referred to as the "over-all" quantum yield.

Equation 30

$$I = \phi_{CL}\, dP/dt = \phi_{EX}\, \phi_{EM}\, dP/dt$$

For chemiluminescent reactions, the quantum yield typically varies from 1 to a maximum of 34%[146], whereas bioluminescent reactions are generally more efficient and can have quantum yields close to 100%[147].

CL is, alongside mass spectrometry, immunological and radiometric methods, among the most sensitive of analytical techniques, capable of yielding detection limits (DL) in the sub-femtomole range. The low DLs are not the only attractive feature of CL methods, other advantages are the wide linear dynamic range and the simplicity of the instrumentation. A dark box with a light sensitive detector (e.g. photomultiplier tube (PMT), charged coupled device (CCD) or photo diode) is all the instrumentation that is required. Since the total amount of light emitted is of interest and the molecules are excited by chemical reactions, no monochromator or light source are required. On the other hand, a more complex flow system, containing additional flow channels might be necessary with CL. Analytical methods based on CL are designed in such a way that the

species to be determined is the limiting reactant i.e. all other reactants are added in excess. The light produced is then a function of the analyte concentration.

The disadvantages of this system include: a small, but still troublesome background emission, which varies with parameters such as pH, solvent composition and temperature. Furthermore, in most cases, the detailed reaction mechanisms are not known. This is obviously a disadvantage from an analytical point of view, as it makes it difficult to predict and control interferences. In addition, the reactions often have complex kinetics, which can lead to non-linear calibration curves. Finally, in some cases, there might be a lack of selectivity. Many CL reactions respond not only to the analyte of interest, but also to other compounds. This disadvantage can be overcome to a large extent by selective sampling, incorporation of a separation step, utilising selective reactors (e.g. immobilised enzyme reactors) or by the use of a masking agent prior to the detection step.

Different instrumental set-ups can be used. In the batch mode, all reagents are mixed in a cuvette and the light emission from the chemical reaction is measured. Since light emission varies with time, it is important to perform these experiments in a reproducible manner. Reproducibility is improved when a flow system is used. Light is measured during a short time as the liquid passes through the detector cell. Optimisation is important (especially in the case of flow systems), since only a fraction of the light is detected. In most cases collection of light should take place when the intensity is at its maximum. Consideration of the time from mixing to detection is important because the intensity of light emission from a CL reaction is transient rather than constant with time. For a CL reaction, the emission intensity I (in photons emitted per second) is directly

proportional to the rate of the chemical reaction dP/dt (in molecules reacting per second)[148],

Equation 31

$$I = \phi_{CL} (dP/dt)$$

where the proportionality constant is the chemiluminescence quantum yield ϕ_{CL} (in photons emitted per molecule reacting). Thus, as the rate of the CL reaction changes with time (due to consumption of reagents), so does the emission intensity. A plot of emission intensity versus time after reagent mixing would appear as shown in Figure 31. To maximise detector sensitivity, one needs to detect near the time of maximum emission intensity. In a flow stream the time taken from reagent mixing to the observation cell is determined by both the volume between these two points and the solution flow rate.

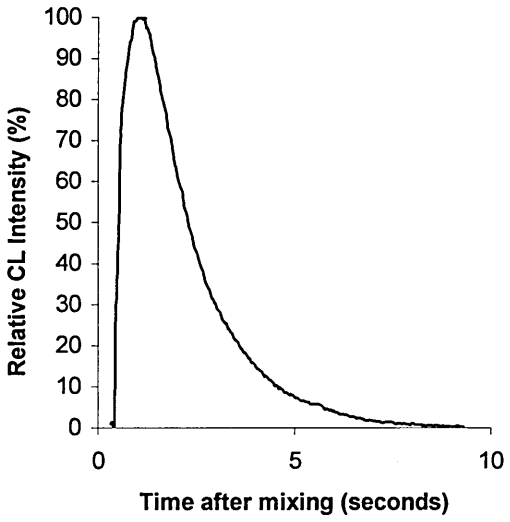

Figure 31: Transient signal of a chemiluminescence reaction.

For most CL detection systems, an eluting analyte causes the CL reaction to proceed at a faster rate than when the analyte is absent. The analyte is detected as an increase in CL emission above a very low background level (see Figure 32 A). However, in some CL detection systems, the eluting analyte interferes with or suppresses the CL reaction, in which case the analyte is detected as a valley or inverted peak, where the CL intensity decreases from a normally high background level (see Figure 32 B).

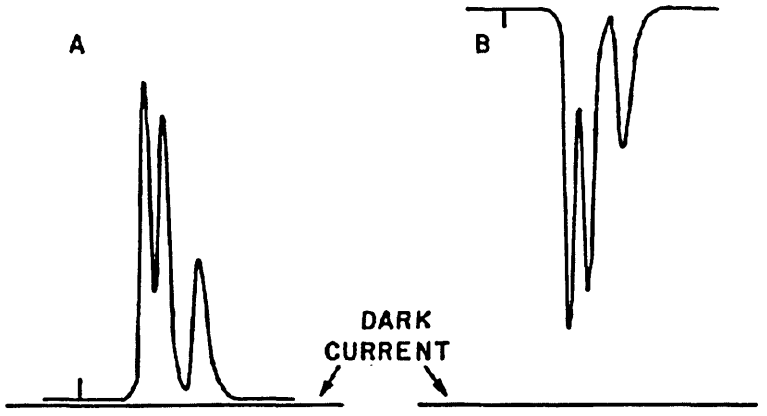

Figure 32: Possible chemiluminescence chromatograms. (A) Analyte peaks appear as signal increases from a low-level background. (B) Analyte peaks appear as signal decreases from a high background.

The luminol chemiluminescence reaction is an example of the type A detection scheme.

3.2 Luminol Chemiluminescence

Luminol (5-amino-2,3-dihydro-1,4-phthalazinedione) is one of the most commonly used CL reagents. In aqueous alkaline solution, luminol is oxidised to 3-aminophthalate with

the emission of light[149] (see Equation 32). The emission is blue, centred about 425 nm and is from excited state 3-aminophthalate[150];

Equation 32

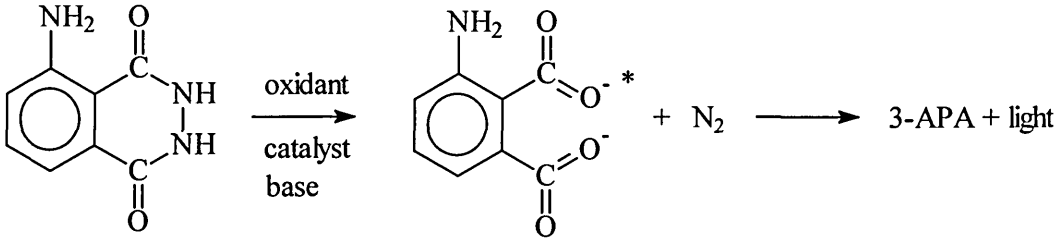

Luminol

3-aminophthalate
(3-APA)

A variety of oxidants may be used, such as permanganate, hypochlorite and iodine[149], but perhaps the most useful oxidant is hydrogen peroxide. A catalyst is required when hydrogen peroxide is used. Typical catalysts include peroxidase, hemin, transition metal ions (Co^{2+}, Cu^{2+}, Fe^{3+}, Cr^{3+}, etc.) or ferricyanide[151,152]. Thus, the luminol CL reaction system most often consists of luminol + H_2O_2 + catalyst + OH^-[153]. Within limits, the CL emission intensity is directly proportional to the concentrations of luminol, H_2O_2 and the catalyst. Thus measurements of CL intensity can be used to determine any of these species. As with most CL systems, any of the reaction components can be viewed as the analyte with the others collectively constituting the reagents. Thus, the luminol CL reaction has been used to determine catalysts or species labelled with catalysts, peroxide or species that can be converted into peroxide and luminol or species labelled with luminol.

3.3 Chemiluminescence Detection

The use of ion chromatography (IC) with chemiluminescence detection (CL) effectively eliminates the need for a derivatisation step and the detection is more selective for trivalent chromium, since this is one of the few metals that catalyse the luminol-hydrogen peroxide reaction[154]. Also, other metals which do catalyse the reaction can be masked by the addition of EDTA[155] to the eluent. The metal-EDTA complexes formed, do not then take part in the reaction. Although a Cr(III)-EDTA complex can also be formed the kinetics of its formation is much slower than for the other metal ions[156,157]. Williams et al.[158] first used this type of ion chromatography method with both an anion and a cation column in parallel in order to effect a separation. Gammelgaard et al.[77] then modified the parameters in order to use a cation-exchange guard column. This however eluted the Cr(VI) in the solvent front. Beere and Jones[159] then improved on this by using an AS4A anion exchange column from Dionex which reportedly had residual cationic groups. In this study a CS5 ion exchange column, which has both anion and cation exchange capacity, was used to separate the chromium species. This gave a good separation of both chromium forms within a reasonable time, along with good sensitivity and linearity. The column stationary phase contains both sulphonic acid (SO_3^-) and quaternary ammonium groups (N^+R_3) on a pellicular stationary phase[160] (see Figure 33). This therefore has an affinity for both the cationic Cr(III) as Cr^{3+} and for the anionic Cr(VI) as CrO_4^{2-}.

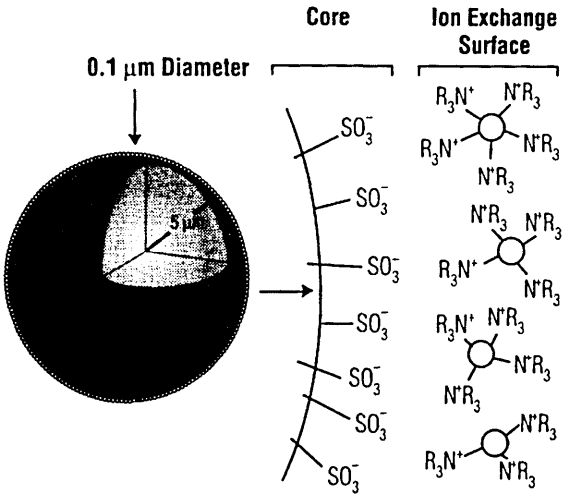

Figure 33: Pellicular anion exchange bead. Taken from Dionex catalogue[160].

Three regions exist in the ion exchange packing.

- An inert, nonporous, chemically and mechanically stable core.
- A surface sulphonated region completely covering the core.
- Outer layers of permanently attached submicron ion exchange beads where the actual chromatography takes place.

This pellicular configuration concentrates a vast number of ion exchange sites into a very narrow layer on the surface of the substrate. Thus, the packing has a high load capacity while maintaining very short diffusion paths. These features combine to give high efficiency and minimal matrix effects.

3.4 Reagents

All chemicals were obtained from Aldrich, Bornem, Belgium and were of ACS reagent grade unless otherwise stated.

Eluent: 0.6 mol L^{-1} potassium chloride [KCl] (99+%) and 0.001 mol L^{-1} EDTA (99+%) to mask any other metal ions present. The pH of the solution was adjusted to 2.5 using hydrochloric acid [HCl] sub-boiled (prepared in the laboratory). The flow rate was 1 mL min^{-1}.

Chemiluminescence reagent solution: 3.4 x 10^{-4} mol L^{-1} 3-aminophthalhydrazide [luminol] (97%), 0.1 mol L^{-1} boric acid [BH_3O_3] (99.99%) as buffer and 0.01 mol L^{-1} hydrogen peroxide [H_2O_2] (27%), Mobi-Lab, Zutendaal, Belgium. The H_2O_2 was cleaned by passing through a maxi-clean IC-Ba cartridge, Alltech, Laarne, Belgium, Cat.No. 30268 in order to remove any cationic impurities. The pH of the solution was adjusted to 11.5 with sodium hydroxide [NaOH] (98%). The flow rate was 1.8 mL min^{-1}.

Reducing solution: Initially 0.015 mol L^{-1} sodium sulphite [Na_2SO_3] was used, but subsequently all studies were carried out using 0.015 mol L^{-1} potassium sulphite [K_2SO_3] (97%). No difference was observed between the two reagents. The pH of the solution was adjusted to 3 with concentrated nitric acid sub-boiled. The flow rate was 0.5 mL min^{-1}.

Both the chemiluminescence reagent and reducing solutions were kept under a helium atmosphere in order to prevent any degradation due to oxidation by air.

Standard Solutions: Chromium(VI) standard solutions were prepared by dilution of a 1 g L^{-1} stock solution prepared by dissolving 3.735 g of potassium chromate [K_2CrO_4] (99.7%) in 1 litre of water. Chromium (III) standard solutions were prepared by dilution of a 1 g L^{-1} stock solution prepared by dissolving 7.695 g of chromium(III)nitrate nonahydrate [$Cr(NO_3)_3.9H_2O$] (99.99+%) in 1 litre of water. All solutions were prepared using ultrapure 18MΩ deionised water obtained from a MilliQ plus 185 system (Millipore, Milford, MA, USA).

Interferences: Magnesium nitrate hexahydrate [$Mg(NO_3)_2.6H_2O$] (99%); zinc nitrate hexahydrate [$Zn(NO_3)_2.6H_2O$] (98%); calcium nitrate tetrahydrate [$Ca(NO_3)_2.4H_2O$] (99%), iron(II)sulphate heptahydrate [$FeSO_4.7H_2O$] (98+%); aluminium nitrate nona-hydrate [$Al(NO_3)_3.9H_2O$] (98+%); manganese(II)nitrate hexahydrate [$Mn(NO_3)_2.6H_2O$] (98%); nickel(II)nitrate hexahydrate crystal [$Ni(NO_3)_2.6H_2O$]; copper(II) nitrate hemipentahydrate [$Cu(NO_3)_2.2.5H_2O$] (98+%); cobalt(II)nitrate hexahydrate [$Co(NO_3)_2.6H_2O$] (98+%); iron(III)nitrate nonahydrate [$Fe(NO_3)_3.9H_2O$] (98+%).

3.5 Instrumentation

3.5.1 Ion Chromatography (IC) System

A metal free Dionex DX500 Chromatography System (Dionex n.v., Mechelen, Belgium) was used incorporating Peaknet control and utilising Dionex Peaknet integration software (see Figure 34). A GP40 Gradient Pump with vacuum degasser was used to pump the eluent through the column at 1 mL min^{-1}. An Ismatec peristaltic pump (Zürich, Switzerland) was used to add the reducing solution at a flow of 0.5 mL min^{-1} and a post column reagent delivery module (Dionex PC10 pneumatic controller) added the chemiluminescence reagent at a flow of 1.8 mL min^{-1}. Injection was carried out using an AS3500 autosampler (Dionex). The injection volume was 50 µL. The separation column was a Dionex Ionpac CS5 4 x 250mm analytical column. PEEK tubing and connectors were used throughout. A 375 µL knitted reaction coil enabled thorough mixing of the reducing solution and the effluent from the column after separation. This ensured complete reduction of Cr(VI) to Cr(III). A Foxy 200 fraction collector (ISCO, Belgium) was also connected after the detector. This enabled the collection of fractions eluting from the column for further analysis by ICP-MS or ETAAS.

3.5.2 Chemiluminescence Detector (CL)

A Jasco FP920 Intelligent Fluorescence detector with chemiluminescence option (Jasco Corporation, Tokyo, Japan) incorporating a flat wound PTFE cell with reflective back-plate in order to direct the maximum amount of light emitted towards the photo multiplier tube which was placed end on to the cell, was used.

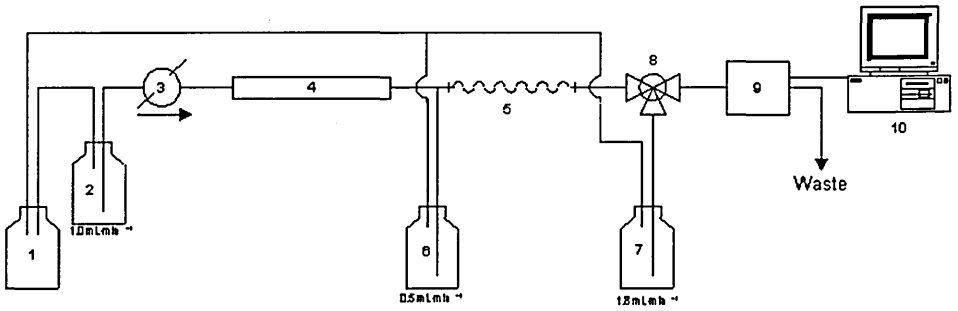

1 Helium
2 Eluent (KCl,EDTA)
3 Injection port
4 Analytical column(CS5)
5 Mixing coil (375µL)
6 Reducing Solution (K_2SO_3)
7 Chemiluminescence reagent (luminol, H_2O_2)
8 Mixing tee
9 Chemiluminescence detector
10 Data processor (Computer)

Figure 34: Schematic diagram of the ion chromatograph with chemiluminescence detection.

A peristaltic pump was used to deliver the reducing solution at a flow rate of 0.5 mL min^{-1}. High pump speed and a small internal diameter (i.d.) of the tubing, 90 rpm and 0.51 mm respectively, were used in order to reduce pump pulsation. High pump speeds reduce the lifetime of the tubing and it is essential that the tubing is replaced regularly so that the flow rate is not altered.

3.5.3 Electro Thermal Atomic Absorption Spectrophotometer (ETAAS)

Validation of the results obtained by IC-CL was carried out by ETAAS. The instrument used for all ETAAS analysis was a Perkin Elmer 5100PC atomic absorption

spectrophotometer with Perkin Elmer 5100ZL Zeeman furnace module (Perkin Elmer, Beaconsfield, Bucks, UK). The furnace program used is shown in Table 20. A chromium hollow cathode lamp was used at a wavelength of 357.9 nm. A 15 µg addition of magnesium nitrate ($Mg(NO_3)_2$) modifier was also used in order to ensure complete atomisation of the different species of chromium.

Table 20: Graphite furnace operating parameters.

Step	Temperature (°C)	Ramp Time (seconds)	Hold Time (seconds)
1 : Drying	110	1	30
2 : Drying	130	5	40
3 : Ashing	1500	10	20
4 : Atomisation	2300	0	5
5 : Cleaning	2400	1	2

3.5.4 Inductively Coupled Plasma - Mass Spectrometer (ICP-MS)

The ICP-MS instrument used was a Fisons PQ2+ quadrupole instrument with a micro concentric nebuliser, for sample introduction at a flow rate of 50 µL min^{-1}, and a Meinhard concentric ICP torch with a double pass spray chamber and recirculating pump (Micromass Int., Manchester, UK). See Table 21 for operating conditions. The ICP-MS instrument was used to investigate the elemental content of liquid aliquots collected after samples were run through the IC-CL instrument.

Tuning of this instrument was carried out daily using a multielement standard (Merck, Darmstadt, Germany) containing Be, Mg, Co, In, Ce, Tm, Pb and U at a concentration of 10 µg L^{-1} in 2% nitric acid. The determination of chromium was carried out at m/z

values of 52 and 53. Although 53 has a lower abundance it also suffers much less from interferences, especially from Ar-C (see Table 5). This was an important consideration here as there is likely to be a considerable amount of carbon present in the extracted soil samples. Relative abundances are shown below:

m/z	Chromium	Ar-C
52	83.79%	98.5%
53	9.50%	1.10%

Table 21: ICP-MS operating conditions.

Parameter	Setting
Forward Power	1400 watts
Reflected Power	0 watts
Torch	Meinhard Concentric Torch
Spray Chamber	Double Pass
Nebuliser	Micro Concentric
Sample introduction	Peristaltic pump
Solution uptake rate	50 µL min^{-1}
Coolant gas flow rate	15 L min^{-1} Argon
Nebuliser gas flow rate	0.7 L min^{-1} Argon
Nebuliser gas pressure	207 Pa (30 psi)
Sample cone material	Nickel
Skimmer cone material	Nickel
No. of sweeps per replicate	50
No. of replicates	6
Masses	^{52}Cr ^{53}Cr
Measurement mode	Peak jumping
Integration time	3 s
Detector mode	Pulse counting

3.5.5 Filtration

Filtration of samples was carried out using 0.45 μm cellulose acetate sterile syringe filters (Alltech, Lokeren, Belgium).

3.6 Procedure

A schematic diagram of the analytical arrangement can be seen in Figure 34. All samples were filtered through 0.45 μm cellulose acetate sterile syringe filters prior to injecting 50 μL onto the column. The column separation of Cr(III) and Cr(VI) is then followed by reduction of Cr(VI) to Cr(III) by sodium sulphite. The chemiluminescence reagent was added, at an optimised distance, just before the detector. The retention times for the Cr(VI) and Cr(III) were 2.5 and 6.2 minutes respectively. All analyses were performed in triplicate. Standards and samples were stored in PTFE containers, as it was found that storage in glass caused the Cr(III) concentration to decrease due to adsorption on the surface (see section 3.7.6).

3.7 Results and Discussion

3.7.1 Trial of AS4A Column

The properties of the columns tested are shown in Table 22. These columns were used in combination or singularly in order to influence the position and resolution of the peaks eluted.

Table 22: Information and specifications for columns tested.

Column	Dimensions (mm)	Functional Group(s)	Type of ion exchange
CS5 Analytical	4 x 250	Sulphonic acid and quaternary ammonium	Cation and some anion
CG5 Guard	4 x 50	Sulphonic acid and quaternary ammonium	Cation and some anion
AS4A Analytical	4 x 250	Alkyl quaternary ammonium	Anion
AG4A Guard	4 x 50	Alkyl quaternary ammonium	Anion

The following column combinations were tested: CG5 + CS5, CG5 + AS4A, AG4A + AS4A, CS5 alone and AS4A alone. The AS4A column was first used for chemiluminescence analysis of chromium by Beere and Jones[159], however the results reported by the authors could not be repeated here. The authors reported that Cr(VI) was eluted first on the AS4A column, but Cr(VI) is likely to be present as CrO_4^{2-} or $Cr_2O_7^{2-}$, and Cr(III) as Cr^{3+}. Since this is an anion exchange column, the Cr(VI) species would have more affinity for the stationary phase and therefor be retained for longer. Chromatograms of the individual species (See Figure 35 to Figure 37) confirm that Cr(III) is eluted first, and in fact in the solvent front, i.e. showing no affinity for the stationary phase.

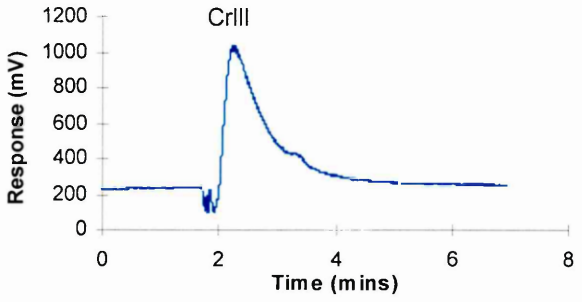

Figure 35: Chromatogram of Cr(III) 20 μg L^{-1} using an AS4A Column and IC-CL detection.

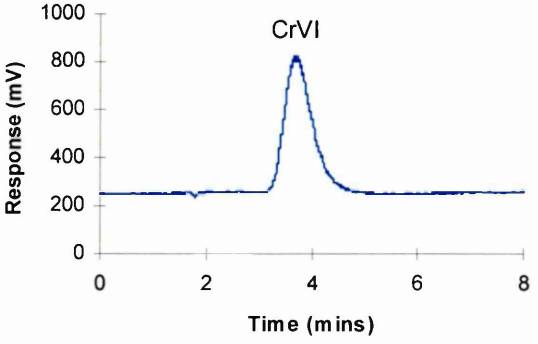

Figure 36: Chromatogram of Cr(VI) 10 μg L^{-1} using an AS4A Column and IC-CL detection.

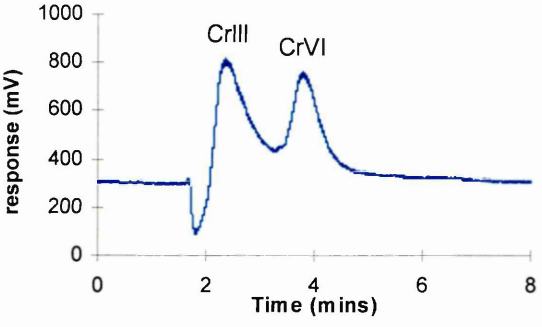

Figure 37: Chromatogram of Cr(III) 10 μg L^{-1} & Cr(VI) 5 μg L^{-1} using an AS4A Column and IC-CL detection.

The explanation given for the order reversal was that there were residual cationic groups present. However it appears somewhat remarkable that an anion exchange column with residual cationic groups should delay a cationic peak for more than seven minutes and until after the anion peak.

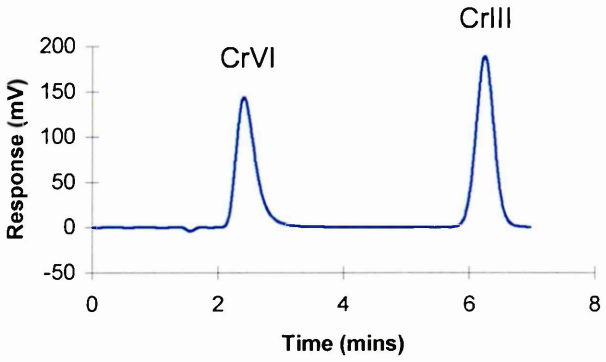

Figure 38: Chromatogram of CrIII/VI 10 µg L^{-1} in 0.6 mol L^{-1} KCl mobile phase using a CS5 Column and IC-CL detection.

Excellent resolution of the two chromium species was obtained with the CS5 column, which contains both cationic and anionic groups (see Figure 38). The calibration graph was found to be linear over more than 3 orders of magnitude (from 0.01 to 50 µg L^{-1}) as shown in Figure 39.

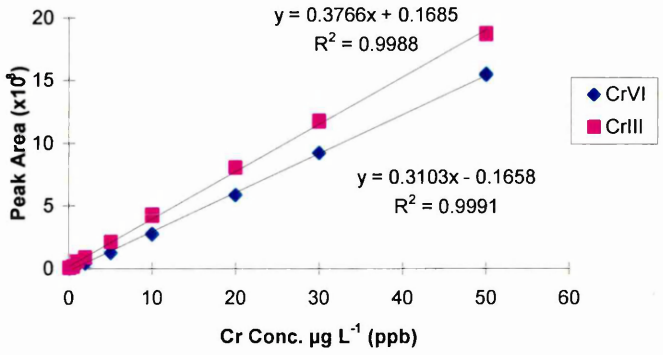

Figure 39: Optimised CrIII/VI calibration from 0.01 to 50 µg L^{-1} by IC-CL using a CS5 column and 0.6 mol L^{-1} KCl mobile phase.

3.7.2 Univariate Optimisation

In order to optimise the chemiluminescence signals the effect of the following conditions were investigated: flow rates of luminol and reducing solution; pH of luminol and reducing solution; concentration of luminol, reducing solution and EDTA; point of luminol introduction and type of mixing coil used.

A comparison was also carried out between the classic univariate optimisation procedure and that of multivariate data analysis using an experimental modelling program. Multivariate data analysis is a powerful optimisation technique when there are interactions between experimental variables. In the classic univariate approach, interactions between variables cannot be allowed for without unreasonable numbers of experiments. In contrast, when using multivariate data analysis these interactions are taken into account without having to perform a large number of experiments.

3.7.2.1 Introduction of Luminol

In order to obtain the maximum amount of light emitted and therefore the best sensitivity the time at which the luminol is added before the detector is critical. This is an important consideration since chemiluminescent reactions and therefore signals are transient and not constant with time[161]. The chemiluminescence reaction will not have had time to reach completion if the luminol is introduced at a point too close to the detector. The maximum signal intensity will also be missed if the distance chosen is too far from the detector. Three different lengths of tubing were tested (5, 27 and 53 cm) with a Cr(VI) concentration of 1 mg L^{-1} in order to vary the time that the luminol reaction had before the detector. The results are shown in Figure 40. As can be seen, the

optimum time before the detector at which to add the luminol was found to be 31 seconds (27 cm of PEEK tubing with an internal diameter of 0.50 mm).

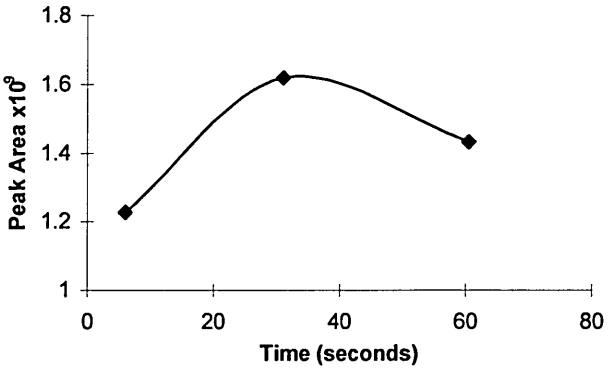

Figure 40: Effect of varying luminol addition time before detector.

3.7.2.2 Luminol Flow Rate

The flow rate of the luminol solution was varied in order to optimise the rate at which the maximum signal for both Cr(III) and Cr(VI) was obtained. The flow had to be such that there was an excess of luminol solution thereby enabling complete reaction of the chromium present, but making sure that excessive dilution did not cause a reduction in signal intensity. Another important consideration was that too large sample 'plugs' could result in double peaks if there was insufficient mixing. Flow rates of 1.2, 1.65, 2.0 and 2.4 mL min^{-1} were tested using a CrIII/VI concentration of 1 mg L^{-1}. As can be seen in Figure 41 the optimum flow rate was found to be 1.8 mL min^{-1}.

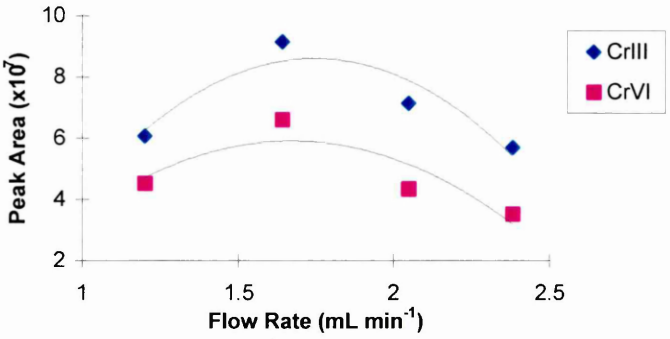

Figure 41: Effect of luminol flow rate on the chemiluminescence signal intensities of Cr(III) (♦)and Cr(VI) (■).

3.7.2.3 Reducing Solution Flow Rate

The reducing solution flow rate was optimised in order to obtain a quantitative reduction of the Cr(VI) into Cr(III). Chromium(III) is the species which takes part in the luminol-hydrogen peroxide reaction as a catalyst and therefore any Cr(VI) which is not reduced will not be detected.

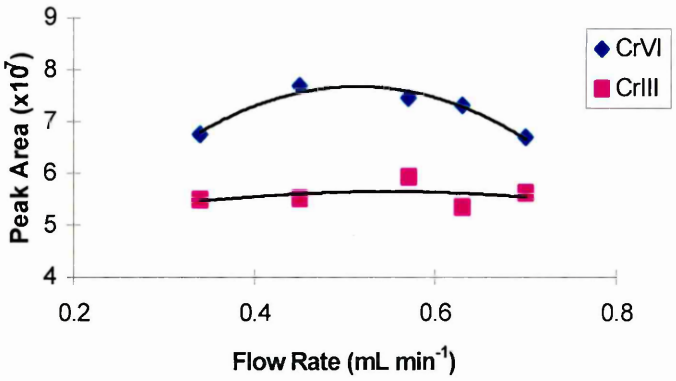

Figure 42: Effect of reducing solution flow rate on the Cr(VI) (♦)and Cr(III) (■) chemiluminescence signals.

In order to achieve quantitative reduction it is important to have thorough mixing of the reducing solution with the effluent from the column, hence this was also studied (see below). For the flow rate optimisation several different flow rates were used and a 5 μg L^{-1} CrIII/VI standard. The results show that the flow rate giving the best (i.e. highest) peak areas for the sample used was at 0.5 mL min^{-1} (see Figure 42).

3.7.2.4 Reducing Solution Mixing

It was important to have thorough mixing of the effluent from the column and the reducing solution in order to effect complete reduction of the Cr(VI) to Cr(III). Two mixing coils were tested; a 375 μL knitted coil (knit) and a 500 μL beaded coil (bead). Using a Cr(VI) standard of 500 μg L^{-1} the results obtained (see Figure 43) showed that the best mixing was obtained using the 375 μL knitted coil. No broadening of the peaks was observed when a coil was inserted in the reaction manifold, but better peak heights and therefore sharper, well-resolved peaks were obtained.

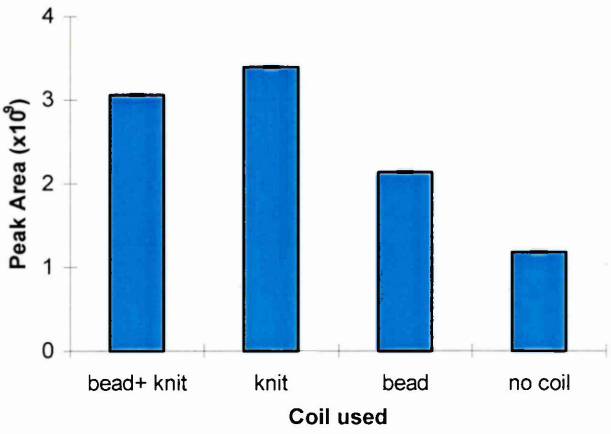

Figure 43: Effect of reducing solution mixing on the chemiluminescence signal intensity.

3.7.2.5 Reducing Solution Concentration

The concentration of potassium sulphite required to give the maximum reduction of Cr(VI) to Cr(III) was also optimised. Concentrations of 0.008, 0.015, 0.03 and 0.06 mol L^{-1} were tested. A concentration of 0.015 mol L^{-1} as shown in Figure 44 gave the maximum signal. It is interesting to note that the reducing solution concentration also affects the Cr(III) peak area. This could be due to the reduction of Cr(III) to Cr(II).

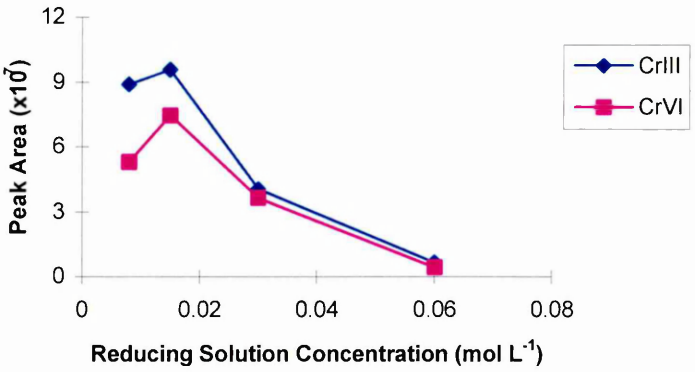

Figure 44: Effect of varying the reducing solution concentration on the Cr(III) (♦)and Cr(VI) (■) chemiluminescence signals.

3.7.2.6 EDTA

Two different concentrations of EDTA were tested: 0.01 mol L^{-1} and 0.001 mol L^{-1}. No difference was observed in peak areas, however it was decided to use 0.001 mol L^{-1} since the 0.01 mol L^{-1} gave a higher background signal.

3.7.3 Conclusions of Univariate Optimisation

The optimised conditions found using the univariate method of optimisation were as shown in Table 23:

Table 23: Univariate optimised conditions.

Parameter	Optimised conditions
Introduction of luminol before detector	31 secs (27 cm of 0.5 cm i.d. tubing)
Luminol flow rate	1.8 mL min^{-1}
Reducing solution flow rate	0.5 mL min^{-1}
Reducing solution mixing	375 µL knitted coil
Reducing solution concentration	0.015 mol L^{-1}
EDTA concentration	0.001 mol L^{-1}

3.7.4 Multivariate Optimisation

Traditionally a univariate optimisation approach is applied in order to obtain an optimised output[162] (e.g. peak area, yield, response etc.). Variables are optimised individually whilst keeping other variables fixed. This approach to optimisation involves a large number of experiments. A more fundamental problem with this type of optimisation is that it assumes that the factors are *independent*. This assumption is not always true.

Multivariate optimisation uses the principles of chemometrics, a discipline in which mathematical and statistical approaches are used to determine parameters that would otherwise be very difficult to measure[163]. Methods of statistical experimental designs have evolved since the pioneering work of Fisher in 1926. These methods, further refined by Box, Hunter & Hunter[162], Scheffé, Tagushi and others[164-167], provide the users with a powerful technique for efficient experimentation. This type of optimisation

involves the use of an experimental design program followed by a multivariate data analysis, enabling the maximum amount of information to be extracted from the fewest number of experimental runs. This is possible by varying all the relevant factors at the same time and then connecting the results using a mathematical model. The model can be used for the interpretation, prediction and optimisation of the experimental conditions. The following information can be obtained from the use of such a model:

- factors that influence the signal responses
- factors with significant interactions (whether positive or negative)
- the best experimental settings to achieve the optimum conditions for the best performance
- the predicted values of the responses for given experimental settings of the factors.

The stages of a multivariate approach to optimisation involve the following steps:

1. Identification of factors to be investigated.
2. Screening to identify which of these factors are important.
3. Full experimental (quadratic) model using only the critical factors in order to find the optimum experimental settings to be used.

Screening is the first stage of an investigation where the goal is to identify the critical factors. A critical factor is one that causes substantial changes (effects) in the response when it varies. At the screening stage simple models (linear or linear with interactions), and experimental designs that allow the identification of the factors with the largest effects in the fewest possible number of experimental runs are used. This can be carried out by the use of full factorial, fractional factorial, L-designs, Plackett-Burman or D-optimal designs. Full and fractional factorial designs were used in this study and will therefore be discussed further in sections 3.7.4.1 and 3.7.4.2 respectively.

After screening, the goal of an investigation is usually to approximate the response by a quadratic polynomial (model) in order to:

- understand in more detail how the factors influence the response
- make predictions, optimise or find a region of operation.

This can be carried out by use of a three-level full factorial, central composite (CCC and CCF), Box Behnken or D-optimal design. The central composite design was used in this study and is described in more detail in section 3.7.4.3.

3.7.4.1 Factorial Designs

Single factor designs with one or more blocking factors are useful when one particular parameter is of more interest than the others, however when the effects of more than one parameter are of equal importance then factorial designs with more than one factor are employed.

These designs require an experiment to be carried out at all possible combinations of the levels of each of the factors considered. A two level, three factor design is represented as 2^3 and involves investigation of three different factors, each at two levels i.e. high and low levels for each factor. This requires 8 experiments, i.e. 2 x 2 x 2, and can be shown diagrammatically in Table 24, where + represents a high value and - a low value, A, B and C represent the three factors and y represents the response.

Table 24: Design matrix for a full factorial 2^3 design.

Run	A	B	C	Response
1	+	+	+	y_1
2	+	+	-	y_2
3	+	-	+	y_3
4	+	-	-	y_4
5	-	+	+	y_5
6	-	+	-	y_6
7	-	-	+	y_7
8	-	-	-	y_8

A 3^4 design on the other hand involves four factors at 3 levels and requires 81 experiments (3 x 3 x 3 x 3). The experiments are carried out in a random manner in order not to generate artefacts in the conclusions.

If we consider factor A in Table 24; in experiments 1 and 5 the levels of B and C are the same, but A is at the + and - level respectively. The difference between y_1 and y_5 is therefore an estimate of the effect of A when B and C are both at the + level. The difference between y_4 and y_8 is an estimate of the effect of A when B and C are both at the - level. In total four estimates of the effect of A can be obtained and the average effect of A can therefore be estimated as:

Equation 33

$$\text{Effect A} = [(y_1-y_5)+(y_2-y_6)+(y_3-y_7)+(y_4-y_8)]/4$$

or $$\text{Effect A} = [(y_1+y_2+y_3+y_4)-(y_8+y_5+y_6+y_7)]/4$$

i.e. $$\text{Effect A} = (\Sigma \text{ positive level runs} - \Sigma \text{ negative level runs})/4$$

In general, for k factors one can write:

Equation 34

$$\text{Effect A} = (\Sigma \text{ positive level runs} - \Sigma \text{ negative level runs})/(2^{k-1})$$

For a 3 level design 2^{k-1} becomes 2^k. From these results it can be seen whether the effect of A on the response is positive or negative.

The interaction effects can be estimated in the same way. If we compare the effect from y_1-y_5 and from y_3-y_7 we can see that both differences estimate the effect of A at the same (+) level of C. However the former does this at the + level of B and the latter at the - level. This interaction effect can then be estimated as:

Equation 35

$$\text{Interaction of B on A} = [(y_1-y_5)-(y_3-y_7)]/2 = [(y_1+y_7)-(y_3+y_5)]/2$$

This is the same for the interaction of A on B:

Equation 36

$$\text{Interaction of A on B} = [(y_1-y_3)-(y_5-y_7)]/2 = [(y_1+y_7)-(y_3+y_5)]/2$$

It can be verified that, at the lower value of C, a second estimate of the AxB interaction can be obtained by:

Equation 37

$$\text{AxB} = [(y_2+y_8)-(y_6+y_4)]/2$$

Averaging the two estimates gives:

Equation 38

$$\text{AxB} = [(y_1+y_2+y_7+y_8)-(y_3+y_4+y_5+y_6)]/4$$

All the interactions for all the factors can be written down in this way. Interactions between three or more factors can also be estimated in the same way.

When there is any possibility of an interaction between factors, an experimental design, such as a factorial design, is required which will estimate both the main effects and the interactions.

3.7.4.2 Fractional Factorial Designs

In a full factorial design the number of experiments increases exponentially with the number of factors, k. For a 2^k design, where $k = 2$, 3, 4 or 7, the number of experiments required is 4, 8, 16 and 128 respectively[168]. The 128 experiments of the 7 factor factorial design are used to estimate the mean value, 7 main effects and 21 two-factor, 35 three-factor, 35 four-factor, 21 five-factor, 7 six-factor and 1 seven-factor interactions. If we consider the interactions between three or more factors to be negligible then the number of experiments can be reduced, by taking one half, one quarter, one eighth etc. of the original full factorial design. These types of designs are referred to as fractional factorials.

The designs must be balanced and chosen so that the experiments map the experimental domain as well as possible and orthogonality is preserved. A 2^{3-1} factorial design is shown in Table 25. It consists of only half of the experiments of the 2^3 design shown in Table 24. The 2^{3-1} design can be considered as $2^2 = 2 \times 2 = 4$ experiments instead of the $2 \times 2 \times 2 = 8$ experiments in the full 2^3 design.

Table 25: A 2^{3-1} fractional factorial design.

Run	A	B	C	Response
1	+	+	+	y_1
2	-	+	-	y_2
3	+	-	-	y_3
4	-	-	+	y_4

The experiments in this design are located such that they describe a tetrahedron, see Figure 45, which is the most efficient way of mapping the experimental domain with only 4 experiments. Each factor is twice at the + level and twice at the - level, so that a balanced design results.

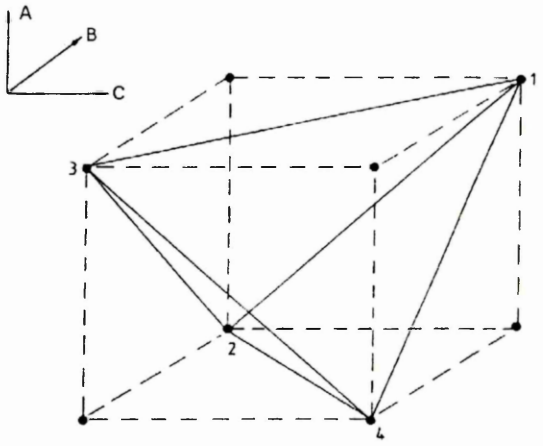

Figure 45: A half replica of a three factor design (2^{3-1} design). Adapted from Massart et al.[169].

3.7.4.3 Central Composite Designs

Another way to overcome the problem of the increasing number of experimental runs required for a full factorial design with three levels is to use a central composite design. This type of design was first introduced by Box and Wilson, who added star designs to

2^f factorials (where f is the number of factors). Central composite designs always consist of the following three parts:

1. A two-level factorial design. In Table 26 the first four experiments constitute a full 2^2 design.
2. A star design. This adds more points in order to be able to describe curvature. In Table 26 points 5-8 are the star points, these are positioned at a distance α from the centre of the design.
3. The centre point. This is often replicated in a design. For this reason it is designated as 9 etc. in Table 26.

Table 26: A two-factor central composite design.

Run	x_1	x_2
1	1	-1
2	+1	-1
3	-1	+1
4	+1	+1
5	$-\sqrt{2}$	0
6	$+\sqrt{2}$	0
7	0	$-\sqrt{2}$
8	0	$+\sqrt{2}$
9 etc.	0	0

Three types of central composite designs are possible. The design is termed *central composite circumscribed* (CCC) when the distance from the centre α for the star points is larger than one. When the star points are located within the boundaries of the factorial, i.e. $\alpha < 1$, then the design is a *central composite inscribed* (CCI). Finally when $\alpha = 1$ then the design is *central composite face-centred* (CCF). This is the type of design shown in Figure 46.

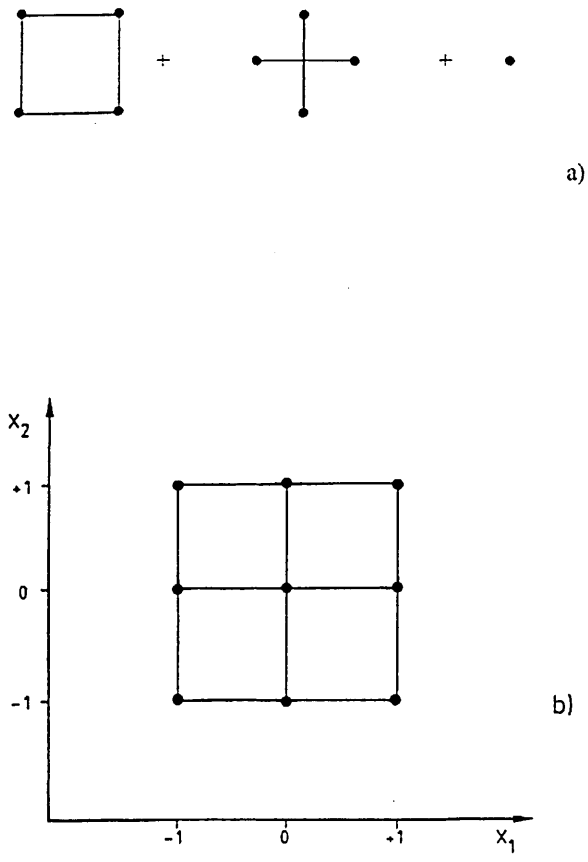

Figure 46: Two-factor central composite design. (a) The individual components of the design i.e. a 2^2 factorial design, a star design and the centre point. (b) The composite design. Adapted from Massart et al.[169].

Central composite designs are useful in that they do not require an excessive number of runs. Designs based on complete factorial designs require at least $2^f + 2^f + 1$ runs. They can also be carried out based on fractional factorial designs. The minimum number of experimental runs required for a given number of factors by 3^f factorial designs and central composite designs is shown in Table 27. This table shows that composite designs can achieve a great saving in the number of experimental runs required, especially when the number of factors is large.

Table 27: Comparison of full factorial and central composite designs. Taken from Morgan[170].

Number of factors f	Treatment combinations	
	Three level factorials 3^f	Composite $2^f + 2^f + 1$
2	9	9
3	27	15
4	81	25
5	243	43
5	81 (1/3 fraction)	27 (1/2 fraction)
6	729	77
6	243 (1/3 fraction)	45 (1/2 fraction)

3.7.4.4 Linear and Quadratic Response Surfaces

Designs at two levels can describe only lines or planes. Designs with three or more levels however can produce curves and from these curves a response surface can be produced. A response surface can be defined as a graph of a response as a function of one or more factors[171]. In general, one has a choice between mechanistic and empirical modelling. Mechanistic models, such as with the Beer-Lambert spectrometric law ($A = \varepsilon bc$), have well understood relationships between the response and the variable(s), whereas models that are empirical in nature have poorly understood relationships and have to be modelled by developing general rules. In the context of experimental design, empirical models are almost always used and the models are mainly second order i.e. quadratic. For a single factor, first order model the equation will be as follows:

Equation 39

$$\eta = \beta_0 + \beta_1 x_1$$

where η is the dependent variable e.g. response, β_0 is the y intercept at factor level $x_1 = 0$, β_1 is the straight line slope for factor x_1. This is the same as the expression $y = mx+c$.

For a quadratic model, the equation must include a constant term, first and second order terms and the interaction between factors (usually limited to two-factor interactions). For two variables, the model can be represented as:

Equation 40

$$\eta = \beta_0 + \beta_1 x_1 + \beta_2 x_2 + \beta_{11} x_1^2 + \beta_{22} x_2^2 + \beta_{12} x_1 x_2$$

This equation now includes an effect due to a second factor x_2 and a second-order interaction term ($\beta_{12} x_1 x_2$). The design leads to the estimation of the β-coefficients, by *b*-values, resulting in the following equation:

Equation 41

$$y = b_0 + b_1 x_1 + b_2 x_2 + b_{11} x_1^2 + b_{22} x_2^2 + b_{12} x_1 x_2$$

where y is the response. For three variables the quadratic equation becomes:

Equation 42

$$y = b_0 + b_1 x_1 + b_2 x_2 + b_3 x_3 + b_{11} x_1^2 + b_{22} x_2^2 + b_{33} x_3^2 + b_{12} x_1 x_2 + b_{13} x_1 x_3 + b_{23} x_2 x_3$$

Equation 42 now includes a third factor x_3 and three interaction terms ($b_{12} x_1 x_2$, $b_{13} x_1 x_3$ and $b_{23} x_2 x_3$). The *b*-coefficients are given by:

Equation 43

$$b = (X^T X)^{-1} X^T y$$

where b is the column vector of coefficients, y is the column vector of n measurements, X is the *independent variable matrix*, sometimes called *model matrix* and X^T is the transpose of X. When the *b*-coefficients have been obtained by multiple regression they can be used to predict the response y as a function of the *x*-factors. This leads to the

construction of so-called *response surfaces* of the type shown in Figure 47 for two factors.

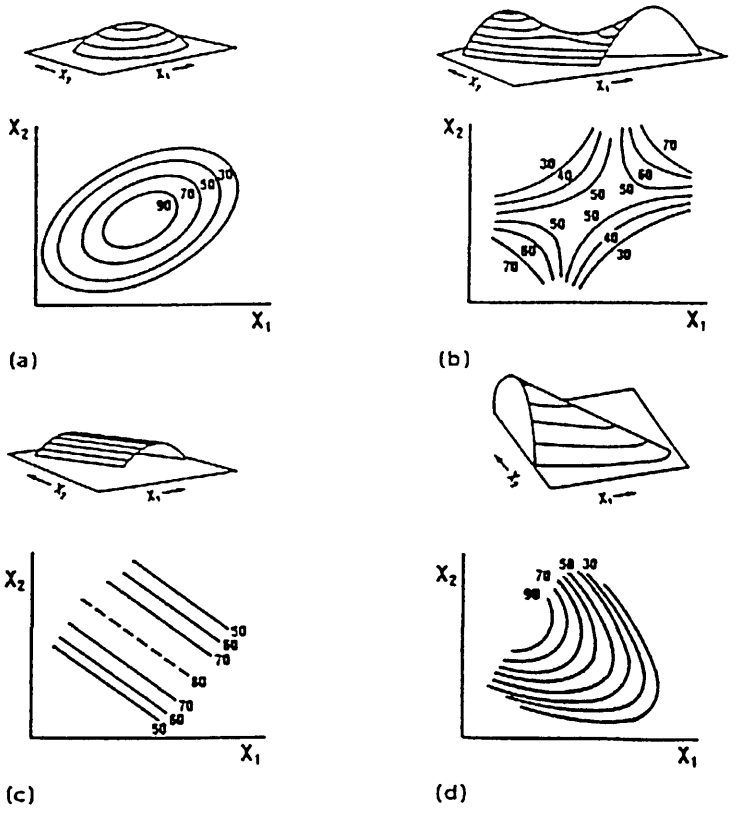

Figure 47: Some examples of contour plots and response surfaces for quadratic 2 factor designs. Taken from Massart et al.[169].

These response surfaces are very attractive descriptions for systems in which two or more variables are important. It is generally necessary to utilise a computer program in order to produce such diagrams.

In this work the computer program used was the Umetri Modde 4.0. Screening was carried out using a linear model fractional factorial design, after which a quadratic model central composite design was utilised which enables response areas to be

expressed. The interactions between several different experimental parameters can be studied using this model[172].

Initially seven parameters were chosen which were thought to be important in determining the optimum amount of light released by the chemiluminescence reaction and the initial screening model was applied. Once this had been completed the results were studied and then the four parameters which were seen to have the most significant effect were taken through a full experimental model.

3.7.4.5 Initial Screening

For each parameter three levels corresponding to high, middle and low values were chosen for use in the computer model (see Table 28).

Table 28: Parameters used for initial screening.

Parameter	Units	High	Middle	Low
Tube length (between luminol addition and detector)	cm	53	27	5
Luminol flow rate	mL min^{-1}	2.4	2.0	1.6
Luminol pH	units	12.5	11.5	10
Luminol concentration	mol L^{-1}	$7x10^{-4}$	$3.4x10^{-4}$	$1x10^{-4}$
Reducing solution flow rate	mL min^{-1}	0.7	0.5	0.3
Reducing solution pH	units	5	3	1
Reducing solution concentration	mol L^{-1}	0.020	0.015	0.010

The tube length before the detector, along with the flow rates are critical for obtaining the maximum signal output. Therefore it is important that these parameters are at their true optimum so that the maximum amount of light falls on the detector.

High, low and middle values for each parameter were entered into the linear program and an experimental model was then produced. This detailed the conditions of each of the experiments to be carried out as shown in Table 29.

The aim of carrying out an initial screening process is to find out which factors are important. This approach is used at the beginning of an investigation in order to reduce the number of variables to those with the largest effect on the response and to modify their ranges if necessary. For this study, a linear model fractional factorial design was used which is a balanced subset of the full factorial design.

Table 29: Results from the initial screening.

Expt No.	Run order	Variables							Responses ($x10^6$)	
		TL cm	LF mL min^{-1}	LpH	LC mol L^{-1}	RSF mL min^{-1}	RSpH	RSC mol L^{-1}	Cr(III)	Cr(VI)
1	8	5	1.6	10	0.0001	0.3	1	0.01	0	0
2	14	53	1.6	10	0.0001	0.7	1	0.02	0	0
3	9	5	2.4	10	0.0001	0.7	5	0.01	10.9	5.2
4	2	53	2.4	10	0.0001	0.3	5	0.02	20.5	13.8
5	18	5	1.6	12.5	0.0001	0.7	5	0.02	242.9	189.3
6	3	53	1.6	12.5	0.0001	0.3	5	0.01	0.6	0
7	10	5	2.4	12.5	0.0001	0.3	1	0.02	229.9	196.5
8	4	53	2.4	12.5	0.0001	0.7	1	0.01	46.8	35.9
9	19	5	1.6	10	0.0007	0.3	5	0.02	36.8	31.4
10	6	53	1.6	10	0.0007	0.7	5	0.01	52.5	40.9
11	16	5	2.4	10	0.0007	0.7	1	0.02	0	0
12	17	53	2.4	10	0.0007	0.3	1	0.01	0	0
13	12	5	1.6	12.5	0.0007	0.7	1	0.01	100.9	17.6
14	13	53	1.6	12.5	0.0007	0.3	1	0.02	10.7	0
15	1	5	2.4	12.5	0.0007	0.3	5	0.01	222.7	158.0
16	5	53	2.4	12.5	0.0007	0.7	5	0.02	25.2	15.2
17	7	29	2.0	11.25	0.0004	0.5	3	0.015	212.7	180.8
18	15	29	2.0	11.25	0.0004	0.5	3	0.015	219.2	178.1
19	11	29	2.0	11.25	0.0004	0.5	3	0.015	224.7	180.0

TL = tube length, LF = luminol flow rate, LpH = luminol pH, LC = luminol concentration, RF = reductant solution flow rate, RpH = reductant solution pH, RC = reductant solution concentration, responses for Cr(III) and Cr(VI) were measured as peak area in arbitrary units.

As can be seen from Figure 48 the fit is reasonably close to 1 (i.e. a good fit), but it could be closer. This means that the model may not accurately predict the optimum. In order to improve this, the individual values were investigated to see if there were any

outliers. A good model should have R^2 and Q^2 values greater than 0.7 and as close to 1 as possible.

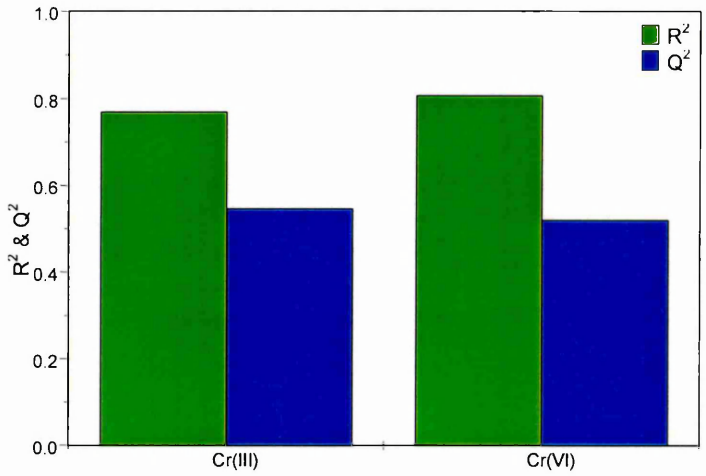

Figure 48: Summary of fit plot (with outliers).

R^2 is the fraction of variation of the response explained by the model according to:

Equation 44

$$R^2 = \frac{SS_{REG}}{SS}$$

SS_{REG} = the sum of squares of Y corrected for the mean, explained by the model.

SS = the total sum of squares of Y corrected for the mean.

Q^2 on the other hand is the fraction of variation of the response that can be predicted by the model, according to:

Equation 45

$$Q^2 = 1 - \frac{PRESS}{SS}$$

PRESS = the prediction residuals sum of squares.

From Figure 49 we can see that both result numbers 13 and 7 are not very close to the line of predicted values from the model.

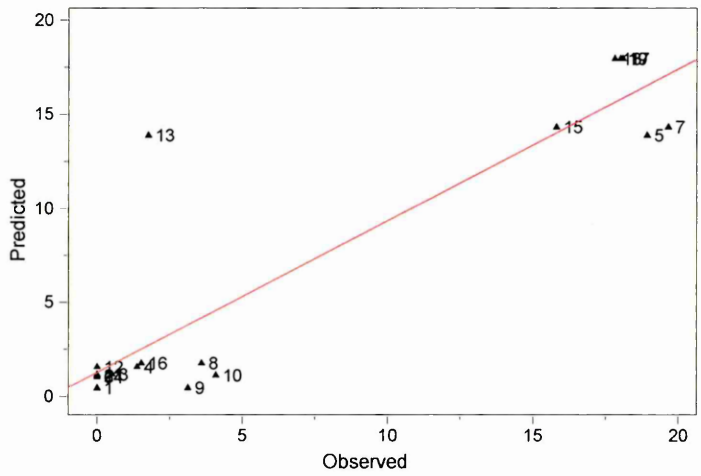

Figure 49: Observed values versus those predicted by the model.

The lack of fit of results 13 and 7 is perhaps seen more clearly in Figure 50, which shows the difference in the standardised residuals (i.e. taking into account standard deviations) for each run from those predicted by the model in the form of a bar chart. Therefore the closer the value to zero the closer the result to the predicted one. The raw data used to obtain these plots can be found in appendices 1 and 2. The standardised residuals are obtained by dividing the raw residual by the residual standard deviation.

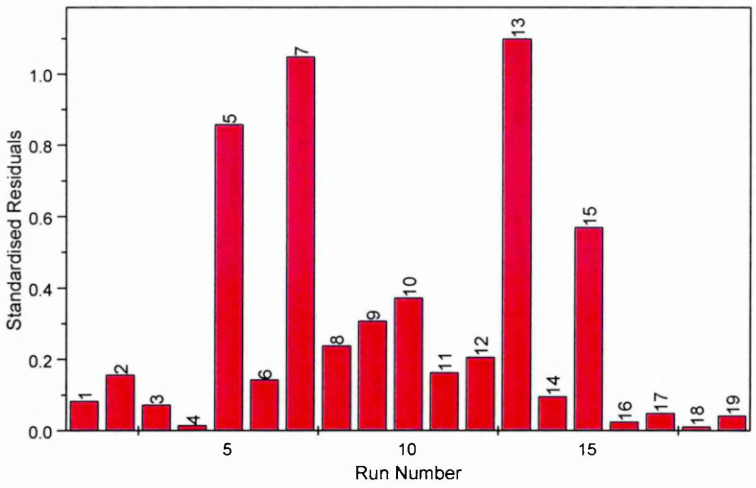

Figure 50: Difference in the observed values from those predicted by the model.

These two experimental runs were rejected using an outlier rejection test 'Dixon's Q' at a 95% confidence limit. When these two values are removed the model is a much better fit for the results obtained, according to R^2 and Q^2, as can be seen in Figure 51. This enables the model to make a much better prediction of the optimum. However should we wish to use the model in order to predict unknown values then we would also have to take into account both the slope and the intercept of the regression line in Figure 49. Runs 5 and 15 are also somewhat far from the predicted values, although they were not rejected by the outlier test and were therefore not removed. It is essential not to remove too many points, as information will be lost and the model will no longer be an accurate predictor.

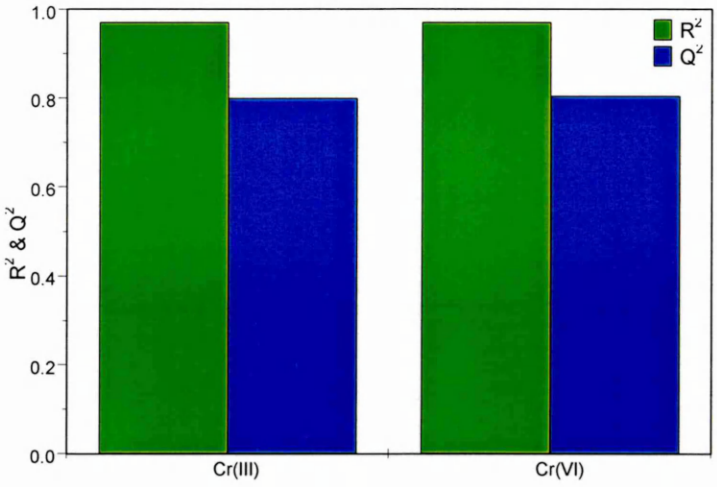

Figure 51: Summary of fit plot (with outliers removed).

As can be seen from the summary of fit plot the values for Q^2 and R^2 are 0.80 and 0.97 respectively for both responses. These values are close to 1, which indicates a good fit to the model. This means that the model has excellent predictive power for the optimisation. The ANOVA tables for Cr(III) and Cr(VI) containing the raw data for the calculation of R^2 and Q^2 can be found in appendices 1 and 2.

The values of R^2 and Q^2 are usually numbers between 0 and 1. The closer the values are to 1 the better the fit of the model and the stronger the predictive power of that model. These values give the best measure of the goodness of fit of the model.

Figure 52 shows the effect that the different factors have upon the Cr(III) and Cr(VI) signals. As we can see the most important effects are LF*LF, TL, LP and LF*RSF. Therefore from the results of the initial screening process the most influential parameters in obtaining the best response were found to be the luminol flow rate, the tube length, the luminol pH and the reductant solution flow rate. It also confirmed that

the luminol flow rate (LF) and the reductant solution flow rate (RSF) were interactive. These four parameters were then used in a full experimental model, to accurately determine the optimum settings for these factors.

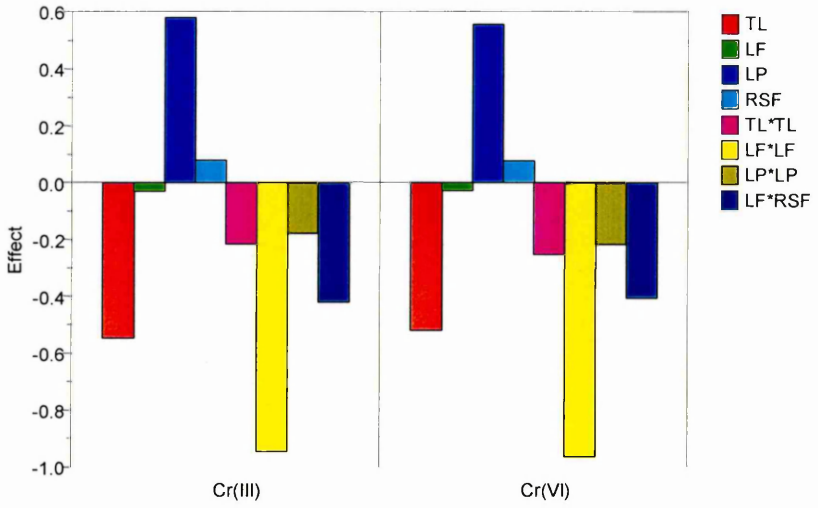

Figure 52: Diagram showing the effects of the investigated factors and the interactions between these factors for the initial screening (see Table 29 for abbreviations).

A response surface graph (Figure 53) was used to display the various different factors. This type of graph enables the optimisation of more than one factor at a time. Response surface methods are fairly efficient and can indicate the likely position of an optimum in very few experimental runs.

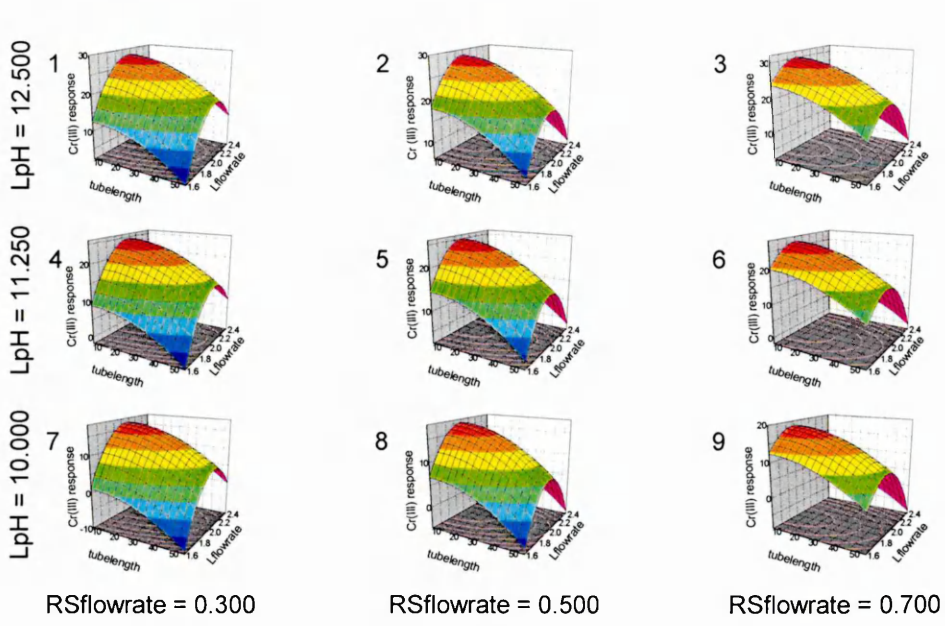

x axis = tube length (cm), y axis = response (peak areas), z axis = luminol flow rate (mL min^{-1}). Outer axis = 3 levels of luminol pH and 3 levels of reductant solution flow rate (mL min^{-1}).

Figure 53: 4D Response surface for Cr(III).

As can be seen from the plot for the Cr(III) response (Figure 53) (a similar plot is available for the Cr(VI) response, see Appendix 3) the tube length has not yet reached its optimum. We must therefore choose values lower than 5 cm for the full experimental model in order to find the optimum. This is also shown in Figure 54, which shows the effect of the tube length on the Cr(VI) signal (a similar plot is available for Cr(III), see Appendix 4).

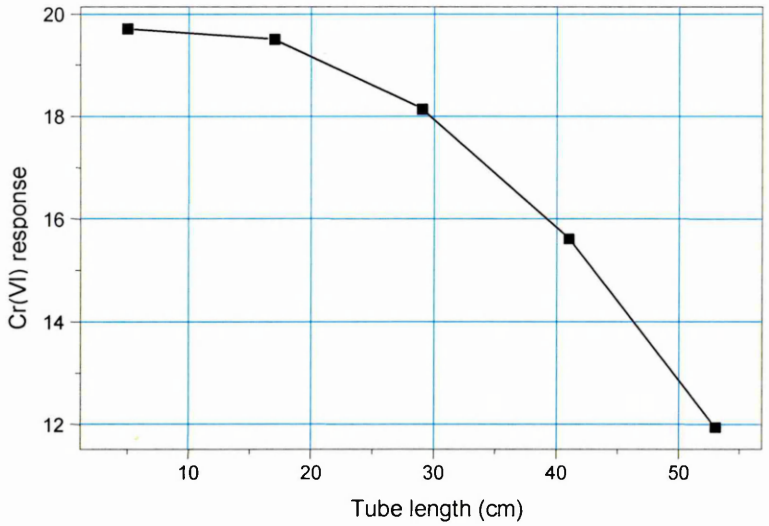

Figure 54: Effect of tube length on the Cr(VI) response.

3.7.4.6 Full Experimental Model

The four parameters which were found to be of most importance were: tube length (TL); luminol flow rate (LF); luminol pH (LpH) and reducing solution flow rate (RSF).

These parameters were then used in order to carry out a full experimental model, the results of which are displayed in Table 30. This was carried out by a partial least squares analysis (PLS) on a quadratic model, using a face centred central composite design, which incorporates a 2^4 full factorial design along with star points and centre points, for the full experimental model. The centre point was replicated three times in order to enable the model to estimate experimental precision. Therefore for four factors and three replicates of the centre point 27 experiments were required, i.e. $2^4 + (2 \times 4) + 3 = (2 \times 2 \times 2 \times 2) + (2 \times 4) + 3 = 16 + 8 + 3 = 27$. This was calculated according to the central composite design of $2^f + 2f + 3$, where f = number of factors (see Table 27 and section 3.7.4.3).

Table 30: Results from the quadratic model, face centred central composite design.

Expt No.	Run order	Variables				Responses ($x10^6$)	
		TL cm	LF mL min^{-1}	LpH	RSF mL min^{-1}	Cr(III)	Cr(VI)
1	22	3	1.6	11	0.5	51.7	30.8
2	23	7	1.6	11	0.5	31.6	770.8
3	21	3	2.4	11	0.5	191.5	147.7
4	2	7	2.4	11	0.5	255.2	183.9
5	9	3	1.6	11	0.7	205.1	163.8
6	24	7	1.6	11	0.7	81.5	46.8
7	3	3	2.4	11	0.7	242.5	175.3
8	5	7	2.4	11	0.7	270.9	196.0
9	13	3	1.6	13	0.5	101.7	79.8
10	1	7	1.6	13	0.5	29.2	62.7
11	4	3	2.4	13	0.5	56.1	41.0
12	26	7	2.4	13	0.5	111.5	77.6
13	7	3	1.6	13	0.7	101.2	83.6
14	19	7	1.6	13	0.7	171.3	104.5
15	14	3	2.4	13	0.7	65.1	51.4
16	16	7	2.4	13	0.7	88.6	57.8
17	8	3	2.0	12	0.6	652.1	500.1
18	6	7	2.0	12	0.6	611.7	484.4
19	27	5	1.6	12	0.6	242.4	204.7
20	17	5	2.4	12	0.6	490.9	353.2
21	15	5	2.0	12	0.5	412.5	340.5
22	12	5	2.0	12	0.7	617.7	487.7
23	18	5	2.0	11	0.6	126.4	83.4
24	25	5	2.0	13	0.6	159.9	113.3
25	11	5	2.0	12	0.6	640.4	503.4
26	10	5	2.0	12	0.6	640.8	500.6
27	20	5	2.0	12	0.6	530.0	333.4

TL = tube length, LF = luminol flow rate, LpH = luminol pH, RSF = reductant solution flow rate, responses for Cr(III) and Cr(VI) were measured as peak area in arbitrary units.

The summary of fit plot (Figure 55) shows that the model is a good prediction of the optimum, since the values of R^2 and Q^2 are close to 1. The raw data used to obtain these plots can be found in appendices 5 and 6.

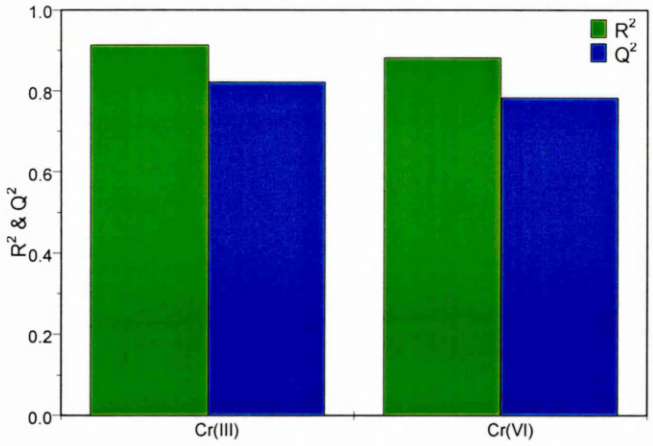

Figure 55: Summary of fit plot.

As can be seen from Figure 56 for the Cr(III) response (a similar plot is available for the Cr(VI) response) the tube length has now reached its optimum, along with the other factors to give the optimum response for both Cr(III) and Cr(VI). The optimum values obtained for all the factors can be seen in Table 31.

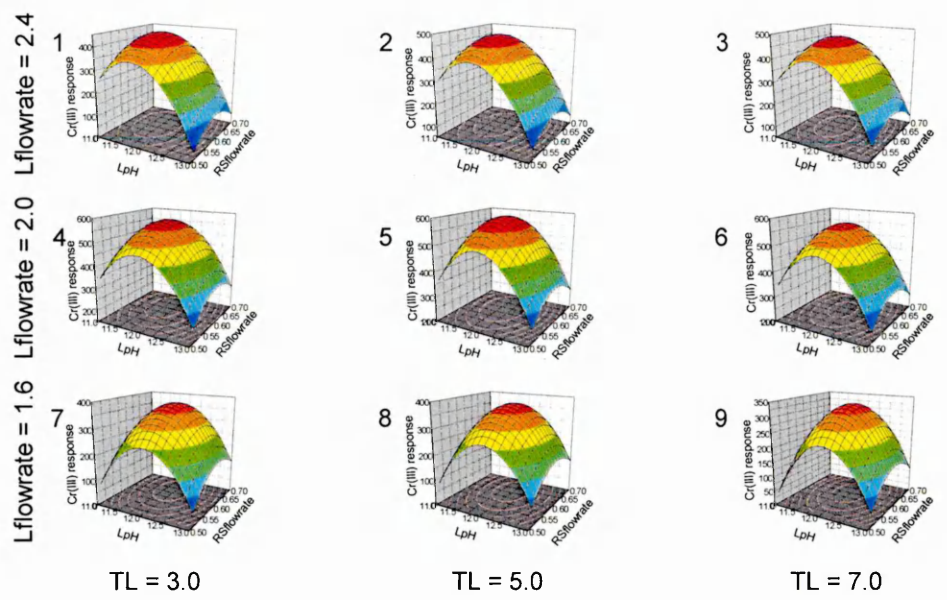

Figure 56: 4D Response surface for Cr(III); x axis = luminol pH, y axis = response (peak areas), z axis = reductant solution flow rate (mL min^{-1}). Outer axis = 3 levels of luminol flow rate (mL min^{-1}) and 3 levels of tubelength (cm).

3.7.5 Comparison of the Univariate and Multivariate Optimisations

A comparison of the results obtained using the two different optimisation approaches is summarised in Table 31.

Table 31 shows that the four most important parameters have different values for the two different methods of optimisation. The critical parameter is the tube length, which determines the time from the luminol addition until it reaches the detector. A shorter tube length of 5 cm was found to be the optimum using the multivariate approach as compared to 27 cm in the univariate optimisation.

Table 31: Comparison of univariate and multivariate optimisation procedures.

Parameter	Univariate	Multivariate
Tube length	27 cm	5 cm
Luminol flow	1.8 mL min^{-1}	2.1 mL min^{-1}
Luminol pH	11.5	11.8
Luminol concentration	$3.4x10^{-4}$ mol L^{-1}	$3.4x10^{-4}$ mol L^{-1}
Reducing solution flow	0.5 mL min^{-1}	0.6 mL min^{-1}
Reducing solution pH	3.0	3.0
Reducing solution conc.	0.015 mol L^{-1}	0.015 mol L^{-1}

A comparison of the Cr(III) and Cr(VI) signals obtained using the two optimised sets of conditions for the analysis of a mixed standard solution containing 10 µg L^{-1} is shown in Figure 57.

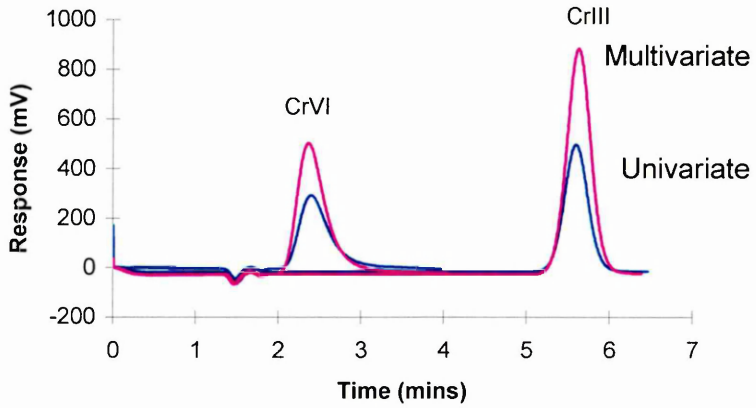

Figure 57: Comparison of the chromatograms obtained of 10 µg L^{-1} CrIII/VI using a CS5 column and IC-CL detetction using the optimised conditions from the multivariate and univariate procedures.

When the multivariate set-up is used the signals from the Cr(III) and Cr(VI) are increased by 43 and 32%, respectively. This allowed smaller peaks to be detected and

therefore also reduced the limit of detection for the analysis. The limit of detection determined for this analysis was improved from 0.08 μg L^{-1} for both Cr(III) and Cr(VI) initially, determined using the univariate optimisation, to 0.002 μg L^{-1} with the multivariate optimisation (see chapter 3.7.10). This clearly advocates the use of multivariate methods in order to optimise experiments of this type. This difference between the two optimisation approaches is explained by the fact that the univariate approach does not allow for interactions between parameters, whereas the multivariate approach does. This means that the true optimum has not been reached in the univariate approach.

3.7.6 Cr(III) Adsorption to Glass

In preliminary trials to calibrate the method, varying results were obtained for Cr(III) whilst the Cr(VI) results gave good linear responses (r^2 = 0.9995) (see Figure 58). At first it was thought that perhaps the pH of the solutions was affecting the calibration for Cr(III) since this is most stable at acidic pHs and the standards so far had been prepared in water. Acidic Cr(III) standards were therefore prepared using 0.14 mol L^{-1} nitric acid, but these still gave RSDs of more than 40%. Sparging the luminol solution with helium was also tried without effect.

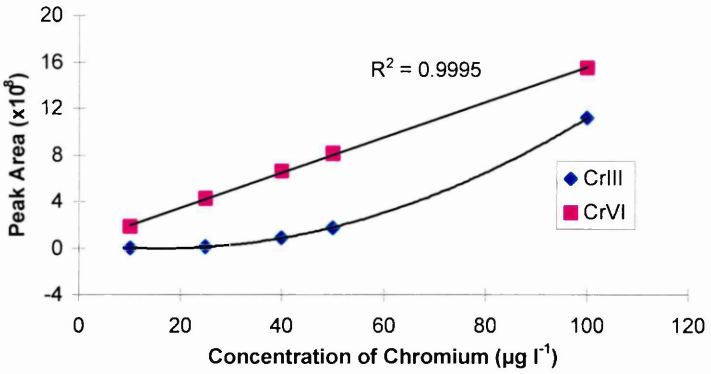

Figure 58: CrIII/VI calibration graph showing the effect of Cr(III) adsorption to glass autosampler vials using IC-CL.

In order to eliminate the possibility of non-specific adsorption on the column as the cause of the non-linearity of the Cr(III) calibration graphs the standards were run without the column. However the effect was similar to that previously observed (see Figure 59).

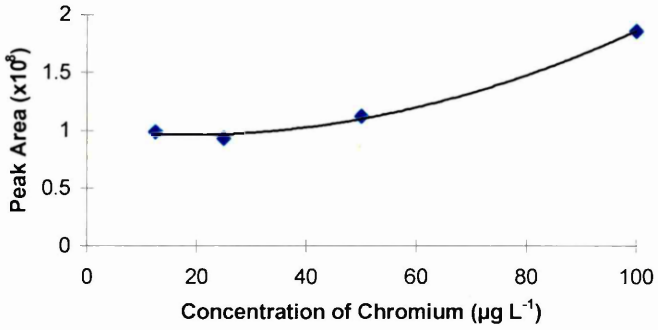

Figure 59: Cr(III) Calibration without a column using IC-CL.

Further trials, using manual injection, eliminated the glass syringe as a possible cause of the problem (see Figure 60).

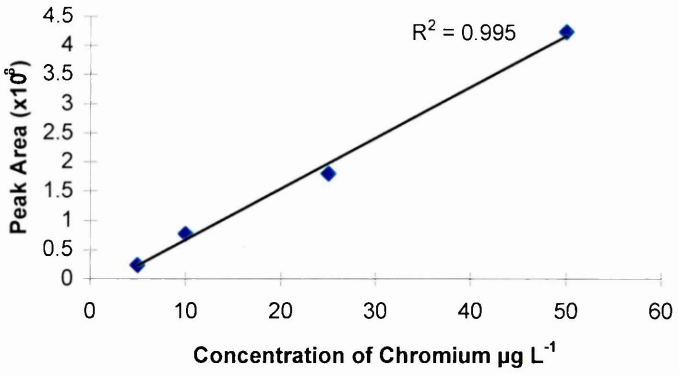

Figure 60: Cr(III) Calibration using manual injection and without a column using IC-CL.

Substitution of the glass autosampler vials with PTFE bottles showed that the former was the cause of the problem. Non-specific adsorption of Cr(III) as Cr^{3+} on the negatively charged silicate groups was the most likely explanation for the reduced Cr(III) response and non-linearity of the calibration graph. This effect can clearly be seen in Figure 61, where a comparison is made between standards prepared in glass autosampler vials and PTFE bottles using manual injection. The decrease in Cr(III) response when stored in a glass vial can be seen Figure 61.

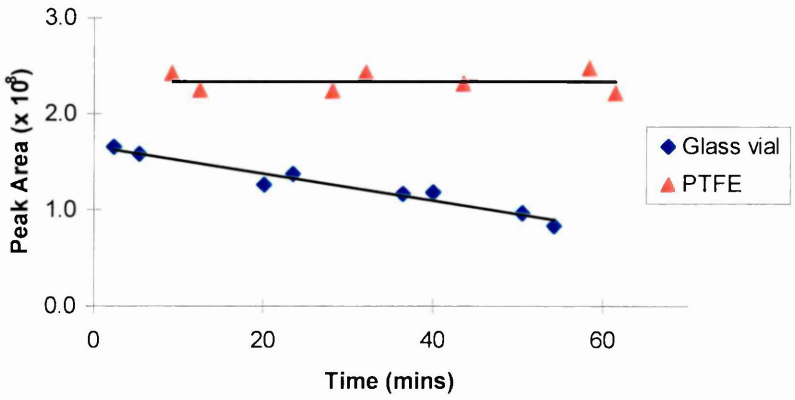

Figure 61: Variation with time for 50 µg L^{-1} Cr(III) out of glass autosampler vials and PTFE bottles using IC-CL.

Results of the determination of 10 μg L^{-1} Cr(III) solutions stored in silanised vials were relatively constant with time (see Figure 62). Silanisation was carried out by soaking the vials overnight in a solution of 5% dimethyldichlorosilane (DMDCS) in toluene (P/N 2233 Alltech, Lokeren, Belgium) then rinsing thoroughly with deionised water and leaving to dry. Good linearity was now observed with both Cr(III) and Cr(VI), r^2 = 0.9988 and 0.9991 respectively (see Figure 39).

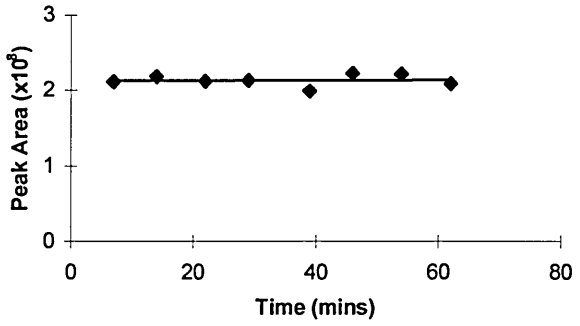

Figure 62: Variation of concentration with time for Cr(III) 10 μg L^{-1} out of silanised glass vials using IC-CL.

3.7.7 Chemiluminescence Reagent and Reducing Solutions Degradation

It was observed that both the chemiluminescence reagent and reducing solution degraded if left overnight i.e. no signal was observed the next day unless both solutions were made up fresh. This degradation could be prevented by storing the solutions under a helium atmosphere. No change was then observed for the chemiluminescence reagent and only a slight change for the reducing solution. Nevertheless, fresh solutions were prepared daily, but the helium atmosphere was retained in order to prevent degradation during analysis.

This effect in the chemiluminescence reagent can be explained by Equation 46[173]:

Equation 46

$$H_2O_2\,(aq) \rightarrow H_2O + \tfrac{1}{2}O_2\,(g)$$

For the sodium sulphite there is also a tendency to gain an oxygen atom to become the more stable sodium sulphate[173,174]:

Equation 47

$$NaSO_3 + H_2O \rightarrow NaSO_4 + 2H^+ + 2e^-$$

Sodium sulphate does not reduce Cr(VI) to Cr(III) and therefore this is an undesirable reaction.

3.7.8 Halide Ion Enhancement

It has been reported[175] that the use of halide ions can enhance the chemiluminescence signal obtained. Chang and Patterson[176] found a 6-fold increase of the chemiluminescence signal generated by the Cr(III)-luminol reaction in the presence of bromide ions.

Trials were carried out with the addition of 0.3 mol L^{-1} potassium bromide (KBr) or potassium chloride (KCl) to the eluent. The solutions were prepared by accurately weighing 1.428 g of KBr or 0.895 g of KCl into 40 mL of deionised water. Further trials were also carried out by preparing the Cr(III) and Cr(VI) standard solutions (30 µg L^{-1}) in the 0.3 mol L^{-1} KCl or KBr solutions and also by addition of the halide solutions to the chemiluminescence reagent. All results (see Table 32) are the mean of 2 separately prepared experiments each injected three times (6 injections in total).

The results obtained (Table 32) when using the halide enhancement were found not to be significantly different to when no halide enhancement was used. The significance

was tested using both one and two-tailed students' t-test at a 95% confidence limit. Since KCl was already present in the sample stream, halide enhancement may already have occurred, so further halide additions did not have an effect.

Table 32: Results of halide enhancement trials.

Enhancement	Solution	Mean Peak Area (x 10^6)	
		Cr(III)	Cr(VI)
None	-	849.3 ± 18.2	637.1 ± 12.6
Bromide	Eluent	838.1 ± 16.4	634.9 ± 11.9
Bromide	Standard	831.8 ± 15.7	642.0 ± 13.0
Bromide	Luminol	836.4 ± 16.1	648.4 ± 13.4
Chloride	Eluent	803.7 ± 14.3	641.7 ± 12.9
Chloride	Standard	833.2 ± 14.8	636.3 ± 12.5
Chloride	Luminol	841.0 ± 17.3	646.6 ± 13.2

3.7.9 Interferences

The effects of other metal ions present in environmental samples on the chromium chemiluminescence signal were investigated. The metal ions and the levels examined are summarised in Table 33.

Both Fe^{3+} and Fe^{2+} were found to interfere with the Cr(VI) signal. Fe^{2+} reduces Cr(VI) to Cr(III) as shown in the equation below. The interference caused by the Fe^{3+} could be due to the presence of Fe^{2+} in the commercially available iron(III)nitrate.

Equation 48

$$Cr^{VI} + 3Fe^{2+} \rightarrow Cr^{III} + 3Fe^{3+}$$

This is not direct interference with the method, since this would have already occurred before the detection step. Also at high concentrations (10 & 100 mg L^{-1}) a peak also occurred at approximately 1.7 minutes, close to where the Cr(VI) occurred when extracted with acetic acid from BCR CRM 483 (see later).

Table 33: Interference effects of other metal ions on the chemiluminescence signals of a solution containing 10 μg L^{-1} Cr(III) and Cr(VI).

Element	Concentration mg L^{-1}	Cr(III) %	Cr(VI) %	Other peaks
Fe^{3+}	1	94 ± 2	34 ± 6	-
Fe^{3+}	10	88 ± 6	0	-
Fe^{3+}	100	114 ± 1	0	yes
Fe^{2+}	1	99 ± 1	0	-
Fe^{2+}	10	99 ± 1	0	yes
Fe^{2+}	100	99 ± 1	0	yes
Ca^{2+}	1	103 ± 4	96 ± 3	-
Ca^{2+}	10	98 ± 2	95 ± 4	-
Ca^{2+}	100	94 ± 1	95 ± 5	-
Zn^{2+}	1	103 ± 1	102 ± 1	-
Zn^{2+}	10	101 ± 4	101 ± 2	-
Zn^{2+}	100	104 ± 1	103 ± 1	-
Mn^{2+}	2	100 ± 1	103 ± 1	-
Mn^{2+}	20	103 ± 1	112 ± 1	-
Mn^{2+}	40	106 ± 1	115 ± 1	-
Co^{2+}	0.01	100 ± 1	99 ± 1	-
Co^{2+}	0.1	99 ± 1	95 ± 3	-
Co^{2+}	1	97 ± 1	99 ± 2	-
Al^{3+}	0.1	100 ± 5	110 ± 4	-
Al^{3+}	1	93 ± 2	99 ± 2	-
Al^{3+}	10	126 ± 1	100 ± 3	-
Mg^{2+}	1	98 ± 1	94 ± 6	-
Mg^{2+}	10	98 ± 1	101 ± 1	-
Mg^{2+}	20	95 ± 2	101 ± 1	-
Ni^{2+}	0.1	96 ± 2	99 ± 1	-
Ni^{2+}	1	97 ± 2	89 ± 1	-

Element	Concentration mg L^{-1}	Cr(III) %	Cr(VI) %	Other peaks
Ni^{2+}	10	94 ± 1	86 ± 2	-
Cu^{2+}	0.1	118 ± 2	107 ± 4	-
Cu^{2+}	1	111 ± 7	104 ± 1	-
Cu^{2+}	10	100 ± 1	99 ± 1	-

Upon reduction of the Fe^{2+} or Fe^{3+} no Cr(III) peak occurred, therefore there was no problem, although this advocated the use of reduction in order to avoid this interference as will be discussed in section 4.5.

For the Ca^{2+} the Cr(VI) was subject to a negative interference i.e. a reduction in the expected peak size. This is probably due to the formation of a complex with Ca^{2+} e.g. $CaCrO_4$. Also for Ni^{2+} a negative interference was observed i.e. the chemiluminescent signal was reduced.

For the rest of the interferences tested no significant effects were noted. The significance was tested using a two-tailed students' t-test at a 95% confidence limit.

3.7.10 Accuracy/Limit of Detection

The accuracy of the analysis was determined using a simulated water sample containing 10 µg L^{-1} of both Cr(III) and Cr(VI). Values of 10.6 ±0.52 µg L^{-1} (4.9%) and 10.1 ±0.50 µg L^{-1} (4.9%) (n = 6) were obtained for Cr(III) and Cr(VI) respectively. The detection limit was established by following the IUPAC - recommended criterion $S\sigma_N = 3$[177] via an algorithm that determined σ_N, the standard deviation of the baseline noise, by a least-

squares fit to a normal (Gaussian) distribution. The limit of detection was found to be 0.002 μg L^{-1} for both Cr(III) and Cr(VI).

The limit of determination[77], defined as being $S\sigma_N = 10$, was found to be 0.02 μg L^{-1} for both Cr(III) and Cr(VI). For practical purposes and due to baseline drift which sometimes occurred, the limit of determination was taken as the lowest detectable amount. Figure 63 shows Cr(III)/Cr(VI) at around the limit of determination (0.05 μg L^{-1}) along with a Gaussian approximation of the baseline noise.

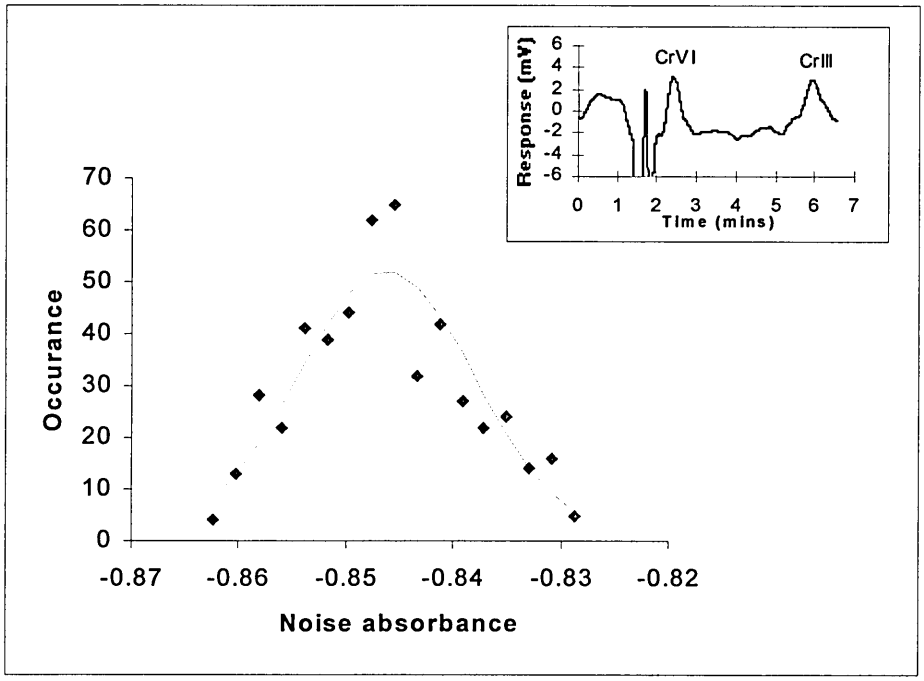

Figure 63: Least squares Gaussian fit of the baseline fluctuation and chromatogram of Cr(III)/(VI) at close to the limit of determination for IC-CL (inset).

3.7.11 BCR CRM 544 CrIII/VI in Water

A lyophilised water solution certified reference material (CRM), BCR CRM 544 (European Commission), certified for Cr(III), Cr(VI) and total chromium content was tested using this system. A glass vial containing 2 mg of the freeze-dried powder was reconstituted as instructed with 20 mL of a HCO_3^-/H_2CO_3 buffer at pH 6.4[178]. A broad band, probably due to the buffer, was observed in the chromatogram at approximately 8 minutes. Reconstitution in 0.01 mol L^{-1} HNO_3 avoided this problem. However, extremely low results for Cr(III) were obtained when the reconstituted sample was stored in the glass vial. This is probably due to the adsorption of the Cr(III) to the glass. Higher Cr(III) results were obtained when the sample was transferred to a PTFE bottle, but still lower than expected. Values of 19 ± 2 µg L^{-1} (n=6) were obtained compared to the certified value of 26.8 ± 1.0 µg L^{-1}. For Cr(VI) reasonable results were obtained 21 ± 2 µg L^{-1} (n=6) compared to the certified value of 22.8 ± 1 µg L^{-1}.

Column fractions collected after ion chromatography of BCR CRM 544 (reconstituted in 0.01 mol L^{-1} HNO_3) were analysed for chromium by ETAAS. The chromatogram, Figure 64, shows lower Cr(III) levels, an indication that chemiluminescence detection did not underestimate the levels of Cr(III).

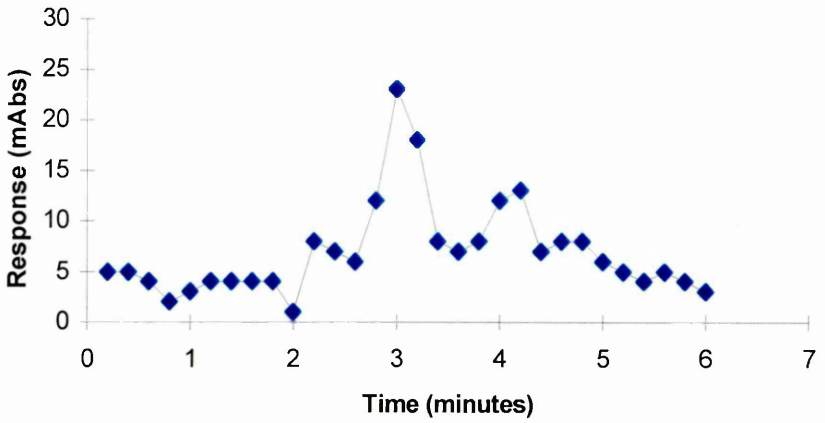

Figure 64: ETAAS analysis of fractions collected of BCR CRM 544 after IC.

A total chromium content of 54.8 ± 2.2 µg L^{-1} compared to the certified value of 49.4 µg L^{-1} ± 0.9 µg L^{-1} was found when the reference material (reconstituted in buffer) was analysed by ETAAS. However the buffer when tested alone also gave a reading for chromium. In an attempt to explain the low Cr(III) results obtained for the reference material when ion chromatography with chemiluminescence detection is used, Beere and Jones[159] suggested that the chloride complex, $[Cr(H_2O)_4Cl_2]^+Cl^-$, is formed. The chloride complex is not oxidised by hydrogen peroxide and as a result cannot be detected by chemiluminescence. Results obtained using ETAAS in this study indicate that the reduction of the Cr(III) signal is not due to the inability of the chloride complex to form the luminescent compound.

Separate chromatograms of solutions of $Cr(NO_3)_3$ and $CrCl_3$ in water were obtained after separation by ion chromatography and ETAAS detection after collection of fractions showed a single peak at 4.5 minutes (see Figure 65 and Figure 66).

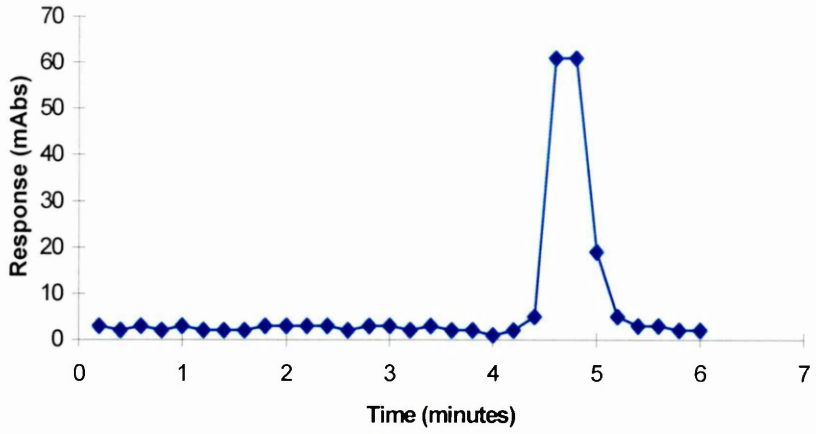

Figure 65: ETAAS analysis of fractions collected of a solution containing 50 μg L^{-1} chromium as $Cr(NO_3)_3$ in H_2O after IC.

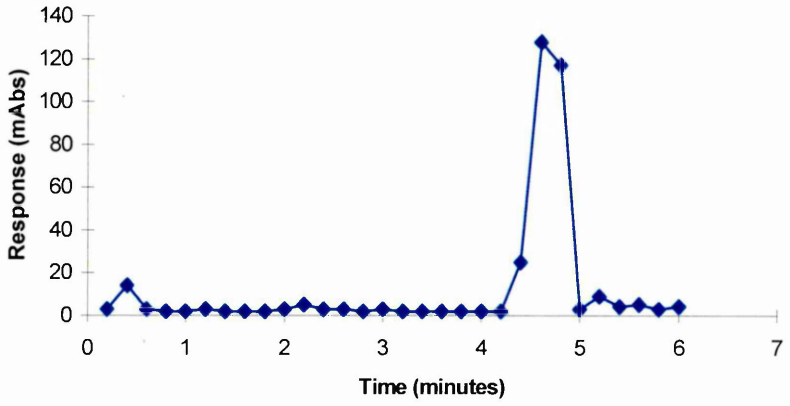

Figure 66: ETAAS analysis of fractions collected of a solution containing 50 μg L^{-1} Cr as $CrCl_3$ in H_2O after IC.

However, when $CrCl_3$ was prepared in 0.1 mol L^{-1} HCl the peak at 4.5 minutes had almost disappeared and a new peak had appeared at approximately 2 minutes (see Figure 67).

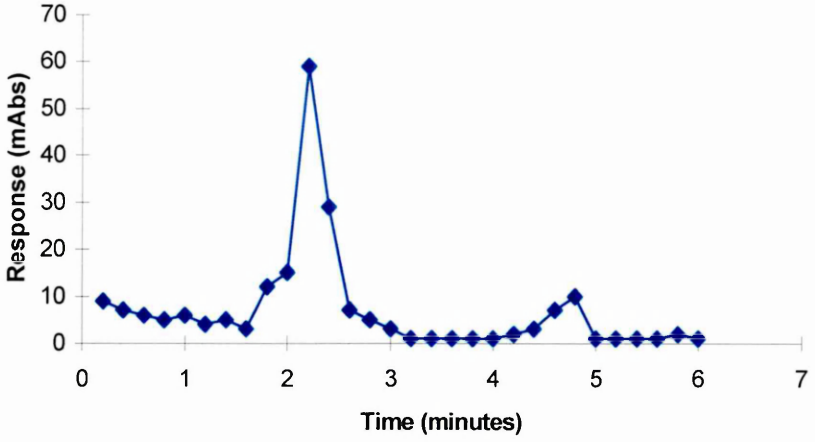

Figure 67: ETAAS analysis of fractions collected of a solution containing 50 μg L^{-1} Cr as $CrCl_3$ in 0.1 mol L^{-1} HCl after IC.

This result was also confirmed by ion chromatography with chemiluminescence detection of a 50 μg L^{-1} Cr(III) standard which was prepared in both 0.1 mol L^{-1} HCl and 0.6 mol L^{-1} KCl, see Figure 68 & Figure 69.

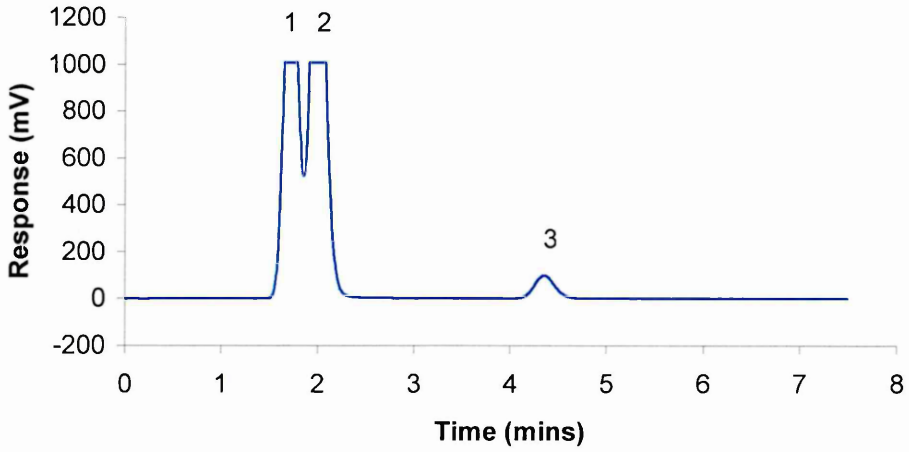

Figure 68: Ion chromatography with chemiluminescence detection of 50 μg L^{-1} Cr as $CrCl_3$ in 0.6 mol L^{-1} KCl.

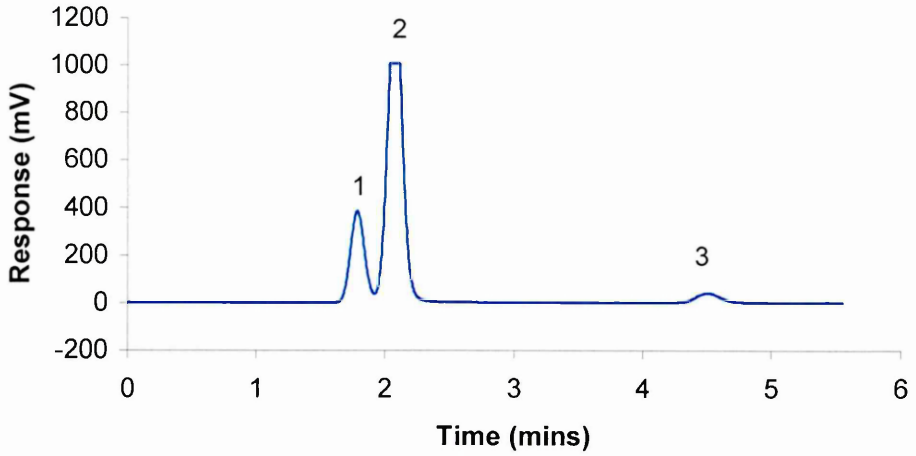

Figure 69: Ion chromatography with chemiluminescence detection of 50 µg L^{-1} Cr as $CrCl_3$ in 0.1 mol L^{-1} HCl.

These chromatograms clearly show that in the presence of an excess of chloride ions the $CrCl_3$ species are formed that can be separated by ion chromatography and detected by both chemiluminescence and ETAAS. Figure 70 shows a standard prepared in deionised water.

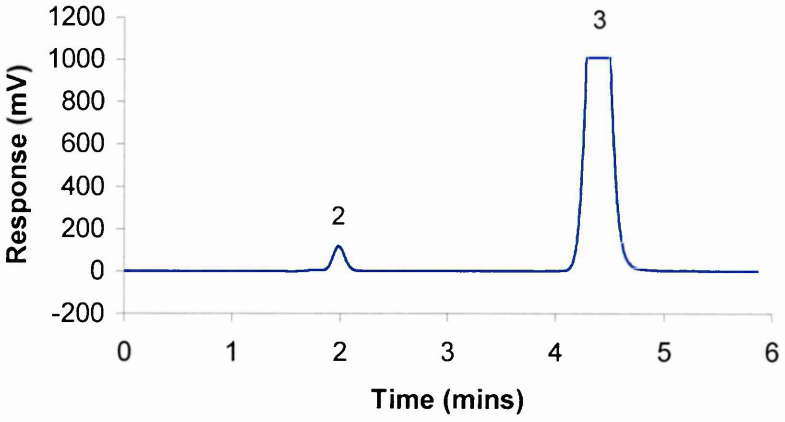

Figure 70: Ion chromatography with chemiluminescence detection of 50 µg L^{-1} Cr as $CrCl_3$ in H_2O.

Trials were then carried out using different concentrations of the eluent (KCl) and also varying the time from preparation of the samples to analysis. $CrCl_3$ samples of 10 μg L^{-1} were prepared in 0.6, 0.3, 0.15 and 0.075 mol L^{-1} KCl to determine how decreasing chloride ion content affected the nature of the species detected (see Figure 71).

Species 1, 2 and 3 in the chromatograms are probably the isomers $[Cr(H_2O)_4Cl_2]^+$, $[Cr(H_2O)_5Cl]^{2+}$ and $[Cr(H_2O)_6]^{3+}$ respectively. The order of elution from the ion chromatograph is largely determined by charge. In addition, as the chloride concentration increases species 1, $[Cr(H_2O)_4Cl_2]^+$, predominates. This can be clearly seen in Figure 71, in which the increasing concentration of KCl used in the column mobile phase determines the nature of the chromium species that are detected.

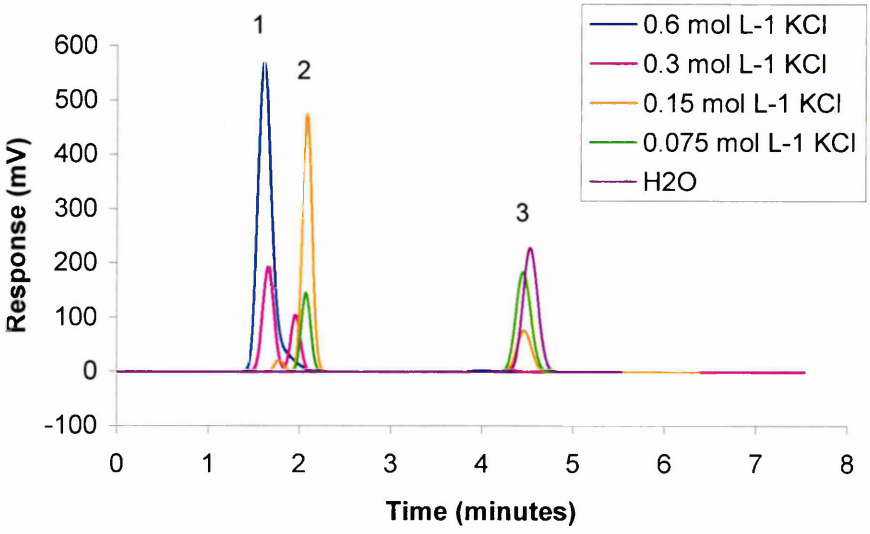

Figure 71: Ion chromatography with chemiluminescence detection of 10 μg L^{-1} Cr as $CrCl_3$ in 0.6, 0.3, 0.15 and 0.075 mol L^{-1} KCl compared to H_2O.

A summary of the distribution of chromium species as the KCl concentration is varied is presented in Figure 72.

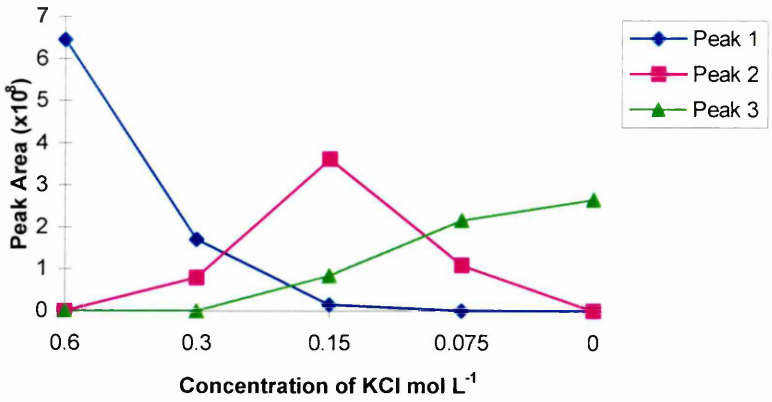

Figure 72: Variation of the peaks detected for 10 μg L^{-1} Cr as $CrCl_3$ in varying concentrations of KCl by IC-CL.

Changes in the distribution of the chromium species in 0.075 mol L^{-1} KCl with time are shown in Figure 73. As peaks 2 and 3 increase with time, peak 1 decreases. This decrease in peak 1 corresponds to the increase in peaks 2 and 3 i.e. no chromium is lost just the form in which it is detected is changed.

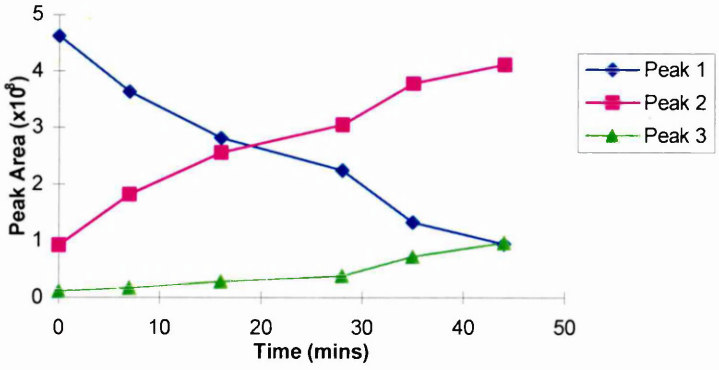

Figure 73: Variation with time of the peaks detected for 10 μg L^{-1} Cr as $CrCl_3$ in 0.075 mol L^{-1} KCl by IC-CL.

The amount of species 2 and 3 present in the equilibrated sample of 10 μg L^{-1} Cr as $CrCl_3$ in 0.075 mol L^{-1} KCl also decreased when left for long periods of time (see Figure 74). This could again be due to the adsorption of Cr(III) to the walls of the vessel.

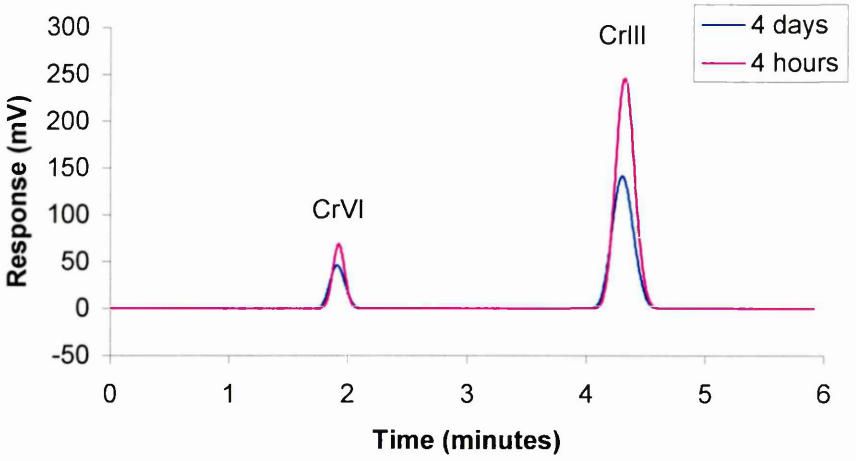

Figure 74: Ion chromatography with chemiluminescence detection of 10μg L^{-1} Cr as $CrCl_3$ in 0.075 mol L^{-1} KCl.

3.7.12 CRM 6010 and SRM 1643d Certified Water Reference Materials

Two certified reference materials for water; LGC (laboratory of the government chemist) CRM 6010 and NIST SRM 1643d were analysed in order to validate the method. The chromatograms of both samples showed that Cr(III) was the predominant species present (see Figure 75).

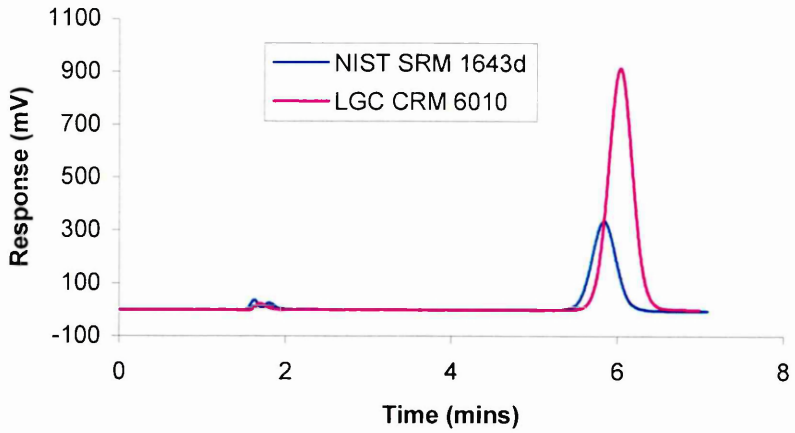

Figure 75: IC-CL chromatogram of water reference materials NIST SRM 1643d and LGC CRM 6010.

Results obtained for the Cr(III) determinations were 49.2 ± 1.8 μg L^{-1} and 19.0 ± 1.5 μg L^{-1} compared to the certified values of 49 ± 4 μg L^{-1} and 18.53 ± 0.20 μg L^{-1} for LGC CRM 6010 and NIST SRM 1643d, respectively. A comparison of the results obtained with the certified values using both one and two-tailed Student t-tests at 95% confidence limit showed that the differences were not statistically significant[179].

CHAPTER 4 EXTRACTION OF CHROMIUM FROM SOLID MATRICES

Metal cations in soils may be present in several different physico-chemical forms, for example as simple or complex ions, easily exchangeable ions, organically bound, occluded by or co-precipitated with metal oxides or carbonates or phosphates and secondary minerals, or ions in crystal lattices of primary minerals. Sequential extraction systems[33,34] have been proposed which reflect these differences in binding of the metal to the matrix.

Generally, sequential extraction procedures apply chemical extractants successively to the sample. In this way a number of fractions are obtained, each of which is associated with a particular type of metal-solid interaction[33,34] , e.g.:

1 Exchangeable (adsorbed metals) e.g. extracted by $CaCl_2$, $MgCl_2$.

2 Carbonate (bound to carbonates) e.g. extracted by EDTA, CH_3COOH.

3 Reducible (bound to Fe and Mn oxides) e.g. extracted by NH_3OHCl, citrate.

4 Oxidisable (bound to organic & sulphidic compounds) e.g. extracted by H_2O_2, H_2O_2/HNO_3, $H_2O_2/CH_3CO_2NH_4$.

5 Residual (bound to the mineral lattice) e.g. extracted by mixtures of strong acids such as $HNO_3/HClO_4/HF$.

Since chromium species are very sensitive to pH changes and can easily be reduced or oxidised (see section 1.2), the extractants used have to be chosen carefully. Therefore, chemicals such as NH_3OHCl and H_2O_2, used for the extraction of reducible and oxidisable fractions, are not suitable.

4.1 Reagents

All chemicals were obtained from Aldrich, Bornem, Belgium and were of ACS reagent grade unless otherwise stated. Chromium(III)nitrate nonahydrate [$Cr(NO_3)_3.9H_20$] (99.99+%); potassium chromate [K_2CrO_4] (99.7%); calcium chloride [CaCl] (99.9+%); sodium diethyldithiocarbamate [NaDDTC] (99+%); potassium hydrogen phosphate [KH_2PO_4] (98+%); ammonium sulphate [$(NH_4)_2SO_4$] (99+%); acetic acid [CH_3COOH] (100%) Aristar grade, BDH Poole, Dorset, UK; hydroxylammonium chloride [$HO.NH_3Cl$] (99%), spectrosol grade, BDH Poole, Dorset, UK; hydrochloric acid fuming [HCl] (37%), G.R., Merck, Darmstadt, Germany; 18MΩ deionised water, MilliQ Plus 185 Ultrapure Water System, Millipore, Milford, MA, USA.

4.2 Instrumentation

4.2.1 Ion Chromatography (IC) System

A metal free Dionex DX500 Chromatography System (Dionex n.v., Mechelen, Belgium) was used incorporating Peaknet control and utilising Dionex Peaknet integration software (see Figure 76). A GP40 Gradient Pump with vacuum degasser was used to pump the eluent through the column at 1 mL min^{-1}. An Ismatec peristaltic pump (Zürich, Switzerland) was used to add the reducing solution at a flow of 0.5 mL min^{-1} and a post column reagent delivery module (Dionex PC10 pneumatic controller) added

the chemiluminescence reagent at a flow of 1.8 mL min^{-1}. Injection was carried out using an AS3500 autosampler (Dionex). The injection volume was 50 µL. The separation column was a Dionex Ionpac CS5 4 x 250mm analytical column. PEEK tubing and connectors were used throughout. A 375 µL knitted reaction coil enabled thorough mixing of the reducing solution and the effluent from the column after separation. This ensured complete reduction of Cr(VI) to Cr(III). A Foxy 200 fraction collector (ISCO, Belgium) was also connected after the detector. This enabled the collection of fractions eluting from the column for further analysis by ICP-MS or ETAAS.

4.2.2 Chemiluminescence Detector (CL)

A Jasco FP920 Intelligent Fluorescence detector with chemiluminescence option (Jasco Corporation, Tokyo, Japan) incorporating a flat wound PTFE cell with reflective back-plate in order to direct the maximum amount of light emitted towards the photo multiplier tube which was placed end on to the cell, was used (see Figure 76).

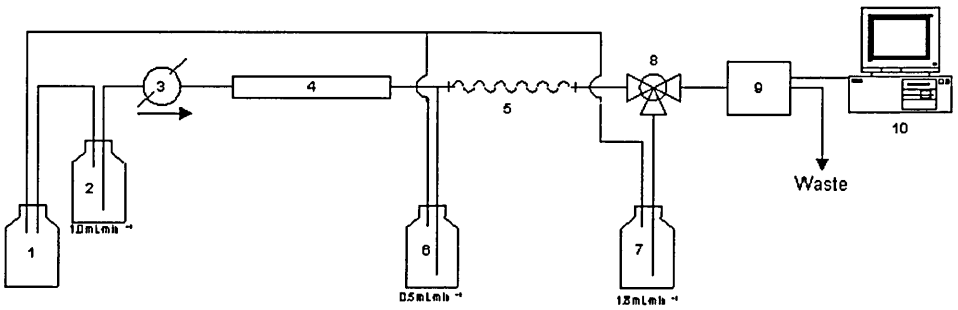

1 Helium
2 Eluent (KCl,EDTA)
3 Injection port
4 Analytical column(CS5)
5 Mixing coil (375µL)
6 Reducing Solution (K_2SO_3)
7 Chemiluminescence reagent (luminol, H_2O_2)
8 Mixing tee
9 Chemiluminescence detector
10 Data processor (Computer)

Figure 76: Schematic Diagram of the ion chromatograph with chemiluminescence detection.

A peristaltic pump was used to deliver the reducing solution at a flow rate of 0.5 mL min^{-1}. High pump speed and a small internal diameter (i.d.) of the tubing, 90 rpm and 0.51 mm respectively, were used in order to reduce pump pulsation. High pump speeds reduce the lifetime of the tubing and it is essential that the tubing is replaced regularly so that the flow rate is not altered.

4.2.3 Electro Thermal Atomic Absorption Spectrophotometer (ETAAS)

Validation of the results obtained by IC-CL was carried out by ETAAS. The instrument used for all ETAAS analysis was a Perkin Elmer 5100PC atomic absorption spectrophotometer with Perkin Elmer 5100ZL Zeeman furnace module (Perkin Elmer, Beaconsfield, Bucks, UK). The furnace program used is shown inTable 34. A chromium hollow cathode lamp was used at a wavelength of 357.9 nm. A 15 µg addition of magnesium nitrate ($Mg(NO_3)_2$) modifier was also used in order to ensure complete atomisation of the different species of chromium.

Table 34: Graphite furnace operating parameters.

Step	Temperature (°C)	Ramp Time (seconds)	Hold Time (seconds)
1 : Drying	110	1	30
2 : Drying	130	5	40
3 : Ashing	1500	10	20
4 : Atomisation	2300	0	5
5 : Cleaning	2400	1	2

4.2.4 Inductively Coupled Plasma - Mass Spectrometer (ICP-MS)

The ICP-MS instrument used was a Fisons PQ2+ quadrupole instrument with a micro concentric nebuliser, for sample introduction at a flow rate of 50 $\mu L\ min^{-1}$, and a Meinhard concentric ICP torch with a double pass spray chamber and recirculating pump (Micromass Int., Manchester, UK). See Table 35 for operating conditions. The ICP-MS instrument was used to investigate the elemental content of liquid aliquots collected after samples were run through the IC-CL instrument.

Tuning of this instrument was carried out daily using a multielement standard (Merck, Darmstadt, Germany) containing Be, Mg, Co, In, Ce, Tm, Pb and U at a concentration of 10 $\mu g\ L^{-1}$ in 2% nitric acid. The determination of chromium was carried out at m/z values of 52 and 53. Although 53 has a lower abundance it also suffers much less from interferences, especially from Ar-C (see Table 5). This was an important consideration here as there is likely to be a considerable amount of carbon present in the extracted soil samples. Relative abundances are shown below:

m/z	**Chromium**	**Ar-C**
52	83.79%	98.5%
53	9.50%	1.10%

Table 35: ICP-MS operating conditions.

Parameter	**Setting**
Forward Power	1400 watts
Reflected Power	0 watts
Torch	Meinhard Concentric Torch
Spray Chamber	Double Pass
Nebuliser	Micro Concentric

Parameter	Setting
Sample introduction	Peristaltic pump
Solution uptake rate	50 µL min^{-1}
Coolant gas flow rate	15 L min^{-1} Argon
Nebuliser gas flow rate	0.7 L min^{-1} Argon
Nebuliser gas pressure	207 Pa (30 psi)
Sample cone material	Nickel
Skimmer cone material	Nickel
No. of sweeps per replicate	50
No. of replicates	6
Masses	^{52}Cr ^{53}Cr
Measurement mode	Peak jumping
Integration time	3 s
Detector mode	Pulse counting

4.2.5 Filtration

Filtration of samples was carried out using 0.45 µm cellulose acetate sterile syringe filters (Alltech, Lokeren, Belgium).

4.3 Extraction Procedure

Approximately 0.25 g of solid soil sample was accurately weighed into a 30 mL PTFE centrifuge tube. A 10 mL portion of 0.43 mol L^{-1} acetic acid or trial solution was added and the tube was shaken for 16 h (overnight) at 300 rotations min^{-1} on an IKA Labortechnik KS-501 orbital bench shaker (Jancke & Kunkel GmbH, Staufen, Germany) at room temperature. The sample was then centrifuged in a Heraeus Megafuge 1.0R bench top centrifuge at 6000 g and 21°C for 15 minutes. The supernatant liquid was then pipetted into a clean 30 mL PTFE bottle and the volume made up to 25 mL with deionised water.

4.4 Results and Discussion

Trials were carried out using seven different extraction media, with detection by IC-CL, in order to investigate the changes in speciation. The results obtained with the extraction media were compared to that in water when mixtures of CrIII/VI were shaken overnight (16hrs) on an orbital bench shaker at 300 rotations min^{-1} at room temperature.

$CaCl_2$

Solutions of 0.05 mol L^{-1} calcium chloride ($CaCl_2$)[128] were investigated. This extracts the exchangeable fraction, as shown in Equation 49.

Equation 49

$$R\text{-}M^{2+} + Ca^{2+} \rightarrow R\text{-}Ca^{2+} + M^{2+}$$

The pH of the solution was found to be 4.05. The results obtained (see Table 36) were 114% and 70% for Cr(III) and Cr(VI) respectively. This infers that some conversion of Cr(VI) to Cr(III) has occurred, and that this is the reason for the increased amount of Cr(III) and the reduced amount of Cr(VI).

CH_3COOH

Acetic acid (0.43 mol L^{-1}) extracts the exchangeable and carbonate bound fractions. The pH of the solution was found to be 2.64. The results obtained were 98% and 96% for Cr(III) and Cr(VI) respectively (see Table 36), therefore we can conclude that the extraction media was found not to change the species present.

NaDDTC

Trials were carried out using 0.002 mol L^{-1} sodium diethyldithiocarbamate (NaDDTC)[71], a complexing agent, at pH 4.0 and 5.6. Dithiocarbamates form strong

and mostly neutral complexes with a large number of heavy metals, which can be separated from a large excess of alkaline and alkaline earth elements. The NaDDTC required a clean-up step prior to use[180], which was carried out by passing the NaDDTC solution through a 3cm C_{18} column (Packard OCH Klar Polygosil C_{18} 40-63µm). At pH 4.0 Cr(VI)-DDTC is formed, but not the Cr(III) complex. Both complexes are formed at pH 5.6. The results obtained here (see Table 36) showed good recoveries of Cr(VI) (95% at pH 4.0 and 104% at pH 5.6), however the Cr(III) complex was too stable to be broken down by the reducing agent and therefore no peak was detected for Cr(III) at pH 5.6 and a reduced peak at pH 4.0. The reduced peak at pH 4.0 (49%) probably indicates that there is some formation of the Cr(III) complex, which can then not be broken down. The Cr(VI) complex, being neutral, was detected in the solvent front.

KH_2PO_4

A trial was carried out using 0.015 mol L^{-1} KH_2PO_4[181] which extracts soluble chromium and Cr(VI). The result obtained for Cr(VI) was very good (98%), however, for Cr(III) only a very small amount was detected (7%). This indicates that there is a possible reaction of Cr(III) with KH_2PO_4, making it no longer detectable by IC-CL.

HCl

A trial was also carried out using 0.1 mol L^{-1} hydrochloric acid (HCl) with heating of the sample. This would not be expected to retain the species intact since the pH is acidic. It would therefore be expected that the Cr(VI) was reduced to Cr(III). However Gammelgaard et al.[77] showed that in recovery experiments no conversion took place. In the trials carried out here this could not be reproduced. It was found that half of the Cr(VI) was indeed reduced to Cr(III) (see Table 36), giving recoveries of 156% for Cr(III) and 50% for Cr(VI). Gammelgaard et al. carried out their trials on biological

samples, however their method could not be used here because of the reduction of Cr(VI) to Cr(III).

$(NH_4)_2SO_4/NH_3$

When using alkaline $(NH_4)_2SO_4/NH_3$[182] (pH 8) as extraction medium it would be expected that the Cr(III) would be oxidised to Cr(VI). It is claimed, however, that the ammonia reduces the oxidation of Cr(III) to Cr(VI) by 65-95%[183]. The results obtained here showed a recovery of only 80% for Cr(VI) and no Cr(III) peak. See Table 36.

A summary of the results obtained by IC-CL with all the extraction media tested can be seen in Table 36.

Table 36: Comparison of extraction media to water to see if any changes in speciation occur (IC-CL detection).

Extractant	Recovery of Cr(III) % (n=12)	Recovery of Cr(VI) % (n=12)
H_2O	100 ± 1	100 ± 1
CH_3COOH	98 ± 2	96 ± 2
$CaCl_2$	114 ± 2	70 ± 2
NaDDTC pH4.0	49 ± 3	95 ± 4
NaDDTC pH5.6	0 ± 2	104 ± 3
KH_2PO_4	7 ± 1	98 ± 2
HCl	156 ± 2	50 ± 2
$(NH_4)_2SO_4/NH_3$	-	80 ± 2

In order to avoid the problems of decreased recovery or oxidation/reduction that occurred with the other extraction media tested, 0.43 mol L^{-1} acetic acid was used for

further tests of extraction of solid samples since this was the only medium tested which did not alter the distribution of chromium species.

Initial trials with 0.43 mol L^{-1} acetic acid extraction and IC-CL detection were carried out using a sewage sludge amended soil: BCR CRM 597, but very little chromium was extracted and only as Cr(III). The low total chromium content was also confirmed by ETAAS, an indication that the chromium contained in this sewage sludge amended soil is too strongly bound to be extracted by this extraction technique. This is to be expected, since Cr(III) is strongly adsorbed onto soil surfaces forming strong complexes with soil humus[184]. Therefore the Cr(III) within the soil is not easily mobilised. Cr(VI) on the other hand is only weakly bound and is therefore easily leachable. A reference material certified for total chromium extracted by 0.43 mol L^{-1} acetic acid (BCR CRM 483) was obtained and further trials were carried out using this material.

4.5 BCR CRM 483 Sewage Sludge Amended Soil

A reference material certified by the European Commission, BCR CRM 483, was obtained which was certified for the total chromium extractable by 0.43 mol L^{-1} acetic acid using overnight (16 h) shaking. Initial trials using IC-CL showed that only a small amount of Cr(III) was extracted (peak II, Figure 77) and no Cr(VI). However a large peak (peak I, Figure 77) was also observed at the start of the chromatogram at approximately 1.8 minutes. Cr(VI) would normally be detected at approximately 2.5 minutes.

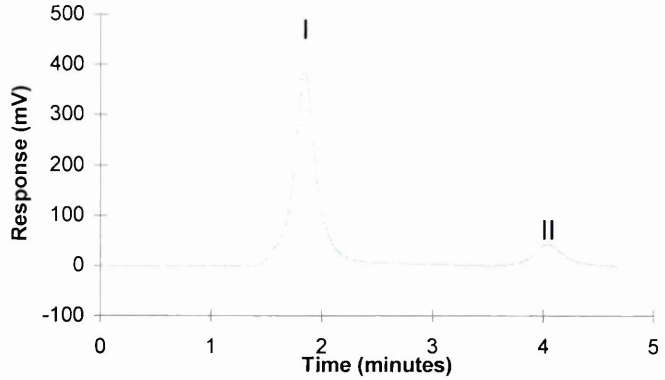

Figure 77: Chromatogram of 0.43 mol L^{-1} acetic acid extraction of BCR CRM 483 using a CS5 column and IC-CL detection.

ETAAS analysis (using chromium hollow cathode lamp) of fractions collected after IC separation proved that this peak was actually due to chromium (see Figure 78). A peak can clearly be seen at approximately 2 minutes.

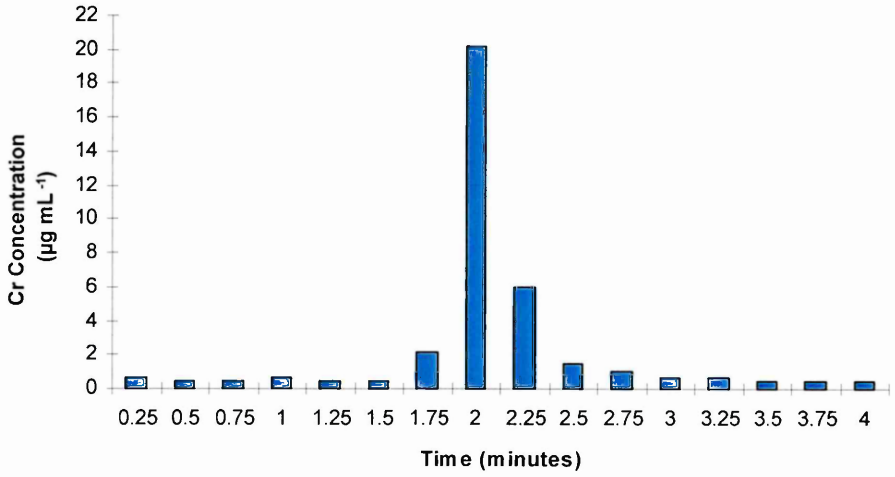

Figure 78: ETAAS analysis of fractions collected after IC of acetic acid extraction of BCR CRM 483.

Standard addition of Cr(VI) was then carried out on acetic acid extractions of the BCR CRM 483 in order to determine if the chromium present at approximately 2 minutes in

the IC chromatogram was due to Cr(VI) or to some other chromium species. Added Cr(VI) appeared at the same position. Further confirmation of the presence of chromium was obtained by ETAAS analysis of fractions collected after standard addition trials.

In order to determine what component of the matrix was affecting the Cr(VI) and causing it to elute at 1.8 minutes, ICP-MS analysis was carried out on fractions collected after IC of the acetic acid extract of BCR CRM 483. The matrix elements Mg, Al, Si, Ca, Mn, Fe, Ni, Co, Cu, and Zn were determined. Figure 79 shows the results obtained.

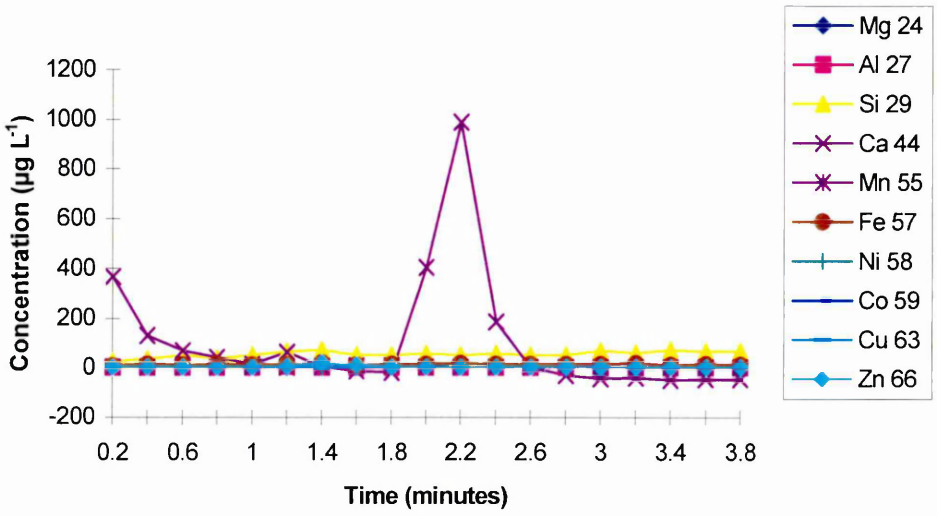

Figure 79: ICP-MS of fractions collected after IC of an acetic acid extraction of BCR CRM 483.

As can be seen in Figure 79, calcium was detected in the fractions containing Cr(VI) indicating that the two elements may be linked. It is likely that the Cr(VI) is associated with Ca^{2+} producing a neutral compound (possibly $CaCrO_4$) during extractions, which then elutes close to the solvent front. Acetic acid will also dissolve calcium carbonates

present in the matrix (according to Equation 50) making calcium available to bind CrO_4^{2-}:

Equation 50

$$CaCO_3 + 2CH_3COOH \rightleftharpoons Ca^{2+} + 2CH_3CO_2^- + CO_2\,(g)^{[173]}$$

A number of attempts using chemical procedures were made to remove the calcium interference. See Table 37.

Table 37: Trials carried out to try and remove calcium interference (detection by IC-CL).

Remedy	Observation
Dilution Significant dilution of samples to see if matrix effects would be reduced before LOD was reached.	In spite of significant dilutions the peak at 1.8 mins remained until no longer detectable.
Oxidation with Potassium Peroxidisulphate ($K_2S_2O_8$)[185] In order to analyse Cr(III) and then total Cr.	This appeared not to be a strong enough oxidising agent as only some Cr(VI) occurred in the correct position. Also Cr(III) was not oxidised as expected.
Complexation with Ethylenediamine tetraacetic acid (EDTA)[131] $Ca^{2+} + EDTA^{4-} \leftrightarrow [Ca(EDTA)]^{2-}$	Cr(VI) peak split and Cr(III) peak reduced in size, possibly due to complexation with EDTA (although this normally occurs slowly due to the kinetics) or due to formation of $Cr(OH)_3$.
Precipitation with Na_2CO_3 It is possible to precipitate carbonates of calcium: $Ca^{2+} + CO_3^{2-} \leftrightarrow CaCO_3$ (white ppt)	No precipitate was observed. No peak was observed for Cr(VI), but Cr(III) peak was increased. Possibly due to reduction of Cr(VI) by the HNO_3 used for acidification.
Precipitation with ammonium carbonate (NH_4HCO_3) In order to obtain a high enough carbonate concentration to precipitate $CaCO_3$ ammonium carbonate should be used in aqueous ammonia solution.	High amounts of chromium impurities were observed, therefore no conclusions could be made. However, it is likely that the Cr(III) would be precipitated as $CrCO_3$.

Remedy	Observation
Chelex 100 chelating resin This is an iminodiacetic acid resin (Na^+ form) consisting of cross-linked polystyrene beads. It can be used for concentrating or removing polyvalent cations from solution. Both batch and column methods were tried.	It appears that the Ca^{2+} is being removed, since the peak at 1.7 mins. is much reduced in size, but along with the Cr(VI) since there is still no peak for this at 2.5 mins. as expected.
Dowex 50WX8 chelating resin This is a sulphonic acid strongly acidic cation exchanger (H^+ form). The resin has an affinity for cations and can therefore retain calcium as shown:[186] $Ca^{2+}(aq) + 2H^+(res) \leftrightarrow Ca^{2+}(res) + 2H^+(aq)$	The peak at 1.7 minutes was almost totally removed and a small peak for Cr(VI) was observed, but this was found to be due to an impurity in the NaOH used.
Formation of a phosphate Sodium salts of condensed phosphates are widely used as water softeners as they form soluble salts with calcium and other metals[131]. $Ca^{2+} + 2PO_4^{3-} \leftrightarrow Ca^{3+}(PO_4)_2$	No Cr(VI) peak was observed and the Cr(III) peak disappeared, probably due to the formation of a phosphate.
Precipitation with ammonium oxalate ($(NH_4)_2C_2O_4$) The addition of ammonium oxalate precipitates calcium oxalate, CaC_2O_4, a white crystalline salt:[173] $Ca^{2+} + C_2O_4 \leftrightarrow CaC_2O_4$ (white ppt)	Precipitation was observed in most samples, but no signal for Cr(VI) was seen. Cr(VI) could be taking part in: $CaCrO_4+(NH_4)_2C_2O_4 \leftrightarrow CaC_2O_4+ (NH_4)_2CrO_4$ or $CaC_2O_4+ HCrO_4^- + NH_3$ (NH_3 has been found to totally quench the CL reaction)
Precipitation with ammonium oxalate Weighing of precipitate	The amount of precipitation was more than could be obtained from the amount of calcium present. CrO_4 is either precipitating with the calcium or as $(NH_4)_2CrO_4$.
Precipitation with ammonium oxalate Removal of ammonium Gaseous ammonia is liberated upon addition of a strong non-volatile base e.g. NaOH[173] $NH_4^+ + OH^-$ (from NaOH) $\leftrightarrow NH_3(g) + H_2O$ This can be detected by moist red litmus.	When moist red litmus paper was placed over the heated bottles the pH was alkaline, indicating that ammonia was being evolved. The heating was continued until no further alkalinity was detected, but still no peak for Cr(VI) was observed.
Calcium Hydroxide This is used in the treatment of hard water and causes the precipitation of $CaCO_3$:[187] $Ca(OH)_2(aq) + Ca(HCO_3)_2(aq) \leftrightarrow 2CaCO_3(s) + 2H_2O$	This method also precipitated the Cr(III) as $Cr(OH)_3$.

Remedy	Observation
Reduction of Cr(VI) with K_2SO_3 It was decided to try and reduce the Cr(VI) as at least then a value for the total chromium could be obtained. Both 0.015 mol L^{-1} and 0.3 mol L^{-1} K_2SO_3 were tried.	No reduction of the Cr(VI) was observed.
Reduction of Cr(VI) with HNO_3 Although HNO_3 normally acts as an oxidising agent, Cr(VI) is reduced to Cr(III) in acidic solutions due to the pH as can be seen from the Eh-pH diagram for chromium (see Figure 1): $Cr_2O_7^{2-}(aq) + 14H^+(aq) + 6e^- \leftrightarrow 2Cr^{3+} + 7H_2O$[188]	For Cr(VI) alone reduction occurred, but in the presence of Ca^{2+} the Cr(VI) peak disappeared, but there was no increased Cr(III) peak. A stronger reduction was required in order to break the Cr(VI)/Ca^{2+} association.
Reduction of Cr(VI) using HNO_3 and H_2O_2 This provides a better source of hydrogen ions for the reduction of Cr(VI) to Cr(III): $Cr_2O_7^{2-}(aq) + 14H^+(aq) + 6e^- \leftrightarrow 2Cr^{3+} + 7H_2O$[188]	The results proved that quantitative reduction of Cr(VI) to Cr(III) could be achieved.
Standard addition of chromium along with addition of calcium to the samples It was found that upon standard addition the Cr(VI) was additive at 1.7 mins, until a certain amount, then it occurred at 2.5 mins, i.e. the Ca^{2+} is of a finite amount. Calcium addition could keep the Cr(VI) at 1.7mins.	Extra calcium at various amounts was added to samples. A Ca^{2+} addition of 10 mg L^{-1} was found to be sufficient.

Out of all the methods tested in Table 37, the methods which actually worked were the standard addition (with added calcium) and the reduction of the Cr(VI) to Cr(III) with HNO_3/H_2O_2.

A comparison of the results obtained for Cr(III), Cr(VI) and total chromium for several analyses using either standard addition (with added calcium) or reduction can be seen in Table 38. These results obtained by the two methods are in good agreement with the certified total chromium amount. Figure 80 shows the results obtained. These were

found not to be significantly different from the certified values. The significance was tested using both one and two-tailed students' t-test at a 95% confidence limit. Since there appeared to be no difference in the use of the two methods, reduction was chosen due to this procedure being simpler to perform.

Table 38: Determination of Cr(III) and Cr(VI) in BCR CRM 483 acetic acid extractions using standard addition or reduction (IC-CL detection unless otherwise stated).

Sample	Cr(III) mg L^{-1}	± 1 s.d. (n = 6)	Cr(VI) mg L^{-1}	± 1 s.d. (n = 6)	Total Cr mg L^{-1}	± 1 s.d. (n = 6)
Certified value	-	-	-	-	18.7	1.0
Standard Addition 1	0.37	0.1	20.5	1.3	20.9	1.3
Standard Addition 2	0.71	0.1	17.4	3.0	18.1	3.0
Reduction 1	0.37	0.1	18.5	0.6	18.9	0.6
Reduction 2	0.71	0.1	17.1	0.5	17.8	0.5
Reduction 3	0.73	0.1	17.4	0.5	18.2	0.5
ETAAS 1	-	-	-	-	18.8	0.3
ETAAS 2	-	-	-	-	18.9	0.4

Standard addition = standard addition of Cr(VI) with added calcium
Reduction = reduction of Cr(VI) using HNO_3 and H_2O_2
ETAAS = electrothermal atomic absorption spectrometry
s.d.=standard deviation

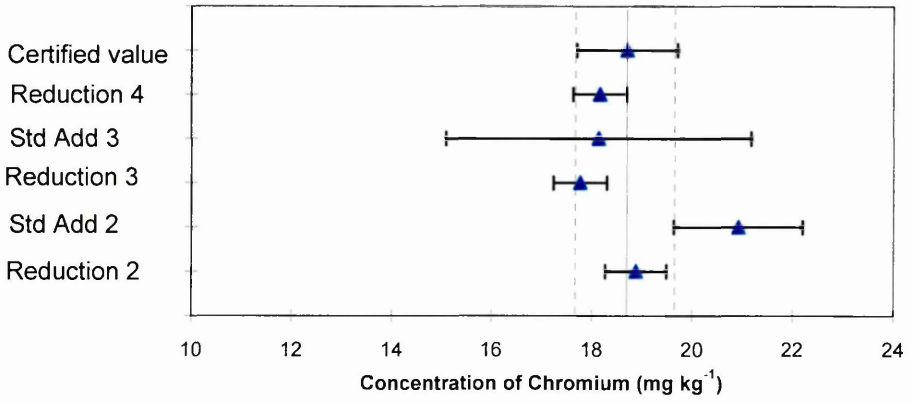

Figure 80: Comparison of results for acetic acid extraction of BCR CRM 483 (IC-CL detection).

4.6 Conclusion

An extraction method was found that extracted chromium species without changing the speciation in the process. Acetic acid extracts the exchangeable chromium species particularly Cr(VI), which is not tightly bound in soils. Good agreement was obtained between both the IC-CL and the ETAAS methods for total chromium in the soil samples. ETAAS is an established and reliable method for the analysis of total chromium. In this study the IC-CL method was shown to obtain the same results for total chromium and give reproducible values for the two species. The developed method can be used to assess the amount of bioavailable Cr(VI) in soils.

CHAPTER 5 SAMPLING AND ANALYSIS OF A FIELD SOIL

A representative sample of soil from a farmer's field was collected in order to carry out several of the procedures that are common in the preparation of reference materials. The aim was to be able to obtain reproducible results for the extraction of chromium species from a real sample.

5.1 Introduction to Soil Sampling

Sampling is a critical but often overlooked stage in an analytical process. It is essential that the sample collected is representative of the particular location[189]. Important considerations for soil sampling include[190]:

- to define the site (location, place and position of sample removal)
- to ensure a representative sample of the area is taken (pattern of sampling)
- to define the sampling depth to be used
- size of the sample to be taken (size of each core and total size of bulk sample)
- number of samples to be taken
- selection of appropriate sampling equipment (different tools for moist or dry soil)
- handling, storage and transport of samples after collection
- to ensure the possibility of reproducing sampling conditions for repeat analysis.

The heterogeneous nature of soil makes it difficult to sample. The two commonly accepted sampling procedures for sampling of fields include sampling along a 'W' track[191] and the zigzag method[192]. In the first method 20-30 samples are taken along a 'W' shaped track for each 1-4 hectares (See Figure 81A) (1 hectare = 10,000

square metres). In the second, around 24 samples are taken along a zigzag path, taking one sample from each sampling unit, as shown in Figure 81B.

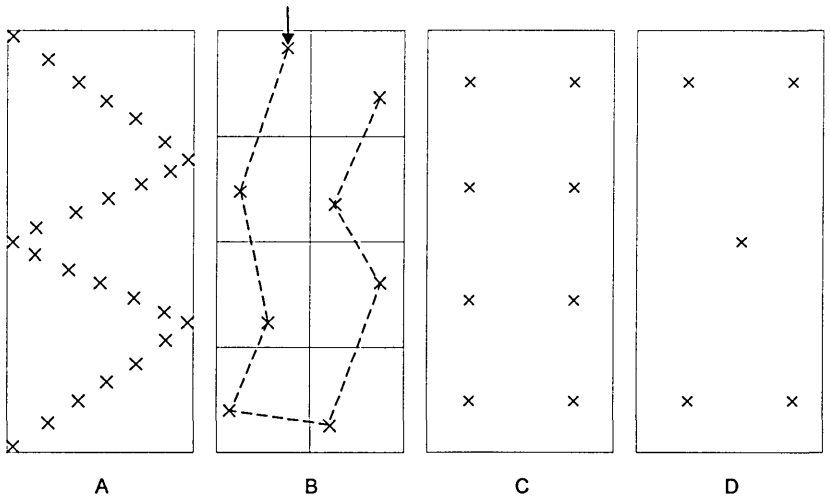

Figure 81: Methods for soil sampling of fields.

The sampling patterns C and D are unsuitable, since they will not result in a representative sample of the whole field. In procedure C the centre of the field is not sampled and the results are likely to be biased by row applications and in procedure D the samples are biased towards the end of the plot, and too few cores have been taken.

Since pollution distribution is not likely to be homogeneous, it is important to use composite samples. A composite sample can be said to 'give a mean analytical value representative of the soil sampling volume from which the composite sample was drawn'[193]. The fundamental requirements of a valid composite sample are:

- Each core should be of the same volume and represent the same cross section of the sampling volume.
- The cores should be taken at random with respect to the sampling volume.
- Enough cores should be taken to adequately represent the whole sampling volume.

The sample should include a sufficient number of cores to ensure that the composite samples are representative of the area sampled. Increasing the number of cores lowers the variability of the sample characteristics. In practice, combining 20 to 30 cores is usually sufficient in providing representative samples of a given area[194].

Soil is not uniform with depth, but is divided into bands termed horizons. Therefore when sampling soils, it is important to specify the depth at which the samples are collected. Since soil characteristics vary with depth, arable land should be sampled by auger to plough depth (around 20 cm) and permanent pasture to a depth of around 10 cm. Two types of auger are available for soil sampling (see Figure 82). The closed cylinder type auger is suitable for dry soils, whereas moist or clay-type soils are sampled with the standard 8 or 10 cm post-hole auger[195].

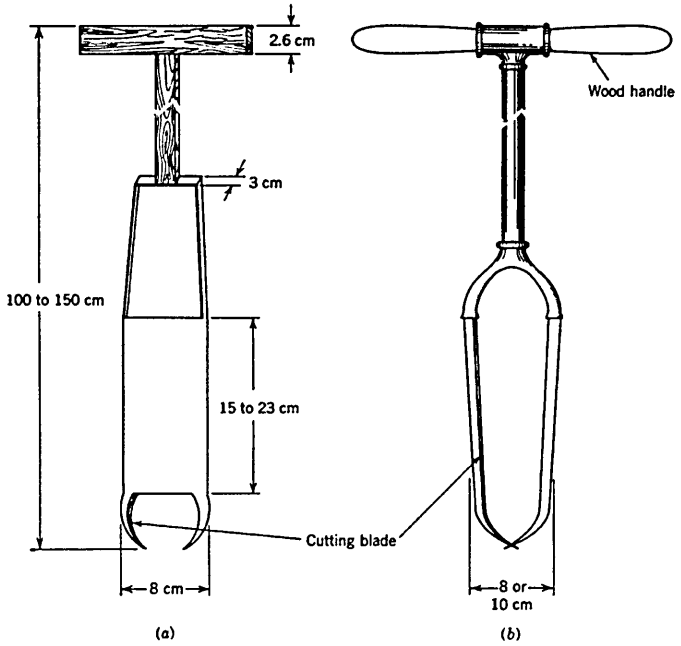

Figure 82: Post-hole type sampling augers: (a) closed cylinder auger; (b) standard post-hole auger. Taken from Jackson[193].

The bulked or composite sample, made up by combining the individual sampling units, should consist of at least 1-2 kg of moist soil, i.e. sufficient to provide 0.5 kg of dried soil. The samples should be stored in polyethylene, or other inert material, bags, and externally labelled with an identifying number for transport to the laboratory for drying and further treatment. It is important to label externally to the sample, as tapes, labels and inks may introduce metal contamination[196].

Once the bulk sample has been obtained it is then necessary to take smaller sub-samples for analysis that are still representative of the whole. This can be achieved in a number of ways (see Figure 83). Scoop sampling is not ideal, as soil undergoes partial fractionation according to particle size, thus causing sub-division in the elemental composition and subsequent errors in the analysis. Mechanical rifflers may not always be suitable for trace element analysis as they are constructed from materials that are likely to introduce contamination. Coning and quartering, on the other hand, requires little apparatus and is adaptable to any bulk sample size.

In the coning and quartering procedure the bulk material is thoroughly mixed and this is poured on to a clean sheet of polythene to form a cone. The cone is divided into four quarters and the two opposite quarters combined and mixed to form a sub-sample of approximately half the original weight. This half sample is again coned and quartered and the process repeated until a sub-sample of a little over the desired analytical sample weight is obtained.

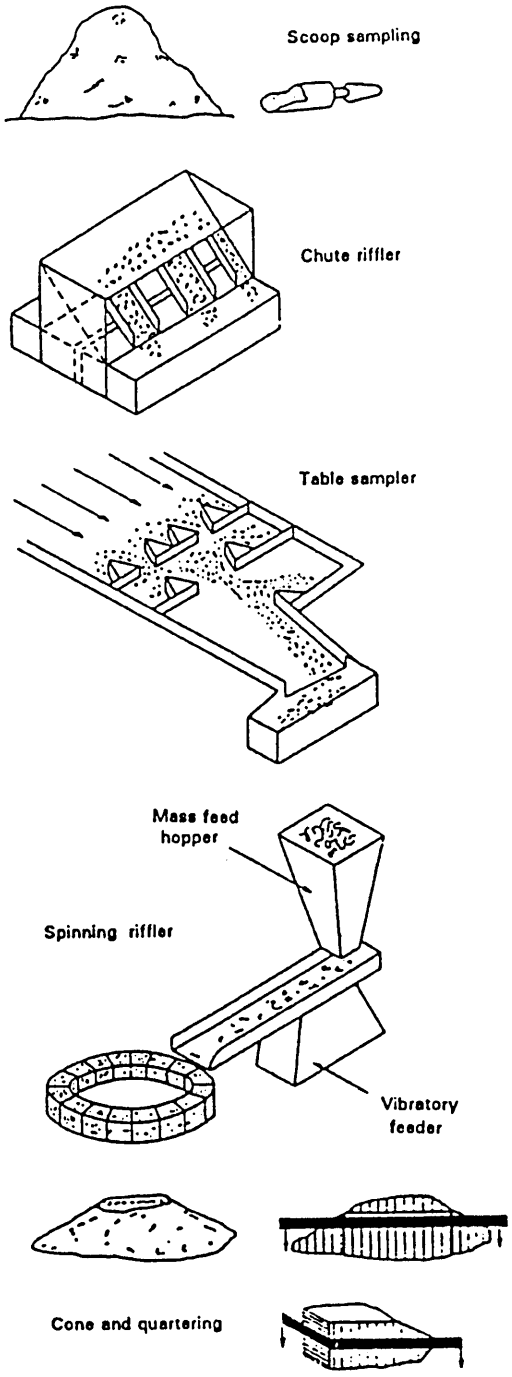

Figure 83: Techniques for sub-sampling of soils. Taken from Allen & Khan[197].

5.2 *Field Moist Soil Sampling*

A field moist soil was collected from a farmer's field in Tenaart, Geel, Belgium, the dimensions of which are shown in Figure 84. The field had previously been planted with sweetcorn and various fertilisers and pesticides had been applied to the plants and soil. The soil was sampled by use of a specially designed PTFE coated 20 cm standard post-hole auger (see Figure 82) with an aperture of 8 cm. It was important to avoid the use of the standard stainless steel tools, as they contain chromium. A composite sample, consisting of twenty seven core samples, was taken by sampling along the 'W' shaped pattern shown in Figure 84. The soil was stored in polyethylene bags with press closures, which were subsequently stored in labelled plastic bags sealed with elastic bands. The samples were then kept in a cool dark place until required. Samples were also taken and frozen for reference.

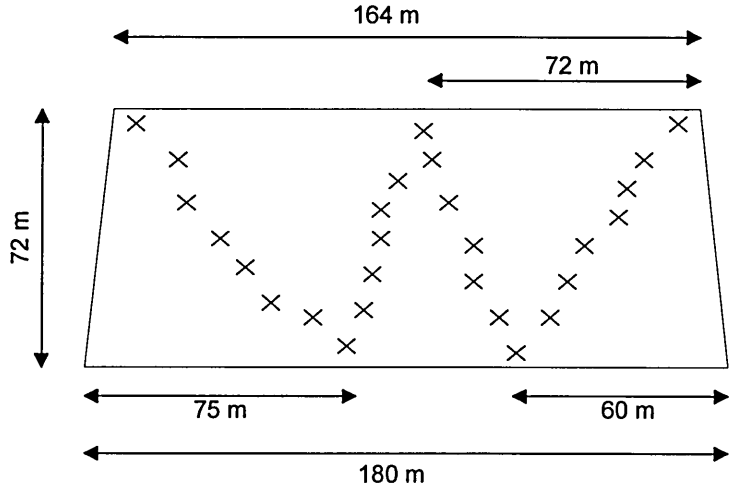

Figure 84: Plan for soil sampling of a farmer's field in Tennart Belgium.

In order to obtain a representative smaller sample (0.25 g per sample) for analysis, coning and quartering was carried out on the main (composite) sample[198]. This method

is normally successfully employed, so long as the original sample size is not too large. The method was carried out as follows:

- The composite sample was mixed by pouring the sample onto a polythene sheet and by moving the heap from one place to another.
- The top of the cone formed was then flattened and a cross marked on the surface.
- Opposite quarters were selected, combined and the procedure repeated again on this smaller sample until a sample of the required size was obtained.
- This procedure was repeated to obtain further samples as required.

The acetic acid extraction procedure detailed in section 4.3 was used on the soil sub-samples followed by ion chromatography with chemiluminescence detection (IC-CL) (see section 3.5.4) for the determination of the chromium species. Samples were also analysed by ETAAS (see section 3.5.3) for total chromium content in order to validate the results obtained by IC-CL. A total of seven different samples were extracted with acetic acid and analysed. All analyses were carried out in triplicate.

5.3 Results and Discussion

The results obtained from the acetic acid extraction and IC-CL analysis of this soil are shown in Figure 85. As can be seen good agreement is obtained between the different samples taken, all of which agree to within their standard deviation. The values were found not to be significantly different when tested using both one and two-tailed students' t-test at a 95% confidence limit. The average concentration for total chromium was found to be 0.15 ± 0.01 mg kg^{-1}.

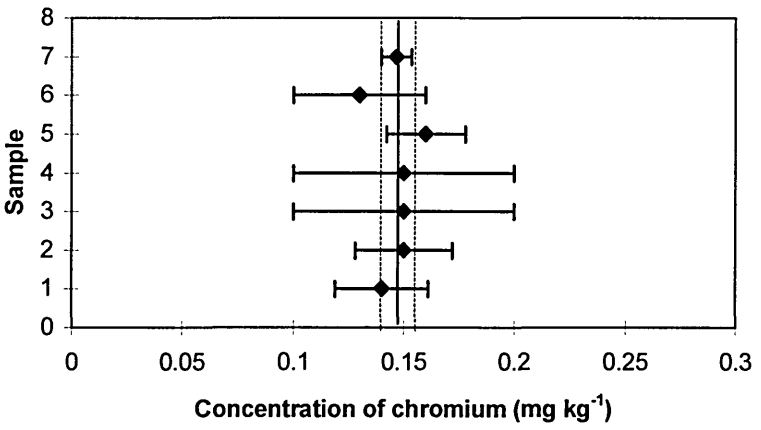

Samples 1-6 = separate samples of 0.25 g field soil extracted with 0.43 mol L^{-1} acetic acid, each analysed in triplicate.
Sample 7 = average ± std. dev. of 1-6.

Figure 85: Results of soil acetic acid extractions with analysis by IC-CL.

The total concentration of chromium determined by IC-CL also agrees well with that determined by ETAAS (see Figure 86). Here the individual concentrations of Cr(III) and Cr(VI) are also shown. Again good agreement was obtained between the seven different samples analysed and the values were found not to be significantly different when tested using both one and two-tailed students' t-test at a 95% confidence limit. The total chromium content determined by ETAAS was 0.14 ± 0.02 mg kg^{-1}. The levels of Cr(III) and Cr(VI) were 0.02 ± 0.004 and 0.13 ± 0.01 mg kg^{-1} respectively.

This characterised soil was subjected to the various steps used in the production of reference materials in order to study likely changes in chromium speciation in the sample (see CHAPTER 6).

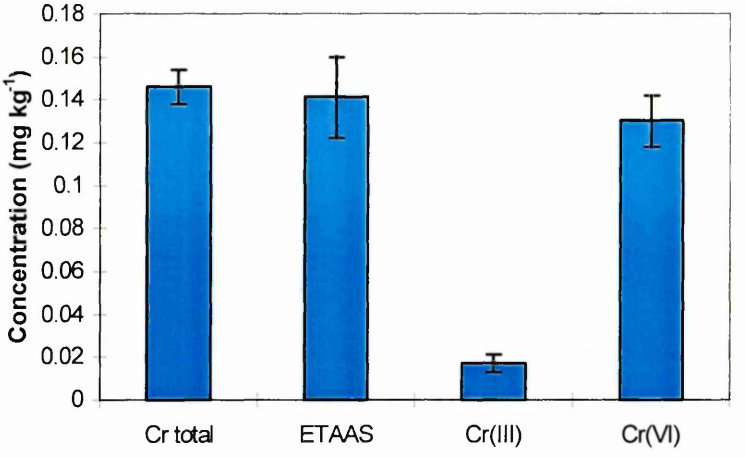

Figure 86: Distribution of chromium species in a field soil and comparison of total chromium analysed by IC-CL and ETAAS (n=7; 3 replicates per sample).

CHAPTER 6 PRODUCTION OF REFERENCE MATERIALS

6.1 Introduction

The role that certified reference materials (CRMs) play in analytical practice is in principle well recognised and has been widely discussed[199-201]. Over the last twenty years the European Commission has supported improvements in the quality of chemical measurements by means of reference materials (RMs), through its Standards, Measurements and Testing programme[202]. A review of their use and prospects in Europe has recently been published[203] and the role that they will play in the future has also been discussed by Rasberry[204]. Generally, there are two types of reference material[205,206], according to the following ISO definitions[207,208].

Reference Material (RM)

A material or substance, one or more properties of which are sufficiently well established to be used for the calibration of an apparatus, the assessment of a measurement method or for assigning values to materials.

Certified Reference Material (CRM)

A reference material, for which one or more property values are certified by a technically valid procedure, accompanied by or traceable to a certificate or other documentation that is issued by a certifying body.

The fundamental difference between RMs and CRMs is that some parameters in CRMs are known with great accuracy and the CRM represents a higher metrological standard,

since it must be accompanied by a certificate which gives the certified value and its uncertainty at a specified confidence limit.

RMs can be divided into the following categories[205,209]:

- *Pure substances or solutions* for identification and/or calibration purposes; pure substances are generally certified by establishing the maximum amount of impurities present.
- *Materials of known matrix composition* for the calibration of comparative measuring instruments; certified calibration solutions have to be prepared on a mass basis in experienced laboratories by specially trained personnel.
- *Matrix RMs* which, as far as possible, represent the matrix of the sample being analysed and whereby the content of a certain number of components are certified; such materials are mainly used for verification of a measurement process.
- *Methodologically defined RMs*; the certified value is defined by a given method and is not traceable to a primary standard.

The manufacture and certification of RMs are extremely labour intensive and time consuming[210], with regular changes being made in order to meet international standards[211-213]. Production guidelines[214] are constantly being amended[215] and updated[216].

The analytes of interest must be specified in advance and losses or contamination of the material should be avoided. The concentration level may represent a natural non-contaminated, contaminated or artificially spiked material at a level corresponding to a regulatory limit.

The materials produced must satisfy many, often rigorous, criteria. The most important of these are stability, homogeneity and representativeness [205,209,217].

6.1.1 Stability

The stability of a RM is one of its most important characteristics. Certified values of the RM should remain unchanged during transportation (short-term stability) and during storage (long-term stability). RMs can be sensitive to degradation due to temperature, light, humidity, microbial activity etc. Therefore stability testing is necessary. Short-term degradation studies (of a few months, at conditions that can be met during transportation) are carried out in order to determine the best conditions for transport. These studies are generally carried out at relatively high temperatures e.g. 40, 18, 4 and -20°C. Long-term stability studies on the other hand are aimed at determining storage conditions. RMs are stored at temperatures of for example 4 and -20°C, and lower temperatures (e.g. liquid nitrogen) and analysed periodically over a period of at least two years.

6.1.2 Homogeneity

Homogeneity is an important attribute of the sample, and ensures that all subsamples taken for measurement will produce the same analytical result, within the measurement uncertainty. The contribution of detectable heterogeneity to the overall uncertainty of the individual RMs has been discussed by Kane[218]. The RM should be homogeneous or re-homogenised easily; this means that within bottle or between bottles there is no significant difference in the certified values or in the matrix.

Materials composed of many phases (e.g. soils) are never homogeneous with respect to trace and ultra-trace components. For this reason, a minimum sample size representative of the whole, is generally recommended by the producer. The minimum sample size depends on the material and can vary from hundreds of milligrams to around a gram. Kurfurst et al.[219] have discussed the micro-heterogeneity present within some RMs.

6.1.3 Representativeness

The RM should be representative of the actual sample being analysed with respect to the matrix composition, contents of the analytes of interest, nature of their binding, fingerprint pattern of interfering substances and physical status.

RMs are necessary in order to assure analytical quality. They are necessary in all types of analytical laboratories and their applications include the following:

- Testing the skill of analytical laboratory personnel.
- Routine control of the quality of analytical laboratory work.
- Testing detectors and sensors used in analytical instruments.
- Testing applicability of a new method to new matrices.
- Validation of new analytical methods.

It is essential that extreme care is taken during the preparation of the RM and that quality guidelines are followed[220] in order to ensure that a stable, homogenous and representative sample is obtained[221]. It is also essential to ensure traceability[222-225] of the measurements made when certifying RMs in order to ensure measurement

reliability. Currently there is a move towards linking laboratory accreditation[226] to metrology[227,228].

6.2 Production Steps

Several typical production stages were carried out on the previously characterised field moist soil sample in order to observe any changes in the speciation that might occur during these types of manipulations. The production stages selected were drying, jet milling, ball milling, sieving, homogenisation and bottling, as shown in the flow diagram (Figure 87).

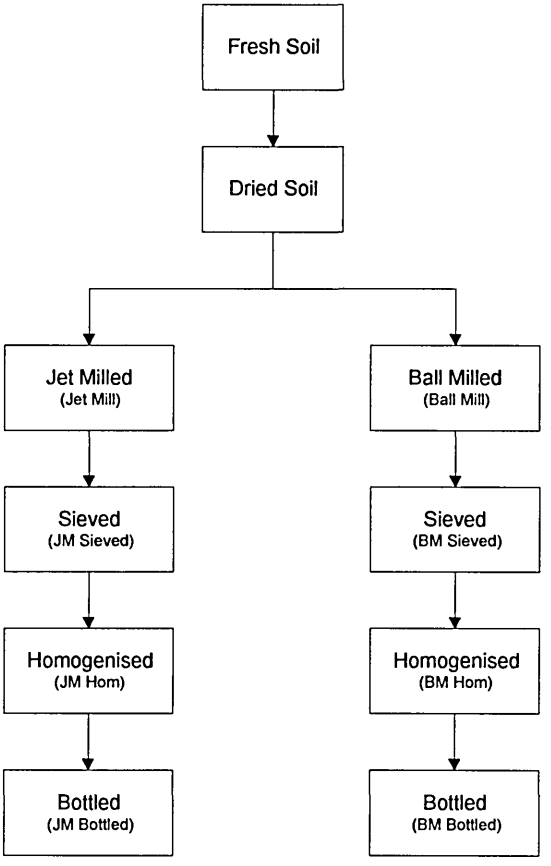

Figure 87: Flow diagram showing production steps.

6.2.1 Drying

The field moist soil sample was placed in a PTFE lined tray. This was then placed in a Heraeus Thermicon P drying oven (Laborbedarf Saarbrücken, Saarbrücken, Germany) at a constant temperature of 105°C overnight (16hrs). The soil was then removed and any large aggregates crushed using a nylon rolling pin. Drying is carried out in order to reduce and preferably prevent microbiological degradation, which would cause the RM to be unstable and it would be impossible to certify the values of the constituents. In general, microbiological degradation can be minimised by reducing the water content of the material to levels below 1%[229]. A Karl Fischer analysis was carried out on the dried material in order to determine the residual water content.

6.2.2 Karl Fischer Titration

A titration for the determination of water in solids e.g. soil[230] can be carried out with good specificity by use of a Karl Fischer reagent[231]. This reagent was in the past composed of iodine, sulphur dioxide, pyridine and methanol[232]. However, pyridine is a known carcinogen, and therefore in recent years safer Karl Fischer reagents using alternative bases in place of the pyridine have been developed. The mixture reacts with water according to Equation 51[233]:

Equation 51

$$CH_3OH + SO_2 + RN \rightarrow [RNH]SO_3CH_3$$

$$H_2O + I_2 + [RNH]SO_3CH_3 + 2RN \rightarrow [RNH]SO_4CH_3 + 2[RNH]I$$

where RN = base (in this case imidazole).

The sulphur dioxide reacts with the alcohol to form an ester, which is neutralised by the base. The anion of the alkyl sulphurous acid is the reactive component. The titration of water constitutes the oxidation of the alkyl sulphite by the iodine.

There are therefore two prerequisites in order to ensure a stoichiometric course for the Karl Fischer reaction[234]. The first is the presence of a suitable alcohol to completely esterify the sulphur dioxide and the second is a suitable base. A suitable base is necessary for the complete neutralisation of the acids produced during the reaction. The basicity of pyridine is too low to completely neutralise the acid and is the cause of the "sluggish" titration observed using the "classic" Karl Fischer reagents. If the base is too strong, the solution becomes too alkaline and an end point will not be reached. A titration in the pH range of 5-7 is preferred and this can be optimised with the use of imidazole[235].

The end point of the reaction is detectable by a colour change from the yellow of the reaction products to the brown of an excess of pyridine. The colour is intense enough for a visual end point determination, however greater accuracy can be obtained by the use of an automated potentiometric determination. This is carried out using a pair of platinum electrodes, which maintain a constant current (around 5-10 μA) between them. Prior to the end point the current flows at a low applied voltage, because the solution contains I_2 from the Karl Fischer reagent and I^- as a product of the reaction shown in Equation 51. The following reactions occur at the anode and cathode.

Equation 52

Anode: $2I^- \rightarrow I_2 + 2e^-$

Cathode: $I_2 + 2e^- \rightarrow 2I^-$

At the end point all of the iodine (I_2) has been consumed and, in order to maintain the current, the cathode potential changes dramatically as methanol is now reduced.

Equation 53

$$CH_3OH + e^- \rightleftharpoons CH_3O^- + \frac{1}{2}H_2O$$

This sudden change in voltage can be easily read and marks the end point.

6.2.2.1 Experimental

Two hundred milligrams of soil was taken and added to 30 mL of dry methanol (titrated to dryness with the titrant solution). The mixture was stirred for a few minutes to ensure a homogeneous mixture. The titrant solution (Hydranal Composite 5, Riedel-de Haën, Germany) was added until the end point was reached, at which point the solution had turned from pale yellow to dark brown. This titration was automated with the use of a 701 KF Titrino automated titration equipment from Metrohm, Switzerland (see Figure 88). The titration procedure was repeated three times.

The results (mean = 0.65% moisture content by weight) showed that the water content had been reduced sufficiently i.e. was below 1%. A sample calculation is shown in Appendix 7.

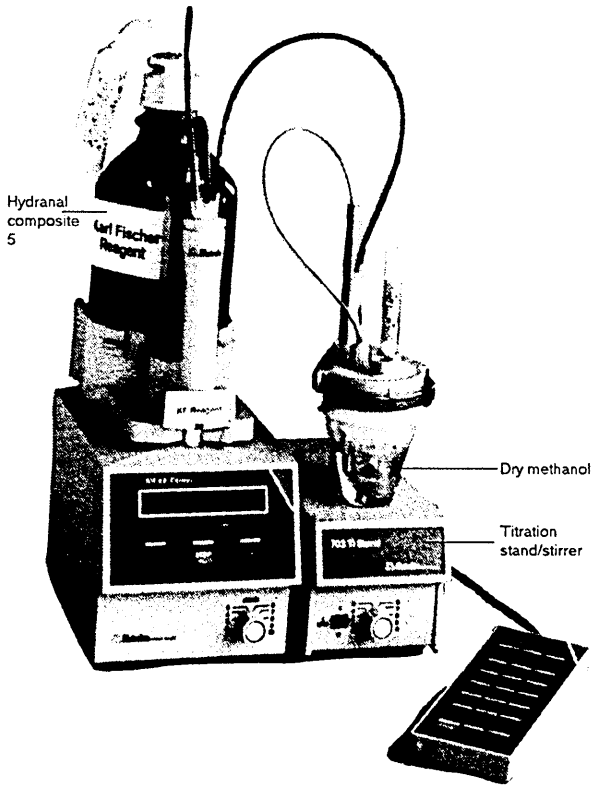

Figure 88: Karl Fischer titration apparatus (adapted from product manual[236]).

6.2.3 Jet milling

Fine grinding of the soil was carried out using a Multi Processing System (100 AFG Jet Mill/50 ZPS Impact Mill/50 ATP Ultrafine Classification System), Alpine, Augsburg, Germany, see Figure 89.

The bottom section of the jet mill consists of three nozzles (see Figure 90), through which an air pressure of 6 bar is blown. The three dimensional nozzle arrangement combines opposing air streams with a flow bed (2), thus enabling the feed material to be completely ground virtually without residue. The air is used to accelerate the feed

material particles, which impact on each other and generate size reduction, without contamination of the material.

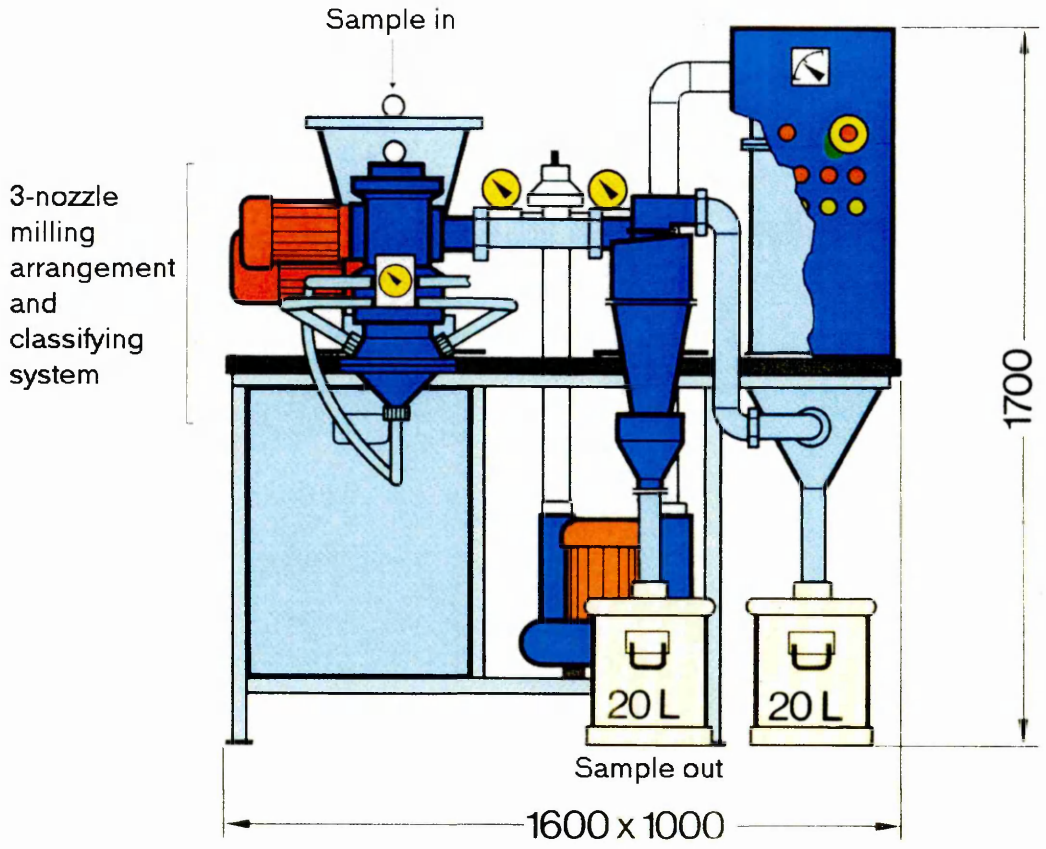

Figure 89: Alpine Jet-Mill (adapted from manual[237]) showing approximate dimensions in mm.

Fine particles are blown up by the lower air jet stream and extracted through the classifying wheel (1) at the top of the chamber. Larger particles are separated by the classifying wheel, fall down and are re-milled in the circulation loop. Depending upon the feed material and the speed of the classifying wheel, particles between 5 and 20 µm, characterised by closely defined size distribution, can be extracted. The faster the classifying wheel spins the smaller the aperture through which particles may pass and therefore the smaller the final particle size collected. After jet milling the particle size of

the resulting material was determined, using a Sympatec Helos particle size analyser (Sympatec GmbH, Zellenfeld, Germany), as <63 μm for 98 % of the particles (see Appendix 8).

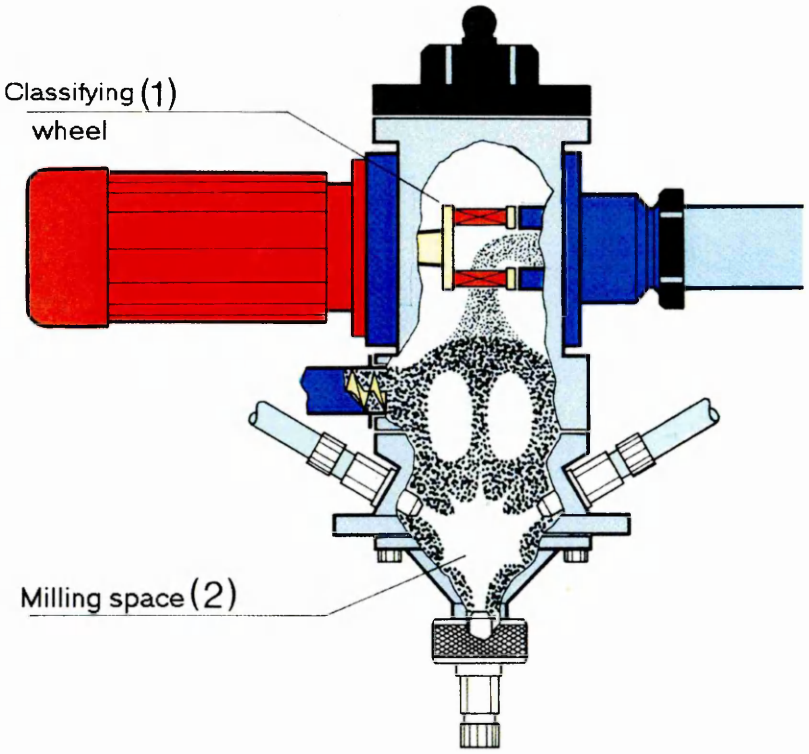

Figure 90: Jet Mill nozzle arrangement and classifying system (adapted from manual[237]).

6.2.4 Ball milling

A portion of the dried soil was taken and ball milled. The ball milling was carried out using a Fritsch Pulverisette 5 Labor-Planeten-Kugelmüh (Fritsch GMBH, Idar-Oberstein, Germany) planetary ball milling apparatus, which could accommodate four porcelain ball mills of 500 mL capacity (see Figure 91). The balls used were of 30 mm

diameter and were made of agate (an extremely hard stone). Optimum milling conditions were established by varying the number of balls, the speed and the time.

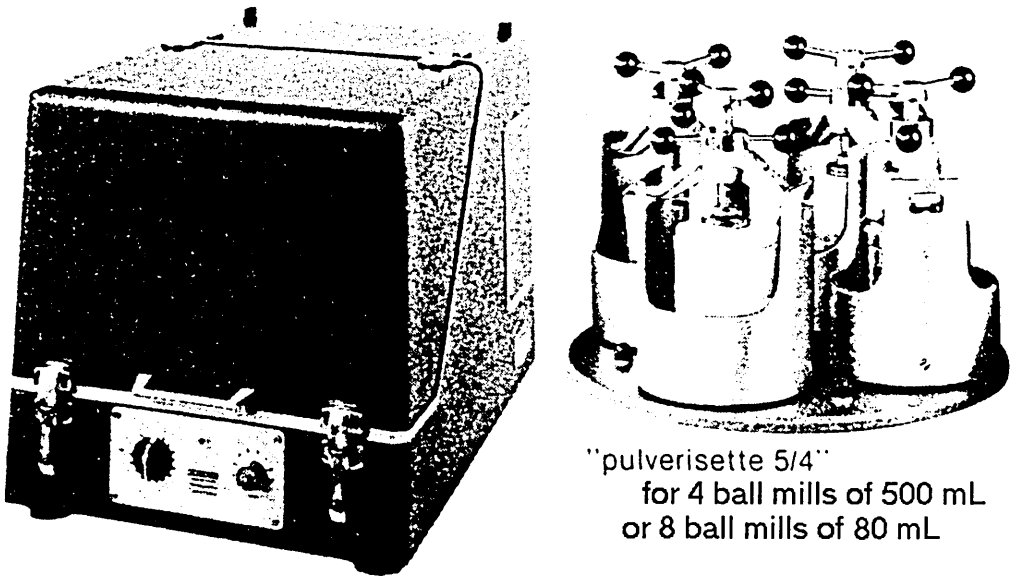

Figure 91: Fritsch Pulverisette 5 ball milling apparatus (from manual[238]).

The grinding balls of a planetary mill reach much higher energy in comparison to conventional ball mills e.g. gravitational and centrifugal ball mills. The grinding medium and grinding balls are released from the inner wall of the grinding vessel and the effective centrifugal acceleration reaches approximately twelve times the acceleration due to gravity. Therefore, a high grinding performance in a planetary mill, is achieved in a relatively short time.

Centrifugal forces are present due to the bearing plate (*"disk"*) and the rotation of the grinding vessel on the grinding medium. Because of the opposing rotational directions of the bearing plate and the grinding vessel, centrifugal forces act alternately in parallel and in opposition. This fact leads alternately to a run down of the grinding balls and a free crossing of grinding balls and grinding medium in the grinding vessel. The grinding

medium is ground by stroking and by rolling off (friction). Figure 92 shows the mode of operation of the planetary ball mill.

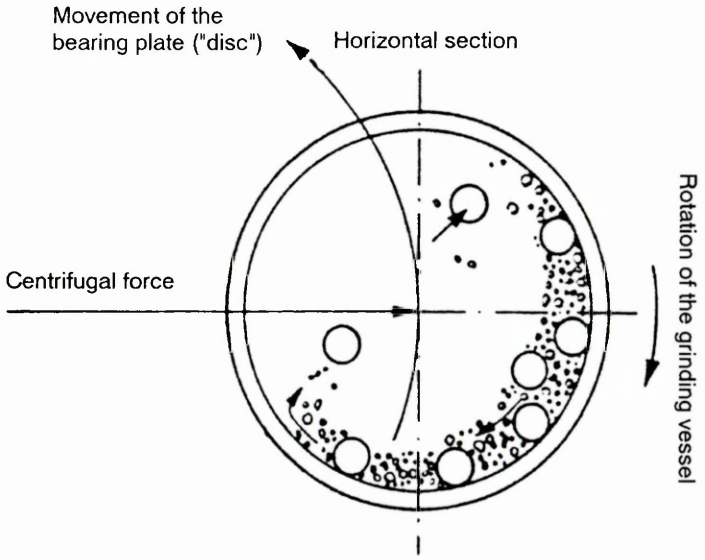

Figure 92: Mode of operation of a planetary mill (adapted from manual[238]).

Several trials were carried out using differing times, speed settings and number of balls (see Table 39).

Table 39: Ball milling trials.

Number of balls	Rotation speed rpm	Time (mins)	Particles < 125 µm (%)	Particles < 63 µm (%)
6	170	4	79	48
8	170	5	90	65
9	210	5	95	75
9	245	6	97	80
9	320	6	98	82

The milling conditions which gave the best particle size were those in which nine agate balls were used in each mill for a period of six minutes at a speed of 320 rpm. It was not possible to use more balls, because this would have hindered free rotation within the ball mill. The particle size of the resulting material was determined using a Sympatec Helos particle size analyser (Sympatec GmbH, Zellenfeld, Germany) (see Appendix 9). This gave a particle size of <125 μm for 98 % of the particles.

6.2.5 Particle Size Analysis

Analysis of the particle size of the ball milled or jet milled materials was carried out using a Sympatec Helios particle size analyser, Sympatec, Etten-Leur, The Netherlands (see Figure 93). A reference measurement was first taken of methanol alone. Then 15 mg of sample was taken and added to 10 mL of methanol. The cuvette containing the mixture was then placed in the instrument and the particle size was determined by laser diffraction. Stirring of the sample was carried out magnetically during analysis to ensure a homogenous distribution of particles. Resulting particle size graphs can be seen in appendices 8 and 9.

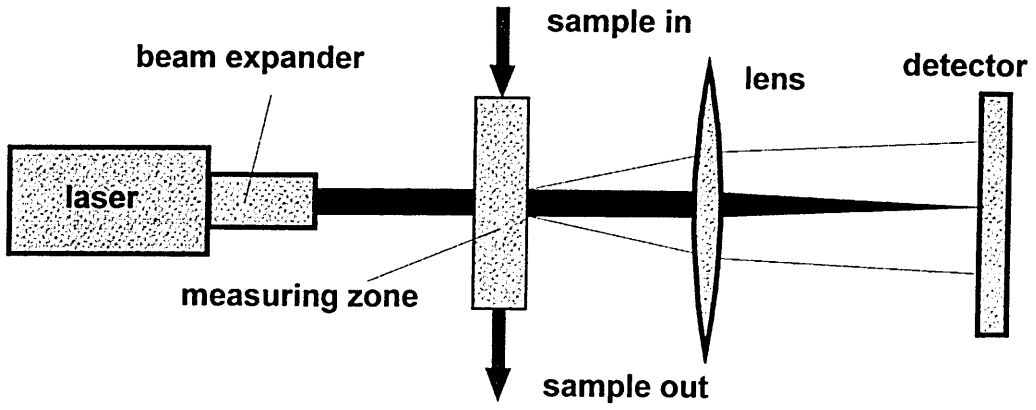

Figure 93: Diagrammatic representation of the laser diffraction instrument (from user notes[239]).

Laser diffraction is an advanced method for the determination of particle size distributions in a size range of about 0.1-3500 μm[240]. The theory behind this procedure is that of Fraunhofer diffraction physics. The instrumentation is demonstrated in Figure 93. It consists of a light source, in this case a He-Ne laser was used as a high energy, monochromatic, coherent parallel light beam for the generation of particle-light interactions. This is followed by a beam expander, which produces an extended and almost ideal wave field for the illumination of the dispersed particles. The particles interact with the incident light by means of diffraction, refraction, absorption and deflection. This generates an angular-dependent intensity distribution, which is converted by the lens into a spatial intensity distribution. This is then measured by a multi-element photo-detector and, after application of the Fraunhofer approach and Mie theory, distribution graphs are produced.

6.2.6 Sieving

Sieving was carried out by passing the ball milled or jet milled soil through a nylon sieve with a mesh size of 125 μm. Any particles that did not pass through the sieve were discarded. (These were few in number and constituted only a fraction of a percent of the bulk sample). Sieving can affect the mixing of the soil[193], causing partitioning, and it is therefore essential that it is thoroughly mixed before sampling.

6.2.7 Homogenisation

Portions of the jet milled and sieved soil or the ball milled and sieved soil were taken and homogenised. This homogenisation was carried out by placing a sample of the soil in a plastic container, which was then placed into a Turbula Shaker Mixer Type T200A (WAB, Switzerland), see Figure 94. This mixer is very efficient due to the use of the

motions of rotation, translation and inversion. These motions cause energetic ratios in the vessel which continually displace the substance within with alternate pulsing motions. These motions have a thickening and thinning effect on the material to be processed. The resulting eddies have a changing energy gradient which causes effective mixing, even of substances of different specific weights.

The mixer was operated at a speed of 90 rpm, turning through several different axes in order to ensure thorough mixing. The mixing was carried out for 6 hours.

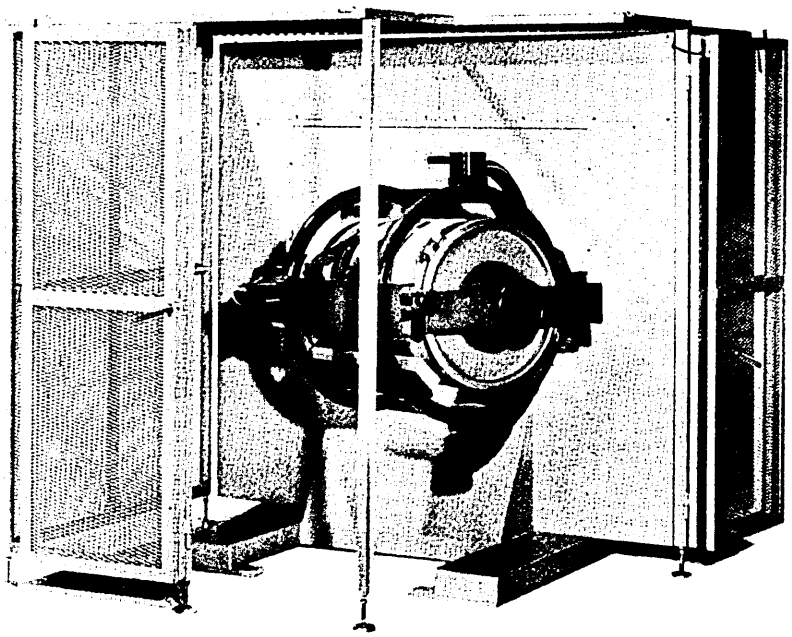

Figure 94: Turbula shaker mixer type T200A (from manual[241]).

6.2.8 Bottling

Bottling was carried out automatically using a tailor-made fully automated filling machine for powders type DM-1, Transmatic Fyllan Limited, Bedford, England (see Figure 95). The machine is composed of a turntable connected to a conveyor belt, which

conveys the bottles to the lift and load cell. Above this cell is positioned a hopper capable of holding 28 L of powder which is continuously stirred during filling. The powder is dispensed into the bottle by use of a motor-driven vertical screw. The mass of powder in each bottle is continuously monitored and recorded. All parts in contact with the material are made of or protected with Teflon, in order to avoid the risk of contamination by trace metals.

In each case (after jet milling, sieving and homogenising or ball milling, sieving and homogenising) six bottles were filled. Samples for testing were then taken from each bottle.

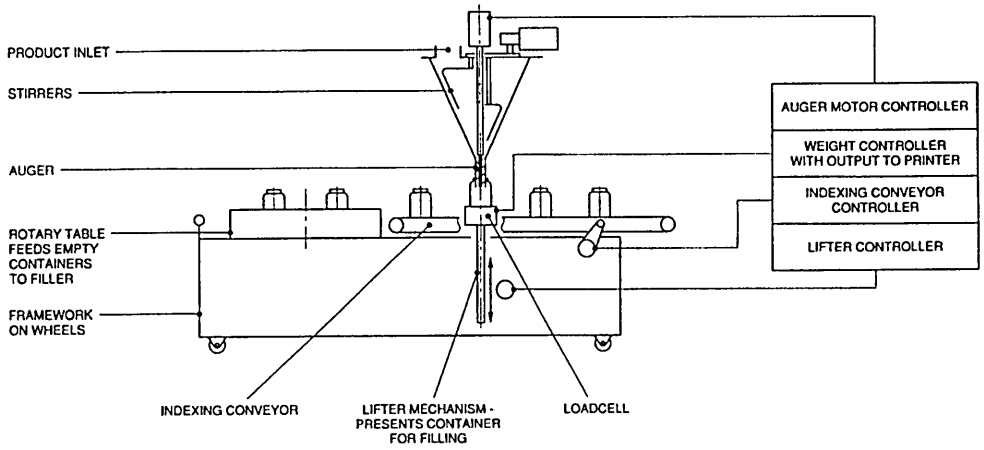

Figure 95: Fully automated filling machine type DM1 (taken from Kramer et al.[242]).

6.2.9 Handling under Protective Atmosphere

All procedures were carried out under a dry air atmosphere in order to prevent re-adsorption of moisture after drying and to prevent biological degradation of the

material. This was achieved by the use of glove boxes containing air purification systems. The main characteristics of the air purification system are shown in Table 40.

Table 40: Main characteristics of the gas purification system.

Gas supply (m^3/h)	5-55
Residual moisture content (vpm)	< 100
Residual oxygen content (vpm)	< 20
Removal of water	Molecular sieve type 4A Grace MS 512
Removal of oxygen	Copper catalyst type BASF R3-11

6.3 Results and Discussion

Figure 96 shows the results of the various production stages on the Cr(III) and Cr(VI) distribution within the soil. The results are the mean of six different analyses from two separate batches of soil. The results from the fresh moist soil have been corrected for the dried mass.

Drying of the soil did not affect the chromium concentration or speciation. The results from the fresh and dried soil when tested statistically using both one and two-tailed students' t-tests were not found to be significantly different.

Several changes in the speciation of chromium can be seen in Figure 96. Notably, after jet milling, the amount of chromium increases significantly, i.e. by 0.22 mg kg^{-1}, from approximately 0.15 mg kg^{-1} when fresh or dried to 0.37 mg kg^{-1} after jet milling. This could be due to contamination from the equipment used. However during jet milling the material is milled against itself, so unless the equipment had residues of another material, this is unlikely to be the cause. A more likely explanation is that the increase

in surface area of the soil particles due to their reduced size enables more chromium to be extracted.

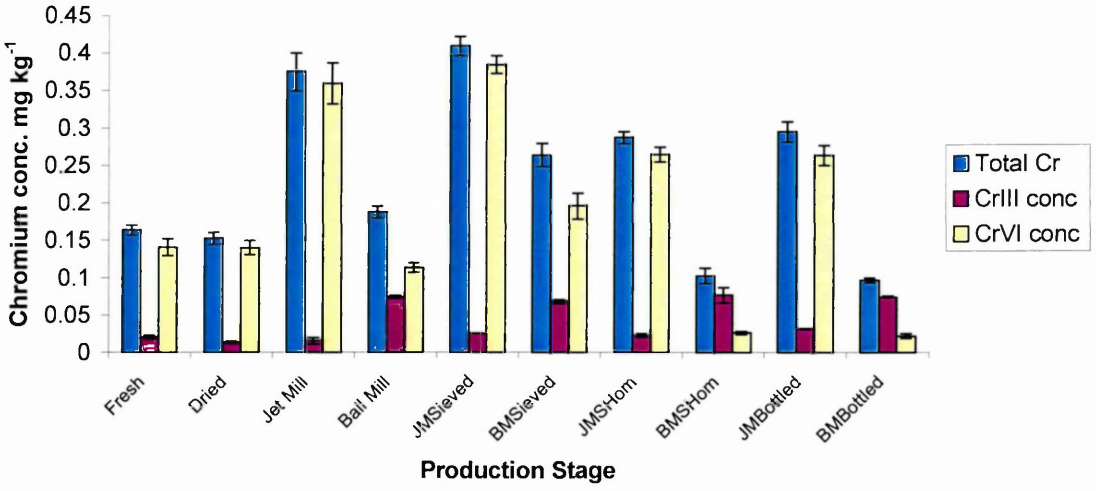

Fresh = fresh, moist field soil, before any procedures were carried out
Dried = soil after oven drying
Jet mill = soil after drying and jet milling
Ball mill = soil after drying and ball milling
JMSieved = soil after drying, jet milling and sieving
BMSieved = soil after drying, ball milling and sieving
JMSHom = soil after drying, jet milling, sieving and homogenisation
BMSHom = soil after drying, ball milling, sieving and homogenisation
JMBottled = soil after drying, jet milling, sieving, homogenisation and bottling
BMBottled = soil after drying, ball milling, sieving, homogenisation and bottling

Figure 96: Changes in chromium speciation in a soil during the production of a reference material.

Another change occurs after ball milling. Here the total chromium is again increased slightly, by 0.04 mg kg^{-1}, although not nearly as much as when the jet milling was used (0.22 mg kg^{-1} increase). This is in keeping with the explanation proposed above, since the particles after ball milling are not so small as those that have been jet milled. When the soil was jet milled this produced 98% of particles with a diameter of less than 63 µm (See Appendix 2). Whereas when the soil was ball milled this produced 98% of particles with a diameter less than 125 µm (See Appendix 1).

The distribution of Cr(III) to Cr(VI) has also changed after ball milling. The amount of Cr(III) has increased by 0.05 mg kg^{-1} from around 0.02 mg kg^{-1} in the fresh and dried soil to 0.07 mg kg^{-1} in the ball milled soil. The amount of Cr(VI) has also decreased slightly from approximately 0.14 mg kg^{-1} in the fresh and dried soil to 0.11 mg kg^{-1} in the ball milled soil, a decrease in Cr(VI) concentration of 0.03 mg kg^{-1}. This indicates that some reduction of the Cr(VI) has occurred during the ball milling procedure.

After sieving the total chromium content in both ball and jet milled soil samples increased by 0.07 and 0.04 mg kg^{-1} respectively. The increased surface area of the smaller particles (<125 μm) produced during both steps result in increased chromium extractions. This increase is more pronounced in the ball milled samples, in which a greater proportion (2%) of particles larger than 125 μm have been removed.

After homogenisation the amount of Cr(III) remained constant (no significant difference using a two-tailed students' t-test), but the Cr(VI) concentration decreased in both the ball and jet milled samples, with more loss being observed in the former. A decrease of 0.015 and 0.02 mg kg^{-1} was observed for the ball and jet milled samples respectively. These chromium concentrations remain constant for six months after bottling (no significant difference using a two-tailed students' t-test).

It is clear from these observations that the manipulations carried out in order to produce a CRM do affect both the concentration and distribution of chromium species in a soil sample. It is important to consider these changes when trying to produce a CRM which is representative of actual chromium concentrations in a real soil sample.

Jet milling is to be recommended over ball milling due to the reduction of Cr(VI) which occurs during ball milling and also due to the significant loss of Cr(VI) during homogenisation after ball milling. Further investigation of the homogenisation process needs to be carried out in order to determine the reason for the loss of Cr(VI).

CHAPTER 7 CONCLUSIONS

Literature on the extraction, separation, identification and determination of chromium (III) and (VI) have been critically reviewed. Single and sequential extraction schemes, HPLC and IC separations, and ICP-MS, as well as visible, UV and chemiluminescence detection were investigated.

The coupled techniques IC with ICP-MS and HPLC or IC with visible detection were evaluated. Extraction procedures with ICP-MS detection were investigated using two CRMs: BCR CRM 596 and BCR CRM 597; an aquatic plant material and a sewage sludge amended soil respectively, certified for total chromium content.

The resolution of the IC with ICP-MS method was poor, whilst the HPLC method was slow and a number of side products were formed, giving rise to multiple peaks in the chromatograms. The extraction trials showed changes in chromium speciation indicating that a single 'mild' extractant may be suitable in order to retain species integrity. Stronger extractants, such as HNO_3 or HNO_3/H_2O_2, either oxidised or reduced the chromium species. The IC with visible detection method proved to be the most promising, however the detection limit was high, therefore a more sensitive detector was required.

In order to improve sensitivity a chemiluminescence detector was obtained and directly coupled to the IC instrument. This method was simple and free from most interferences.

Initially a univariate optimisation was used to optimise the instrumental parameters but when the settings were found not to vary independently, multivariate optimisation was

applied. Comparison of the two procedures showed an improvement in peak areas of 43% and 32% for Cr(III) and Cr(VI) respectively when multivariate optimisation was used. Improvement in the detection limit from 0.08 μg L^{-1} to 0.002 μg L^{-1} was achieved.

A linear calibration was obtained from 0.01 to 50 μg L^{-1}. Limits of detection were found to be 0.002 μg L^{-1} for both Cr(III) and Cr(VI). Limits of determination were found to be 0.02 μg L^{-1} for both Cr(III) and Cr(VI). The precision, determined using a 10 μg L^{-1} solution of Cr(III) and Cr(VI) was 10.6 ± 0.52μg L^{-1} (4.9%) for Cr(III) and 10.1 ± 0.50 μg L^{-1} (4.9%) for Cr(VI) (n=6). Validation of the method was carried out using two water reference materials certified for total chromium content: LGC CRM 6010; 49 μg L^{-1} ± 4 μg L^{-1} and NIST SRM 1643d; 18.53 μg L^{-1} ± 0.20 μg L^{-1}. Results obtained showed good agreement with the certified values: 49.21 μg L^{-1} ± 1.81 μg L^{-1} and 19.03 μg L^{-1} ± 1.50 μg L^{-1} respectively. These results gave improvements on previously published results.

The developed analytical method was used to determine both Cr(III) and Cr(VI) after extraction from solid matrices. Initially BCR CRM 483, which was certified for total extractable chromium concentration, was used to test the extraction procedures. Several extraction methods were investigated for their suitability, i.e. which methods extracted the chromium species without change in the concentration or distribution of species. The extraction methods investigated were CH_3COOH, $CaCl_2$, NaDDTC at pH4.0 and pH5.6, KH_2PO_4, HCl and $(NH_4)_2SO_4/NH_3$. The only method that was found not to change the chromium species present in the sample upon extraction was 0.43 mol L^{-1} acetic acid. Only a fraction of the chromium contained in soil was extracted by this method. However it is this fraction that is likely to be mobile and hence bioavailable.

This single extraction procedure, in conjunction with the IC-chemiluminescence method developed, was then used to assess the amount of acetic acid extractable chromium in a 'real sample'. A field soil was collected from a farmer's field using a post-hole sampling auger and a 'W' sampling pattern of the field, in order to obtain a representative sample. Cone and quartering was then used in order to reduce the volume to obtain a smaller representative sample of the bulk sample for analysis. The Cr(III) and Cr(VI) concentrations determined in the field moist soil were 0.02 ± 0.004 mg kg^{-1} and 0.13 ± 0.01 mg kg^{-1} respectively. These results were in good agreement with the total chromium concentration determined by ETAAS (0.14 ± 0.02 mg kg^{-1}).

The field soil was taken through some of the different procedures that are often used for the production of reference materials. The production stages selected were drying, jet milling, ball milling, sieving, homogenisation and bottling. This investigation showed no change in the chromium species distribution after drying of the soil or after bottling. However changes in either the amount or distribution of chromium species were observed after jet milling, ball milling, sieving and homogenisation.

It was clear from these observations that the manipulations carried out in order to produce a CRM affect both the concentration and distribution of chromium species in a soil sample. It is important to consider these changes when trying to produce a CRM which is representative of actual chromium concentrations in a real soil sample.

Jet milling is to be recommended over ball milling due to the reduction of Cr(VI) which occurs during ball milling and also due to the significant loss of Cr(VI) during homogenisation after ball milling. Further investigation of the homogenisation process needs to be carried out in order to determine the reason for the loss of Cr(VI).

CHAPTER 8 FURTHER WORK

In analytical chemistry there is an ever-increasing demand for rapid, sensitive, low-cost and selective detection methods. The IC-CL method developed in this study meets these requirements for the determination of chromium species. Further study of chromium containing samples taken through different production stages of reference materials such as lyophilisation of liquid samples should also be performed. Methods of prevention of the loss or interconversion of the chromium species also need to be investigated in order to enable representative CRMs to be produced.

Different matrices such as plant materials could also be studied, along with other important elements, such as selenium, arsenic, antimony and vanadium, which exist in a number of oxidation states.

CHAPTER 9 APPENDICES

9.1 Appendix 1: Raw Data for Cr(VI) - Initial Screening

9.1.1 Residual Table

Cr(VI) Exp. No.	Observed	Predicted	Obs - Pred	Std.err(±)
1	2.000e-03	0.507	-0.505	0.556
2	2.000e-03	2.215	-2.213	0.801
3	0.526	1.176	-0.649	0.603
4	1.385	0.534	0.851	0.934
5	18.927	18.218	0.709	1.292
6	2.000e-03	1.011	-1.009	0.646
8	3.594	1.679	1.915	0.745
9	3.141	0.507	2.633	0.556
10	4.090	2.215	1.875	0.801
11	2.000e-03	1.176	-1.174	0.603
12	2.000e-03	0.534	-0.532	0.934
14	2.000e-03	1.011	-1.009	0.646
15	15.797	16.537	-0.739	1.220
16	1.524	1.679	-0.155	0.745
17	18.084	17.964	0.120	1.023
18	17.807	17.964	-0.157	1.023
19	18.003	17.964	0.039	1.023
N = 17	Q2 =	0.8038	CondNo =	Infinite
DF = 8	R2 =	0.9747	Y-miss =	0
Comp= 3	R2Adj =	0.9494	RSD =	1.7758

R^2 adjusted = $\frac{1 - \text{residual MS}}{\text{Total MS}}$

R^2 adjusted utilises mean square (MS) rather than sums of squares. This takes into account the number of residual degrees of freedom in the polynomial regression. R^2 adjusted is always smaller then R^2.

9.1.2 Anova Table

Cr(VI)	DF	SS	MS	F	p	SD
			(variance)			
Total	17	1620.042	95.297			
Constant	1	622.730	622.730			
Total Corrected	16	997.312	62.332			7.895
Regression	8	972.085	121.511	38.534	1.348e-05	11.023
Residual	8	25.227	3.153			1.776
Lack of Fit	6	25.186	4.198	205.979	4.839e-03	2.049
(Model Error)						
Pure Error	2	0.041	0.020			0.143
(Replicate Error)						
N = 17	Q2 =	0.8038	CondNo =	Infinite		
DF = 8	R2 =	0.9747	Y-miss =	0		
Comp= 3	R2Adj =	0.9494	RSD =	1.7758		
			ConfLev=	0.95		

DF = degrees of freedom
SS = sum of squares
MS = mean square
F = ratio of explained variance and unexplained variance
p = number of terms in the model including the constant
SD = standard deviation

9.2 *Appendix 2: Raw Data for Cr(III) - Initial Screening*

9.2.1 Residual Table

Cr(III) Exp. No.	Observed	Predicted	Obs - Pred	Std.err(±)
1	2.000e-03	0.938	-0.936	0.671
2	2.000e-03	2.894	-2.892	0.965
3	1.086	1.767	-0.682	0.727
4	2.052	0.731	1.321	1.127
5	24.295	24.340	-0.045	1.558
6	0.059	1.530	-1.471	0.779
8	4.677	2.360	2.317	0.898
9	3.683	0.938	2.745	0.671
10	5.245	2.894	2.352	0.965
11	2.000e-03	1.767	-1.765	0.727
12	2.000e-03	0.731	-0.729	1.127
14	1.066	1.530	-0.464	0.779
15	22.273	22.176	0.096	1.471
16	2.520	2.360	0.160	0.898
17	21.270	21.892	-0.622	1.233
18	21.923	21.892	0.031	1.233
19	22.474	21.892	0.583	1.233
N = 17	Q2 =	0.7998	CondNo =	Infinite
DF = 8	R2 =	0.9766	Y-miss =	0
Comp= 3	R2Adj =	0.9531	RSD =	2.1411

$$R^2 \text{ adjusted} = \frac{1 - \text{residual MS}}{\text{Total MS}}$$

R^2 adjusted utilises mean square (MS) rather than sums of squares. This takes into account the number of residual degrees of freedom in the polynomial regression. R^2 adjusted is always smaller then R^2.

9.2.2 Anova Table

Cr(III)	DF	SS	MS	F	p	SD
			(variance)			
Total	17	2600.272	152.957			
Constant	1	1034.748	1034.748			
Total Corrected	16	1565.524	97.845			9.892
Regression	8	1528.850	191.106	41.687	9.959e-06	13.824
Residual	8	36.674	4.584			2.141
Lack of Fit	6	35.947	5.991	16.481	0.058	2.448
(Model Error)						
Pure Error	2	0.727	0.364			0.603
(Replicate Error)						
N = 17	Q2 =	0.7998	CondNo =	Infinite		
DF = 8	R2 =	0.9766	Y-miss =	0		
Comp= 3	R2Adj =	0.9531	RSD =	2.1411		

DF = degrees of freedom
SS = sum of squares
MS = mean square
F = ratio of explained variance and unexplained variance
p = number of terms in the model including the constant
SD = standard deviation

9.3 Appendix 3: 4D Response surface for Cr(VI)

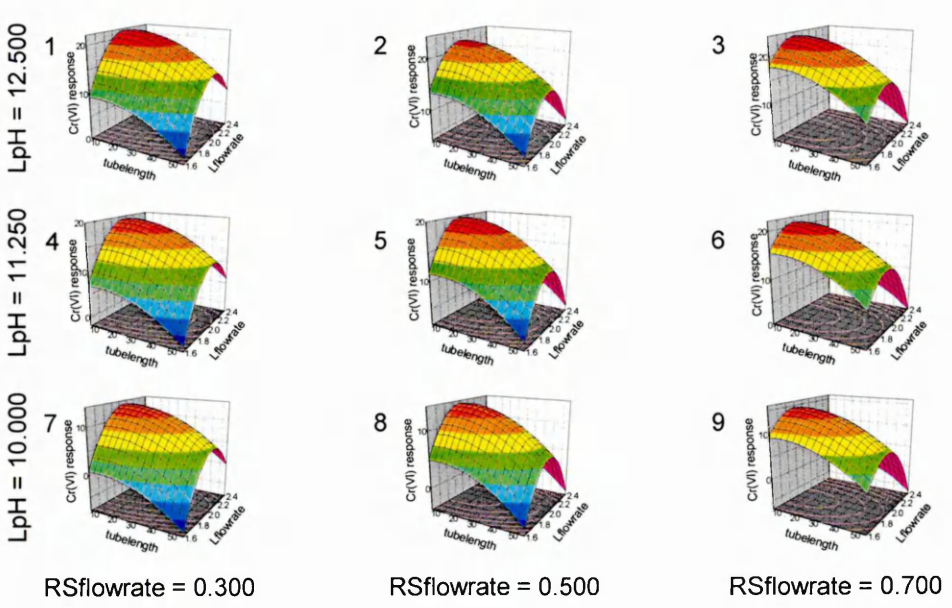

x axis = tube length (cm), y axis = response (peak areas), z axis = luminol flow rate (mL min^{-1}). Outer axis = 3 levels of luminol pH and 3 levels of reductant solution flow rate (mL min^{-1}).

9.4 Appendix 4: Effect of tube length on the Cr(III) response

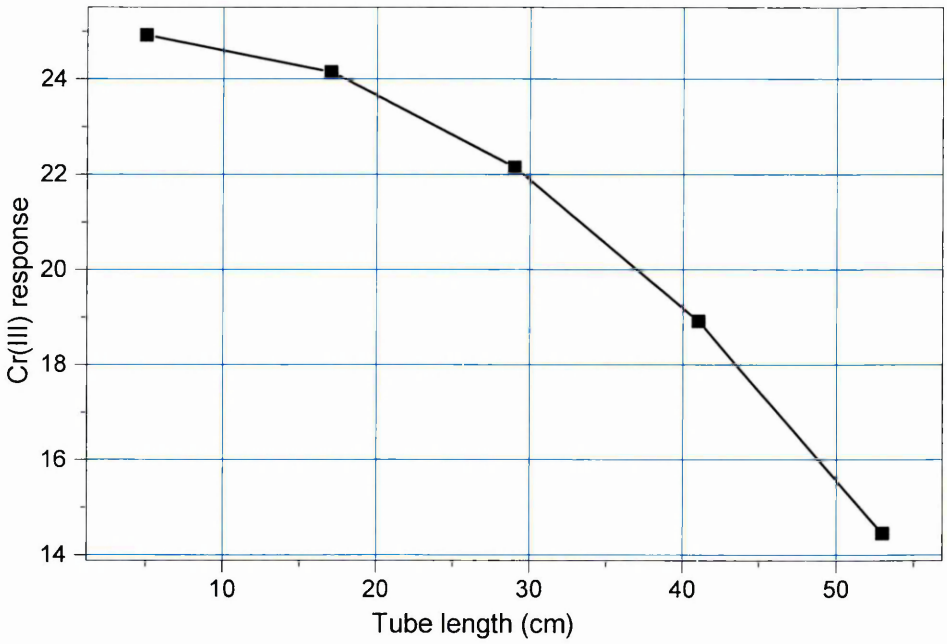

9.5 Appendix 5: Raw Data for Cr(III) - Full Experiment

9.5.1 Residual Table

Cr(III) Exp. No.	Observed	Predicted	Obs - Pred	Conf.int(±)
1	51.672	48.979	2.693	176.445
2	31.567	11.018	20.548	176.445
3	191.473	235.808	-44.335	176.445
4	255.188	279.444	-24.256	176.445
5	205.087	195.302	9.785	176.445
6	81.532	120.083	-38.551	176.445
7	242.530	313.848	-71.318	176.445
8	270.880	320.226	-49.346	176.445
9	101.740	30.085	71.655	176.077
10	29.195	23.690	5.505	176.077
11	56.097	13.515	42.581	176.077
12	111.524	88.717	22.807	176.077
13	101.186	129.860	-28.674	176.077
14	171.282	86.206	85.076	176.077
15	65.147	45.007	20.140	176.077
16	88.594	82.950	5.644	176.077
17	652.087	559.266	92.821	154.494
18	611.693	559.257	52.436	154.494
19	242.442	367.654	-125.212	154.494
20	490.883	459.440	31.443	154.494
21	412.453	465.338	-52.885	154.494
22	617.689	535.616	82.073	154.494
24	159.858	335.431	-175.573	195.952
25	640.379	582.071	58.308	85.231
26	640.828	582.071	58.757	85.231
27	529.950	582.071	-52.121	85.231
N = 26	Q2 =	0.8230	CondNo =	8.1166
DF = 11	R2 =	0.9138	Y-miss =	0
Comp= 2	R2Adj =	0.8040	RSD =	98.1844

$$R^2 \text{ adjusted} = \frac{1 - \text{residual MS}}{\text{Total MS}}$$

R^2 adjusted utilises mean square (MS) rather than sums of squares. This takes into account the number of residual degrees of freedom in the polynomial regression. R^2 adjusted is always smaller then R^2.

9.5.2 Anova Table

Cr(III)	DF	SS	MS	F	p	SD
			(variance)			
Total	26	3.14275e+06	120874.844			
Constant	1	1.91324e+06	1.91324e+06			
Total Corrected	25	1.22951e+06	49180.328			221.766
Regression	14	1.12347e+06	80247.602	8.324	5.886e-04	283.280
Residual	11	106041.875	9640.171			98.184
Lack of Fit	9	97878.977	10875.441	2.665	0.303	104.285
(Model Error)						
Pure Error	2	8162.899	4081.450			63.886
(Replicate Error)						
N = 26	Q2 =	0.8230	CondNo =	8.1166		
DF = 11	R2 =	0.9138	Y-miss =	0		
Comp= 2	R2Adj =	0.8040	RSD =	98.1844		

DF = degrees of freedom
SS = sum of squares
MS = mean square
F = ratio of explained variance and unexplained variance
p = number of terms in the model including the constant
SD = standard deviation

9.6 Appendix 6: Raw Data for Cr(VI) - Full Experiment

9.6.1 Residual Table

Cr(VI) Exp. No.	Observed	Predicted	Obs - Pred	Conf.int(±)
1	30.803	41.527	-10.724	156.524
2	77.078	13.984	63.094	156.524
3	147.675	177.140	-29.465	156.524
4	183.883	208.810	-24.927	156.524
5	163.770	147.731	16.039	156.524
6	46.816	93.140	-46.324	156.524
7	175.339	233.795	-58.456	156.524
8	196.016	238.417	-42.401	156.524
9	79.826	28.942	50.884	156.197
10	62.734	24.305	38.429	156.197
11	40.962	16.914	24.048	156.197
12	77.570	71.490	6.080	156.197
13	83.640	101.342	-17.702	156.197
14	104.477	69.656	34.821	156.197
15	51.372	39.765	11.607	156.197
16	57.765	67.292	-9.527	156.197
17	500.129	422.406	77.723	137.052
18	484.374	422.398	61.976	137.052
19	204.683	283.637	-78.954	137.052
20	353.171	350.262	2.909	137.052
21	340.488	354.360	-13.872	137.052
22	487.715	405.363	82.352	137.052
24	113.290	260.734	-147.444	173.828
25	503.351	442.495	60.856	75.608
26	500.559	442.495	58.064	75.608
27	333.408	442.495	-109.087	75.608
N = 26	Q2 =	0.7837	CondNo =	8.1166
DF = 11	R2 =	0.8831	Y-miss =	0
Comp= 2	R2Adj =	0.7343	RSD =	87.0993

$$R^2 \text{ adjusted} = \frac{1 - \text{residual MS}}{\text{Total MS}}$$

R^2 adjusted utilises mean square (MS) rather than sums of squares. This takes into account the number of residual degrees of freedom in the polynomial regression. R^2 adjusted is always smaller then R^2.

9.6.2 Anova Table

Cr(VI)	DF	SS	MS	F	p	SD
			(variance)			
Total	26	1.83567e+06	70602.539			
Constant	1	1.12191e+06	1.12191e+06			
Total Corrected	25	713756.125	28550.244			168.968
Regression	14	630307.000	45021.930	5.935	2.651e-03	212.184
Residual	11	83449.094	7586.281			87.099
Lack of Fit	9	64506.465	7167.385	0.757	0.686	84.660
(Model Error)						
Pure Error	2	18942.629	9471.314			97.321
(Replicate Error)						
N = 26	Q2 =	0.7837	CondNo =	8.1166		
DF = 11	R2 =	0.8831	Y-miss =	0		
Comp= 2	R2Adj =	0.7343	RSD =	87.0993		
			ConfLev=	0.95		

DF = degrees of freedom
SS = sum of squares
MS = mean square
F = ratio of explained variance and unexplained variance
p = number of terms in the model including the constant
SD = standard deviation

9.7 Appendix 7: Calculation of the results of a Karl Fischer Titration

Once the end point has been reached the amount of the Karl Fischer reagent used is known. The water content is calculated from the consumption and its water equivalent (WE) of the reagent[233]:

$$mg\,H_2O = a \cdot WE$$

$$\%\,H_2O = \frac{a \cdot WE}{100 \cdot e}$$

where: a = the consumption of reagent in mL

WE = water equivalent of the reagent in mg H_2O/mL

e = weight of the sample in g

The following formula is applied for the statistical evaluation of a series of titrations:

$$\text{Mean} \quad M = \frac{1}{n} \quad X_i$$

$$\text{Standard deviation} \quad S_{abs} = \sqrt{\frac{X_i^{\,2} - \frac{1}{n}\left(X_i\right)^2}{n-1}}$$

$$S_{rel} = \frac{100 \cdot S_{abs}}{m}\%$$

where: x_i = result of each analysis

n = number of analyses

M = mean

s = standard deviation

Sympatec GmbH
System-Partikel-Technik

WINDOX

HELOS Particle Size Analysis

Sympatec HELOS (H0262) CUVETTE: sediment **10/01/98 / 13:40:3**

dispersant Methanol

sonication duration 0.00 s
pause 0.00 s
stirring rate 50.00 %

Measuring conditions: sediment
measuring range: R5: 0.5/4.5...875
measuring duration: 10.00
cycle time: 1000
start when: % at
reference measurement: 00:06:06 , 0.00
evaluation: HRLD (V 3.1 Rel.1
parameter 4 :

operator : oostra
identifier : 3175K.
Comments: 3175K.
SEDIMENT, JET MILLED 4200 rpm.
M.Derbyshire.

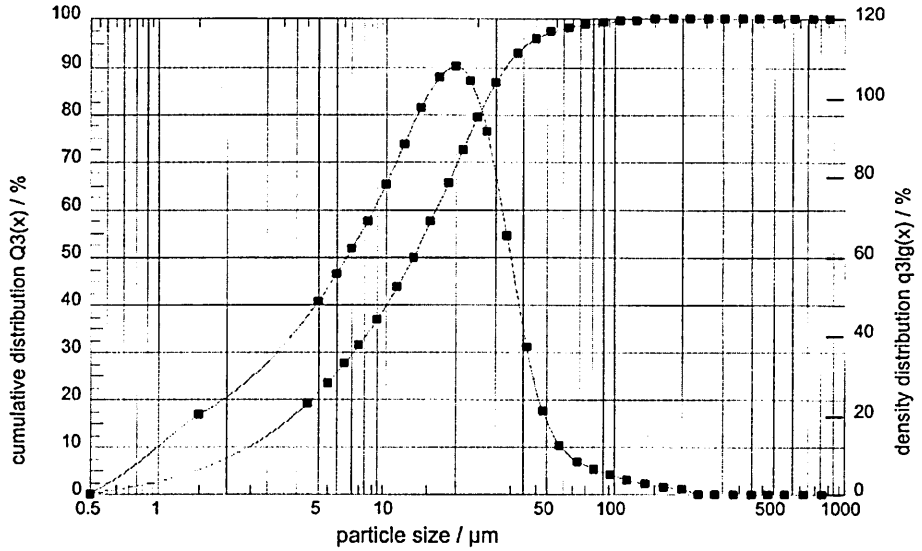

Volume Size Distribution

x0/µm	Q3/%	x0/µm	Q3/%	x0/µm	Q3/%	x0/µm	Q3
4.50	18.99	18.50	65.24	75.00	98.52	305.00	100.0
5.50	23.22	21.50	72.26	90.00	99.02	365.00	100.0
6.50	27.25	25.00	79.08	105.00	99.34	435.00	100.0
7.50	31.09	30.00	86.32	125.00	99.60	515.00	100.0
9.00	36.53	37.50	92.64	150.00	99.79	615.00	100.0
11.00	43.33	45.00	95.56	180.00	99.92	735.00	100.0
13.00	49.74	52.50	96.95	215.00	100.00	875.00	100.0
15.50	57.18	62.50	97.89	255.00	100.00		

x10 =	2.61 µm	x50 =	13.09 µm	x90 =	34.3
x16 =	3.87 µm	x84 =	28.40 µm	x99 =	89.5
VMD =	17.2 µm	Sv =	0.82587 m2/cm3	c_opt =	42.4

9.9 Appendix 9: Ball Mill Particle Size Determination

Sympatec GmbH
System-Partikel-Technik

HELOS Particle Size Analysis

WINDOX

Sympatec HELOS (H0262) CUVETTE: sediment **10/23/98 / 10:32:3**

dispersant water

sonication duration 0.00 s
pause 0.00 s
stirring rate 50.00 %

Measuring conditions: 10.000s,
measuring range: R5: 0.5/4.5...875
measuring duration: 10.00
cycle time: 1000
start when: % at
reference measurement: 00:40:11 , 0.00
evaluation: HRLD (V 3.1 Rel.1
parameter 4 :

operator : oostra
identifier :
Comments: SEDIMENT MICHELE.
6` Ball Milling Rotation 8.

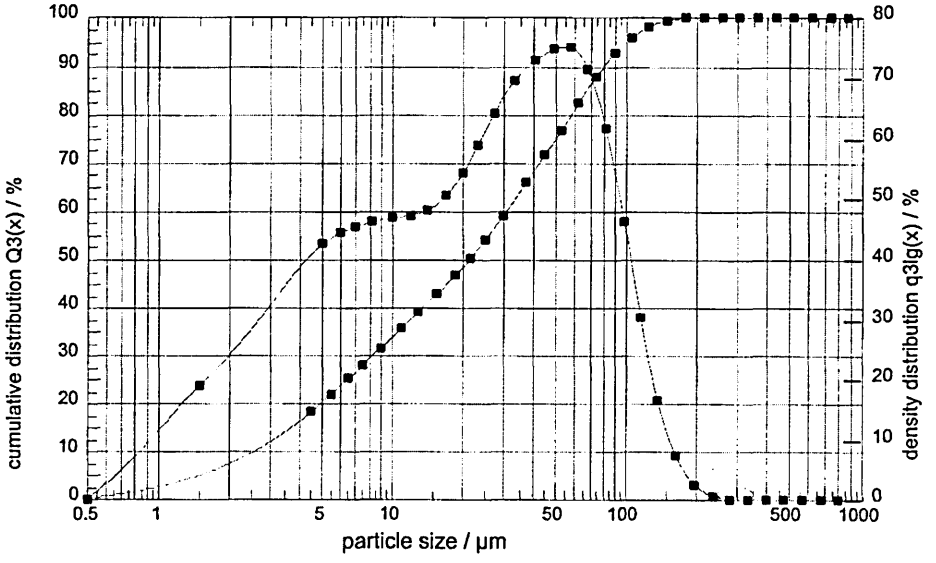

Volume Size Distribution

x0/µm	Q3/%	x0/µm	Q3/%	x0/µm	Q3/%	x0/µm	Q3
4.50	18.06	18.50	46.41	75.00	87.66	305.00	100.0
5.50	21.74	21.50	49.94	90.00	92.52	365.00	100.0
6.50	24.95	25.00	53.78	105.00	95.61	435.00	100.0
7.50	27.76	30.00	58.86	125.00	97.90	515.00	100.0
9.00	31.41	37.50	65.59	150.00	99.20	615.00	100.0
11.00	35.47	45.00	71.35	180.00	99.78	735.00	100.0
13.00	38.88	52.50	76.34	215.00	99.96	875.00	100.0
15.50	42.55	62.50	82.01	255.00	100.00		

x10 =	2.72 µm	x50 =	21.55 µm	x90 =	82.2
x16 =	4.04 µm	x84 =	66.90 µm	x99 =	146.1
VMD =	33.4 µm	Sv =	0.70717 m2/cm3	c_opt =	37.8

9.10 Appendix 10: Publications

9.10.1 Optimization of the Simultaneous Determination of Cr(III) and Cr(VI) by Ion Chromatography with Chemiluminescence Detection

Anal. Chem. 1999, *71*, 4203–4207

Optimization of the Simultaneous Determination of Cr(III) and Cr(VI) by Ion Chromatography with Chemiluminescence Detection

Michelle Derbyshire[†] and Andrée Lamberty

European Commission Joint Research Centre (JRC), Institute for Reference Materials and Measurements (IRMM), Retieseweg, B-2440 Geel, Belgium

Philip H. E. Gardiner*

Division of Chemistry, School of Science and Mathematics, Sheffield Hallam University, Howard Street, Sheffield, S1 1WB, UK

An optimized method for the simultaneous determination of Cr(III) and Cr(VI) in aqueous solutions using ion chromatography with chemiluminescence detection is described. Excellent resolution of the two chromium species was obtained using a single mixed-bed ion-exchange column with continuous elution. After postcolumn reduction of Cr(VI) to Cr(III), the light emitted during the Cr(III)-catalyzed oxidation of luminol with hydrogen peroxide was measured. Parameters affecting the post-column reactions such as reductant concentration, reductant mixing, point of luminol introduction, and luminol flow rate were optimized. The calibration curves in the range tested (0.01–50 $\mu g\ L^{-1}$) were linear, and detection limits of 0.002 $\mu g\ L^{-1}$ for both Cr(III) and Cr(VI) were obtained. The results of the analyses of the water reference materials LGC CRM6010 and NIST SRM1643d with certified chromium values of 49 ± 4 and 18.53 ± 0.20 $\mu g\ L^{-1}$ and found to contain only Cr(III) were 49.2 ± 1.8 and 19.0 ± 1.5 $\mu g\ L^{-1}$, respectively. Values of 10.6 ± 0.5 and 10.1 ± 0.5 $\mu g\ L^{-1}$ were obtained when a simulated water sample containing 10 $\mu g\ L^{-1}$ Cr(III) and Cr(VI) was analyzed.

In 1972, Seitz et al.[1] described the instrumentation and optimized the chemical conditions for the chemiluminescence detection of Cr(III) in water using a flow system. The method was based on the measurement of the intensity of light emitted when luminol (5-amino-2,3-dihydro-1,4-phthalazinedione) is oxidized by hydrogen peroxide in the presence of Cr(III). Under the experimental conditions, the intensity of the light emitted was found to be directly proportional to the metal ion concentration. Potential interference effects caused by other metal ions that similarly catalyze the same reaction were masked by adding EDTA to the sample stream. The developed method was very selective and sensitive. Free Cr(III) ions were found to be the only chromium species that catalyze the reaction, and in contrast to other metal ions, the rate of formation of the Cr(III)–EDTA complex is slow such that Cr(III) is still in the free state when the luminol reaction occurs. The low detection limit (0.025 $\mu g\ L^{-1}$) is still comparable to values obtained with current instrumental techniques.

In a further development, Chang and Patterson[2] showed that the chemiluminescence signal generated by the Cr(III)–luminol reaction is enhanced 6-fold in the presence of bromide ions. Recently the addition of bromide ions has been used with flow injection analysis (FIA) and chemiluminescence detection for the determination of Cr(III) in tap water.[3]

Williams et al.[4] demonstrated that ion chromatography with chemiluminescence detection could be adapted to the study of the distribution of Cr(III) and Cr(VI) species in aqueous solutions. The species are separated by ion chromatography followed by postcolumn reduction of Cr(VI) to Cr(III) before detection. Subsequent work [5,6] to improve this method highlighted the importance of selecting an appropriate column for the separation of the two species.

Ion chromatography with chemiluminescence detection is a much less costly alternative to most currently available instrumental methods for the study of the distribution of Cr(VI) and Cr(III) species in aqueous solutions. This combination of techniques is cost-effective, readily automated, can handle a large sample throughput, and is very sensitive. In this study, we investigate the application of a variety of columns to the separation of Cr(III) and Cr(VI) species, optimize the conditions for the chemiluminescence detection of both species, and validate the method using two water reference materials.

EXPERIMENTAL SECTION

Apparatus. Figure 1 shows the schematic diagram of the ion chromatography system with the postcolumn manifold coupled

[†] Ph.D. student, Sheffield Hallam University.

(1) Seitz, W. R.; Suydam, W. W.; Hercules, D. M. *Anal. Chem.* **1972**, *44*, 957–963.

(2) Chang, C. A.; Patterson, H. H. *Anal. Chem.* **1980**, *52*, 653–656.

(3) Economou, A.; Clark, A. K.; Fielden, P. R. *Anal. Commun.* **1998**, *35*, 389–390.

(4) Williams, T.; Jones, P.; Ebdon, L. *J. Chromatogr.* **1989**, *482*, 361–366.

(5) Gammelgaard, B.; Jøn, O.; Nielsen, B. *Analyst* **1992**, *117*, 637–640.

(6) Beere, H. G.; Jones, P. *Anal. Chim. Acta* **1994**, *293*, 237–243.

10.1021/ac9902751 CCC: $18.00
Published on Web 08/24/1999

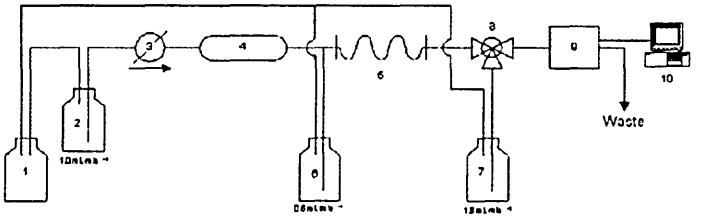

1 = Helium
2 = Eluent (KCl,EDTA)
3 = Injection port
4 = Analytical column(CS5)
5 = Mixing coil (375μl)
6 = Reducing Solution (K_2SO_3)
7 = Chemiluminescence reagent (luminol, H_2O_2)
8 = Mixing tee
9 = Chemiluminescence detector
10 = Data processor (Computer)

Figure 1. Configuration of the combined ion chromatography and chemiluminescence detector system.

to the chemiluminescence detector. Measurements were carried out on a metal-free Dionex DX 500 system (Dionex Corp., Sunnyvale, CA) equipped with a Dionex Ionpac CS5 (4 × 250 mm) analytical column, Peaknet control, and integration software. Signal detection was carried out on a Jasco FP920 Intelligent fluorescence detector (Jasco Corp., Tokyo, Japan) equipped with a chemiluminescence option and incorporating a flat wound PTFE cell with a reflective back plate to maximize the amount of emitted light reaching the photomultiplier. PEEK tubings and mixing tees were used for all the postcolumn connections.

The eluent flow rate through the separation column was 1 mL min^{-1}. The reductant solution (0.5 mL min^{-1}) was added via a Ismatec peristaltic pump (Ismatec, Zürich, Switzerland), and the luminol solution was introduced at a flow rate of 1.8 mL min^{-1} using a postcolumn reagent delivery module (Dionex PC 10 pneumatic controller). The AS 3500 autosampler (Dionex) introduced 50-μL sample injections onto the column. Thorough mixing of the reductant solution with the column effluent was achieved by using a 375-μL knitted reaction coil.

Reagents. All chemicals used, except where stated, were certified ACS grade and purchased from Sigma-Aldrich (Bornem, Belgium).

All solutions were prepared with ultrapure 18 MΩ water obtained from a MilliQ Plus 185 system (Millipore, Milford, MA).

Eluent. A mixture of 0.6 mol L^{-1} potassium chloride and 0.001 mol L^{-1} EDTA with pH adjusted to 2.5 using hydrochloric acid was used as the eluent solution.

Chemiluminescence Reagent. A mixture of 3.4×10^{-4} mol L^{-1} luminol, 0.1 mol L^{-1} boric acid, and 0.10 mol L^{-1} hydrogen peroxide (supplied by Mobi-Lab, Zutendaal, Belgium) with pH adjusted to 11.5 with sodium hydroxide was used. Before use, the hydrogen peroxide solution was passed through a Clean IC-Ba cartridge (Alltech, Laarne, Belgium) in order to remove cationic impurities.

Reductant. A 0.015 mol L^{-1} solution of potassium sulfite with pH adjusted to 3 with nitric acid was used.

The column eluent and postcolumn reagents were kept under a helium atmosphere.

Standard Solutions. Separate 1 g L^{-1} stock solutions containing Cr(VI) and Cr(III) were prepared by dissolving 3.735 g of K_2CrO_4 and 7.695 g of $Cr(NO_3)_3 \cdot 9H_2O$ in 1 L of water, respectively. **Care must be taken in preparing these solutions particularly in handling the more toxic K_2CrO_4, which is a carcinogen.**

Interferences. Solutions of each of the following compounds: magnesium nitrate hexahydrate, zinc nitrate hexahydrate, calcium nitrate tetrahydrate, iron (II) sulfate heptahydrate, aluminum nitrate nonahydrate, manganese (II) nitrate hexahydrate, nickel (II) nitrate hexahydrate, copper (II) nitrate hemipentahydrate, cobalt (II) nitrate, and iron (III) nitrate nonahydrate were prepared.

Preparation of Autosampler Vials. To prevent the adsorption of Cr(III), the autosampler vials were soaked overnight in 5% (v/v) dimethyldichlorosilane (DMDCS) in toluene, rinsed thoroughly with 18 MΩ deionized water, and dried before use.

Procedure. All samples were filtered through 0.45-μm cellulose acetate sterile syringe filters (Alltech, Laarne, Belgium) prior to injecting 50 μL onto the column. Column separation of Cr(III) from Cr(VI) was followed by postcolumn reduction of Cr(VI) to Cr(III) with potassium sulfite. The chemiluminescence reagent was added just before the detector. All analyses were performed in triplicate. Standards and samples were stored in PTFE containers.

Table 1. Type and Dimensions of Columns Tested

column	dimensions (mm)	functional group(s)	type of ion exchange
CS5 analytical	4 × 250	sulfonic acid and quaternary ammonium	cation and some anion
CG5 guard	4 × 50	sulfonic acid and quaternary ammonium	cation and some anion
AS4A analytical	4 × 250	alkyl quaternary ammonium	anion
AG4A guard	4 × 50	alkyl quaternary ammonium	anion

RESULTS AND DISCUSSION

(i) Separation Columns. Four different columns and column combinations were tested to find the most suitable for the separation of Cr(III) and Cr(VI). Information about the column types are summarized in Table 1.

The column combinations, CG5 + CS5, AG4A + AS4A, and CG5 + AS4A, and the single columns, CS5 and AS4A, were investigated. Beere and Jones[5] found that when the AS4A column

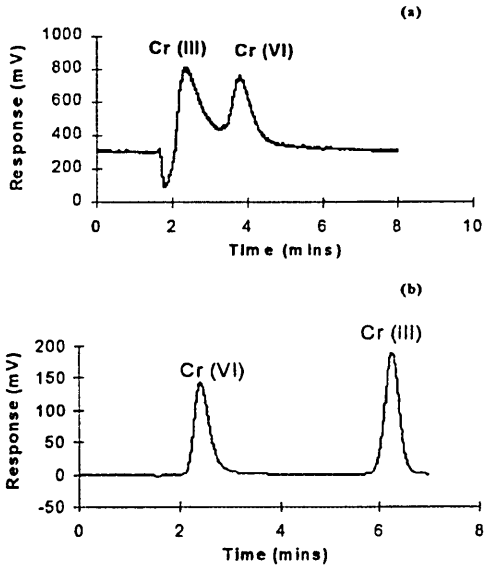

Figure 2. (a) Chromatogram of 10 μg L^{-1} Cr(III) and 5 μg L^{-1} Cr-(VI) using an AS 4A column. (b) Chromatogram of mixed 10 μg L^{-1} Cr(III) and Cr(VI) using a CS 5 column.

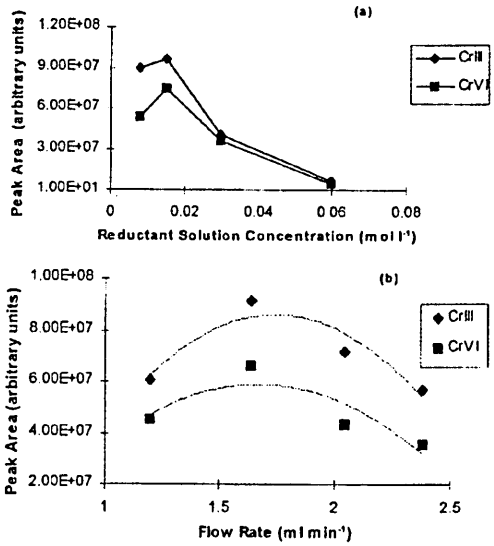

Figure 3. (a) Effect of varying redundant solution concentration on the Cr(III) (◆)and Cr(VI) (■) chemiluminescence signals. (b) Effect of luminol flow rate on the chemiluminescent signal intensities of Cr-(III) (◆) and Cr(VI) (■).

is used Cr(VI) is eluted first. In contrast, our results with a similar column showed the reverse (Figure 2a). AS4A is an anion-exchange column, and therefore it will retain Cr(VI) in either of its two forms—CrO_4^{2-} or $Cr_2O_7^{2-}$ but not Cr^{3+}. As a result, Cr^{3+} will be expected to elute first. This order of elution is confirmed in Figure 2a. The explanation given for the order reversal is that the column contains residual anionic groups that retain Cr^{3+}. While the presence of small amounts of residual anionic groups could increase the Cr^{3+} retention time, it is highly unlikely that complete reversal would occur. Changing separation conditions did not lead to much improvement in the resolution of the two peaks. Of the columns tested the best resolution was obtained with the CS5 column, which is a mixed cation and anion exchanger (Figure 2b). There was no need to use either discontinuous elution[12] or more than one column[4] in order to resolve the chromium species.

(ii) Optimization of the Postcolumn Reaction Conditions. *Reductant Concentration.* Figure 3a shows that the maximum chemiluminescence signal intensities for both Cr(III) and Cr(VI) were obtained at a potassium sulfite concentration of 0.015 mol L^{-1}. Note that at this potassium sulfite concentration the Cr(VI) peak area is about 90% of that of Cr(III). This may be due to incomplete reduction of Cr(VI). However, this concentration was chosen because of the 3-fold increase in sensitivity over signals at 0.03 mol L^{-1} where the peak areas are the same. The implication of this choice is that the slopes of the calibration curves for the two chromium species are different (see later).

Reductant Mixing. To achieve complete reduction of Cr(VI) to Cr(III), it was important to mix thoroughly the column effluent with the reductant solution. Two coil types: 375 μL knitted and 500 μL beaded coils were investigated. Compared to when no coil was used, the chemiluminescence signals for Cr(VI) were enhanced by 320% and 200% for the knitted and beaded coils, respectively.

Introduction of Luminol. To ensure that the maximum amount of emitted light produced by the reaction is measured, the point at which luminol is introduced into the flow stream before the detector is critical. Emitted light from chemiluminescent reactions decay with time.[7] Of the three distances investigated, 5, 27, and 53 cm from the detector, 27 cm gave maximum intensity. From this distance, the sample–luminol mixture carried in a 0.50 mm internal diameter tubing reached the detector in 31 s. Although the signal intensity at 53 cm was higher than at 5 cm, there was a 15% loss in intensity compared to that at 27 cm.

Luminol Flow Rate. In the presence of excess luminol, the intensity of the chemiluminescent signal is proportional to the chromium concentration.[1] However, the amount of excess luminol has to be kept to a minimum in order to prevent the decrease of the chemiluminescent signal caused by dilution of the Cr(III). Figure 3b shows that a flow rate of 1.8 mL min^{-1} is optimum.

(iii) Cr(III) Adsorption to Glass. In preliminary trials, it was observed that the calibration graph for Cr(III) was nonlinear, and the relative standard deviation (RSD) of the analytical results was

(7) Nieman, T. A. In Detection Based on Solution-Phase Chemiluminescence Systems In *Chemiluminescence and Photochemical Reaction Detection in Chromatography*; Birks, J. W., Ed.; VCH Publishers: New York, 1989.
(8) Aue, W. A.; Sun, X. *J. Chromatogr.* **1993**, *633*, 151–162.
(9) Prokisch, J.; Kovács, B.; Györi, Z.; Loch, J. *J. Chromatogr., A* **1994**, *683*, 253–260.
(10) Arar, E. J.; Long, S. E.; Martin, T. D.; Gold, S. *Environ. Sci. Technol.* **1992**, *26*, 1944–1950.
(11) Powell, M. J.; Boomer, D. W.; Wiederin, D. R. *Anal. Chem.* **1995**, *67*, 2474–2478.
(12) Barnowski, C.; Jakubowski, N.; Stuewer, D.; Broekaert, A. C. *J. Anal. At. Spectrom.* **1997**, *12*, 1155–1161.

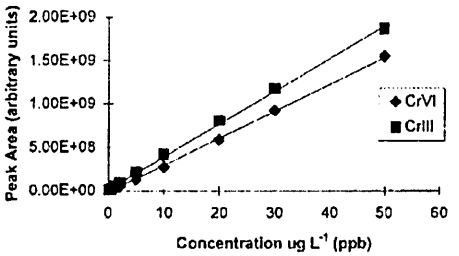

Figure 4. Calibration graphs for Cr(III) (■), $y = 4.0 \times 10^7x - 2.0 \times 10^7$, and Cr(III) (◆), $y = 3.0 \times 10^7x - 2.0 \times 10^7$, in the concentration range 0.01–50 $\mu g\ L^{-1}$.

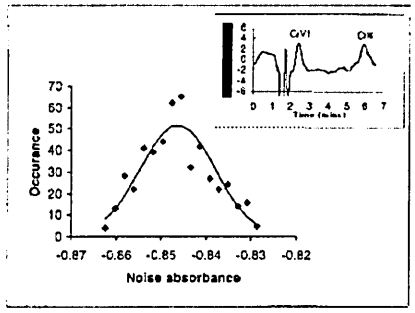

Figure 5. Chromatogram of solution containing 0.05 $\mu g\ L^{-1}$ Cr(III) and Cr(VI) (inset), and least-squares Gaussian fit of the baseline fluctuation.

greater than 40%. Addition of 0.14 mol L^{-1} nitric acid to standards to prevent sorption of Cr(III) on to the autosampler glass vials, and the removal of the analytical column in order to eliminate the possibility of adsorption to the column, did not solve the problem. A linear calibration graph was obtained when the standards prepared in PTFE were manually injected onto the column. These results seemed to indicate that the glass autosampler vials might be the cause of the problem. A study of the stability over time of a 50 $\mu g\ L^{-1}$ Cr(III) solution in a glass autosampler vial and a PTFE container was carried out. In contrast to the signals from the solution in the PTFE container, the signals from the standard glass vial had decreased by over 60% in less than 1 h. Subsequent measurements were carried out in silanized glass vials in order to prevent the loss of Cr(III).

(iv) Method Validation. *Calibration Graph and Detection Limits.* As shown in Figure 4, the calibration graphs for both Cr(III) and Cr(VI) are linear in the range 0.01–50 $\mu g\ L^{-1}$ with correlation coefficients (r^2) of 0.9988 and 0.9991, respectively.

The detection limits for both Cr(III) and Cr(VI) were found to be 0.002 $\mu g\ L^{-1}$ using the IUPAC recommended criteria[6] (see Figure 5). An improvement in detection limits of between 8 and 50-fold has been obtained with the present setup over other existing chemiluminescence detector-based systems.[1,4-6] Inferior detection limits have been reported for systems in which ion chromatography or HPLC is coupled to more expensive detectors: inductively coupled plasma spectrometer;[9] inductively coupled plasma-mass spectrometer;[10-12] and the recently developed diode laser atomic absorption spectrometer.[13]

Table 2. Interference Effects of Other Metal Ions on the Chemiluminescence Signals of a Solution Containing 10 $\mu g\ L^{-1}$ Cr(III) and Cr(VI)

element	concn, mg L^{-1}	Cr(III)% ± %	Cr(VI)% ± %	other peaks
Fe^{3+}	1	94 ± 1.6	34 ± 5.6	
Fe^{3+}	10	88 ± 5.6	0	
Fe^{3+}	100	114 ± 1.3	0	yes
Fe^{2+}	1	99 ± 0.9	0	
Fe^{2+}	10	99 ± 1.1	0	yes
Fe^{2+}	100	99 ± 0.7	0	yes
Ca^{2+}	1	103 ± 4.0	96 ± 3.5	
Ca^{2+}	10	98 ± 1.9	95 ± 4.1	
Ca^{2+}	100	94 ± 0.6	95 ± 4.9	
Zn^{2+}	1	103 ± 0.3	102 ± 0.5	
Zn^{2+}	10	101 ± 3.7	101 ± 2.0	
Zn^{2+}	100	104 ± 0.8	103 ± 0.8	
Mn^{2+}	2	100 ± 0.6	103 ± 0.3	
Mn^{2+}	20	103 ± 0.3	112 ± 0.7	
Mn^{2+}	40	106 ± 0.1	115 ± 0.1	
Co^{2+}	0.01	100 ± 1.1	99 ± 0.9	
Co^{2+}	0.1	99 ± 1.3	95 ± 3.5	
Co^{2+}	1	97 ± 0.7	99 ± 2.1	
Al^{3+}	0.1	100 ± 4.6	110 ± 4.0	
Al^{3+}	1	93 ± 2.4	99 ± 2.0	
Al^{3+}	10	126 ± 1.0	100 ± 3.2	
Mg^{2+}	1	98 ± 0.7	94 ± 5.9	
Mg^{2+}	10	98 ± 1.1	101 ± 1.0	
Mg^{2+}	20	95 ± 1.9	101 ± 0.4	
Ni^{2+}	0.1	96 ± 2.2	99 ± 0.8	
Ni^{2+}	1	97 ± 2.1	89 ± 0.9	
Ni^{2+}	10	94 ± 0.4	86 ± 1.8	
Cu^{2+}	0.1	118 ± 2.2	107 ± 4.2	
Cu^{2+}	1	111 ± 6.7	104 ± 1.4	
Cu^{2+}	10	100 ± 0.1	99 ± 1.2	

Interferences. This method was developed with a view to using it to study the distribution of chromium species in the environment. The cations chosen for study were those commonly found in environmental samples. Table 2 lists the cations and concentration levels at which they were tested. Only ferrous and ferric ions were found to interfere with the determination Cr(VI). Fe^{2+} reduces Cr(IV) to Cr(III) and as a result no Cr(VI) signal was detected. In the presence of 10 and 100 mg L^{-1} Fe^{2+}, an unidentified peak with a retention time of 1.7 min was detected. This peak was probably due to excess Fe^{2+} catalyzing the luminol reaction. To eliminate this effect, a higher EDTA concentration may have to be used. Significant signal depression followed by complete elimination of the Cr(VI) peak at higher Fe^{3+} concentration was also observed. However, this is probably due to the presence of Fe^{2+} impurities in commercially available iron(III) nitrate. Of the other cations studied, none interfered directly with the chemiluminescence signal at the concentration levels tested. This is in contrast to the findings of Gammelgaard et al.,[5] who reported the appearance of double peaks in the presence of similar levels of Co^{2+} and Mn^{2+}.

Analysis of Certified Reference Materials. Two water certified reference materials LGC CRM 6010 and NIST SRM 1643d were analyzed in order to validate the method. The chromatograms of both samples showed that only Cr(III) was present. Results obtained for the Cr(III) determinations were 49.2 ± 1.8 and 19.0 ± 1.5 compared to the certified values of 49 ± 4 $\mu g\ L^{-1}$ and 18.53

(13) Zyish, A.; Schaldach, G.; Berndt, H.; Nieman, K. *Anal. Chem.* **1998**, *70*, 5093–5096.

± 0.20 $\mu g\ L^{-1}$ for CRM 6010 and SRM 1643d, respectively. A comparison of the results obtained with the certified values using a Student t test at 95% confidence limit showed that the differences were not statistically significant. The results of the analysis of a solution containing a mixture of 10 $\mu g\ L^{-1}$ Cr(III) and Cr(VI) were 10.6 ± 0.5 and 10.1 ± 0.5 $\mu g\ L^{-1}$ ($n = 6$), respectively.

CONCLUSION

The optimized method described here is simple, readily automated and more sensitive than any currently available for the study of the distribution of Cr(III) and Cr(VI) species in aqueous solutions. The equipment is relatively inexpensive, and in contrast to the UV/visible detection of Cr(VI) using the measurement of absorbance of the 1,5 diphenylcarbohydrazide–chromium complex, this method can provide information on the levels of both Cr(III) and Cr(VI).

ACKNOWLEDGMENT

Financial support from the European Commission is gratefully acknowledged.

Received for review March 15, 1999. Accepted June 25, 1999.

AC9902751

9.10.2 Comparison of Univariate and Multivariate Procedures for the Optimisation of the Determination of Cr(III) and Cr(VI) by Ion Chromatography with Chemiluminescence Detection

To be published in Analytica Chimica Acta

Comparison of Univariate and Multivariate Procedures for the Optimisation of the Determination of Cr(III) and Cr(VI) by Ion Chromatography with Chemiluminescence Detection.

Michelle Derbyshire*, Magnus Johansson, Philip Gardiner† & Andrée Lamberty.

European Commission, Joint Research Centre, Institute for Reference Materials and Measurements, Retieseweg, B – 2440 Geel, Belgium.

† Division of Chemistry, School of Science and Mathematics, Sheffield Hallam University, Howard Street, Sheffield, S1 1WB, UK.

* Corresponding Author

Abstract

A comparative study of the univariate and multivariate optimisation of the determination of Cr(III) and Cr(VI) by ion chromatography with chemiluminescence detection is described. The multivariate analysis was performed by employing an experimental design program, Umetri Modde version 4.0. Seven variables were optimised for maximum peak area response. After initial screening, the four most influential variables were selected. These four variables were then optimised using a 2^4 full factorial design. The multivariate optimised parameter settings resulted in a peak area increase of 43 and 32% for Cr(III) and Cr(VI) respectively when compared to the univariate optimised settings. The limit of detection determined for this analysis was also improved from 0.08 μg L^{-1} for both Cr(III) and Cr(VI) initially, determined using the univariate optimisation, to 0.002 μg L^{-1} with the multivariate optimisation.

Introduction

Chromium in the environment occurs mainly as chromium(III) and chromium(VI). The two different oxidation states have very different effects on living organisms. Cr(VI) is toxic whereas Cr(III) is non-toxic and considered to be an essential nutrient. It is therefore of utmost importance to perform species specific determinations of chromium at trace levels in environmental samples. Methods developed for this purpose often involve the combination of ion chromatography or HPLC coupled with an element selective detector, such as ICP-MS[1,2,3]. An alternative, highly sensitive and low cost method, is chemiluminescence, which has been used for determination of chromium in a variety of environmental samples[4,5,6].

Chemiluminescence can be defined as light emitted from chemical reactions. Chemiluminescence is, alongside mass spectrometry, immunological and radiometric methods, among the most sensitive of analytical techniques, capable of yielding detection limits in the sub-femtamole range. Ion chromatography with chemiluminescence detection can be used for the ultratrace determination of Cr(III) and Cr(VI) in aqueous solution without the need for extensive chemical pretreatment since chromium is one

[1] E.J. Arar, S.E. Long, T.D. Martin and S. Gold, Environ. Sci. Technol., 26 (1992) 1944-1950.
[2] M.J. Tomlinson and J.A. Caruso, Anal. Chim. Acta, 322 (1996) 1-9.
[3] M.J. Powell and D.W. Boomer, Anal. Chem., 67 (1995) 2474-2478.
[4] A. Economou, A.K. Clark and P.R. Fielden, Anal. Commun., 35 (1988) 389-390.
[5] R. Li and D.M. Hercules, Anal. Chem., 46 part 7, (1974) 916-919.
[6] R. Escobar, M.S. García-Domínguez and A. Guiraúm F.F. de la Rosa, Fres. J. Anal. Chem., 361 (1998) 509-511.

of the few metals that catalyse the luminol-hydrogen peroxide reaction[7]. Other metals that catalyse the reaction can be masked by the addition of EDTA[8].

Traditionally, a univariate optimisation approach is used[9,10,11] for the optimisation of the signal output[12]. This approach does not allow for interactions between variables without performing an excessive numbers of experiments. In contrast, multivariate optimisation, based on the principles of chemometrics, uses mathematical and statistical means to determine parameters that would otherwise be very difficult to measure[13] separately. An experimental design program in which multivariate data analysis is used enables the maximum amount of information to be extracted from the fewest number of experimental runs. This is possible by varying all the relevant factors at the same time and then connecting the results by use of a mathematical model. This model can then be used for interpretations, predictions and optimisation. The following information can be obtained from use of such a model: which factors have an influence on the responses; which factors have significant interactions (whether positive or negative); what are the best settings to achieve the optimum conditions for the best performance and what are the predicted values of the responses for given settings of the factors.

This study was therefore carried out to compare the two different techniques of optimisation for an ion chromatography with chemiluminescence detection system for the determination of chromium species.

[7] M.P. Neary, R. Seitz and D.M. Hercules, Analytical Letters, 7 parts 8&9, (1974), 583-590.
[8] R.E. Hamm, J., Am. Chem. Soc., 75 (1953) 5670-5672.
[9] T. Williams, P. Jones and L. Ebdon, J. of Chromatography, 482 (1989) 361-366.
[10] B. Gammelgaard, O. Jøns and B. Nielsen, Analyst, 117 (1992) 637-640.
[11] H.G. Beere and P. Jones, Anal. Chim. Acta, 293 (1994) 237-243.
[12] G.E.P. Box, W.G. Hunter and J.S. Hunter, Statistics for Experimenters, John Wiley, 1978.
[13] B.K. Lavine, Anal. Chem., 72 (2000) 91R-97R.

Experimental

Apparatus

Figure I shows the set-up of the ion chromatography system. A metal free Dionex DX500 chromatography system (Dionex Corp., Sunnyvale, CA) was used along with a Dionex Ionpac CS5 (4 x 250mm) analytical column, peaknet control and integration software. The chemiluminescence signals were detected with a Jasco FP920 Intelligent Fluorescence detector (Jasco Corp., Tokyo, Japan) incorporating a flat wound PTFE cell with reflective back-plate. This enables the maximum amount of light emitted to be directed towards the photo multiplier tube.

The eluent flow rate through the column was 1 mL min^{-1}. The reductant solution was added via an Ismatec peristaltic pump (Ismatec, Zürich, Switzerland) and the luminol was introduced using a post column reagent delivery module (Dionex PC 10 pneumatic controller). The samples (50 µL) were introduced onto the column by injections from an AS 3500 autosampler (Dionex) from silanised sample vials. A 375 µL knitted reaction coil was used in order to achieve thorough mixing of the reductant solution and the column effluent.

Reagents

All chemicals used, except where stated, were certified ACS grade and purchased from Sigma-Aldrich (Bornem, Belgium). All solutions were prepared using ultrapure 18 MΩ deionised water obtained from a MilliQ Plus 185 system (Millipore, Milford, MA).

Eluent. The eluent solution was composed of a mixture of 0.6 mol L^{-1} potassium chloride and 0.001 mol L^{-1} EDTA with the pH adjusted to 2.5 with concentrated hydrochloric acid.

Chemiluminescence Reagent. A mixture of 3.4 x 10^{-4} mol L^{-1} 3-aminophthalhydrazide (luminol) 97%, 0.1 mol L^{-1} boric acid and 0.1 mol L^{-1} hydrogen peroxide (Mobi-Lab, Zutendaal, Belgium), with the pH adjusted to 11.8 (optimum) with sodium hydroxide was used. Prior to use the hydrogen peroxide was passed through a Clean IC-Ba cartridge (Alltech, Laarne, Belgium) in order to remove cationic impurities.

Reductant Solution. A 0.015 mol L^{-1} solution of potassium sulphite with the pH adjusted to 3 with nitric acid was used. The eluent and

postcolumn reagents were kept under a helium atmosphere in order to prevent any degradation.

Standard Solutions. Separate stock solutions containing 1 g L^{-1} Cr(VI) and Cr(III) were prepared by dissolving 3.735 g of K_2CrO_4 and 7.695 g of $Cr(NO_3)_3.9H_2O$ in 1 L of water, respectively. **Appropriate precautions must be taken when handling the carcinogen K_2CrO_4.**

Preparation of autosampler vials. To prevent the adsorption of Cr(III), the autosampler vials were soaked overnight in 5% (v/v) dimethyldichlorosilane (DMDCS) in toluene, rinsed thoroughly with deionised water and dried before use.

Figure I. Schematic diagram of the ion chromatography system with chemiluminescence detection.

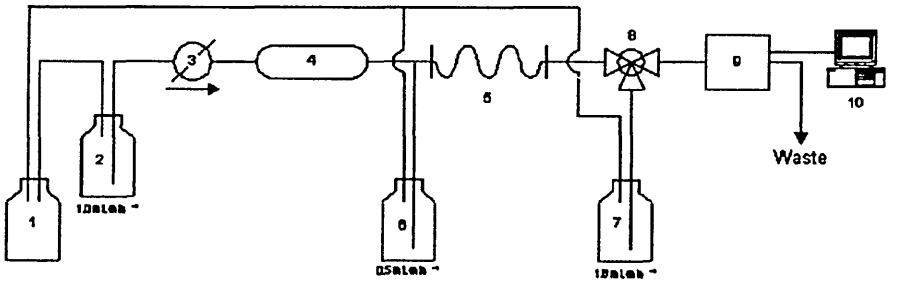

1 = Helium
2 = Eluent (KCl, EDTA)
3 = Injection port
4 = Analytical column (CS5)
5 = Mixing coil (375 µL)
6 = Reductant solution (K_2SO_3)
7 = Chemiluminescence reagent (luminol, H_2O_2)
8 = Mixing tee
9 = Chemiluminescence detector
10 = Data processor (computer)

Procedure

Samples of 50 µL were injected onto the column. The separation of Cr(III) from Cr(VI) was carried out on the column followed by reduction of the Cr(VI) to Cr(III) by potassium sulphite. The chemiluminescence reagent was added just before the detector. All analyses were carried out in triplicate. All solutions were stored in PTFE containers.

Univariate Optimisation

The following parameters were optimised using a univariant procedure. This has been described in more detail previously[14]. Each parameter was varied individually whilst keeping the other variables fixed.

Reductant Solution Concentration (RSC) and pH (RSpH). It is important to obtain the maximum reduction of Cr(VI) to Cr(III) in order to obtain quantitative results and the maximum sensitivity. Both the concentration and the pH of the reductant solution can influence the amount of conversion of Cr(VI) to Cr(III).

Reductant solution (RSF) and Luminol solution flow rates (LF) These flow rates are critical since they determine the time it takes for the solution plug to reach the detector, and also the time spent in the detector after the introduction of the luminol solution.

Tube length (TL). Optimisation of the tube length is essential in order to detect the maximum amount of light emitted from the reaction.

Luminol solution concentration (LC) and pH (LpH). These are critical for the production of intense chemiluminescence signals.

For the detection of Cr(VI) a reduction to Cr(III) must be performed after the separation of the two species. Here the RSC and RSpH are the most critical parameters. The flow rates of both the reductant and luminol solutions influence the overall flow rate and thus the final stage of detection. Solution additions cause peak broadening, and distortion of the chromatographic peak shape and ultimately decrease the detection limit. All these aspects

[14] M. Derbyshire, A. Lamberty and P.H.E. Gardiner, Anal. Chem., 71 (1999) 4203-4207.

are interconnected and therefore the multivariate approach for optimisation has a much better chance of taking these interactive effects into consideration and eventually finding better optimum settings.

Multivariate Optimisation

The Modde 4.0 software (Umetri, Umeå, Sweden) was used for experimental design and multivariate analysis applied for screening and optimisation of parameters influencing the analyte response from the IC-CL system. This procedure enables the interactions for different parameters to be studied through a limited number of experiments, whilst changing several variables at one time. For the initial screening all seven variables thought to influence the chemiluminescence signal were studied. Then after studying the results from these experiments the four parameters identified as having the most influence were chosen and a full experimental model based on the results developed in order to obtain the optimum conditions.

Results and discussion

Univariate Optimisation

Each parameter was taken individually and varied whilst keeping the rest of the parameters constant. Once a parameter had been optimised this value was kept constant and the next parameter was taken. Table I shows the optimised values for each parameter.

Table I. Optimised parameters for the univariate procedure.

Parameter	Optimised Value
Tube length	27 cm
Luminol flow	1.8 mL min^{-1}
Luminol pH	11.5
Luminol concentration	$3.4x10^{-4}$ mol L^{-1}
Reducing solution flow	0.5 mL min^{-1}
Reducing solution pH	3.0
Reducing solution conc.	0.015 mol L^{-1}

Multivariate Optimisation

A linear model using a fractional factoral design was utilised for the intitial screening. This was followed by a partial least squares analysis (PLS) on a quadratic model, using a face centred central composite design, which incorporates full factorial, star points and replicated centre points, for the full experimental model.

Initial Screening

The aim of carrying out an initial screening process is to find out which factors are important. This approach is used at the beginning of an investigation in order to reduce the number of factors to those with the largest effect on the response and to modify their ranges if necessary. For this study a linear model fractional factorial design was used which is a balanced subset of the full factorial design. Each experiment was carried out three times and the average response for both the Cr(VI) and Cr(III) peaks is given in Table **II**.

As can be seen from the summary of fit plot (Figure II) the values for Q^2 and R^2 are close to 1, 0.80 and 0.97 respectively for both responses. This indicates that the results are a good fit to the model, and means that the model has excellent predictive power for the optimisation.

Figure II. Summary of fit plot for initial screening (with outliers removed).

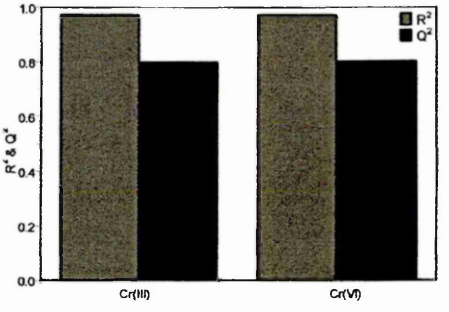

Table II. Results from the initial screening experiments.

Exp. No.	Run order	Variables							Responses ($x10^6$)	
		TL cm	LF mL min^{-1}	LpH	LC mol L^{-1}	RSF mL min^{-1}	RSpH	RSC mol L^{-1}	Cr(III)	Cr(VI)
1	8	5	1.6	10	0.0001	0.3	1	0.01	0	0
2	14	53	1.6	10	0.0001	0.7	1	0.02	0	0
3	9	5	2.4	10	0.0001	0.7	5	0.01	10.9	5.2
4	2	53	2.4	10	0.0001	0.3	5	0.02	20.5	13.8
5	18	5	1.6	12.5	0.0001	0.7	5	0.02	242.9	189.3
6	3	53	1.6	12.5	0.0001	0.3	5	0.01	0.6	0
7	10	5	2.4	12.5	0.0001	0.3	1	0.02	229.9	196.5
8	4	53	2.4	12.5	0.0001	0.7	1	0.01	46.8	35.9
9	19	5	1.6	10	0.0007	0.3	5	0.02	36.8	31.4
10	6	53	1.6	10	0.0007	0.7	5	0.01	52.5	40.9
11	16	5	2.4	10	0.0007	0.7	1	0.02	0	0
12	17	53	2.4	10	0.0007	0.3	1	0.01	0	0
13	12	5	1.6	12.5	0.0007	0.7	1	0.01	100.9	17.6
14	13	53	1.6	12.5	0.0007	0.3	1	0.02	10.7	0
15	1	5	2.4	12.5	0.0007	0.3	5	0.01	222.7	158.0
16	5	53	2.4	12.5	0.0007	0.7	5	0.02	25.2	15.2
17	7	29	2.0	11.25	0.0004	0.5	3	0.015	212.7	180.8
18	15	29	2.0	11.25	0.0004	0.5	3	0.015	219.2	178.1
19	11	29	2.0	11.25	0.0004	0.5	3	0.015	224.7	180.0

TL = tube length, LF = luminol flow rate, LpH = luminol pH, LC = luminol concentration, RSF = reductant solution flow rate, RSpH = reductant solution pH, RSC = reductant solution concentration, responses for Cr(III) and Cr(VI) were measured as peak area in arbitrary units.

The results from experiments 13 and 7 were not very close to those predicted by the model. These two experimental runs were rejected using an outlier rejection test 'Dixon's Q' at a 5% confidence limit. When these two values are removed the model is a much better fit for the results obtained. This enables the model to make much better predictions.

R^2 is the fraction of variation of the response explained by the model according to:

$$R^2 = \frac{SS_{REG}}{SS}$$

SS_{REG} = the sum of squares of Y corrected for the mean, explained by the model.
SS = the total sum of squares of Y corrected for the mean.

Q^2 on the other hand is the fraction of variation of the response that can be predicted by the model, according to:

$$Q^2 = 1 - \frac{PRESS}{SS}$$

PRESS = the prediction residuals sum of squares.

The values of R^2 and Q^2 are usually numbers between 0 and 1, with negative values being possible for very poorly fitting models. The closer the values are to 1 the better the fit of the model and the stronger the predictive power of that model. These values give the best measure of the goodness of fit of the model.

Figure III. Diagram showing the effects of the investigated factors and the interactions between these factors for the initial screening (see **Table II** for abbreviations).

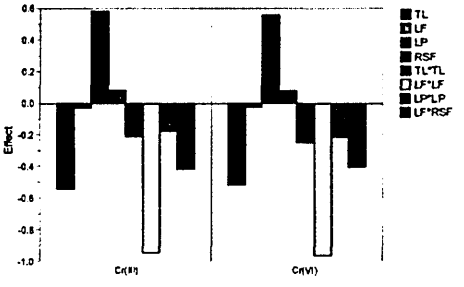

Figure III shows the effect that the different factors have upon the Cr(III) and Cr(VI) signals. As we can see the four most important effects are LF*LF, TL, LP, LF*RSF. Therefore from the results of the initial screening process the most influential factors in obtaining the best response were found to be the luminol flow rate, the tube length, the luminol pH and the reductant solution flow rate. These four parameters were then used in a full experimental model, in order to accurately determine the optimum settings for these factors.

Figure IV. 4D Response surface for Cr(III); x axis = tube length (cm), y axis = response (peak areas), z axis = luminol flow rate (mL min^{-1}). Outer axis = 3 levels of luminol pH and 3 levels of reductant solution flow rate (mL min^{-1}).

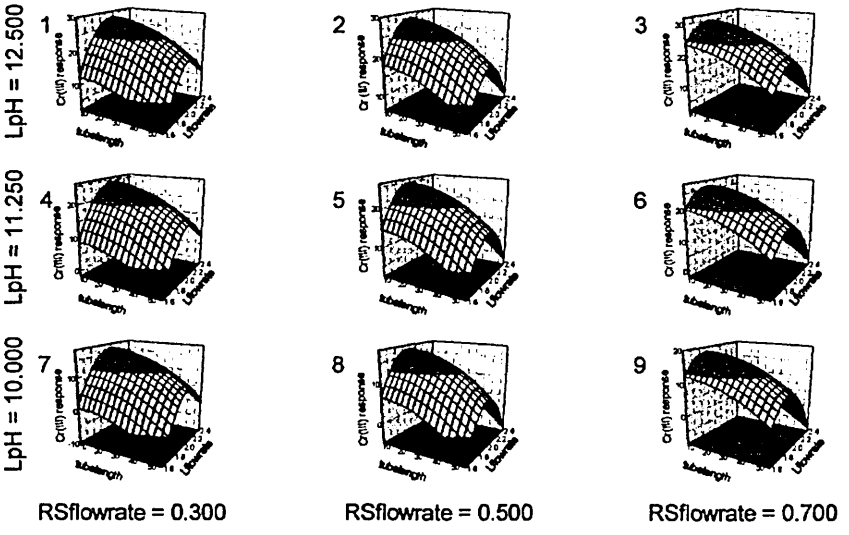

As can be seen from Figure IV for the Cr(III) response (a similar plot is available for the Cr(VI) response) the tube length has not yet reached its optimum. We must therefore choose values lower than 5 cm for the full experimental model in order to find the optimum.

Full Experimental Model

The four parameters that were seen to be the most influential in obtaining the best response from Cr(III) and Cr(VI), from the results of the initial screening, were then taken and a full experimental model was carried out on them. For the full experimental model a quadratic model utilising a face centred central composite design was used. Each experiment was carried out three times and the average responses for both the Cr(VI) and Cr(III) peak areas are given in Table III.

Table III. Results from the quadratic model, face centred central composite design.

Exp. No.	Run order	Variables				Responses ($x10^6$)	
		TL cm	LF mL min^{-1}	LpH	RSF mL min^{-1}	Cr(III)	Cr(VI)
1	22	3	1.6	11	0.5	51.7	30.8
2	23	7	1.6	11	0.5	31.6	770.8
3	21	3	2.4	11	0.5	191.5	147.7
4	2	7	2.4	11	0.5	255.2	183.9
5	9	3	1.6	11	0.7	205.1	163.8
6	24	7	1.6	11	0.7	81.5	46.8
7	3	3	2.4	11	0.7	242.5	175.3
8	5	7	2.4	11	0.7	270.9	196.0
9	13	3	1.6	13	0.5	101.7	79.8
10	1	7	1.6	13	0.5	29.2	62.7
11	4	3	2.4	13	0.5	56.1	41.0
12	26	7	2.4	13	0.5	111.5	77.6
13	7	3	1.6	13	0.7	101.2	83.6
14	19	7	1.6	13	0.7	171.3	104.5
15	14	3	2.4	13	0.7	65.1	51.4
16	16	7	2.4	13	0.7	88.6	57.8
17	8	3	2.0	12	0.6	652.1	500.1
18	6	7	2.0	12	0.6	611.7	484.4
19	27	5	1.6	12	0.6	242.4	204.7
20	17	5	2.4	12	0.6	490.9	353.2
21	15	5	2.0	12	0.5	412.5	340.5
22	12	5	2.0	12	0.7	617.7	487.7
23	18	5	2.0	11	0.6	126.4	83.4
24	25	5	2.0	13	0.6	159.9	113.3
25	11	5	2.0	12	0.6	640.4	503.4
26	10	5	2.0	12	0.6	640.8	500.6
27	20	5	2.0	12	0.6	530.0	333.4

TL = tube length, LF = luminol flow rate, LpH = luminol pH, RSF = reductant solution flow rate, responses for Cr(III) and Cr(VI) were measured as peak area in arbitrary units.

As can be seen from the summary of fit plot (Figure V) for the Cr(III) response (similar plots for the Cr(VI) response are available) the tube length has now reached its optimum, along with the other factors to give the optimum response for both Cr(III) and Cr(VI). The optimum values obtained for all the factors using both optimisation techniques are summarised in Table V.

Figure V. Summary of fit for full experimental model.

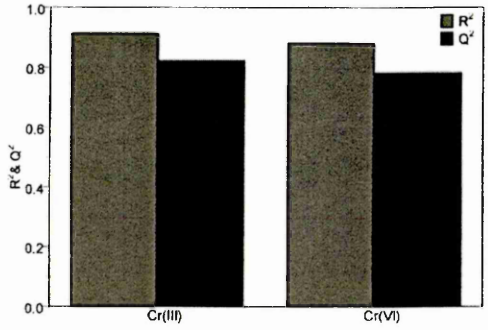

Figure VI. 4D Response surface for Cr(III); x axis = luminol pH, y axis = response (peak areas), z axis = reductant solution flow rate (mL min^{-1}). Outer axis = 3 levels of luminol flow rate (mL min^{-1}) and 3 levels of tube length (cm).

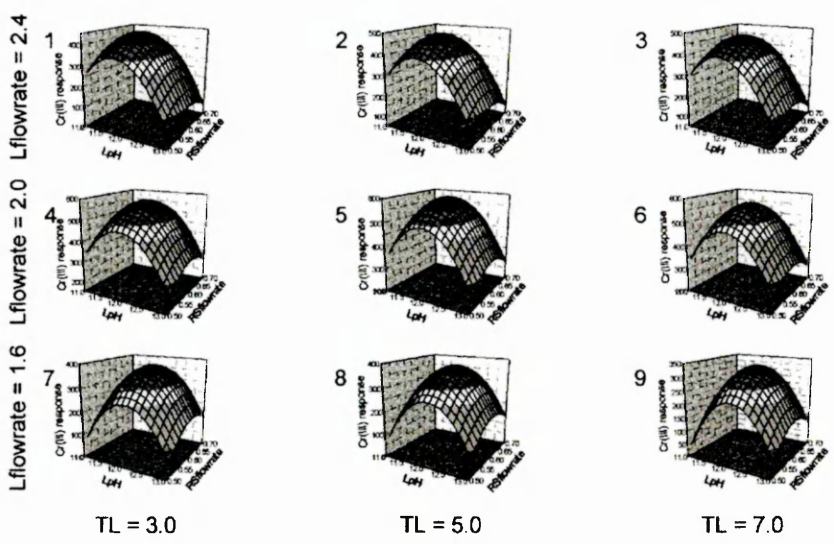

Comparison of Multivariate and Univariate Procedures

Table V shows that the four most important parameters have different values from the two different methods of optimisation. Most significant however is the fact that the most critical aspect of the chemiluminescent experiment i.e. the tube length, which determines the time from the luminol addition until it reaches the detector, is significantly different; 27 cm in the univariate method and only 5 cm in the multivariate method.

Table V. Comparison of univariate and multivariate optimisations.

Parameter	Univariate	Multivariate
Tube length	27 cm	5 cm
Luminol flow	1.8 mL min^{-1}	2.1 mL min^{-1}
Luminol pH	11.5	11.8
Luminol conc.	$3.4x10^{-4}$mol L^{-1}	$3.4x10^{-4}$ mol L^{-1}
Red. Flow	0.5 mL min^{-1}	0.6 mL min^{-1}
Red. pH	3.0	3.0
Red. conc.	0.015 mol L^{-1}	0.015 mol L^{-1}

The difference between the observed signal from the two methods can clearly be seen in Figure VII. This chromatogram is a comparison of the Cr(III) and Cr(VI) signals obtained using the two optimised sets of conditions for the analysis of a mixed standard solution containing 10 μg L^{-1}. When the multivariate set-up is used the signals from the Cr(III) and Cr(VI) are increased by 43 and 32% respectively. The limit of detection determined for this analysis was improved from 0.08 μg L^{-1} for both Cr(III) and Cr(VI) initially, determined using the univariate optimisation, to 0.002 μg L^{-1} with the multivariate optimisation. These detection limits were found using the IUPAC recommended criteria[15] of three times the standard deviation of the baseline noise. The effect of the interactions between the various instrumental and chemical parameters could be responsible for the differences in the optimised conditions obtained by both methods. Clearly the multivariate approach is to be preferred for the optimisation of analytical systems in which the output signal is determined by a number of interdependent parameters.

Figure VII: Comparison of multivariate and univariate optimisations.

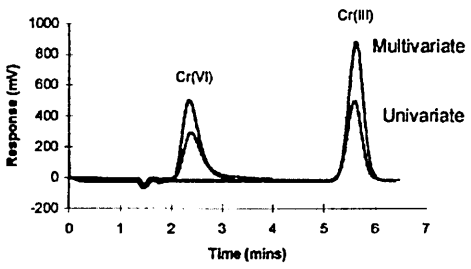

The Modde software is a powerful means of carrying out statistical experimental design. It is windows based and is not just useful for optimisation purposes, as was the case here, but may also be used for method development and validation in laboratories as well as process modelling and process development in industry.

Acknowledgement

MD would like to thank Håkan Emteborg, Malin Stigbrand and Einar Pontin for their help with the chemiluminescence analysis, and Jørgen Vinther Nørgaard for editorial assistance.

Work was carried out at the Joint Research Centre, Institute for Reference Materials and Measurements, Geel, Belgium as part of a Community Training Project financed by the Commission Programme "Reference Materials and Measurements".

[15] W.A. Aue and X.J. Sun., J. Chromatogr. A, 683 (1994) 253-260.

CHAPTER 10 Literature Cited

1 Ure, A.M., *Mikrochimica Acta*, 1991, **II**, 49-57.

2 Ure, A., Quevauviller, Ph., Muntau, H. & Griepink, B., Improvements in the Determination of Extractable Contents of Trace Metals in Soil and Sediment Prior to Certification, Commission of the European Communities, Report No. EUR 14763 EN, 1993.

3 Nakos, G., 1982, *Plant Soil*, **66**, 271-277.

4 Mitchell, R.L., 1971, Technical Bulletin No.21, Her Majesties State Office, London.

5 Schueneman, T.J., Plant Response to and Soil Immobilization of Increasing Levels of Zn^{2+} and Cr^{3+} Applied to a Catena of Sandy Soils, PhD Dissertation, Michegan State University, East Lansing, 1974.

6 Adriano, D.C., Trace Elements in the Natural Environment, *Springer-Verlag*, New York, 1986.

7 Morrison, G.M.P., Batley, G.E. & Florence, T.M., *Chemistry in Britain*, 1989, **25**, 791.

8 Ure, A.M. & Davidson, C.M. (eds.), Chemical Speciation in the Environment, 1st ed., *Blackie*, London, 1995.

9 Jeejeebhoy, K.N., Chu, R.C., Marliss, E.B., Greenberg, G.R. & Bruce-Robertson, A., *American Journal of Clinical Nutrician*, 1977, **30**, 531-538.

10 Berman, E., Toxic Metals and their Analysis, *Heyden*, London, 1980.

11 Anderson, R.A., *Science of the Total Environment*, 1989, **86**, 75-81.

12 Cox, A.G., Determination of Chromium in Natural Waters by Flow Injection Inductively Coupled Plasma Emission Spectrometry, PhD Dissertation, Sheffield Hallam University, School of Science, 1992.

[13] Townshend, A. (ed.), Encyclopaedia of Analytical Science, 1st ed., *Academic Press Ltd.,* London, 1995.

[14] Forstner, U. & Wittman, G.T.W., Metal Pollution in the Aquatic Environment, *Springer-Verlag*, New York, 1979.

[15] Gad, S.C., *Science of the Total Environment*, 1989, **86**, 149-157.

[16] Sittig, M., Handbook of Toxic and Hazardous Chemicals and Carcinogens, Vol. 1, 3rd ed., *Noyes*, New Jersey, 1991.

[17] Levis, A.G. & Bianchi, V., Mutagenic and Cytogenic Effects of Chromium Compounds. In; Langard, S. (ed), Topics in Environmental Health, Vol. 5, Biological and Environmental Aspects of Chromium, *Elsevier Biomedical Press*, New York, 1982.

[18] Pacyna, J.M. & Nriagu, J.O., Atmospheric Emmissions of Chromium from Natural and Anthropogenic Sources In: Nriagu, J.O. & Nieboer, E. (eds.), Chromium in the Natural and Human Environments Vol. 20 Advances in Environmental Science and Technology, *John Wiley & Sons*, New York, 1988.

[19] Cranston, R.E. & Murray, J.W., *Analytica Chimica Acta*, 1974, **99**, 275-282.

[20] Panklow, J.F. & Janauer, G.E., *Analytica Chimica Acta*, 1974, **69**, 97-104.

[21] Krull, I.S., Panero, K.W. & Gersham, L.L., *Journal of Chromatographic Science*, 1983, **21**, 460-472.

[22] Losi, M.E., Amrhein, C. & Frankenberger, W.T., *Reviews of Environmental Contamination and Toxicology*, 1994, **136**, 91-121.

[23] Schroeder, D.C. & Lee, G.F., *Water, Air and Soil Pollution*, 1975, **4**, 355-365.

[24] James, B.R. & Bartlett, R.J., *Journal of Environmental Quality*, 1983, **12**, 177-181.

[25] Richard, F.C. & Bourg, A.C.M., *Water Research*, 1991, **25**, 807-816.

[26] Goodgame, D.M.L., Hayman, P.B. & Hathway, D.E., *Inorganic Chimica Acta*, 1984, **91**, 113-115.

[27] Cary, E.E., Allaway, W.H. & Olson, O.E., *Journal of Agriculture and Food Chemistry*, 1977, **25**, 305-309.

[28] Cotton, F.A. & Wilkinson, G., Advanced Inorganic Chemistry, 4th ed., *John Wiley & Sons*, New York, 1980.

[29] Palmer, C.D. and Wittbrodt, P.R., *Environmental Health Perspectives*, 1991, **92**, 25-40.

[30] Rai, D., Sass, B.M. and Moore, D.A., *Inorganic*, 1987, **26**, 345-349.

[31] Dionex Technical Note 26, Determination of Cr(VI) in Water, Wastewater and Solid Waste Extracts, Dionex, Sunnyvale CA, USA, May 1990.

[32] Bartlett, R.J. & James, B.R., *Journal of Environmental Quality*, 1979, **8**, 31-35.

[33] Morabito, R., *Fresenius Journal of Analytical Chemistry*, 1995, **351**, 378-385.

[34] Li, X., Coles, B.J., Ramsey, M.H. & Thornton, I., *Chemical Geology*, 1995, **124**, 109-123.

[35] Prokisch, J., Kovacs, B., Gyori, Z. & Loch, J., *Communications in Soil Science and Plant Analysis*, 1995, **26**, 2051-2065.

[36] James, B.R., Petura, J.C., Vitale, R.J. & Mussoline, G.R., *Environmental Science & Technology*, 1995, **29**, 2377-2381.

[37] Greene, D.C., Pepe, S., Dolinsek, F. & Katz, S.A., *Journal of Environmental Science and Health*, 1992, **A27**, 577-586.

[38] Das, A.K., Chakraborty, R., Cevera, M.L. & Guardia, M., *Talanta*, 1995, **42**, 1007-1030.

[39] Tessier, A., Campbell, P.G.C. & Bisson, M., *Analytical Chemistry*, 1979, **51**, 844-851.

[40] Davidson, C.M., Thomas, R.P., McVey, S.E., Perala, R., Littlejohn, D. & Ure, A.M., *Analytical Chimica Acta*, 1994, **291**, 277-286.

[41] James, B.R., *Environmental Science and Technology*, 1996, **30**, 248A-251A.

[42] Vitale, R.J., Mussoline, G.R., Petura, J.C. & James, B.R., *Journal of Environmental Quality*, 1994, **23**, 1249-1256.

[43] Vitale, R.J., Mussoline, G.R., Rinehimer, K.A., Petura, J.C. & James, B.R., *Environmental Science and Technology*, 1997, **31**, 390-394.

[44] James, B.R., Petura, J.C., Vitale, R.J. & Mussoline, G.R., *Environmental Science and Technology*, 1995, **29**, 2377-2381.

[45] Nivas, T.B., Sabatini D.A., Shiau, B & Harwell, J.H., *Water Research*, 1996, **30**, 511-520.

[46] Houba, V.J.G. & Novozamsky, I., *Fresenius Journal of Analytical Chemistry*, 1998, **360**, 362-365.

[47] Pasullean, B., Davidson, C.M. & Littlejohn, D., *Journal of Analytical Atomic Spectrometry*, 1995, **10**, 241-246.

[48] Cantle, J.E. (ed.), Techniques and Instrumentation in Analytical Chemistry Volume 5: Atomic Absorption Spectrometry, *Elsevier*, New York, 1982.

[49] Kabil, M.A., *Journal of Analytical Atomic Spectrometry*, 1995, **10**, 733-738.

[50] Zybin, A., Schaldach, G., Berndt, H. & Niemax, K., *Analytical Chemistry*, 1998, **70**, 5093-5096.

[51] Oktavec, D., Lehotay, J. & Hornackova, E., *Atomic Spectroscopy*, 1995, **16**, 92-96.

[52] Manzoori, J.L., Sorouraddin, M.H. & Shemirani, F., *Talanta*, 1995, **42**, 1151-1155.

[53] Kubrakova, I., Kudinova, T., Formanovsky, A., Kuzmin, N., Tysin, G. & Zolotov, Y., *Analyst*, 1994, **119**, 2477-2480.

[54] Beceiro-Gonzalez, E., Barciela-Garcia, J., Bermejo-Barrera, P. & Bermejo-Barrera, A., *Fresenius Journal of Analytical Chemistry*, 1992, **344**, 301-305.

[55] Lameiras, J., Elisa Soares, M., Lourdes Bastos, M. & Ferreira, M., *Analyst*, 1998, **123**, 2091-2095.

[56] Manzoori, J.L. & Shemirani, F., *Journal of Analytical Atomic Spectrometry*, 1995, **10**, 301-305.

[57] Isozaki, A., Narukawa, T. & Okutani, T., *Bunseki Kagaku*, 1995, **44**, 111-115.

[58] Cox, A.G. & McCleod, C.W., *Mikrochimica Acta*, 1992, **109**, 161-164.

[59] Heltai, G., Jozsa, T. & Percsich, K., *Fresenius Journal of Analytical Chemistry*, 1996, **355**, 638-641.

[60] Tomlinson, M.J. & Caruso, J.A., *Analytica Chimica Acta*, 1996, **322**, 1-9.

[61] Tomlinson, M.J., Wang, J & Caruso, J.A., *Journal of Analytical Atomic Spectrometry*, 1994, **9**, 957-964.

[62] Powell, M.J. & Boomer, D.W., *Analytical Chemistry*, 1995, **67**, 2474-2478.

[63] Pantsar-Kallio, M. & Manninen, P.K.G., *Analytica Chimica Acta*, 1996, **318**, 335-343.

[64] Inoue, Y., Sakai, T. & Kumagai, H., *Journal of Chromatography A*, 1995, **706**, 127-136.

[65] Byrdy, F.A., Olson, L.K., Vela, N.P. & Caruso, J.A., *Journal of Chromatography A*, 1995, **712**, 311-320.

[66] Saverwyns, S., Van Hecke, K., Vanhaecke, F., Moens, L. & Dams, R., *Fresenius Journal of Analytical Chemistry*, 1999, **363**, 490-494.

[67] Zhang, X. & Koropchak, J.A., *Microchemical Journal*, 1999, **62**, 192-202.

[68] Nusko, R. & Heumann, K.G., *Analytica Chimica Acta*, 1994, **286**, 283-290.

[69] Andrle, C.M. & Broekaert, J.A.C., *Fresenius Journal of Analytical Chemistry*, 1993, **346**, 653-658.

[70] Eijärvi, E., Lajunen, L.H.J. & Heikha, M., *Finnish Chemical Letters*, 1985, **12**, 225-230.

[71] Tande, T., Petterson, J.E. & Torgrimsen, T., *Chromatographia*, 1980, **13**, 607-610.

[72] Schwedt, G., *Fresenius Zeitschrift Analytical Chemistry*, 1979, **295**, 382-387.

[73] Padarauskas, A. & Schwedt, G., *Talanta*, 1995, **42**, 693-699.

[74] Tian, S. & Schwedt, G., *Fresenius Journal of Analytical Chemistry*, 1996, **354**, 447-450.

[75] Sikovec, M., Novic, M., Hudnik, V. & Franko, M., *Journal of Chromatography A*, 1995, **706**, 121-126.

[76] Dionex, Dionex Ion Chromatography Cook Book: A Practical Guide to Quantitative Analysis by Ion Chromatography, Issue 1, Dionex, Sunnydale, CA, USA, 1987.

[77] Gammelgaard, B., Jøns, O. & Nielsen, B., *Analyst*, 1992, **117**, 637-640.

[78] Economou, A., Clark, A.K. & Fielden, P.R., *Analytical Communications*, 1998, **35**, 389-390.

[79] Li, R. & Hercules, D.M., *Analytical Chemistry*, 1974, June, **46**, 916-919.

[80] Escobar, R., García-Domínguez, M.S. & Guiraúm F.F. de la Rosa, A., *Fresenius Journal of Analytical Chemistry*, 1998, **361**, 509-511.

[81] Johnstone, R.A.W. and Rose, M.E., Mass Spectrometry for Chemists and Biochemists, 2nd ed., *Cambridge University Press*, Cambridge, 1996.

[82] Becker, J.S. & Dietze, H.J., *Spectrochimica Acta Part B*, 1998, 1475-1506.

[83] Chait, E.M., *Analytical Chemistry*, 1972, March, **44**, 77A-91A.

[84] Milne, G.W.A. & Lacey, M.J., *CRC Critical Reviews in Analytical Chemistry*, 1974, July, 45-104.

[85] Lichtman, D., *Research and Development*, 1964, **15**, 52.

[86] Nørgaard, J.V., Application and Charaterisation of a Micro Concentric Nebuliser for use in Inductively Coupled Plasma Mass Spectrometry, Degree Thesis, Technical University of Denmark, January 1996.

[87] Jarvis, K.E., Gray, A.L. & Houk, R.S., Handbook of Inductively Coupled Plasma Mass Spectrometry, *Blackie*, London, 1992.

[88] Jarvis, I. & Jarvis, K.E., *Chemical Geology*, 1992, **95**, 1.

[89] Fassel, V.A., *Analytical Chemistry*, 1979, **51**, 1290A-1308A.

[90] Montaser, A. (ed.), Inductively Coupled Plasma Mass Spectrometry, *Wiley-VCH*, New York, USA, 1998.

[91] Vanhoe, H., *Journal of Trace Elements and Electrolytes Health Discussion*, 1993, **7**, 131.

[92] Date, A.R. & Gray, A.L., Applications of Inductively Coupled Plasma Mass Spectrometry, *Blackie*, London, 1989.

[93] Sargent, M. & Webb, K., *Spectroscopy Europe*, 1993, **5**, 21-28.

[94] Beauchemin, D., *Trends in Analytical Chemistry*, 1991, **10**, 71-77.

[95] Nørgaard, J.V., Determination of Rubidium in Natural Waters by Using Inductively Coupled Plasma - Isotopic Dilution Mass Spectrometry, Internal Report, European Commission, Joint Research Centre, Institute for Reference Materials and Measurements, Geel, Belgium, June 1994.

[96] Dymott, T., *LabPlus International*, 2000, September/October, 22-24.

[97] Šťastná, M., Němcová. I. & Zýka, J., *Analytical Letters*, 1999, **32**, 2531-2543.

[98] Vandecasteele, C., Vanhoe, H. and Dams, R., *Journal of Analytical Atomic Spectrometry*, 1993, **8**, 781-786.

[99] Cantle, J.E. (ed.), Techniques and Instrumentation in Analytical Chemistry - Volume 5: Atomic Absorption Spectrometry, *Elsevier*, New York, 1982.

[100] Wollaston, W.A., *Philosophical Transactions of the Royal Society of London, Series A*, 1802, **92**, 365-370.

[101] Brewster, D., Report 2nd meeting, British Association, 1832, 320-331.

[102] West, P.W., Folse, P. & Montgomery, D., *Analytical Chemistry*, 1950, **22**, 667-670.

[103] Peters, D.G., Hayes, J.M. & Hieftje, G.M., Chemical Separations and Measurements: Theory and Practice of Analytical Chemistry, *Saunders College Publishing*, Orlando, 1985.

[104] Woodriff, R., *Applied Spectroscopy*, 1974, **28**, 413-417.

[105] Ewing, G.W., Instrumental Methods of Chemical Analysis, 5th edition, *McGraw Hill,* New York, 1985.

[106] Koirtyohann, S.R. & Kaiser, M.L., *Analytical Chemistry*, 1982, **54**, 1515A-1524A.

[107] L'vov, B.V., *Spectrochimica Acta*, 1961, **17**, 761-770.

[108] L'vov, B.V., *Spectrochimica Acta Part B*, 1978, **33B**, 153-193.

[109] Dresser, R.D., Mooney, R.A., Helthmar, E.M. & Plankey, F.W., *Journal of Chemical Education*, 1975, **52**, A451-A508.

[110] Skoog, D.A., West, D.M. & Holler, F.J., Fundamentals of Analytical Chemistry, 7th edition, *Saunders College Publishing*, Orlando, 1996.

[111] Slavin, W., *Analytical Chemistry*, 1982, **54**, 685A-694A.

[112] Peters, D.G., Hayes, J.M. & Hieftje, G.M., Chemical Separations and Measurements. Theory and Practice of Analytical Chemistry, *Saunders College Publishing*, Orlando, 1984.

[113] Maugh, T.H., *Science*, 1983, **220**, 183-188.

[114] Brown, S.D., *Analytical Chemistry*, 1977, **49**, 1269A-1281A.

[115] Fernandez, F.J., Myers, S.A. & Slavin, W., *Analytical Chemistry*, 1980, **52**, 741-746.

[116] Maugh, T.H., *Science*, 1977, **198**, 39-41.

[117] Zander, A.T., *American Laboratory*, 1976, **11**, 11-22.

[118] Sturgeon, R.E., *Analytical Chemistry*, 1977, **49**, 1255A-1267A.

[119] Tswett, M.S., Khromofilly v Rastitel'nom I Zhivotnom Mire (Chromophylls in the Plant and Animal World), *Karbasnikov Publishers*, Warsaw, 1910.

[120] Martin, A.J.P. & Synge, R.L.M., *Biochem. J.*, 1941, **35**, 1358.

[121] Ettre, L.S., & Zlatkis, A. (eds.), 75 Years of Chromatography - A Historical Dialogue, *Elsevier*, Amsterdam, 1979.

[122] Small, H., *Analytical Chemistry*, 1983, **55**, 235A-242A.

[123] Heftmann, E. (ed.), Chromatography, 3rd edition, *Van Nostrand Reinhold*, New York, 1975.

[124] Walton, H.F. (ed.), Ion-Exchange Chromatography, *Dowden, Hutchinson and Ross, Inc.*, Stroudsburg, PA, 1976.

[125] Fritz, J.S., *Analytical Chemistry*, 1987, **59**, 335A-344A.

[126] Reed, N.M., Cairns, R.O. and Hutton, R.C., *Journal of Analytical Atomic Spectrometry*, 1994, **9**, 881-896.

[127] IUPAC, Isotopic Compositions of the Elements 1989, *Pure and Applied Chemistry*, 1991, **63**, 991-1002.

[128] Ure, A.M., Quevauviller, Ph., Muntau, H. & Griepink, B., *International Journal of Environmental Analytical Chemistry*, 1993, **51**, 135-151.

[129] Dionex Technical Note 24, Determination of Chromium by Ion Chromatography: Method A, Dionex, Sunnyvale CA, USA, July 1991.

[130] Krishnamurty, K.V., Shpirt, E. & Reddy, M.M., *Atomic Absorption Newsletter*, 1976, **15**, 68-70.

[131] Cotton, F.A., Wilkinson, G. & Gaus, P.L., Basic Inorganic Chemistry, 2nd ed., *John Wiley & Sons*, New York, 1987.

[132] Eijärvi, E., Lajunen, L.H.J. & Heikha, M., *Chromatographia*, 1980, **13**, 607-610.

[133] Hope, J.M., Martin, R.L. & Taylor, D., *Journal of the American Chemical Society Chemical Communications*, 1977, bbnmm,.99-100.

[134] Andrle, C., Speziation von Chrom mittels Hochdruckflüssigkeitschromatographie (HPLC), Diplomarbeit, Universität Dortmund Fachbereich Chemie, Arbeitskreis Analytische Chemie, Juli 1992.

[135] Dionex Technical Note 24, Determination of Chromium by Ion Chromatography: Method A, Dionex, Sunnyvale CA, USA, July 1991.

[136] Willems, G.J., Blaton, N.M., Peeters, O.M. & De Router, C.J., *Analytica Chimica Acta*, 1977, **88**, 345-352.

[137] Harzdorf, A.C., *International Journal of Environmental Analytical Chemistry*, 1987, **29**, 249-261.

[138] Nriagu, J.O. & Nieboer, E., Chromium in the Natural and Human Environments, *John Wiley and Sons*, New York, 1988.

[139] Baeyens, W.R.G. & Ling, B.L., Potentials of Luminescence Analysis: An Overview In Baeyens, W.R.G., De Keukeleire, D. & Korkidis, K. (eds.), Luminescence Techniques in Chemical and Biochemical Analysis, *Marcel Dekker Inc.*, New York, 1991.

[140] Wiedemann, E., *Annalen der Physik und Chemie*, 1888, **34**, 446-463.

[141] Cambell, A.K. Chemiluminescence Principles and Applications in Biology and Medicine, *Ellis Horwood Ltd.,* Chichester, England, 1988.

[142] Schulman, S.G., Molecular Luminescence Spectroscopy. Methods and Applications: Part 1, *John Wiley and Sons*, New York, 1985.

[143] Nieman, T.A., Analytical Chemiluminescence in Flowing Streams: FIA and HPLC In Baeyens, W.R.G., De Keukeleire, D. & Korkidis, K. (eds.), Luminescence Techniques in Chemical and Biochemical Analysis, *Marcel Dekker Inc.*, New York, 1991, Chapter 17, 523-565.

[144] Robards, K. & Worsfold, P.J., *Analytica Chimica Acta*, 1992, **266**, 147-173.

[145] Emteborg, M., Theory and Applications of Imidazole-Mediated Peroxylate Chemiluminescence, PhD Dissertation, Umeå University, Umeå, Sweden, 1997.

[146] Tseng, S.S., Mohan, A.G., Haines, L.G., Vizcarra, L.S. & Rauhut, M.M., *Journal of Organic Chemistry*, 1979, **44**, 4113-4116.

[147] Kricka, L.J. & Thorpe, G.H.G., *Analyst*, 1983, **108**, 1274-1296.

[148] Nieman, T.A, Detection Based on Solution-Phase Chemiluminescence Systems In Birks, J.W. (ed.), Chemiluminescence and Photochemical Reaction Detection in Chromatography, *VCH Publishers Inc.,* New York, 1989.

[149] Seitz, W.R., *CRC Critical Reviews in Analytical Chemistry*, 1981, **13**, 1-58.

[150] White, E.H. & Roswell, D.F., Luminol Chemiluminescence In Burr, J.G. (ed.), Chemi- and Bioluminescence, *Marcel Dekker*, New York, 1985.

[151] Cormier, M.J., Hercules, D.M. & Lee, J. (eds.), Chemiluminescence and Bioluminescence, *Plenum Press*, New York, 1973.

[152] Burdo, T.G. and Seitz, W.R., *Analytical Chemistry*, 1975, **47**, 1639.

[153] Burr, J.G. (ed.), Chemi- and Bioluminescence, *Marcel Dekker*, New York, 1985.

[154] Neary, M.P., Seitz, R. & Hercules, D.M., *Analytical Letters*, 1974, **7**, 583-590.

[155] Hamm, R.E., *Journal of the American Chemical Society*, 1953, **75**, 5670-5672.

[156] Seitz, W.R., Suydam, W.W. & Hercules, D.M., *Analytical Chemistry*, 1972, **44**, 957-963.

[157] Hoyt, S.D. & Ingle, J.D. Jr., *Analytica Chimica Acta*, 1976, **87**, 163-175.

[158] Williams, T., Jones, P. & Ebdon, L., *Journal of Chromatography*, 1989, **482**, 361-366.

[159] Beere, H.G. & Jones, P., *Analytica Chimica Acta*, 1994, **293**, 237-243.

[160] Dionex, Dionex Consumables Selection Guide, Dionex, Sunnyvale CA, USA, 1995-96.

[161] Nieman, T.A., Detection Based on Solution-Phase Chemiluminescence Systems In Birks, J.W. (ed.), Chemiluminescence and Photochemical Reaction Detection in Chromatography, *V.C.H. Publishers Ltd.*, U.S.A., 1989.

[162] Box, G.E.P., Hunter, W.G. and Hunter, J.S., Statistics for Experimenters, *John Wiley & Sons*, New York, 1978.

[163] Lavine, B.K., *Analytical Chemistry*, 2000, **72**, 91R-97R.

[164] Davies, O.L. (ed.), Statistical Methods in Research and Production Design and Analysis of Industrial Experiments, *Oliver & Boyd*, Edinburgh, 1947.

[165] Davies, O.L. (ed.), The Design and Analysis of Industrial Experiments, *Oliver & Boyd*, Edinburgh, 1954.

[166] Box, G.E.P. & Draper, N.R., Impirical Model-Building and Response Surfaces, *John Wiley & Sons*, New York, 1987.

[167] Kiefer, J.C., Jack Carl Kiefer Collected Papers III, *Springer*, New York, 1985.

[168] Morgan, E., Burton, K.W. & Church, P.A., *Chemometrics and Intelligent Laboratory Systems*, 1989, **5**, 283-302.

[169] Massart, D.L., Vandeginste, B.G.M., Buydens, L.M.C., De Jong, S., Lewi, P.J. & Smeyers-Verbeke, J., Handbook of Chemometrics and Qualimetrics: Part A, *Elsevier*, Amsterdam, 1997.

[170] Morgan, E., Chemometrics: Experimental Design, Analytical Chemistry by Open Learning, *John Wiley & Sons*, New York, 1991.

[171] Atkinson, A.C., *Chemometrics and Intelligent Laboratory Systems*, 1995, **28**, 35-47.

[172] Umetri AB, Users guide to Modde 4.0, Manual edition 1997-06-13, Umetri AB, Umeå, Sweden, 1997.

[173] Holtzclaw, H.F., Robinson, W.R. & Odom, J.D., General Chemistry with Quantitative Analysis, 9th edition, *D.C. Heath & Co.*, Toronto, 1991.

[174] Holleman, A.F. & Wiberg, E., Lehrbuch der Anorganischen Chemie, 34th edition, de Gruyter & Co., Berlin, 1995.

[175] Economou, A., Clark, A.K. & Fielden, P.R., *Analytical Communications*, 1998, **35**, 389-390.

[176] Chang, C.A. & Patterson, H.H., *Analytical Chemistry*, 1980, **52**, 653-656.

[177] Aue, W.A. & Sun, X., *Journal of Chromatography*, 1993, **633**, 151-162.

178 Vercoutre, K., Cornelis, R. & Quevauviller, Ph., The Certification of the Contents of the Cr(III), Cr(VI) Species and Total Cr in a Lyophilised Solution CRM544, Commission of the European Communities, Report No. EUR 17605 EN, 1997.

179 Miller, J.C. & Miller, J.N., Statistics for Analytical Chemistry, 3rd edition, *Ellis Horwood*, New York, 1993.

180 Sperling, M., Yin, X. & Welz, B., *Journal of Analytical Atomic Spectrometry*, 1991, **6**, 295-300.

181 Kozuh, N., Stupar, J., Milacic, R. & Gorenc, B., *International Journal of Environmental Analytical Chemistry*, 1994, **56**, 207-217.

182 Wang, J., Ashley, K., Kennedy, E.R. & Neumeister, C., *Analyst*, 1997, **122**, 1307-1312.

183 Karwas, C.P., *Journal of Environmental Science and Health, Part A.*, 1995, **30**, 1223-1235.

184 Bartlett, R.J. & Kimble, J.M., *Journal of Environmental Quality*, 1976, **5**, 379-383.

185 Örnemark, U., Pettersson, J. & Olin, Å., *Talanta*, 1992, **39**, 1089-1096.

186 Skoog, D.A., West, D.M. & Holler, F.J., Fundamentals of Analytical Chemistry, 7th edition, *Saunders College Publishing*, Orlando, 1996.

187 Daintith, J.(ed.), Oxford Dictionary of Chemistry, *Oxford University Press*, Oxford, 1996.

188 Zumdahl, S.S., Chemistry, 3rd edition, *D.C. Heath & Co.*, U.S.A., 1993.

189 Lepretre, A. & Martin, S., *Analusis*, 1994, **22**, M40-M43.

190 Fortunati, G.U., Banfi, C. & Pasturenzi, M., *Fresenius Journal of Analytical Chemistry*, 1994, **348**, 86-100.

191 Sampling of Soils, Soiless Growing Media, Crop Plants and Miscellaneous Substances for Chemical Analysis, Booklet No. 2082, Ministry for Agriculture, Forests and Fisheries, UK.

192 Rubio, R., & Ure, A.M., *International Journal of Environmental Analytical Chemistry*, 1993, **51**, 205-217.

193 Jackson, M.L., Soil Chemical Analysis, *Constable & Co. Ltd.*, London, 1958.

194 Reed & Rigney, *Journal of the American Society of Agronomy*, 1947, **39**, 26-32.

195 Piper, Soil and Plant Analysis, *Interscience Publishers Inc.*, New York, 1944.

196 Scott, R.O & Ure, A.M., *Analyst Proceedings*, 1972, **10**, 288-293.

197 Allen, T. & Khan, A.A., *The Chemical Engineer*, 1970, **5**, 108-112.

198 Hoffmann, P., *Nachrichten aus Chemie, Technik und Laboratorium: Zeitschrift der GDCh.*, 1992, **40**, M2-M7.

199 Griepink, B., *Fresenius Journal of Analytical Chemistry*, 1990, **338**, 486-488.

200 Maier, E.A., *Trends in Analytical Chemistry*, 1991, **10**, 340-347.

201 Quevauviller, Ph., *Analusis*, 1993, **21**, M47-M53.

202 Maier, E.A., Boenke, A. & Meriguet, P., *Trends in Analytical Chemistry*, 1997, **16**, 496-503.

203 Quevauviller, Ph., *Trends in Analytical Chemistry*, 1999, **18**, 76-85.

204 Rasberry, S.D., *Fresenius Journal of Analytical Chemistry*, 1998, **360**, 277-281.

205 Griepink, B., *Fresenius Journal of Analytical Chemistry*, 1990, **337**, 812-816.

206 Thompson, M. & Wood, R., *Pure and Applied Chemistry*, 1993, **65**, 2123-2144.

207 Hasselbarth, W., *Fresenius Journal of Analytical Chemistry*, 1996, **354**, 263-265.

208 Quevauviller, Ph., *Analyst*, 1995, **120**, 597-602.

209 Quevauviller, Ph., *Spectrochimica Acta Part B*, 1998, **53**, 1261-1279.

[210] Quevauviller, P. & Maier, E.A., Interlaboratory Studies and Certified Reference Materials for Environmental Analysis, *Elsevier*, Amsterdam, 1999.

[211] ISO Guide 30, Terms and Definitions used in Connection with Reference Materials, 2nd edition, ISO, Geneva, Switzerland, 1992.

[212] ISO Guide 35, Certification of Reference Materials - General and Statistical Principles, 2nd edition, ISO, Geneva, Switzerland, 1989.

[213] ISO Guide 34, General Requirements for the Competence of Reference Material Producers, 2nd edition, ISO, Geneva, Switzerland, 2000.

[214] BCR/48/93, Guidelines for the Production and Certification of BCR Reference Materials, European Commission, Standards, Measurements and Testing Programme, Brussels, Belgium, 15 December 1994.

[215] BCR/12/96, List of Suggested Amendments of the Guidelines, Scientific Evaluation Group SMT, European Commission, Brussels, 1996.

[216] BCR01/97-Part A, Guidelines for the Production and Certification of BCR Reference Materials Part A: Recommendations to Proposers of Reference Material Projects, European Commission, Standards, Measurements and Testing Programme, Brussels, Belgium, 1 September 1997.

[217] Quevauviller, P. & Maier, E.A., Quality Assurance and Quality Control for Environmental Monitoring In: Quevauviller, P. (ed.) Quality Assurance in Environmental Monitoring. Sampling and Sample Pretreatment, *VCH Publishers*, New York, 1995.

[218] Kane, J.S., *Analyst*, 1997, **122**, 1289-1292.

[219] Kurfurst, U., Pauwels, J., Grobecker, K.H., Stoeppler, M. & Muntau, H., *Fresenius Journal of Analytical Chemistry*, 1993, **345**, 112-120.

[220] Walker, R.F., *Trends in Analytical Chemistry*, 1997, **16**, 9-16.

221 Kramer, G.N. & Pauwels, J., *Mikrochimica Acta*, 1996, **123**, 87-93.

222 De Bievre, P. Mayer, K. & Taylor, P.D.P., *Escarda Bulletin*, **27**, 38-43.

223 De Bievre, P. Kaarls, R., Peiser, H.S., Rasberry, S.D. & Reed, W.P., *Accreditation and Quality Assurance*, 1997, **2**, 168-179.

224 De Bievre, P. Kaarls, R., Peiser, H.S., Rasberry, S.D. & Reed, W.P., *Accreditation and Quality Assurance*, 1997, **2**, 270-274.

225 De Bievre, P. Kaarls, R., Peiser, H.S., Rasberry, S.D. & Reed, W.P., *Accreditation and Quality Assurance*, 1996, **1**, 3-13.

226 Günzler, H. (ed.), Accreditation and Quality Assurance in Analytical Chemistry, *Springer-Verlag*, New York, In publication.

227 De Bievre, P. & Taylor, P.D.P., *AOAC International*, 2000, Nov./Dec.

228 De Bievre, P. & Taylor, P.D.P., *Fresenius Journal of Analytical Chemistry*, 2000, **368**, 567-573.

229 Pauwels, J., Van der Veen, A., Lamberty, A. & Schimmel, H., *Accreditation and Quality Assurance*, 2000, **5**, 95-99.

230 Zellis, M.K., Bell, J.S. & Prunty, L., *Soil Science Society of America Journal*, 1998, **62**, 257-262.

231 Mitchell, J. & Smith, D.M., Aquametry, 2nd edition, *Interscience*, New York, 1977.

232 Harris, D.C., Quantitative Chemical Analysis, 3rd edition, *W.H. Freeman & Co.*, New York, 1991.

233 Hydranal®-Manual. Eugen Scholz Reagents for Karl Fischer Titration, Riedel-de Haën Laborchemikalien GmbH & Co. KG, Seelze, Germany, 1997.

234 Grünke, S. & Wünsch, G., *Fresenius Journal of Analytical Chemistry*, 2000, **368**, 139-147.

[235] Schöffski, K., Coates, A. & Brunet, L., *Analysis Europa*, 1996, Sept./Oct., 39-44.

[236] Metrohm, Instructions for Use: 701 KF Titrino Series 01, Manual No. 8.701.1003, Metrohm Ltd., Herisau, Switzerland.

[237] Operating Instructions 1213/13E for Alpine Grinding and Classifying System, Alpine AG, Ausburg, Germany.

[238] Rumpf, I., Fritsch Pulverisette 5 Labor-Planeten-Kugelmüh Manual, Fritsch GMBH, Idar-Oberstein, Germany.

[239] Sympatec User Meeting Notes, Sympatec GmbH, Etten-Leur, The Netherlands, 16 April 1997.

[240] Witt, W. & Röthele, S., *Particle and Particle Systems Characterization*, 1996, **13**, 280-286.

[241] Turbula Shaker Mixer Manual 27624, WAB, Basel, Switzerland.

[242] Kramer, G.N., Muntau, H., Maier, E. & Pauwels, J., *Fresenius Journal of Analytical Chemistry*, 1998, **360**, 299-303.